Università degli Studi di Ferrara

DOTTORATO DI RICERCA IN
"BIOCHIMICA BIOLOGIA MOLECOLARE E BIOTECNOLOGIE"

CICLO XXV

COORDINATORE Prof. FRANCESCO BERNARDI

RUOLO DELLE PROTEINE MINORITARIE DEL RETICOLO SARCOPLASMATICO NELL'ACCOPPIAMENTO ECCITAZIONE-CONTRAZIONE DEL MUSCOLO SCHELETRICO.

Settore Scientifico Disciplinare MED/04

Dottorando
Dott. MOSCA BARBARA

Tutore
Prof. ZORZATO FRANCESCO

Anni 2009/2012

INDICE pp.1

1. INTRODUZIONE

1.1. Il TESSUTO MUSCOLARE

Il tessuto muscolare è costituito da cellule muscolari responsabili della contrazione muscolare e da involucri connettivali che nutrono il muscolo e lo ancorano al sistema scheletrico.

Il muscolo si divide in muscolo liscio e muscolo striato. Il MUSCOLO LISCIO possiede fibre fusiformi mononucleate, per contrazioni toniche prolungate, prive di striatura trasversale. I nuclei si trovano in posizione centrale rispetto alla cellula. Il muscolo liscio ha la caratteristica di avere una elevata forza di contrazione con un ridotto consumo di ATP ed alta frazione di accorciamento. La scarsa velocità di contrazione è dovuta alla lenta formazione dei ponti actina-miosina. Le proteine contrattili non sono allineate come nella fibra muscolare scheletrica e cardiaca ed inoltre il controllo della contrazione è indipendente dalla volontà.

Il MUSCOLO STRIATO è il più evoluto, al microscopio ottico presenta una striatura trasversale per l'alternarsi di zone ottiche diverse e si divide in muscolo cardiaco e scheletrico.

Il muscolo cardiaco si contrae ritmicamente in assenza di stimolazione nervosa grazie a cellule pacemaker che si depolarizzano in maniera vigorosa e spontanea. Gli elementi cellulari sono più piccoli e mononucleati di natura non sinciziale e disposti centralmente rispetto alla fibra. Le cellule sono unite tra loro attraverso dischi intercalari, giunzioni intime in modo tale da consentire la propagazione dell'onda di contrazione. Le proteine contrattili sono allineate in modo regolare, creando sarcomeri simili a quelli del muscolo scheletrico.

Il muscolo scheletrico o somatico composto da cellule cilindriche molto lunghe, si contrae sotto il controllo della stimolazione nervosa, presenta fibre e tendini muscolari. In invaginazioni complesse delle membrana plasmatica si inseriscono le fibre collagene dei diversi involucri connettivali, le quali si fondono le une alle altre all'estremità del muscolo formando il tendine.

1.2. FUNZIONI DEL MUSCOLO SCHELETRICO

Sono molteplici le funzioni che svolge il tessuto muscolare scheletrico tra cui:

- servomotore per la ventilazione polmonare e la mobilità di articolazioni e sfinteri viscerali (sono striati oltre ai muscoli della lingua anche quelli della parte superiore dell'esofago);

- pompa per il ritorno venoso dagli arti inferiori;

- bruciatore per la termogenesi (per sostenere la termogenesi normale e patologica);

- riserva di aminoacidi utilizzabili durante il digiuno protratto;

- secretore autocrino e paracrino-endocrino.

1.3. ULTRASTRUTTURA DEL MUSCOLO SCHELETRICO

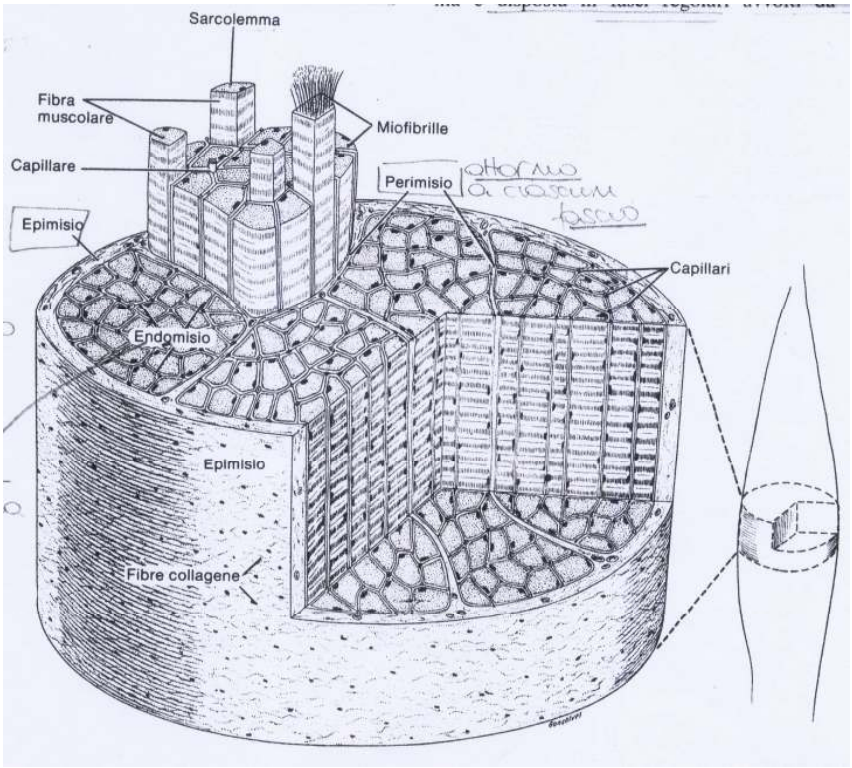

Figura1. Struttura del muscolo scheletrico striato. (Immagine tratta dal libro di testo Compendio di Istologia, L.C. Junqueira;J. Carneiro; R. Kelley)

La cellula muscolare o fibra è un sincizio polinucleato che deriva dalla fusione, durante lo sviluppo, di cellule progenitrici mononucleate embrionali, i mioblasti (cellule staminali muscolari). Ciascuna fibra è avvolta da una membrana connettivale delicata composta

da una lamina basale e da fibre reticolari detta endomisio. Le fibre a loro volta sono riunite in fasci, a formare il fascicolo, avvolto da una membrana detta perimisio. L'insieme dei fascicoli muscolari che formano il muscolo è circondato da una ulteriore guaina di tessuto connettivo denso detta epimisio. Nel tessuto connettivo parallelamente tra una fibra e l'altra penetra una ricca rete di capillari sanguigni e di nervi costituiti da fibre nervose e motorie, mentre i vasi linfatici risiedono nel tessuto connettivo. Ogni fibra muscolare è di forma cilindrica allungata e la lunghezza può variare da alcuni cm ad alcuni m ed il diametro da 10 ai 150 µm a seconda del muscolo.

I NUCLEI ovali si trovano alla periferia della cellula subito sotto la membrana plasmatica anche detta sarcolemma. Ciascuna fibra è costituita da citoplasma (sarcoplasma o mioplasma) contenente gli organelli cellulari tra cui il reticolo endoplasmatico (sarcoplasmatico) liscio, numerosi mitocondri e fasci di filamenti cilindrici detti miofibrille, aventi un diametro di 1-2 µm, le quali si estendono da un lato all'altro della fibra, ed a loro volta sono costituite da fasci di filamenti di natura proteica detti miofilamenti. Le miofibrille costituiscono le UNITA' CONTRATTILI del muscolo scheletrico ed appaiono come una successione di bande chiare e scure, trasversali rispetto all'asse longitudinale della cellula e birifrangenti al microscopio. L'effetto della striatura è dato dall' alternanza delle bande scure A, anisotrope (birifrangenti in luce polarizzata), aventi al centro una zona più chiara detta banda H, che a sua volta è bisecata dalla linea M; e dalle bande chiare I, isotrope (non alterano la luce polarizzata), bisecate dalla linea scura Z. Il tratto compreso tra due linee Z costituisce il sarcomero che è l'unità funzionale del muscolo.

La ***banda A***, lunga 1,5 µm, è la porzione del sarcomero comprendente l'intera lunghezza dei filamenti spessi, compresi i filamenti di actina che vi si sovrappongono alle estremità, è situata in posizione centrale, e non cambia la sua estensione durante la contrazione anche se tende a diventare più elettrondensa per la maggiore sovrapposizione dei filamenti sottili di actina.

La ***banda I*** lunga mediamente 0,8 µm, è la porzione di due sarcomeri adiacenti costituita da soli filamenti sottili di actina. In un sarcomero sono presenti due emibande I, una per ciascuna linea Z e con differente polarità, ma mai una banda I completa. Nel muscolo a riposo al microscopio elettronico appare come una banda larga e chiara, e al microscopio ottico è poco colorabile, ma durante la contrazione diventa più stretta per lo

scorrimento dei filamenti di actina (mentre la banda A rimane uguale) che si sovrappongono per un'estensione maggiore a quelli di miosina.

La ***banda H*** è una porzione della banda A, ed è costituita dalla porzione del sarcomero costituita dai soli filamenti spessi di miosina. Al microscopio elettronico appare come una zona occupata solo da filamenti elettrondensi di miosina, è meno elettrondensa della banda A ma più della banda I. La sua lunghezza diminuisce notevolmente durante la contrazione per la sovrapposizione dei filamenti actinici che si sovrappongono per un'estensione maggiore sui filamenti di miosina.

La ***linea M*** è una stretta banda che si forma all'interno della banda H. È costituita dalle code delle molecole di miosina e da proteine accessorie.

A  B 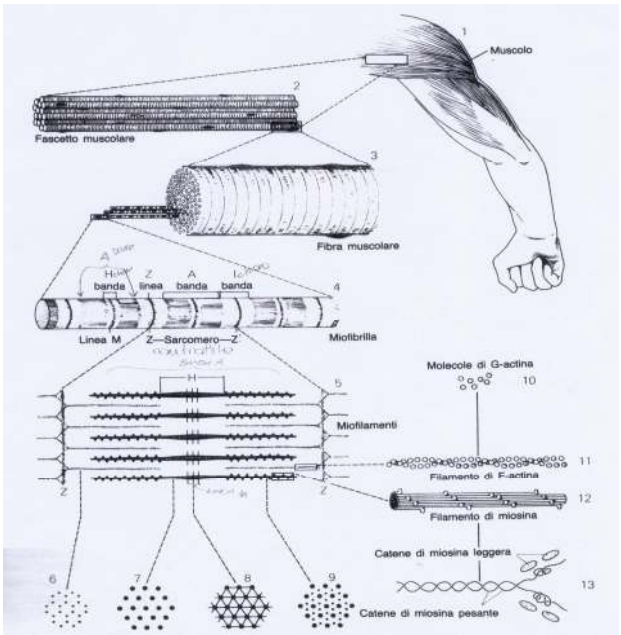

Figura 2. A. Sezione di muscolo scheletrico osservata al microscopio a polarizzazione. Le bande A appaiono come linee birifrangenti brillanti. Ciò è duvuto al fatto che le molecole di miosina dei filamenti spessi sono rigidamente ordinate. Le bande I sono scure.

Figura 2. B. Schema che illustra la struttura e la posizione dei filamenti spessi e sottili nel sarcomero. (Immagine tratta dal libro di testo Compendio di Istologia, L.C. Junqueira;J. Carneiro; R. Kelley)

Le MIOFIBRILLE possiedono una serie ordinata di miofilamenti spessi e di filamenti sottili.

I filamenti spessi sono molecole di miosina avente peso molecolare di 480 KDa, formata da due catene pesanti, cilindriche e sottili avvolte l'una sull'altra, e da quattro catene leggere identiche. La miosina è composta da una parte filamentosa idrofobica detta coda, una zona di flessibilità e da una parte globosa idrofilica detta testa che possiede siti di legame per l'ATP ed anche la capacità enzimatica di idrolizzare l'ATP (attività ATP-asica) e di legarsi alla actina. Ogni miofilamento è composto da circa 200 melecole di miosina orientate in modo contrapposto testa-coda.

I miofilamenti sottili sono composti dalle proteine actina, tropomiosina e troponina.

L'actina ha un peso molecolare di 42 KDa, si presenta come lunghi polimeri filamentosi/fibrosi F-actina consistenti di due filamenti di 300-400 monomeri globulari G-actina avvolti l'uno sull'altro nella configurazione ad elica destrorsa. Quando le molecole di G-actina polimerizzano per formare F-actina si legano "fronte-retro" producendo un filamento con una polarità. Ciascun monomero di G-actina possiede siti per l'ATP ed un sito di legame per la miosina.

La tropomiosina avente un peso molecolare di circa 70 KDa, è di tipo fibroso, bastoncellare sottile lunga 40 nm contenente 2 catene polipeptidiche nella configurazione ad •-elica avvolte l'una sull'altra, ed ha una forte affinità per le scanalature tra le due catene di actina.

La troponina ha un peso molecolare di circa 80 KDa, è di tipo globulare e si trova nei punti di giunzione della tropomiosina. E' composta da tre subunità proteiche: troponina T (TnT) avente la funzione di legare la tropomiosina, subunità I (TnI) che lega il filamento di actina e la subunità C (TnC) o catalitica ad elevata affinità per lo ione calcio. Il sistema troponina-tropomiosina può esser considerato un inibitore dell'apparato contrattile, in quanto a riposo la tropomiosina è legata all'actina coprendo i siti di legame actina-miosina.

1.4. TEORIA DELLO SCORRIMENTO DEI MIOFILAMENTI “SLIDING FILAMENTS” di Huxley

La fase finale della contrazione muscolare può essere divisa in due fasi: 1. aggancio (formazione dei ponti trasversali, crossbridges) tra i filamenti spessi e sottili; 2. scorrimento dei filamenti stessi. L’azione ciclica di queste due fasi determina l’accorciamento dell’ intera miofibra e di conseguenza dell’intero muscolo. La forza generata da un singolo sarcomero varia linearmente con l’entità di sovrapposizione dei miofilamenti, poiché una elevata sovrapposizione determina un elevato numero di crossbridges. La tensione sviluppata dal muscolo dipende quindi dal grado di interazione tra filamenti di actina e miosina.

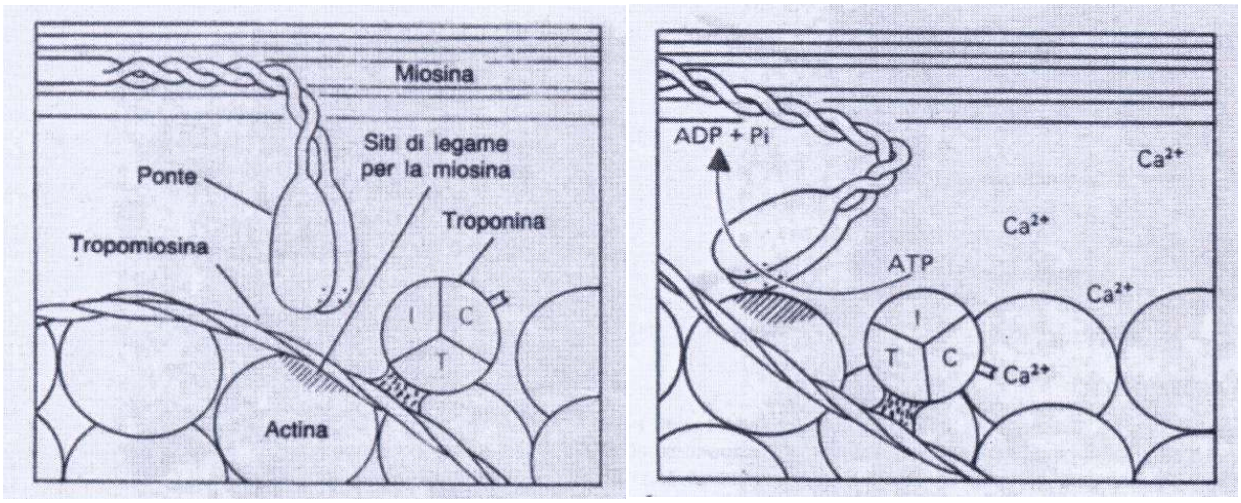

A **B**

Figura 3. La contrazione del muscolo inizia quando il Ca^{2+} si lega alla subunità TnC della Troponina, con la conseguente liberazione nell’actina del sito di legame per la miosina (Figura A, tratteggio obliquo). Figura B: in un secondO stadio la testa della miosina si lega all’actina e l’ATP viene viene demolita in ADP con la cessione di energia che induce il movimento della testa di miosina. In conseguenza delle modificazioni conformazionali, i filamenti sottili scorrono sopra i filamenti spessi. Fenomeno che si ripete più volte durante un’unica contrazione e provoca la completa sovrapposizione dei filamenti, fino all’accorciamento dell’intera miofibra. (Immagine tratta dal libro di testo Compendio di Istologia, L.C. Junqueira;J. Carneiro; R. Kelley)

A riposo i sarcomeri consistono di filamenti spessi e sottili parzialmente sovrapposti, i quali durante la contrazione mantengono la loro lunghezza originaria, ma divengono completamente sovrapposti.

In condizioni di riposo l'ATP si lega al sito contenente ATPasi sulle teste di miosina, ma la velocità di idrolisi è molto lenta. Per demolire rapidamente l'ATP e generare energia la miosina richiede l'actina come cofattore. A riposo però la miosina non può associarsi all'actina poiché i siti di legame per la miosina sulle molecole di actina sono bloccati dal complesso troponina-tropomiosina.

Tuttavia quando la gli ioni calcio divengono disponibili in concentrazione elevata, da innescare la contrazione, si legano alla subunità C della troponina generando una modificazione della configurazione spaziale della intera molecola di troponina consentendo alla tropomiosina di approfondare nell'elica dell'actina. Questa modificazione consente la liberazione del sito di legame per la miosina sull'actina ed i 2 filamenti possono interagire. Come conseguenza dell'interazione, l'ATP si suddivide in ADP + Pi e viene liberata energia. Questa attività provoca un ripiegamento della testa di miosina di 45° che causa lo scorrimento dell'actina lungo il filamento di miosina e ne consegue che il filamento sottile viene spinto in avanti nella banda A. Nel momento in cui le teste di miosina spostano l'actina entrano in funzione nuovi ponti trasversali actina-miosinici, mentre i vecchi ponti si rompono soltanto dopo che la miosina si è legata a una nuova molecola di ATP e ciò provoca il ritorno alla posizione originaria della testa di miosina e la prepara per un altro ciclo di contrazioni. Ogni contrazione muscolare è il risultato di centinaia di cicli di formazione e rottura di ponti trasversali fra actina e miosina. L'attività di contrazione che provoca la completa sovrapposizione dei filamenti sottili e spessi prosegue fino a che gli ioni calcio sono rimossi dal mioplasma ed il complesso troponina-tropomiosina maschera nuovamente i siti di legame della miosina.

Esistono poi altre PROTEINE DI TIPO STRUTTURALE quali:

-Titina che è una sorta di "molla" per mantenere i miofilamenti spessi concentrici con i filamenti sottili di actina;

-Nebulina "molecular ruler" avente la funzione di mantenere costante la lunghezza dei miofilamenti di actina;

-Laminina, una glicoproteina formata da tre diverse catene polipeptidiche legate da ponti disolfuro. Insieme al collagene IV compone reti interconnesse nella membrana basale, conferendo a quest'ultima elasticità e forza.

-Distrofina a forma di bastoncello, lega l'actina a spettrina e •-actinina, che forma filamenti contrattili e paralleli. La distrofina è localizzata sulla superficie interna della membrana plasmatica ed ancora il sarcomero alla membrana;

-Actinina , principale componente della linea Z, e desmina legano tra loro sarcomeri adiacenti, in tal modo mantengono in registro le miofibrille.

La contrazione muscolare dipende dalla disponibilità degli ioni calcio, mentre la decontrazione del muscolo è in rapporto con l'assenza degli ioni. Il RETICOLO SARCOPLASMATICO (SR) regola in modo specifico il flusso di ioni calcio. Dal punto di vista strutturale il reticolo sarcoplasmatico che costituisce approssimativamente il 10% del volume cellulare, appare come una complessa rete tubulare interna che circonda ciascuna miofibrilla e rappresenta il principale deposito di calcio della fibra. Si divide in LONGITUDINALE che decorre lungo tutta la miofibrilla e connette due cisterne terminali e GIUNZIONALE all'estremità dei sarcomeri. La parte giunzionale si presenta come CISTERNE TERMINALI che non sono altro che delle dilatazioni del reticolo sarcoplasmatico, adiacenti ed in associazione con i tubuli trasversi, TUBULI T, ovvero invaginazioni del sarcolemma. Il complesso reticolo sarcoplasmatico (SR)-tubuli T-SR prende il nome di TRIADE che è alla base del meccanismo eccitazione-contrazione, in quanto a livello della triade la depolarizzazione dei tubuli T, contenenti il recettore delle Diidropiridine (DHPR) sensibile al voltaggio, viene trasmessa al reticolo sarcoplasmatico dove sono localizzati i recettori della Rianodina (RyR-1) canali di rilascio del calcio (Mitchell et al., 1983; Rios e Pizarro, 1991; Melzer et al., 1995). La copiosa fuoriuscita di calcio dal reticolo innesca il movimento delle proteine contrattili detto appunto accoppiamento eccitazione-contrazione (**EC coupling**).

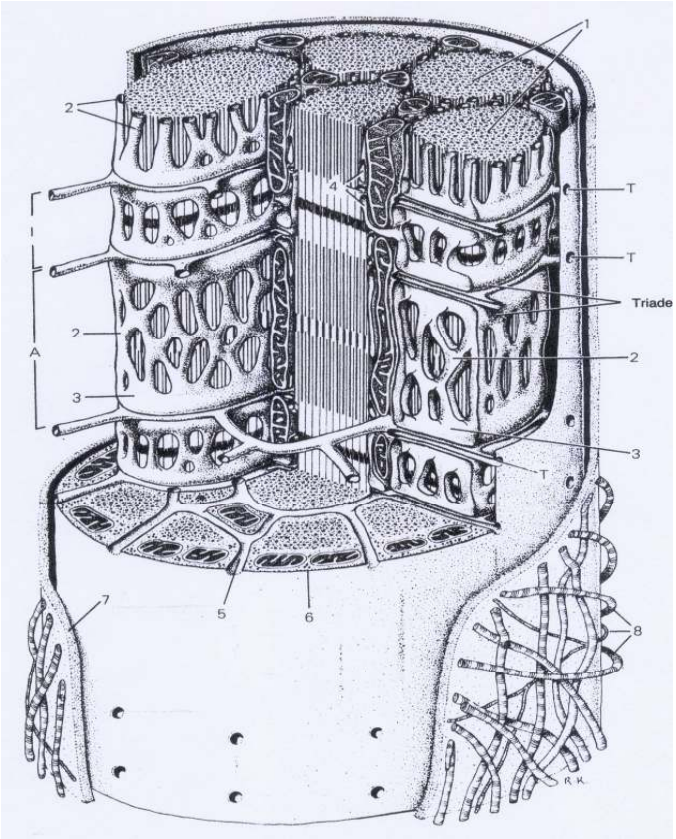

Figura 4. Schema di un segmento di muscolo. Il sarcolemma e le fibrille muscolari sono parzialmente tagliate. Si possono notare: le invaginazioni dei tubuli T (T e 5) a livello della transizione fra le bande A e I, due volte in un sarcomero. Esse si associano alle cisterne terminali del reticolo sarcoplasmatico (3) formando le triadi. Fra le miofibrille vi sono numerosi mitocondri (4). Nelle superfici di taglio delle miofibrille (1) si riconoscono i filamenti spessi e sottili. Il sarcolemma è circondato da una lamina basale (7) e da fibre reticolari (8). (Immagine tratta dal libro di testo Compendio di Istologia, L.C. Junqueira;J. Carneiro; R. Kelley)

Le cellule muscolari mature possiedono quantità trascurabili di reticolo sarcoplasmatico rugoso e di ribosomi.

Altro componente strutturale invece presente in grande quantità è rappresentato dai MITOCONDRI, anche se sono presenti in numero ridotto nelle fibre di tipo rapido. Sono organelli membranosi dotati di un sistema di membrane interne dette creste e ricchi di enzimi del ciclo di Krebs. Questi organelli sono deputati alla respirazione cellulare per il rifornimento energetico delle attività metaboliche cellulari mediante rilascio di ATP.

Nel sarcoplasma si trovano inoltre in abbondanza il GLICOGENO sotto forma di granuli grossolani distribuiti lungo le miofibrille, i quali fungono da deposito di energia utilizzata durante la contrazione muscolare. Sono inoltre presenti i LIPIDI raccolti in vacuoli, anch'essi utilizzati come combustibili cellulari. Un altro componente del sarcoplasma è

la MIOGLOBINA, simile all'emoglobina a cui si deve in gran parte il colore rosso scuro di alcuni muscoli. La mioglobina funge da pigmento che immagazzina l'ossigeno che diffonde dai capillari sanguigni tra le fibre.

1.5. SISTEMA DI PRODUZIONE DELL'ENERGIA

Le cellule muscolari scheletriche sono ben adattate alla produzione discontinua di lavoro meccanico mediante la liberazione di energia, e devono inoltre essere provviste di fonti di energia per soddisfare le esplosioni di attività. Il tessuto muscolare ottiene l' energia più prontamente disponibile dalla demolizione degli acidi grassi e del glucosio e verrà conservata sotto forma di ATP e di fosfocreatina, composti contenenti fosfato (P) ricco di energia. La molecola di glucosio è un eccellente combustibile che viene immagazzinato sotto forma di polimeri che possono venir rapidamente scissi nel caso dell'aumento della domanda energetica e rappresenta un precursore versatile poiché genera diversi intermedi metabolici. Il glucosio viene importato nel muscolo scheletrico attraverso un trasportatore denominato GLUT4 che è insulino dipendente. Pertanto quando la concentrazione di glucosio nel sangue è elevata (dopo un pasto) e vi è rilascio di insulina, il muscolo funge da deposito di glucosio. Oltre a rappresentare una forma di accumolo di energia, il glucosio è anche la forma con la quale l'energia viene trasferita alle cellule. Nel citosol della cellula vi sono complessi multienzimatici che prendono parte alla Glicolisi, la reazione in cui una molecola di Glucosio viene scissa in più passaggi catalizzati da enzimi diversi, in due molecole di Piruvato. Con la Glicolisi si mantiene costante il livello di ATP nel caso dovesse servire rapidamente. Il destino poi del Piruvato dipende dal tipo di cellula e dalle esigenze metaboliche del momento. Questo composto può seguire una via anabolica, che porta alla sintesi dell'aminoacido Alanina, o due vie cataboliche: 1) 2 Acetil CoA che entra nel ciclo di Krebs o ciclo dell'acido citrico per dare $4CO_2$ + $4H_2O$, in condizioni aerobiche; 2) 2 Lattato, fermentazione nel muscolo in condizioni anaerobiche. Quest'ultima via è detta lattica o lattacida ed avviene quando un tessuto, come un muscolo, che si sta contraendo violentemente, deve funzionare in condizioni anaerobiche. Il piruvato non può esser ulteriormente ossidato per la mancanza di ossigeno, e viene così ridotto a Lattato (forma dissociata dell'acido lattico). Nel muscolo l'energia chimica è disponibile anche nei depositi di glicogeno, costituenti circa lo 0.51% del peso del muscolo. Nel muscolo a riposo o durante la ripresa dopo la contrazione, il substrato principale è costituito dagli

acidi grassi, i quali vengono demoliti ad Acetato dagli enzimi della • -ossidazione ubicati nella matrice mitocondriale. L'Acetato viene poi ulteriormente ossidato nel Ciclo dell'Acido Citrico e l'energia risultante viene conservata sotto forma di ATP. Gli acidi grassi sono la principale sorgente di energia nel muscolo scheletrico degli atleti di fondo, come i maratoneti. Quando i muscoli scheletrici sono sottoposti ad uno sforzo breve "sprint", seguono la via descritta precedentemente, metabolizzando rapidamente il glucosio, proveniente dalle riserve muscolari di glicogeno, in Lattato provocando un debito di ossigeno che verrà colmato durante il periodo di ripresa. Il Lattato poi viene esportato dal muscolo al fegato dove viene riconvertito in glucosio.

1.6. CLASSIFICAZIONE DELLE FIBRE MUSCOLARI

Le fibre muscolari conservano la loro organizzazione strutturale di base, ma dal punto di vista morfologico-citologico (rapporto tra citoplasma e miofibrille o struttura del reticolo sarcoplasmatico), istochimico-biochimico (contenuto in mioglobina) e funzionale-metabolico si possono riconoscere principalmente due tipi di fibre muscolari:

- **Fibre di tipo I**, fibre lente o rosse "SLOW TWITCH FIBERS" che formano i muscoli tonici, contengono molta mioglobina e citocromo che impartiscono loro il colore rosso scuro. Sono capaci di utilizzare grandi quantità di ossigeno nell'unità di tempo (minuto), in quanto sono circondate da una fitta rete capillare. Sono le fibre più adatte agli sforzi prolungati poiché si contraggono e rilassano lentamente, ma sono capaci di svolgere un'attività vigorosa e continua. Le fibre di tipo I sono perciò considerate le fibre resistenti alla fatica muscolare (Pette e Spamer,1986; Pette e Staron,1988). La loro energia deriva dalla fosforilazione ossidativa perciò contengono un gran numero di mitocondri, sede del metabolismo aerobico.
- **Fibre di tipo II**, fibre veloci o bianche "FAST TWITCH FIBERS" che fanno parte dei muscoli definiti fasici, per l'attività esplosiva e potente. Appaiono bianche poiché hanno un basso contenuto di mioglobina e citocromo. Sono le fibre più veloci, ma hanno normalmente minore resistenza, infatti non sopportano il lavoro muscolare continuo e pesante.

Si distinguono sottotipi di fibre di tipo II:

- **Fibre di tipo IIA**, veloci ossidative “FAST TWITCH OXIDATIVE” ricche di mioglobina e capaci di utilizzare grandi quantità di ossigeno. Se opportunamente allenate sono in grado di diventare simili alle fibre di tipo I.
- **Fibre di tipo IIB**, veloci glicolitiche “FAST TWITCH GLYCOLYTIC” così definite perché prediligono il metabolismo glicolitico di tipo anaerobico che porta alla produzione di acido lattico. Lo scarso contenuto di mioglobina conferisce loro un colore pallido (Gauthier, 1969). Possiedono una quantità maggiore di miofibrille, il reticolo sarcoplasmatico è ben sviluppato e le attività enzimatiche della miosina e della pompa Ca^{2+}-ATPasi sono ben sviluppate, permettendo così rapida velocità di contrazione e di rilasciamento.
- **Fibre di tipo IIX**, che hanno caratteristiche intermedie tra le IIA e le IIB (dalle quali queste ultime probabilmente prendono origine) presenti in numero limitato.

	Tipo I, "ST"	**Tipo IIA, "FT"**	**Tipo IIB,"FT"**	**Tipo IIX,** in adulti
diametro fibra	piccolo con tanti capillari	grande con pochi capillari	grande con pochi capillari	intermedie tra IIA e IIB
colore	rosso	rosso	bianco	intermedie tra IIA e IIB
mioglobina e mitocondri	elevati	scarsi	scarsi	intermedie tra IIA e IIB
glicogeno	elevato	scarso	scarso	intermedie tra IIA e IIB
tipo di contrazione	scossa lenta	scossa rapida	scossa rapida	intermedie tra IIA e IIB
affaticabilità	scarsa	intermedia	rapida	intermedie tra IIA e IIB
metabolismo produzione ATP	Fosforilazione ossid. Aerobica	Glicolisi alattacida Fosf.ossidativa	Glicolisi alattacida Fosf.ossidativa	intermedie tra IIA e IIB
attività lattica deidrogenasica	scarsa	intermedia o elevata	elevata	intermedie tra IIA e IIB
attività ATPasica	scarsa	elevata	elevata	intermedie tra IIA e IIB

Tabella 1. Caratteristiche dei diversi tipi di fibre del muscolo scheletrico.

In genere la suddivisione delle fibre nei vari tipi e sottotipi è in gran parte determinata geneticamente. Le varie tipologie di fibre possono caratterizzare prevalentemente muscoli diversi, infatti esistono muscoli bianchi ricchi di fibre di tipo II (Extensor Digitorum Longus, EDL) o muscoli rossi composti da fibre di tipo I (Soleus), ma esistono anche muscoli definiti misti (Flexor Digitorum Brevis, FDB) in cui sono presenti entrambe le tipologie di fibre in diverso rapporto, ma con lieve prevalenza delle miofibre di tipo II (Calderon et al. 2009). Inoltre lo stesso muscolo può variare da specie a specie o addirittura tra individui della stessa specie (Johnson et al., 1973) a significare che oltre ai geni sia l'allenamento che l'ambiente possono influenzare la composizione muscolare.

1.7. SISTEMA NERVOSO CENTRALE, INNERVAZIONE E CONTRAZIONE MUSCOLARE

Il sistema nervoso centrale controlla la motilità muscolare scheletrica attraverso diverse vie ed una di queste comprende il motoneurone delle placche muscolari a contatto con le fibre muscolari contrattili. Tale complesso si definisce UNITA' MOTORIA.

Nel muscolo scheletrico i nervi motori mielinici perdono la guaina mielinica e si ramificano nel tessuto connettivo del perimisio formando numerosi ramuscoli terminali. Tali sinapsi che gli assoni dei Motoneuroni stabiliscono con le fibre muscolari vengono definite GIUNZIONI NEUROMUSCOLARI/MIONEURALI O PLACCA MOTRICE. Entro il terminale assonico vi sono numerosi mitocondri e vescicole sinaptiche contenenti il neurotrasmettitore Acetilcolina (Ach).

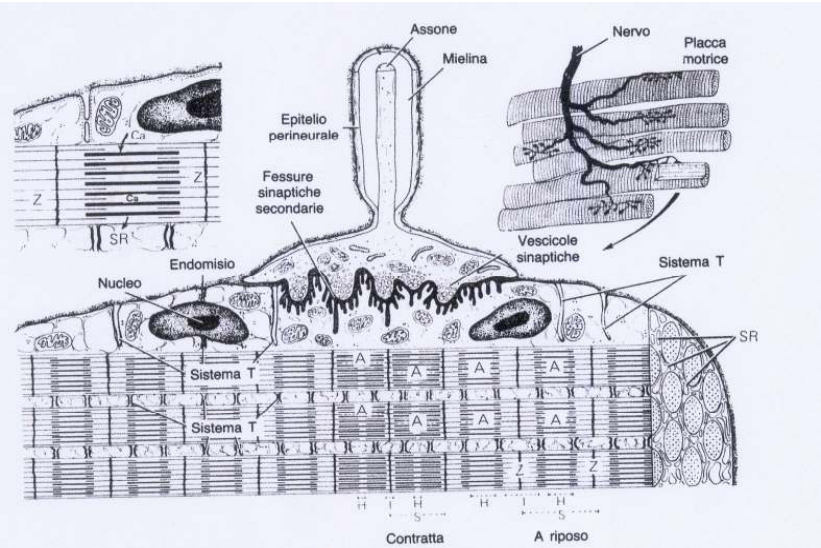

Figura 7: Ultrastruttura della placca motrice e meccanismo della contrazione. In alto a destra si illustra la ramificazione di un piccolo nervo con una placca motrice per ogni fibra muscolare. Nel disegno centrale è ingrandito uno dei terminali bulbosi di una placca motrice, dove si notano le vescicole sinaptiche nel terminale assonico dilatato. Nella regione della membrana plasmatica si notano fessure e creste note come fessure sinaptiche secondarie. L'assone perde la guaina mielinica ed entra in intimo contatto con la fibra. La contrazione inizia quando dalle vescicole sinaptiche viene liberata l'acetilcolina, un neurotrasmettitore che promuove un aumento localizzato della permeabilità del sarcolemma la quale viene successivamente propagata al resto della fibra ed attraverso le invaginazioni dei tubuli T viene trasferita al reticolo sarcoplasmatico (SR). L'aumento di permeabilità del SR favorisce la liberazione del calcio dalle cisterne, il quale innesca il meccanismo dello scorrimento dei filamenti proprio della contrazione muscolare. I filamenti sottili scorrono tra i filamenti spessi riducendo la distanza fra le linee Z, e di conseguenza una riduzione delle dimensioni di tutte le bande, eccettuata la banda A. (Immagine tratta dal libro di testo Compendio di Istologia, L.C. Junqueira;J. Carneiro; R. Kelley)

Quando un potenziale d'azione si propaga dalla fibra motrice alla placca motrice, si ha la depolarizzazione della membrana plasmatica del terminale presinaptico, che provoca l'apertura transitoria dei canali calcio. Gli ioni calcio entrano nel terminale presinaptico secondo il gradiente di potenziale elettrochimico, si fondono con le vescicole sinaptiche e si ha secrezione di Acetilcolina per esocitosi. Il neurotrasmettitore si lega ai recettori adrenergici che si trovano sulla superficie esterna della placca motrice, provocando un aumento transitorio della permeabilità aspecifica del sarcolemma della fibra muscolare per gli ioni sodio e potassio determinando la depolarizzazione del sarcolemma. Contemporaneamente l'acetilcolina eccedente viene idrolizzata rapidamente a colina e acetato grazie all'enzima acetilcolinesterasi, diffuso su tutta la superficie del sarcolemma. Il potenziale di placca viene definito transitorio poichè la demolizione dell'acetilcolina è necessaria per impedire il contatto prolungato del trasmettitore con i recettori sul sarcolemma.

La depolarizzazione innescata si propaga lungo tutta la superficie della fibra muscolare, per conduzione elettrica alla regione limitrofa, ed entro le fibre attraverso il sistema dei tubuli T. In ciascuna triade vi è un aumento della permeabilità e se l'intensità è tale da raggiungere la soglia di eccitabilità, il segnale di depolarizzazione dal recettore delle Diidropiridine (DHPR) voltaggio dipendente viene trasferito alla regione di fronte sul reticolo sarcoplasmatico, dove si trova il canale di rilascio della Ryanodina, al quale è anatomicamente accoppiato, provocando la liberazione degli ioni calcio dal reticolo. Gli ioni calcio si legano alle proteine dei filamenti sottili di actina che scorrono sui filamenti spessi di miosina determinando la contrazione muscolare. Si stima che un singolo potenziale d'azione nel muscolo scheletrico favorisca la liberazione di circa il 10 % del calcio rilasciabile dal SR. La depolarizzazione cessa quando gli ioni calcio vengono attivamente riportati all'interno delle cisterne del reticolo sarcoplasmatico tramite una pompa Ca^{2+}/ATPasi che opera con trasporto attivo in un rapporto stechiometrico pari a 3 Ca^{2+} : 1 ATP. Diminuendo la concentrazione degli ioni calcio nel sarcoplasma, il muscolo si rilascia.

1.8. OMEOSTASI DEL CALCIO NEL MUSCOLO SCHELETRICO

L'omeostasi cellulare è il mantenimento della concentrazione chimica di ioni e molecole tra compartimenti diversi separati da una membrana semipermeabile. L'equilibrio deve mantenersi nel tempo ed al variare delle condizioni esterne permettendo così alle cellule di sopravvivere.

Nelle fibre muscolari elevate quantità di calcio vengono rilasciate dai depositi intracellulari del reticolo sarcoplasmatico ed una piccola quantità proviene dall'esterno, mentre negli altri tipi cellulari, sprovvisti di strutture specializzate, la fonte di calcio è extracellulare ed il flusso della corrente verso l'interno viene mediato da canali specializzati.

La concentrazione di calcio intracellulare libero all'interno del citosol si aggira attorno a livelli estremamente bassi, al di sotto di 10^{-7} M (circa 1000 volte più bassa rispetto all'esterno), contro concentrazioni di calcio extracellulari pari a 10^{-3} M (Makoto, 2006). Tale differenza di concentrazione tra interno ed esterno è dovuta al fatto che il calcio all'interno del citoplasma è a sua volta sequestrato all'interno di organelli di deposito delimitati da membrana, quali il reticolo sarcoplasmatico nelle cellule muscolari, reticolo endoplasmatico e mitocondri nelle altre cellule. I mitocondri sono presenti anche nelle fibre muscolari, ma in condizioni fisiologiche partecipano solamente in minima parte ai flussi di calcio intracellulari, in quanto sono deputati principalmente nella regolazione dell'attività degli enzimi mitocondriali del metabolismo ossidativo. Il SR con il sistema di membrane altamente sviluppato ed essendo l' organello di stoccaggio del calcio, è legato alla omeostasi di questo ione e mantiene al suo interno una elevata concentrazione di calcio che si aggira attorno a 2 mM, grazie a meccanismi di trasporto attivo. La principale proteina responsabile del mantenimento di questo disequilibrio chimico intracellulare è la pompa Ca^{2+}-ATPasi che opera a carattere di uniporto. Il pompaggio degli ioni avviene contro un gradiente di concentrazione elevato e perciò necessita di quantità elevate di energia sotto forma di ATP. La pompa trasferisce due ioni calcio per ogni molecola di ATP che viene idrolizzata. Tale pompa è presente non soltanto sulla membrana degli organelli intracellulari, ma si trova anche sulla membrana citoplasmatica di tutte le cellule mantenendo l'omeostasi cellulare. Queste pompe ubicate in zone diverse della cellula presentano similitudini per quanto riguarda il meccanismo d'azione, ma differiscono a livello strutturale e modulatorio (Reeves et al., 1979).

1.9. PROTEINE COINVOLTE NELL'OMEOSTASI DEL CALCIO

Le proteine che legano calcio e partecipano alla omeostasi del calcio si raggruppano principalmente in due gruppi:

1. Proteine transmembrana o integrali, incorporate nella membrana cellulare, capaci di regolare le correnti del calcio tra interno ed esterno della cellula e tra citosol ed organelli. Si tratta di proteine canali.
2. Proteine solubili o luminali presenti nel sarcoplasma e nel reticolo sarcoplasmatico, capaci di legare il calcio grazie ad un motivo strutturale ad ansa capace di ospitare gli ioni calcio.

A seconda della funzione svolta, queste proteine che legano il calcio si possono suddividere ulteriormente in tre gruppi:

1. Proteine coinvolte nella trasduzione dei segnali intracellulari mediati da calcio come messaggero. Tali proteine cambiano la loro conformazione dopo aver legato il calcio e riescono così ad interagire con altre proteine "target" ed a modulare la loro attivazione;
2. Proteine leganti il calcio con funzione direttamente dipendente da calcio, possiedono perciò attività enzimatica calcio dipendente;
3. Proteine che legano calcio e ne controllano la concentrazione citosolica. Fungono da tamponi intracellulari del calcio.

Esistono inoltre pompe ATPasi o sistemi di estrusione del calcio attraverso la membrana plasmatica:

- Uno scambiatore Na^+/Ca^{2+} che opera in associazione con la pompa Na^+/K^+;
- Le Ca^{2+} -ATPasi descritte precedentemente come le principali pompe per il flusso del calcio.

Partecipano inoltre alla omeostasi del calcio nel muscolo scheletrico:

- i canali per il Ca^{2+} dipendenti dal voltaggio;
- canali per il calcio controllati da ligandi che si aprono in seguito al legame con una molecola segnale;
- i canali controllati da meccanismi intracellulari tipo IP3, cAMP,ecc.

Tutte queste proteine leganti calcio agiscono in sinergia e tramite la rete di interazioni che stabiliscono hanno origine cascate di reazioni che portano al ciclo di contrazione-rilasciamento muscolare. Il calcio è un messaggero molto importante poiché molte funzioni intracellulari sono sensibili alle variazioni di concentrazione del calcio citosolico. Nelle fibre muscolari a riposo la concentrazione di calcio è pari a 0,1 µM (100 nM), mentre al momento dello stimolo la concentrazione di calcio aumenta da 10 a 100 volte fino ad arrivare a 1-10 µM; ma anche piccoli incrementi di concentrazione possono determinare effetti elevati. Oltre alle variazioni di potenziale capaci di aumentare la permeabilità della membrana al calcio, anche stimoli determinati dai cambiamenti dei livelli ormonali determinano un aumento del calcio intracellulare e portano anch'essi all'attivazione di reazioni calcio-sensibili.

1.10. CANALI CALCIO SULLA MEMBRANA PLASMATICA

1.10.1. IL RECETTORE DELLE DIIDROPIRIDINE (DHPR).

Il recettore delle Diidropiridine appartiene alla famiglia di canali calcio sensibili al voltaggio di tipo L (long lasting), che si attiva successivamente ad elevate depolarizzazioni della membrana (High Voltage Activated, HVA). E' maggiormente presente nel muscolo scheletrico, ma lo si trova anche nel cuore e nel cervello. Esistono isoforme diverse in quanto sono codificati da geni diversi che conferiscono loro una regolazione distinta ed una struttura differente, infatti sia nel cuore che nel cervello manca la subunità • (Ertel et al., 2000). Per di più, il DHPR nel cuore funziona da canale del calcio voltaggio dipendente, ma la copiosa quantità di calcio che lascia passare dall'ambiente esterno aumenta la concentrazione citoplasmatica di calcio che va così a legarsi al dominio citoplasmatico del recettore della Ryanodina (tipo 2 nel cuore). Tale legame è responsabile della fuoriuscita ulteriore di calcio dal reticolo sarcoplasmatico (Rilascio Indotto da Calcio, CIRC).

Nel muscolo scheletrico, il recettore delle Diidropiridine si trova sulla membrana plasmatica localizzato sui Tubuli T ed il suo orientamento spaziale lo rende in intima relazione con il recettore della Ryanodina (RyR-1) sul reticolo sarcoplasmatico. Entrambi i recettori, ciascuno sulle proprie membrane, appaiono come delle file

altamente ordinate separate da 12 nm di mioplasma (Block et al., 1988; Franzini-Armstrong & Jorgensen, 1994; Paolini et al., 2004)

Il DHPR del muscolo scheletrico è formato da 5 subunità proteiche distinte:

1. **$Ca_v1.1$ (• 1s)**, la subunità principale che funge da sensore del voltaggio e costituisce il canale ionico. Possiede un peso molecolare di 175 KDa, che prende origine da una forma di 212 KDa tagliata nel dominio carbossiterminale ad opera di proteasi (Catterall, 2000b; Tanabe et al., 1987). La subunità • 1 è sua volta formata da 4 unità ripetute (I,II,III,IV) aventi funzioni diverse, ciascuno composto da 6 segmenti (S1-S6)(Bannister, 2007)

   Il *dominio I* determina le cinetiche di attivazione del canale, che sono lente nel muscolo scheletrico e veloci nel muscolo cardiaco (Tanabe et al., 1991).

   L'*ansa • 1 I-II,* è in contatto con la subunità • del DHPR stessoanche se non è chiaro se la subunità • sia direttamente coinvolta nell'attività di trasduzione del voltaggio. Ciò che è chiaro è che l'interazione • 1 I-II / • migliora la conformazione di membrana del DHPR (Strube et al., 1996; Neuhuber et al., 1998; Schredelseker et al., 2005) rispetto a RyR-1, in quanto vi è una diretta interazione della subunità • con un gruppo di residui carichi positivamente sulla regione del piede di RyR-1 (Cheng et al., 2005) che interagisce con la proteina JP45.

   L'*ansa • 1 II-III*, rappresenta la parte che direttamente interagisce con il recettore RyR-1 e per questo sembra esser l'elemento determinante nel processo di EC coupling (Tanabe et al., 1990a; Protasi et al., 2002). In esperimenti su miotubi disgenici, è stata identificata una regione di 46 aminoacidi (720-765), la quale è necessaria per promuovere il rilascio del calcio da RyR-1 in risposta alla depolarizzazione della membrana, segnale definito ortogrado (Nakai et al., 1998b). Tuttavia, tale ansa sembra esser necessaria per potenziare la corrente del calcio di tipo L poiché proveniente dal DHPR, ad opera di segnali inviati da RyR-1, accoppiamento retrogrado (Nakai et al., 1996,1998; Avila e Dirksen, 2000).

   L'*ansa • 1 III-IV*, sembra esser la parte responsabile di una mutazione del DHPR collegata ad una malattia autosomica dominante detta Ipertermia maligna (MH) che colpisce principalmente il recettore RyR-1. Nonostante questa

partecipazione allo sviluppo della malattia, non è ancora stato studiato il potenziale ruolo dell'ansa III-IV nel'accoppiamento eccitazione-contrazione.

Sul lato mioplasmatico, vi sono inoltre l'estremità *• 1 amino-terminale* (N-terminus), la quale non gioca un ruolo significante nella contrazione muscolare; e l'estremità *• 1 carbossi-terminale* (C-terminus), caratterizzata da diversi motivi che ne facilitano l'interazione con diverse proteine, quali il recettore della Rianodina, Calmodulina (CaM), la proteina trasmembrana JP45 che a sua volta interagisce con la proteina luminale Calsequestrina (CSQ-1) del reticolo sarcoplasmatico, ed in fine con la proteina strutturale AKAP15.

La subunità • 1 rappresenta anche il sito di legame per le molecole antagoniste del recettore, quali il farmaco diidropiridina

2. **Subunità • 2** di 143 KDa;
3. **Subunità •** di 54 KDa;
4. **Subunità •** di 30 KDa;
5. **Subunità •** di 26 KDa.

Nel muscolo scheletrico, la ridotta corrente calcio che attraversa il recettore delle Diidropiridine, si pensa che non intervenga nel meccanismo di eccitazione-contrazione, ma bensì è proprio la depolarizzazione del DHPR che induce cambiamenti nella propria conformazione che sono avvertiti dal recettore RyR-1 determinandone l'apertura ed innescando la contrazione muscolare.

1.10.2. I CANALI IONICI TRP (TRANSIENT RECEPTOR POTENTIAL)

Si tratta di una famiglia di canali ionici permeabili a cationi mono e bivalenti. Se ne conoscono più di 30 tipi (Hardie, 2001) e in base alle omologie di sequenza sono stati raggruppati in 7 sottofamiglie: TRPM (Melastatin); TRPV (Vanilloid); TRPML (Mucolipin); TRPP (Polycystin); TRPA (Ankyrin); TRPN (no mechanoreceptor potential C) e TRPC (Canonical). In base a similitudini strutturali e funzionali la famiglia TRPC è a sua volta suddivisa in 4 sottofamiglie: TRPC1; TRPC2; TRPC3, TRPC6 e TRPC7; TRPC4 e TRPC5 (Ambudkar et al., 2006).

Nel muscolo scheletrico sono espressi i canali TRPC, responsabili dell'influsso di calcio dall'esterno verso l'ambiente cellulare, i quali vengono attivati in seguito a meccanismi

dipendenti dalla fosfolipasi C (PLC) ed in alcuni casi sono direttamente accoppiati a PLC . La fosfolipasi C è responsabile della produzione di Inositolo trifosfato (IP3) e di Diacilglicerolo (DAG), molecole che si comportano come secondi messaggeri in quanto attivano direttamente i canali TRPC sulla membrana cellulare, tramite un meccanismo definito "Receptor-Operated Ca^{2+} entry" (ROC) (Claphan, 2003; Minke & Selinger, 1992). Il ruolo preciso dei canali TRPC non è ancora del tutto chiarito e fino ad ora diversi studi hanno cercato di identificarli. L'inositolo trifosfato (IP3) induce il rilascio di calcio dal reticolo sarcoplasmatico e diversi lavori proponevano che i canali TRPC, tranne l'isoforma TRPC6, si attivassero in seguito a tale deplezione del calcio dai depositi intracellulari secondo un meccanismo detto "Store-operated Ca^{2+} entry" (SOC) (Venkatachalam et al., 2002). Dopo diverse sfide che sostenevano che i TRPC1 potessero costituire un componente dei canali "Store-Operated" (Beech et al., 2003; Ambudkar et al., 2007) associati ad altri canali detti Orai (Kim et al., 2009) e con STIM1, un sensore del calcio intracellulare (Liao et al., 2008); altri sostennero la tesi contraria, ovvero che tale meccanismo fosse indipendente dai canali TRPC1 (DeHaven et al., 2009). Un lavoro recente afferma che esiste una corrente di calcio proveniente dall'esterno che è indipendente dai "store-operated" e che non implica Orai e STIM, ma piuttosto pare provenire attraverso i tubuli T, ma ciò che non è chiaro sono i componenti che vi partecipano (Lyfenko e Dirksen, 2008).

Un recente studio sostiene che i canali TRPC1 siano responsabili in minima parte dell'entrata di calcio dall'esterno nelle fibre a riposo (circa il 12% dell'influsso totale di calcio), ma che siano capaci di modulare un'entrata di calcio maggiore durante contrazioni muscolari ripetute sostenendo così la forza muscolare prodotta. Per di più è stato dimostrato che l'attività dei canali TRPC1 non sia dipendente dal meccanismo "Store-operated Ca^{2+} entry" (Zanou et al., 2009).

1.11. POMPE CALCIO SULLA MEMBRANA PLASMATICA

Le ATPasi ioniche o pompe ioniche trasportano ioni contro gradiente a spese di ATP che viene idrolizzata. La pompa Na^+/K^+ o ATPasi Na^+/K^+- dipendente è un etero dimero, presenta un peptide a catena • con 10 domini trasmembrana, i quali nella parte extracellulare rappresentano il sito di interazione con farmaci capaci di inattivare la pompa; ed un peptide a catena • glicosilato avente funzione regolatoria. Si conoscono

due pompe per il calcio di questo tipo: quella sulla membrana plasmatica (PMCA) che estrude il calcio dal citosol e la pompa sul reticolo sarcoplasmatico (SERCA) che trasporta il calcio dal citosol alle cisterne del reticolo. Entrambe sono etero dimeri e codificate da geni diversi e rappresentano l'80% del contenuto proteico totale del reticolo longitudinale della fibra striata.

Esistono inoltre diverse isoforme di ATPasi protoniche, le quali trasportano ioni contro gradiente accumulando potenziale e acidificando il microambiente ricevente. I due tipi principali sono la ATPasi H^+-dipendente vacuolare o V-H^+-ATPasi tipica dei lisosomi e quella di membrana.

1.11.1. Ca^{2+} -ATPasi SUL PLASMALEMMA O POMPA PMCA

Le Ca^{2+} -ATPasi della membrana plasmatica (PMCA) sono proteine di circa 130 KDa presenti in molte cellule eucariotiche (Guerini et al., 1998). La struttura di queste pompe è costituita appunto da 10 domini di transmembrana e circa l'80% della proteina si affaccia sul citoplasma della cellula, mentre solamente un corto segmento sporge sul lato extracellulare. La funzione di queste pompe è quella di catalizzare il trasporto del calcio dal citoplasma della cellula all'esterno tramite un meccanismo ATP-dipendente. E' in grado di rimuovere dalla cellula 3 moli di calcio/minuto/litro per ogni molecola di ATP idrolizzata (Salviati et al., 1982). L'attivatore fisiologico della pompa è il calcio complessato alla proteina calmodulina. Esistono quattro diverse isoforme di pompe PMCA (PMCA1-PMCA4) codificate da quattro geni diversi. Le isoforme PMCA1 e PMCA4 sono espresse nei tessuti adulti, mentre le PMCA2 e PMCA3 sono principalmente espresse nel sistema nervoso e nel muscolo scheletrico (Fresu et al., 1999; Strehler & Zacharias, 2001).

1.11.2. POMPE O SCAMBIATORI Na^+/Ca^{2+} E POMPE Na^+/K^+ SULLA MEMBRANA PLASMATICA

Sulla membrana plasmatica delle cellule vi è lo scambiatore Na^+/Ca^{2+} che scambia 3 ioni sodio per ogni ione calcio trasportato dal citoplasma verso l'esterno della cellula, utilizzando l'energia proveniente dal co-trasporto del sodio ad opera di un'altra pompa Na^+/K^+. Quest'ultima è un'altra ATPasi capace di estrudere 3 ioni Na^+ fuori dalla cellula e di pompare 2 ioni K^+ nel citoplasma, tramite un meccanismo ATP dipendente. Lo scambiatore Na^+/Ca^{2+}, nella sua forma fosforilata, presenta alta affinità per il calcio intracellulare e per il sodio extracellulare e viene attivato da una concentrazione interna di calcio compresa tra 0,1-1,0 µM. Tale sistema di estrusione è elettrogenico, perciò la direzione in cui vengono trasportati sia il calcio che il sodio dipende dal potenziale di membrana (Reeves et al., 1979).

1.12.CANALI CALCIO SULLA MEMBRANA DEL RETICOLO SARCOPLASMATICO

1.12.1.IL RECETTORE DELLA RYANODINA

Il recettore della Ryanodina (RyR) è una proteina sulla membrana del reticolo sarcoplasmatico, che forma un complesso omotetramerico, composto da 4 subunità identiche. Ogni monomero presenta una sequenza aminoacidica di circa 5000 aa ed un peso molecolare di circa 560 KDa. E' composta da una regione idrofilica amino terminale (NH2) di circa 4000 aa ed una regione idrofobica carbossiterminale (COOH) più piccola, circa 1000 aa, entrambe rivolte sul lato citoplasmatico. La maggior parte del recettore (90%) si trova nel citoplasma e tale porzione di recettore costituisce i piedi giunzionali (Junctional Feet) che si osservano sulle cisterne terminali del reticolo e si affacciano ai recettori delle Diidropiridine sui tubuli T. Esistono diverse isoforme codificate da geni diversi ed espresse in tessuti differenti:

- RyR-1 espressa principalmente nel muscolo scheletrico sia di tipo rapido che lento. Il gene che la codifica si trova sul cromosoma 19 (banda q13.1);
- RyR-2 che si trova nel cuore ed è codificato da un gene sul cromosoma 1. Analisi hanno evidenziato una somiglianza del 60% con l'isoforma RyR-1, che corrisponde ai segmenti transmembrana che formano il canale;

- RyR-3 espressa principalmente nel cervello, ma anche in cellule non eccitabili.

Tutte queste isoforme dimostrano di avere caratteristiche simili ma non identiche di conduttanza e proprietà farmacologiche, in quanto RyR-2 e RyR-3 vengono inibiti da concentrazioni di calcio superiori rispetto a RyR-1 e quest'ultimo è più sensibile all'azione del Mg^{2+} rispetto agli altri 2 tipi.

Il recettore della Ryanodina è modulato da diversi fattori, quali agenti fisiologici (Ca^{2+}, Mg^{2+}, ATP) e diversi processi cellulari (fosforilazione, ossidazione) (Meissner, 1994). Nel muscolo scheletrico il calcio svolge un'azione complessa sul recettore RyR-1, in quanto basse concentrazioni di calcio (1-10 µM) attivano il recettore, mentre alte concentrazioni (1-10 mM) lo inibiscono. Il calcio è inoltre capace di influenzare il recettore attraverso i siti di legame sulla parte luminale del recettore (Copello et al., 1997; Meissner et al., 1997). Il Mg^{2+} inibisce il recettore a concentrazioni millimolari (1 mM) e compete con il calcio sullo stesso legame, abbassando la sensibilità al calcio del recettore (Meissner, 1986). Il recettore è inoltre regolato da agenti farmacologici: la caffeina che attiva il recettore a concentrazioni millimolari e induce la contrazione muscolare a livelli inferiori di 2 mM; la rianodina, un alcaloide estratto dalla pianta Ryana, che è dose dipendente in modo inversamente proporzionale, in quanto basse concentrazioni (10 nM) determinano l'apertura del canale, mentre alte concentrazioni (50-100 µM) bloccano il canale; il rosso rutenio e 4 Cloro-cresolo (Fessenden et al., 2003; Sun et al., 2003).

Il recettore della Ryanodina-1 fa parte della famiglia di canali del rilascio di calcio intracellulare che si trova nel SR. Le funzioni principali sono quindi di regolare i segnali calcio intracellulari modulando la fuoriuscita del calcio dalle cisterne terminali del reticolo al fine della contrazione e quella di regolare il recettore delle Diidropiridine, in quanto l'interazione tra DHPR e RyR-1, essenziale per la contrazione muscolare assieme ad altre proteine accessorie, origina un segnale bidirezionale. La depolarizzazione della membrana plasmatica, innesca un segnale ortogrado, capace di regolare l'accoppiamento eccitazione-contrazione, poichè i cambiamenti conformazionali di $Ca_v1.1$ (• 1s) del recettore DHPR vengono trasmessi fisicamente al recettore della Ryanodina determinandone l'apertura. A sua volta il Recettore della Ryanodina determina un segnale definito retrogrado regolando l'organizzazione del DHPR in tetradi e modulando l'ampiezza della corrente calcio di tipo L entrante dal DHPR stesso (Nakai et al., 1996).

Mutazioni nel recettore della Ryanodina sono implicate in alterazioni dell'omeostasi di calcio e malattie muscolari quali l'ipertermia maligna (MH), central core disease (CCD) ed una forma di multiminicore disease (MmD).

1.12.2. IL RECETTORE DELL'INOSITOLO 1,4,5-TRIFOSFATO (IP3R)

Il recettore dell'Inositolo 1,4,5-Trifosfato è un canale calcio con peso molecolare di 220-260 KDa, composto da 4 subunità ciascuna di circa 2700 residui aminoacidici e da 6 domini trasmembrana. Ogni subunità presenta una regione amino terminale citoplasmatica avente il sito per la molecola Inositolo 1,4,5- trifosfato (IP3), una regione carbossiterminale che contribuisce alla formazione del canale ed una regione intermedia di circa 1700 aa contenente i siti di regolazione del recettore. E' localizzato sulla membrana del reticolo sarcoplasmatico e presenta omologie con il recettore della Ryanodina (Jiang et al., 2002; Serysheva et al., 2003). Si tratta di un canale di rilascio del calcio e la sua regolazione dipende dall'IP3 e dal calcio stesso. L'attivazione del canale comprende una prima fase che vede l'attacco dell'Inositolo Trifosfato (IP3) su tutte le subunità del recettore che attiva il canale e lo rende sensibile maggiormente al calcio ed una seconda fase che prevede l'attacco del calcio al recettore e la sua fuoriuscita verso il citoplasma (Marshall & Taylor, 1994; Taylor & Laude, 2002). Il messaggero IP3 è molto importante e la sua produzione è mediata da un meccanismo di attivazione della proteina G, che si trova sulla membrana citoplasmatica, la quale si dissocia e la subunità • va ad attivare la fosfolipasi C. La fosfolipasi C poi, attraverso la scissione dei fosfolipidi del doppio strato lipidico di membrana, è in grado di produrre Diacilglicerolo e Inositolo Trifosfato che attiva il recettore.

Il recettore è inoltre modulato da proteine leganti il calcio, quali Calmodulina, in quanto a concentrazioni basse di calcio la Calmodulina è associata al recettore inattivandolo, mentre ad alte concentrazioni di calcio la Calmodulina subisce modificazioni conformazionali che la portano ad interagire con regioni diverse del canale determinandone l'apertura (Saimi & Kung, 2002; Schumacher et al., 2001).

Esistono tre diverse isoforme del recettore IP3R e l'espressione è diversa nei diversi tessuti, ma molti tessuti contengono più isoforme (Miwako et al., 2005):

- IP3R1, presente nel cuore, nel fegato, nei reni, nell'ovaio e nelle cellule del Purkinje, nel muscolo liscio e nelle cellule satelliti del muscolo scheletrico;

- IP3R2, predominante nel cervello;
- IP3R3, l'isoforma più comunemente presente in tutti i tessuti, incluso nelle isole pancreatiche, nei reni e nel tratto gastrointestinale.

1.13. POMPE CALCIO SULLA MEMBRANA DEL RETICOLO SARCOPLASMATICO

1.13.1. Ca^{2+}-ATPasi DEL RETICOLO SARCOPLASMATICO (SERCA) (Sarcoplasmic endoplasmatic Reticulum Calcium ATPase)

Le Ca^{2+}-ATPasi SERCA sono una famiglia di proteine aventi un peso molecolare di circa 110 KDa (MacLennan & Toyofuku, 1992; Martonosi & Pikula, 2003; Toyoshima & Nomura, 2002; Toyoshima et al., 2000) e si trovano sulla parte di reticolo sarcoplasmatico longitudinale. La funzione di queste pompe è simile alle pompe PMCA di membrana plasmatica. Le pompe SERCA sono in grado di trasportare all'interno delle cisterne del reticolo 2 ioni calcio per ogni molecola di ATP idrolizzata, scambiando 2-3 protoni luminali. Tutto ciò è possibile grazie al passaggio della Ca^{2+}-ATPasi da uno stato ad alta energia (E1) ad uno stato a bassa energia (E2), che favorisce la traslocazione del calcio dal citosol al lume del reticolo contro gradiente elettrochimico (Inesi et al., 1995; Lee, 2002; Moller et al., 2005). Possiedono un'alta affinità per il calcio (K_d 0,1 µM).

Esistono tre principali isoforme tessuto specifiche SERCA1, SERCA2, SERCA3, che sono codificate da geni diversi (Callen et al., 1995; Dode et al., 1996; Otsu et al., 1993). Le isoforme SERCA1a e SERCA1b sono preferenzialmente espresse nei muscoli neonatali e nei muscoli adulti "Fast Twitch"; la proteina SERCA2a è presente nei muscoli neonatali, in cellule non muscolari, nel muscolo cardiaco e nei muscoli aduti "Slow Twitch"; l'isoforma SERCA2b si trova nei muscoli lisci e nelle cellule non muscolari.

1.14. PROTEINE LEGANTI CALCIO E ACCESSORIE DEL RETICOLO SARCOPLASMATICO

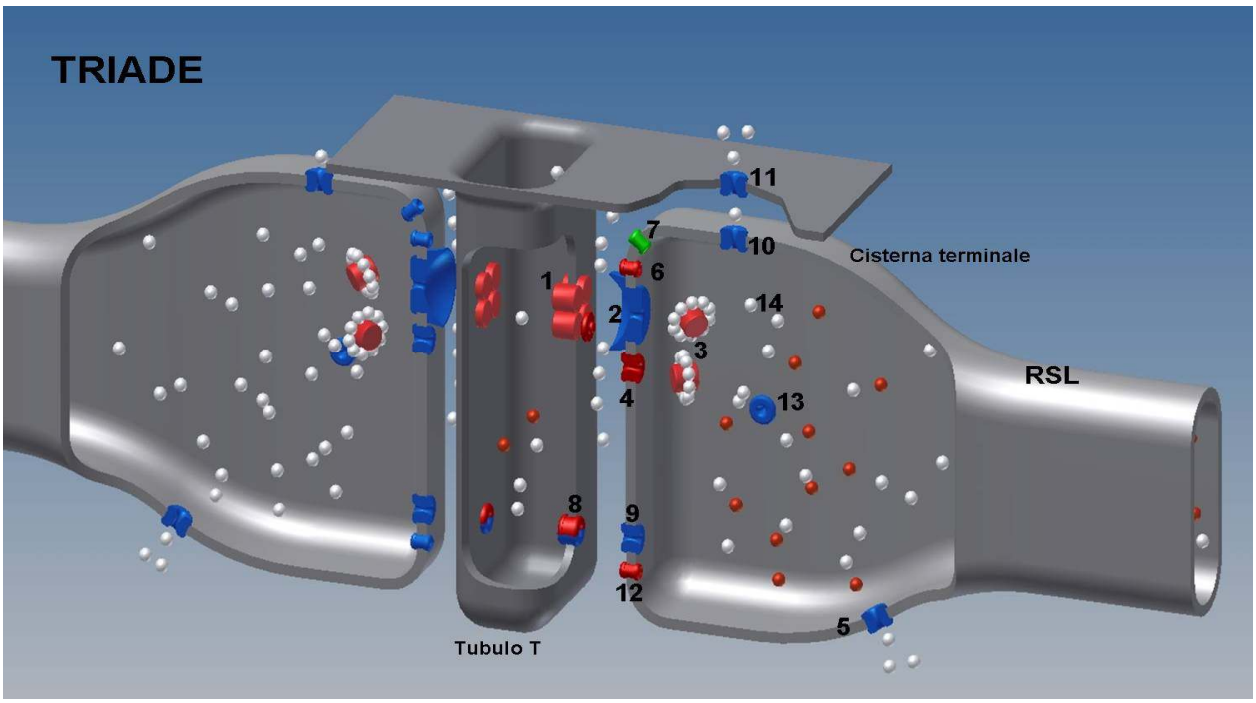

Figura 8: Rappresentazione tridimensionale della TRIADE e di alcune proteine che partecipano al meccanismo EC-coupling: 1.Recettore DHPR, via d'entrata del calcio ECCE; 2.Recettore della Ryanodina-1; 2.Calsequestrina-1; 4.JP45; 5.Ca^{2+}/ATPasi SERCA; 6.Triadina; 7.Giuntina; 8.Orai, via d'entrata del calcio SOCE; 9.STIM1; 10.Recettore dell' Inositolo 1,4,5-Trifosfato (IP3R); 11.Pompa PMCA; 12.SRP-27/TRIC; 13.Calreticulina; 14.ioni calcio. (Immagine realizzata da Adriano e Barbara Mosca)

Tramite esperimenti di frazionamento delle membrane del reticolo sarcoplasmatico che sono ricche in proteine leganti calcio (Meissner et al., 1973; Campbell et al., 1980; Saito et al., 1984) è stato possibile suddividere generalmente le proteine in: componenti delle cisterne terminali (TC) che hanno un ruolo nel rilascio del calcio nel citosol della cellula e proteine del reticolo longitudinale (LSR) specializzate nel recuperare il calcio dal citosol e stoccarlo all'interno del reticolo. Negli anni, sono state identificate le proteine che sono localizzate nelle membrane delle facce giunzionali (JFM) delle cisterne terminali, le strutture adiacenti ai tubuli T che assieme formano la TRIADE, le quali partecipano attivamente al meccanismo dell'accoppiamento Eccitazione-Contrazione (EC coupling). Si tratta di proteine quali: Calsequestrina (CSQ-1); JP45; Giuntina (Junctin); Triadina (Triadin) oltre che al recettore della Ryanodina (RyR-1) di cui abbiamo già discusso, che svolgono la funzione di tampone calcio, trasduzione del

segnale, o siti di legame per la formazione di complessi. Queste proteine vengono definite componenti maggiori, ma esistono anche proteine accessorie o definite componenti proteici minori, quali Sarcalumenina, Phospholamban, Calmodulina (CaM), Mitsugumina29 (MG-29), Junctofilina-1, SRP-27/TRIC-A, Junctate, ed altre proteine nella parte longitudinale del reticolo, che tramite la loro funzione tampone del calcio o modulatoria di altre proteine permettono il corretto coordinamento della contrazione muscolare (Rev. Treves et al., 2009). VEDI ARTICOLO 5 a pp.137.

1.15. PROTEINE NELLA MEMBRANA DELLA FACCIATA GIUNZIONALE (JFM)

1.15.1. CALSEQUESTRINA

La proteina Calsequestrina è la proteina luminale più abbondante del reticolo sarcoplasmatico. Ha un peso molecolare di circa 56 KDa e per la sua moderata affinità per il calcio (K_d 4x10-5M) e la sua elevata capacità di legare il calcio (40-50 mol Ca^{2+}/ mol CSQ) viene considerata principalmente una proteina tampone. La proteina si presenta come un monomero formato da tre domini simili legati da corte sequenze aminoacidiche, ed un terzo della proteina è formata da residui acidi di istidina che conferiscono alla molecola la capacità di legare il calcio. La caratteristica principale di questa molecola è che a concentrazioni elevate di calcio libero nel reticolo (~1mM) la proteina subisce un ripiegamento (Folding Compaction) e forma dei polimeri con anse capaci di intrappolare il calcio; mentre quando le concentrazioni dello ione si riducono (tra 10 e 100 µM) la proteina dimerizza. Quando la Calsequestrina si compatta si attacca con la estremità aminoacidica (NH2) alle proteine accessorie Giuntina e Triadina, anch'esse nella faccia giunzionale della membrana del reticolo (JFM), e si collega al recettore della Ryanodina formando un complesso quaternario. Il sito della CSQ-1, che si presenta con filamenti lineari vicino RyR-1 e filamenti ramificati nella parte luminale del SR, e l'aggregazione di CSQ-1 conferiscono alla proteina il ruolo di connessione con RyR-1 mediato da Triadina e Giuntina (Guo et al., 1994; Zhang et al., 1997) e da altre molecole linkers (Treves, 2009). Esistono due principali isoforme CSQ-1 scheletrica nelle fibre "Fast Twitch" e "Slow Twitch" e l'isoforma CSQ-2 del muscolo cardiaco e nelle fibre di tipo lento (Arai et al., 1992; Biral et al., 1992; Damiani & Margreth, 1994). Tuttavia nelle fibre "Fast Twitch" in via di sviluppo sono presenti entrambe le isoforme, successivamente la CSQ-2 decresce gradualmente nel muscolo

adulto (Park et al., 1998; Sacchetto et al., 1993). La CSQ-2 è simile alla CSQ-1 ma quest'ultima nella regione carbossi-terminale (COOH-term) presenta dei residui acidi o siti di fosforilazione.

Da lavori in letteratura pare che l'azione della Calsequestrina sia contrastante: esperimenti sulla CSQ-1 attaccata alla faccia giunzionale del reticolo hanno proposto una funzione inibitoria della proteina nei confronti del recettore della Ryanodina, in quanto l'attività del canale era bloccata (Beard et al., 1999-2002; Wang et al., 2001); mentre altri hanno proposto una funzione di attivazione del canale di rilascio (Kawasaki & Kasai, 1994; Ohkura et al., 1995). In ogni caso, il cambiamento conformazionale che subisce la Calsequestrina dipendente dalla variazione della concentrazione del calcio luminale suggerisce che la proteina è capace di regolare il canale di rilascio del calcio Ryanodina-1.

1.15.2. TRIADINA

La Triadina è una proteina transmembrana con un peso molecolare di 95 KDa localizzata nella porzione giunzionale delle cisterne terminali del reticolo sarcoplasmatico. La estremità amino terminale (NH2-ter) si affaccia sul citosol della cellula mentre la parte carbossiterminale (COOH-ter) è rivolta verso il lume del reticolo. Quest'ultima è ricca di residui residui aminoacidici carichi positivamente che formano un dominio definito KEKE, ed inoltre presenta un unico sito per la proteina Calsequestrina contenente aspartato. Presenta omologie strutturali e funzionali con la proteina Giuntina, con la quale ancora la Calsequestrina al recettore della Ryanodina.

E' stata scoperta inizialmente nel muscolo scheletrico (Caswell et al., 1991; Knudson et al., 1993a, 1993b), ma esistono altre tre isoforme espresse nel cuore: Triadin 1 di 35 KDa, Triadin 2 di 40KDa e Triadin 3 di 92 KDa (Guo et al., 1996), caratterizzate da un alto grado di omologia nella regione compresa tra gli aminoacidi 1-264, da un corto dominio aminoterminale citoplasmatico e da un lungo segmento carbossiterminale luminale (Jones et al., 1995).

1.15.3. GIUNTINA

La Giuntina è una proteina transmembrana di 26 KDa formata da 210 residui aminoacidici. Colocalizza con Triadina sulle cisterne terminali, e nella parte carbossiterminale rivolta nel lume del reticolo sarcoplasmatico vi sono un'alternanza di aminoacidi carichi positivamente e negativamente (dominio KEKE) e perciò presenta più siti di legame per Calsequestrina. La sua stretta vicinanza nel muscolo scheletrico con Triadina e RyR-1 e l'interazione con il recettore della Ryanodina stesso in maniera calcio indipendente, lascia ipotizzare che per una efficace operazione di rilascio del calcio dal reticolo sarcoplasmatico sia richiesta la formazione del complesso quaternario. Esiste sia la isoforma cardiaca che scheletrica le quali provengono da un unico gene, mediante splicing alternativo.

1.15.4. JP45

La proteina JP45 è un polipeptide di 45 KDa a singolo filamento transmembrana che si trova sulle cisterne terminali del reticolo in prossimità del recettore della Ryanodina. La sua struttura primaria è stata identificata da un cDNA isolato da una libreria di cDNA di muscolo scheletrico di topo, presso il nostro laboratorio (Zorzato et al., 2000). La parte aminoterminale è rivolta sul citoplasma della cellula, mentre la parte carbossiterminale, che si affaccia sul lume del reticolo, presenta 47 aminoacidi carichi positivamente e 30 carichi negativamente.

Da esperimenti si è visto che l'RNA messaggero (mRNA) di JP45 viene espresso già a 17 giorni dalla nascita, seguito da un picco di espressione intorno a due mesi di vita per poi decrescere di circa tre volte con l'invecchiamento (Anderson et al., 2003). Inizialmente si pensava interagire con RyR-1, ma da esperimenti effettuati è emerso che la parte N-ter interagisce con il sensore del voltaggio cav1.1 (• 1s) del recettore delle Diidropiridine, con il quale forma un complesso; mentre la estremità C-ter interagisce con la proteina Calsequestrina (Anderson et al., 2003). Da altri studi (Delbono et al., 2007) si è visto che inattivando la proteina tramite esperimenti in vivo di topi giovani JP45KO, la forza muscolare diminuiva del 20-30%. Il fatto che le proteine contrattili erano comunque presenti, ha fatto supporre che la ridotta fuoriuscita di calcio

dalle cisterne con conseguente diminuzione di forza fosse dovuta all'alterazione del meccanismo di eccitazione-contrazione, causata a sua volta da un'alterazione del complesso JP45-Ca_v1.1(• 1s). In aggiunta si è visto che in tali topi JP45 KO si aveva una riduzione della densità di cav1.1 del DHPR che comportava modifiche elettrofisiologiche delle fibre. Allo stesso modo, in esperimenti di overespressione di JP45, si è notato un accumulo di molecole di JP45 non associate alla proteina Calsequestrina con conseguente ridotta fuoriuscita di calcio dal reticolo durante la contrazione. Questo è dovuto al fatto che la parte N-ter di JP45 non era più in grado di interagire con cav1.1.

Tutti questi motivi fanno pensare che JP45 sia una proteina coinvolta nella trasduzione del segnale, attraverso la quale la Calsequestrina comunica informazioni riguardanti il reticolo sarcoplasmatico (contenuto in Calcio) al recettore DHPR.

1.15.5. CALMUDULINA (CaM)

La Calmudulina è una proteina ubiquitaria di 17 KDa nel lume del reticolo sarcoplsmatico. E' formata da un lobo all' N-terminale con il quale si lega alle proteine bersaglio in maniera calcio-dipendente; un lobo al C-terminale con due mani E-F leganti il calcio che vanno incontro a modifiche conformazionali in seguito al legame; ed una porzione centrale composta da 8 giri di • -elica.

La Calmodulina ha funzione modulatoria dei segnali calcio e quando all'interno del reticolo la concentrazione del calcio aumenta, forma complessi Ca^{2+}-CaM, che a loro volta interagiscono con altre proteine quali adenilato ciclasi, fosfodiesterasi, pompe calcio, chinasi e fosfatasi (Kink et Alii, 1990). Inoltre la calmudulina è responsabile della risposta iniziale ai segnali calcio, e pare regolare l'attività dei Recettori DHPR e di RyR-1, RyR-2, partecipando nel meccanismo di eccitazione-contrazione, anche se il ruolo preciso non è ancora stato identificato.

1.15.6. MITSUGUMIN 29 (MG29)

La proteina Mitsugumin 29 ha un peso molecolare di 29 KDa ed è una proteina integrale di membrana formata da 4 domini, la quale nei muscoli maturi si trova anche nei tubuli trasversali. La funzione è quella di interagire con il recettore della Ryanodina, aumentandone la probabilità di apertura, ma senza alterare l'ampiezza della corrente di canale (Pan et al., 2004).

In esperimenti condotti in topi MG29 KO si sono notati tubuli trasversali rigonfi e un disallineamento delle tetradi.

1.15.7. JUNCTOPHILIN-1

Junctophilin-1 è una proteina intrinseca di membrana di 72 KDa. Possiede una regione citoplasmatica con 14 aminoacidi "repeat motif" (MORNN motif) con affinità per la membrana plasmatica ed una regione carbossiterminale che attraversa il reticolo sarcoplasmatico (Takeshima et al, 2000).

Il suo ruolo è quello di collegare i tubuli trasversali con il reticolo sarcoplasmatico.

Esistono 3 isoforme: Junctophilin-1 espressa nel muscolo scheletrico, Junctophilin-2 nel cuore e Junctophilin-3 nel cervello.

In esperimenti su topi Junctophilin KO, si è vista morte prematura ed incompleta formazione del complesso giunzionale tra i tubuli T ed il SR.

1.15.8. SRP-27 / TRIC-A

Mitsugumin-33 o TRIC-A è un canale cationico selettivo composto da un dominio trimerico che attraversa la membrana (Yazawa et al., 2007), conosciuta anche come SRP-27 Sarcoplasmic Reticulum Protein di 27 KDa (Bleunven et al., 2008). Si trova localizzata sul reticolo sarcoplasmatico vicino, ma distinta, RyR-1. Si può ottenere la proteina tramite esperimenti di coimmunoprecipitazione assieme alla proteima Maurocalcina e RyR-1 appunto, ma non con Maurocalcina da sola, e questo fa pensare che SRP-27 faccia parte del complesso macromolecolare di RyR-1. E' un canale con

selettività per il K^+ sul Na^+, che può essere attivato durante la fuoriuscita di calcio da RyR-1 per bilanciare le cariche tra le membrane.

1.15.9. JUNCTATE

Junctate è una proteina a singolo segmento di 33 KDa composta da 298 residui aminoacidici, che attraversa la membrana del reticolo Sarco ed Endoplasmatico. E' stata clonata presso il nostro laboratorio, analizzando una cDNA-teca di muscolo scheletrico e cardiaco umani (Treves et al., 2000). Appare come una proteina chimera in quanto la regione N-terminale è identica a Giuntina, mentre la porzione C-terminale è identica alla proteina Aspartil •-idrossilasi, che fa parte di una famiglia di enzimi •-chetoglutarato diossigenasi (Treves et al., 2000). Il fatto che possieda una moderata affinità per il calcio (K_d 217 µM) ed una alta capacità a legare tale ione 21 mol Ca^{2+} /mol proteina, fa pensare che Junctate svolga una modulazione fisiologica sull'omeostasi del calcio.

1.16. PROTEINE NEL RETICOLO SARCOPLASMATICO LONGITUDINALE (RSL)

1.16.1. CALRETICULINA

La calreticulina è una proteina luminale legante calcio di 46 KDa. Presenta una regione N-terminale altamente conservata tra le specie, una regione tra gli aminoacidi 181-280 contenente un dominio P ed una regione C-terminale con residui aminoacidici acidi molto simile alla Calsequestrina (Nakamura et al., 2001).

Le funzioni che svolge sono molteplici: tampone calcio per la sua alta capacità di legame (20-30 mol Ca^{2+} / mol proteina), interviene quindi nell'omeostasi stessa e funge da Chaperone molecolare, partecipando in diversi processi di ripiegamento della sequenza proteica in associazione con la proteina Calnexina. L'iperespressione della Calreticulina comporta un accumulo di calcio nei depositi cellulari ed influisce sul meccanismo di Store-operated Ca^{2+} influx (Bastianutto et al., 1995; Mery et al., 1996; Xu et al., 2000).

PROTEINE NEL RSL E NELLE CISTERNE TERMINALI:

1.16.2. SARCALUMENINA

Sarcalumenina è una glicoproteina composta da 436 aminoacidi avente un peso molecolare di 160 KDa localizzata nel lume del reticolo sarcoplasmatico longitudinale e nelle cisterne terminali. Tra la regione N-terminale e C-terminale vi è un dominio legante calcio, mentre nella parte C-terminale si notano siti ATPasici e GTPasici (Yoshida et al., 2005). Il suo gene però codifica tramite "Splicing Alternativo" anche una variante di glicoproteina di 53 KDa, la quale colocalizza con Sarcalumenina stessa. Possiede elevata capacità di legare calcio (35 mol / mol proteina) e moderata affinità (K_d 0,6 mM). E' presente sia nel cuore che nel muscolo scheletrico. Il fatto che colocalizzi con la Ca^{2+}-ATPasi SERCA, fa pensare che oltre alla funzione di tampone del calcio, svolga una funzione di mantenimento della pompa stessa. A tal proposito sono stati svolti esperimenti in topi Sarcalumenina KO e si è notata una riduzione sia dell'attività che del contenuto di SERCA (Leberer et al., 1990; Yoshida et al., 2005).

NUOVE PROTEINE TRANSMEMBRANA DEL RETICOLO SARCOPLASMATICO

1.16.3. SRP-35

SRP-35 (Sarcoplasmic Reticulum di 35 KDa) è una proteina recentemente scoperta nel nostro laboratorio (Treves et al.,2012). Si trova localizzata nel reticolo sarcoplasmatico del muscolo scheletrico ed è stata trovata in molti tessuti coinvolti nel metabolismo degli acidi grassi, quali fegato, tessuto adiposo e reni. Nel muscolo scheletrico si trova precisamente sul reticolo sarcoplasmatico longitudinale (LSR) dove si trovano molti enzimi glicolitici quali la piruvato chinasi, aldolasi, enolasi, e gliceraldeide 3-fosfato deidrogenasi. Analizzando la sequenza proteica si è visto che SRP-35 è un membro della famiglia DHRS (deidrogenasi/riduttasi) a catena corta SDR (short chain dehydrogenase/reductase) appartenente alla sottofamiglia 7C. Come gli altri membri di questa famiglia di enzimi partecipa alla via glicolitica, e lo fa catalizzando la conversione di retinolo (Vitamina A) nell'intermedio retinaldeide (tramite SDR o alcol deidrogenasi) e successivamente ad acido retinoico (tramite aldeide deidrogenasi citosolica) riducendo a sua volta il NAD+ a NADH. Si tratta di una reazione reversibile, infatti a partire da all-trans-retinaldeide viene prodotto acido retinoico con riduzione contemporanea di NAD+.

In generale le SDR fanno parte di un gruppo composto da oltre 46.000 membri, sono espresse ubiquitariamente e sono coinvolte nella riduzione di molti substrati quali: steroli, alcoli, zuccheri, composti aromatici, xenobiotici e retinoli. Gli enzimi SDR differiscono per alcune sequenze nella loro struttura terziaria, ma mantengono inalterato il dominio legante il cofattore NAD+. Negli umani sono state identificate almeto 70 SDR distinte che possiedono una estremità carbossiterminale variabile, ma tutte caratterizzate da un intreccio detto Rossmann-fold e legano i dinucleotidi NAD(P). SRP-35 inoltre contiene nel proprio sito attivo residui di tirosina adiacenti a lisine e serine e si differenzia dalle altre per la sua lunghezza, infatti si presenta con 311 residui invece dei soliti 250, che la classificano come un membro esteso della superfamiglia SDR. Nei vertebrati gli effettori dell'acido retinoico appartengono ad una famiglia di recettori nucleari: RARs (retinoic acid receptor) RAR • /• /• e RXRs (retinoic x receptor) RXR • /• /• e nel momento in cui l'acido retinoico si attacca a RAR, il recettore dimerizza con RXRs e trasloca nel nucleo dove si attacca a sequenze specifiche di DNA note come elementi risposta dell'acido retinoico, promuovendo così la trascrizione di diversi geni coinvolti nella crescita, sviluppo, differenziamento, produzione di citochine e metabolismo.

1.17. VIE D'ENTRATA DEL CALCIO NEL MUSCOLO SCHELETRICO

A differenza del cuore, nel muscolo scheletrico il meccanismo di eccitazione-contrazione prevede principalmente il contributo della depolarizzazione della membrana plasmatica ed il successivo rilascio di calcio dai depositi intracellulari (Melzer et al., 1995), tramite una interazione bi-direzionale tra il recettore DHPR e RyR-1 (Nakai et al., 1996). Da studi del passato è risaputo che la contrazione singola ("twitch") delle fibre muscolari persiste anche in assenza di calcio extracellulare (Armstrong et al., 1972), confermato in esperimenti dove l'entrata di calcio esterno è stata bloccata con farmaci quali diltiazem (Gonzalez-Serratos et al., 1982) o con bloccanti non specifici delle correnti calcio di Tipo L, quali Cd^{2+} o La^{3+} (Nakai et al., 1996). Per di più, a confermare questo vi è la cinetica di attivazione dei canali di Tipo L, come il DHPR (50-100 ms), la quale è troppo lenta per permettere una entrata di calcio significativa durante brevi potenziali d'azione del muscolo scheletrico (2-5 ms). Tuttavia recenti studi mettono in luce la presenza di due vie distinte di entrata del calcio extracellulare: ECCE

(Excitation-Coupled Ca^{2+} Entry) e SOCE (Store-Operated Calcium Entry) (William & Rosenberg, 2002; Cherednichenko et al., 2004).

ECCE è la via di influsso di calcio trans-sarcolemmatica, indipendente dallo svuotamento delle cisterne, che viene attivata in seguito a depolarizzazioni prolungate di membrana. Richiede l'intervento del recettore DHPR, canale ti tipo L sensibile al voltaggio (LTCC, L-Type Calcium Channel) ed il recettore canale della Ryanodina (RyR-1). Anche se il poro attraverso cui passa la corrente calcio proveniente dall'esterno non è ancora stato ben chiarito, da esperimenti sembra coincidere con il recettore DHPR, in quanto sia il canale di Tipo L che ECCE vengono inibiti dai bloccanti La^{3+} e Gd^{3+} e da alte concentrazioni di nifedipina, bloccante specifico delle correnti Calcio di tipo L (Hurne et al., 2005; Bannister et al., 2009).

SOCE è la via di influsso di calcio dall'esterno tramite il canale Orai, che per attivarsi necessita della fuoriuscita di calcio dai depositi intracellulari attraverso il canale STIM1. Orai si trova sulla membrana plasmatica nei Tubuli T e fa parte di una famiglia di canali tetramerici altamente selettivi per il calcio. STIM1 è localizzata di fronte sulla membrana del reticolo sarcoplasmatico ed è una fosfoproteina a singolo segmento transmembrana. Nella estremità N-terminale rivolta nel lume del reticolo, comprende un motivo "Steril-• -motif" (SAM) ed un dominio EF-hand che presenta alta affinità per il calcio (200-600 µM), il quale conferisce alla molecola la attività di sensore del contenuto del lume del SR (Stathopulos et al., 2006). La estremità C-terminale sul lato citoplasmatico è formata da 2 spirali superavvolte con regioni ricche di proline. Questa regione superavvolta pare attivare l'nflusso di calcio attraverso il canale selettivo Orai, in quanto da esperimenti si è visto che, in condizioni di riposo i depositi sono pieni di calcio e le proteine STIM1 sono distribuite diffusamente sulla membrana e stabili grazie al legame col calcio nei motivi EF-hand. Quando viene stimolata la fuoriuscita di calcio dai depositi sarcoplasmatici, il distacco del calcio da STIM1 ne promuove l'oligomerizzazione. Gli oligomeri si aggregano e si convogliano nella parte giunzionale del reticolo, a 10-25 nm di distanza dal sito di contatto con Orai1, sui Tubuli T, attivando l'influsso di calcio SOCE tramite quest'ultimo (Stathopulos et al., 2006; Liou et al., 2007; Muik et al., 2009; Wu et a., 2006).

SOCE, al contrario di ECCE, non viene attivata da potenziali di membrana prolungati, ma sembra essere importante per sostenere il calcio che fuoriesce dai depositi e prevenire la debolezza muscolare.

Ciò che rimane da chiarire è se entrambi ECCE e SOCE operino distintamente o richiedano la cooperazione dei canali TRPC, e se abbiano un ruolo fisiologico nello sviluppo e nell'affaticamento muscolare, nell'anzianità, oltre che nelle malattie muscolari.

2. SCOPO DELLA TESI

Il muscolo scheletrico costituisce circa il 40% della massa corporea e svolge un ruolo importante nella salute umana.

L'attivazione della contrazione muscolare è dovuta alla propagazione del potenziale d'azione all'interno della fibra muscolare attraverso il sistema dei tubuli trasversi (tubuli T). La depolarizzazione dei tubuli T induce il rilascio di calcio accumulato nel lume del reticolo sarcoplasmatico (RS) mediante un processo detto accoppiamento eccitazione-contrazione (EC-coupling) (Rios and Pizarro, rev 1991). Tale meccanismo coinvolge un complesso macromolecolare di proteine principali e minoritarie che cooperano in una fitta rete di segnali. Tra queste un ruolo importante è svolto da Calsequestrina-1 (CSQ-1), proteina luminale del reticolo sarcoplasmatico che oltre alla funzione di tampone del calcio regola il recettore della Rianodina (RyR-1), canale di rilascio del calcio presente sul reticolo sarcoplasmatico e JP45, proteina transmembrana del RS adiacente a RyR-1. JP45 interagisce sia con CSQ-1 che con la subunità cav 1.1 del recettore delle Diidropiridine (DHPR), che agisce come canale calcio e sensore di voltaggio per iniziare la contrazione muscolare attivando i recettori della Rianodina. I complessi meccanismi del processo di EC-coupling non sono ancora del tutto definiti. Ciò, unito al fatto che molti disordini muscolari hanno come comune denominatore una alterazione dell'omeostasi del calcio, ha spinto il nostro gruppo a studiare il ruolo di diverse proteine coinvolte nel meccanismo di EC-coupling, in particolare le proteine JP45 e CSQ-1.

Lo scopo principale di questa tesi è di valutare le proprietà biochimiche e funzionali delle fibre del muscolo scheletrico in topi in cui le singole proteine JP45 e CSQ-1 sono state inattivate (topi JP45 KO e CSQ-1 KO), ma soprattutto quello di esaminare ciò che succede al meccanismo di EC-coupling quando entrambe le proteine vengono delete (topi JP45/CSQ-1 DKO). Abbiamo infatti ipotizzato che il complesso JP45/CSQ-1 sia coinvolto nelle via di segnale tra il lume del reticolo e Ca_v 1.1.

In collaborazione con altri colleghi appartenenti ad altri gruppi di ricerca abbiamo inoltre cercato di:

-approfondire lo studio del fattore di trascrizione PGC-1• , che è coinvolto nella plasticità muscolare promuovendo la conversione delle fibre di "tipo fast" in fibre di "tipo slow" nell'esercizio muscolare, ciò ci ha fatto ipotizzare che PGC-1• sia coinvolto nella

modulazione dei rilasci di calcio dal reticolo sarcoplasmatico attraverso il recettore della Rianodina e che influisca di conseguenza sulla generazione della forza muscolare;

-abbiamo inoltre svolto esperimenti per caratterizzare una proteina scoperta recentemente nel nostro laboratorio, SRP35. Poiché la struttura della proteina ha rivelato essere una deidrogenasi a catena corta (SDR) coivolta nella via glicolitica del muscolo scheletrico abbiamo investigato se SRP35 possa esser coinvolta nella generazione dei segnali intracellulari, intesi come rilasci di calcio dal reticolo sarcoplasmatico attraverso RyR-1 e metabolismo del muscolo scheletrico.

3.MATERIALI E METODI

3.1. SVILUPPO DELLA COLONIA MURINA TRANSGENICA

I topi sono stati nel corso degli ultimi anni modelli importanti per studiare il ruolo fisiopatologico di geni coinvolti nelle malattie e per osservare il fenotipo in seguito a mutazioni in sequenze geniche. Le tecniche di ingegneria genetica sono applicate di frequente ai topi, i quali sono spesso confrontati con gli esseri umani per la condivisione di sequenze geniche e per aspetti fisiologici. Esistono differenti strain murini, aventi ciascuno un diverso patrimonio genetico (genetic background) che può influenzare il fenotipo ad esempio dal punto di vista di caratteristiche fisiologiche e anatomiche diverse o della diversa suscettibilità alle patologie. Per discriminare il fenotipo dato dal transgene di interesse rispetto al fenotipo dato dal background dell'animale, la scelta dello strain murino nella costruzione del modello animale transgenico è molto importante. Per le nostre analisi di laboratorio abbiamo scelto come ceppo ricevente puro "inbred", topi con strain C57BL-6, caratterizzati da una buona breeding performance, elevata sensibilità ad alcol e narcotici e maggiore inclinazione allo sviluppo di cataratta e perdita udito. Diverse sono le tecniche di ingegnerizzazione degli animali da laboratorio, noi abbiamo scelto la tecnica Knock-out (KO) o inattivazione del gene, per studiare il ruolo di geni sequenziali ma con funzione sconosciuta. La tecnica prevede:

1. Il gene che deve essere inattivato è stato isolato da una libreria di geni murini; si è creato un costrutto avente una sequenza di DNA uguale al gene isolato, tranne che per un tratto sufficiente a rendere inoperabile il gene (non si inattiva in gene intero);
2. Le cellule staminali, capaci di crescere in vitro, sono state isolate da una blastocisti di topo con background esempio Balb-c, albini. Il background genetico è inteso come l'insieme di tutti i geni e le rispettive varianti alleliche, che possono interagire con il gene/transgene di interesse ed influenzare il fenotipo. Tali geni infatti possono essere direttamente correlati al gene di interesse, ma possono anche far parte dello stesso processo biochimico o della stessa via di segnale cellulare.

3. Le cellule staminali sono state trattate con elettroporazione per permettere alla sequenza di DNA di entrare. Alcune cellule incorporano la sequenza nuova nel loro cromosoma al posto di quello vecchio per ricombinazione omologa, in quanto le sequenze sono simili. Usando poi un marcatore per il gene della sequenza nuova si possono identificare le cellule che hanno incorporato il nuovo DNA.
4. Dalla coltura cellulare, le cellule staminali con la sequenza nuova sono state incorporate nella blastocisti di un topo con background diverso, esempio C57BL, con manto grigio. Tale blastocisti è stata a sua volta impiantata nell'utero di un topo femmina per completare il periodo gestazionale. La blastocisti possiede 2 corredi cromosomici: le cellule originali di topo grigio, e le cellule ingegnerizzate di topo bianco. I topi nati sono topi CHIMERA ed hanno evidenziato caratteristiche intermedie ai 2 corredi cromosomici.
5. I topi chimera che hanno incorporato la sequenza di DNA ingegnerizzato nelle cellule germinali (ovulo o spermatozoo) sono stati incrociati con topi C57BL-6, Wild-Type (WT). La prole nata che conteneva ancora una copia del gene funzionale (eterozigote per il gene Knok-out) è stata ulteriormente incrociata per produrre topi aventi il gene con entrambi gli alleli inattivati, KO. Ad ogni incrocio con il ceppo puro ricevente (inbred), il background originale viene diluito del 50%. Tale tecnica definita Backcross tradizionale, si basa sulla legge Mendeliana dell'assortimento indipendente degli alleli nello scambio tra cromatidi fratelli durante la meiosi. Sono stati necessari almeno 10-12 incroci successivi in un background ricevente puro per ottenere una percentuale del background genetico di partenza inferiore all'1%, corrispondente ad una differenza di solo 1 centimorgan nella mutazione nel gene di interesse.

I topi sono stati ingegnerizzati per la proteina JP45.

I topi JP45/CSQ-1 DKO sono stati ottenuti incrociando un topo maschio JP45x CSQ-1 KO femmina gentilmente concessa dal professor Protasi F. di Chieti. Nella generazione F1 sono stati ottenuti topi 100% JP45/CSQ-1 doppi eterozigoti. La generazione F1 è stata incrociata tra di loro F1xF1 e si sono ottenuti topi 6,25% (1/16) DKO e WT.

3.2. ESTRAZIONE DEL DNA DA TESSUTO

Per l'estrazione del DNA sono state effettuate delle biopsie di tessuto dalle code dei topini dell'età di 7 giorni di sviluppo postnatale. Il DNA è stato estratto tramite il Kit Nucleospin Tissue (Machery-Nagel) che prevede prima di tutto una lisi iniziale del tessuto overnight in agitazione con 25 µl dell'enzima Proteinase K e 180 µl di buffer di pre-lisi T1. Il tessuto è stato successivamente agitato per un minuto e sono stati aggiunti 200 µl del buffer di lisi B3, agitato ed incubato 10 minuti a 70 °C. Al termine il campione è stato agitato per un minuto ed è stato centrifugato 5 minuti ad 11.000 rpm per eliminare le impurità rappresentate dai peli. Al termine il surnatante è stato trasferito in una provetta nuova e vi sono stati aggiunti 200 µl di etanolo, dopo aver agitato il campione per un minuto è stato caricato completamente in una provetta con colonna e centrifugato 1 minuto a 11.000 rpm per permettere il binding del DNA alla membrana della colonna. Sono stati effettuati 2 passaggi di lavaggio della membrana prima con 500 µl di buffer BW (Guanidine hydrochloride and isopropanol) e con 600 µl del buffer B5 (concentrate powder and ethanol) ognuno seguiti da una centrifugata di 1 minuto a 11.000 rpm. Successivamente il campione è stato sottoposto ad una centrifugata di 1 minuto per asciugare la membrana di silica gel. La colonna con il DNA legato è stata trasferita in una provetta nuova e sono stati aggiunti 100 µl di buffer BE (10 mM Tris/HCl pH=8) precedentemente riscaldato a 70°C, incubato 1 minuto sul bancone e centrifugato 1 minuto a 11.000 rpm. Quest'ultimo passaggio è stato ripetuto due volte per eluire più DNA possibile. I campioni sono stati poi conservati a -20°C.

3.3. QUANTIFICAZIONE DEL DNA

Il DNA è stato quantificato allo spettrofotometro a singolo raggio UV DU7400 Beckman. I campioni sono stati diluiti 1:50 in Tris HCl 10 mM pH=8 e dopo aver sottratto il valore di densità ottica del bianco, è stata misurata la concentrazione del DNA considerando l'assorbanza a 260 nm . Il valore ottenuto a 260 nm è stato moltiplicato per 50 (fattore di diluizione) e per 50 (assorbanza del DNA = 1µg/1ml; 1 OD_{260nm} =50µg/1ml). E' stata letta anche la densità ottica a 280 nm (OD_{280nm}) indicativa della presenza di proteine ed il rapporto tra OD_{260nm}/OD_{280nm} deve esser compreso tra 1,8 e 2 per avere un campione puro.

3.4.REAZIONE DI POLIMERASI A CATENA (PCR)

Le sequenze specifiche di DNA mutato per le proteine JP45 e Calsequestrina sono state amplificate tramite la tecnica della reazione di polimerasi a catena PCR.

Per amplificare il tratto CSQ-1 KO è stato utilizzato il Kit Taq DNA polimerasi Roche. Per un campione, è stata preparata una soluzione master mix contenente 20,7 µl di acqua microfiltrata, 5 µl di buffer + Mg 10x, 4 µl di dNTP 2,5 mM ciascuno, ed i primers CS-F : 5'-CCTTTCTCTTAGCAGAGCCC-3'; CS-R : 5'-CCATCTACCTTCAACAAACCC-3', LTR2 5'-GCGTTACTTAAGCTAGCTTGC-3'. Sono stati aggiunti 0,3 µl di enzima Taq 1U/µl e 10 µl di DNA del campione alla concentrazione di 1ng/µl per un volume finale di 50 µl. Per l'amplificazione al termociclatore è stato impostato il seguente programma: 1 ciclo di denaturazione a 95°C per 15 minuti, 35 cicli ciascuno composto da 40 secondi a 94°C di denaturazione a singola elica, 40 secondi a 60°C di appaiamento del primer e 60 secondi a 72°C di estensione del DNA ad opera dell'enzima. Al termine è stato fatto 1 ciclo a 72°C per 5 minuti. I prodotti di PCR sono stati separati su gel di agarosio 2% tramite elettroforesi 20 minuti a 100 V in TAE 0,5x (Tris 0,4 M, acido acetico glaciale, EDTA 0,01 M pH=8) e colorati con Etidio Bromuro (5 µl/100 ml di TAE 0,5x).

Per amplificare il tratto corrispondente a JP45 KO è stato utilizzato il Kit Roche FastStart Taq Plimerasi ed in un volume totale di 20 µl sono stati messi : 10,8 µl di acqua microfiltrata, 2 µl di buffer + Mg 10x, 2 µl di dNTP, 0,5 µl del F2 5'-TAAAGACAGAGACCACATCCTCCC-3' e 0,5 µl del primer F4 5'-GACAAGGGGTGTGGGGTATGAGGC-3'. Sono stati aggiunti 0,2 µl di enzima FastStart Taq e 4 µl di DNA (1ng/µl). Al termociclatore è stato impostato il seguente programma: 1 ciclo 95°C di 15 minuti, 35 cicli ciascuno composto da denaturazione per 40 secondi a 94°C, appaiamento per 40 secondi a 68°C e estensione per 1 minuto e 20 secondi a 70°C seguiti da un ciclo a 72°C per 7 minuti. Gli amplificati sono stati letti come per CSQ ma in gel di agarosio all'1%.

3.5. Real-Time PCR

Per studiare il profilo dell'espressione genica, l'mRNA viene convertito a cDNA impiegando una trascrittasi inversa e può così servire da stampo nella tecnica di PCR in tempo reale (Vukcevic et al., 2008). Per questa tecnica sono stati utilizzati muscoli interi di Soleo ed EDL estratti e conservati in azoto liquido. L'RNA totale è stato estratto tramite il reagente TRIzol (Invitrogen) e trattato con deossiribonucleasi I per eliminare la contaminazione da DNA nei campioni di RNA (DNase I amplification Grade, Invitrogen). In seguito alla trascrittasi inversa utilizzando 1000 ng di RNA (High capacity cDNA Reverse transcription Kit, Applied Biosystems), il cDNA e stato amplificato tramite la real-time PCR quantitativa utilizzando SYBR Green technology (fast SYBER green master mix, Applied biosystem) e con i seguenti primers: Primers TRPC3: forward, 5•-GCCAAGCGACGGAGGAATTA-3•; reverse, 5• CAGCACACTGGGGTTCAGTT-3•. Primers Cav1.2: forward, 5•- ATGAAAACACGAGGATGTACGTT-3•; reverse, 5• ACTGACGGTAGAGATGGTTGC-3•. Primers ORAI1: forward, 5• AACGAGCACTCGATGCAGG-3•; reverse, 5• GGGTAGTCATGGTCTGTGTCC-3•. Primers STIM1: forward, 5•- TGACAGGGACTGTACTGAAGATG-3•; reverse, 5• TGCCGAGTCAAGAGAGGAGG-3•.

L'espressione genica in ogni tipologia di muscolo è stata ottenuta normalizzando l'incremento della espressione proteica, inteso come numero di cicli di PCR, per l'espressione delle proteine Tata box binding (TBP), la cui espressione rimane invariata sia nei DKO che nei controlli.

3.6. PREPARAZIONE DI VESCICOLE MICROSOMALI DA RETICOLO SARCOPLASMATICO

Sono stati impiegati topi JP45/CSQ-1 DKO e WT di 6-8 settimane di età. I topi sono stati sacrificati uno alla volta per dislocazione cervicale e è stato seguito il protocollo messo a punto da Saito et al (Saito et al., 1984). In camera fredda (4°C) è stato prelevato il tessuto muscolare delle zampe posteriori ed omogenato per 2-3 minuti tramite una sonda dotata di lame. Abbiamo preparato un omogenato al 10% in un tampone contenente: 0,3 mM saccarosio, 5 mM Imidazolo pH=7,4, e gli antiproteolitici 0,2 mM PMSF, 1 mM Iodoacetamide, 1 mM Benzamidine, 1 µM Leupeptina. Successivamente gli omogenati sono stati centrifugati per 10 minuti 4°C a 5000 rpm in

centrifuga sorvall rotore SSB4. Il surnatante è stato raccolto in una nuova provetta, mentre ai pellets sono stati aggiunti gli stessi quantitativi precedenti di tampone per ottenere un omogenato del 10% e sono stati omogenati 2-3 minuti per la seconda volta. E' stata ripetuta la centrifugata di 10 minuti 4 °C a 5000 rpm ed i surnatanti raccolti sono stati aggiunti a quelli precedenti. Successivamente i surnatanti sono stati centrifugati per 15 minuti 4 °C a 11.000 rpm (sorvall rotore SSB4). I nuovi surnatanti ottenuti sono stati poi filtrati su 15-20 strati di garza e centrifugati in ultracentrifuga Beckman rotore 70TI per 1 ora 4°C 40.000 rpm. Sempre lavorando a 4°C, i pellets ottenuti sono stati risospesi in 500-1000 µl del tampone di saccarosio iniziale ed omogenati tramite l'uso di potters ed aliquotati in vials e conservati a -80 °C, tranne una piccola aliquota tenuta per leggere la concentrazione proteica.

3.7. LETTURA DELLA CONCENTRAZIONE PROTEICA

La concentrazione proteica dei campioni JP45/CSQ-1 DKO e WT è stata letta allo spettrofotometro DU7400 Beckman nello spettro del visibile, tramite reazione colorimetrica con metodo Bradford. In seguito ad una retta di taratura dello strumento eseguita con concentrazioni seguenti della proteina sierica bovina (BSA) 1µg/µl in colorante Bradford 1x (Biorad), i campioni sono stati diluiti 1:500 nello stesso colorante. E' stata misurata la densità ottica a 280 nm dopo aver sottratto la densità ottica del bianco.

3.8. WESTERN BLOT

Le vescicole microsomali di JP45/CSQ-1 DKO e WT sono state preparate in una soluzione denaturante composta da 10 µg vescicole, soluzione "O" 2x (sample buffer: 10% glicerolo, 5% • mercaptoetanolo, 2,3% SDS e 62,5 mM Tris pH=8) ed acqua microfiltrata e separate in gel SDS-poliacrilammide, formato da un Running gel 10-12% nella parte inferiore (3-3,6 ml Acrolammide, 1,5 M Tris-HCl, 0,4 % SDS, 20 µl Temed, 40 µl AMPs 10% ed acqua microfiltrata fino a 12 ml) e nella parte superiore da uno Stacking Gel 4% (0,56 ml Acrilammide, 0,5 M Tris-HCl, 0,4% SDS, 15 µl Temed, 30 µl AMPs 10% ed acqua microfiltrata fino a 4 ml). Nel pozzetto più a sinistra è stato

caricato un marcatore di peso molecolare Prestained Protein Marker, Broad Range (BioRad). La corsa elettroforetica su gel delle proteine è avvenuta a temperatura ambiente (RT) 1-2 ore ad amperaggio costante di 200 Volt. Il trasferimento su membrana di nitrocellulosa è avvenuto over night a 4 °C ad amperaggio costante di 200 mA. Il giorno seguente la membrana è stata prima colorata con rosso Ponceau per visualizzare le proteine, decolorata con TBS 1x (TBS 10x: 1,4 M NaCl, 0,1 M Tris) ed incubata 1 ora in agitazione a RT con una Blocking Solution (Roche) diluita 1:10 in TBS 1x, per saturare le regioni della membrana non ancora legate da proteine. Dopo un ciclo di lavaggio con TBS 1x, è stata effettuata l'incubazione di 1 ora con l'anticorpo primario diluito in TBS-Tween (TBS-T). Dopo un ciclo di 3 lavaggi con TBS-T, è stata eseguita una incubazione di 1 ora a RT con l'anticorpo secondario coniugato ad una perossidasi in soluzione TBST-T. Al termine sono stati fatti 3 lavaggi di 5 minuti in agitazione con TBS-T a RT e la membrana è stata poi incubata con il substrato BioChemiluminescence (Roche) per la perossidasi ed esposta a lastra autoradiografica.

Per gli anticorpi primari per JP45 e CSQ-1 sono stati utilizzati rabbit anti-JP45 e chicken anti-CSQ-1 (fatti in casa) e diluiti 0.5µg/ml e 0.3µg/ml finali rispettivamente; mentre per gli anticorpi secondari sono stati scelti Prot G 1:250.000 Protein G-peroxidase strepticoccus sp. (Sigma); Anti mouse HRP Conj. 1:200.000 Anti-mouse IgG (Fab specific) peroxidase conjugate (Sigma); Anti chicken HRP conj. 1:130.000 Anti-chicken IgY (IgG)peroxidase conjugate (Sigma).

Per l'identificazione delle altre proteine di reticolo tramite Western Blot sono stati utilizzati i seguenti anticorpi:

Name	Dilution/Conc.	Compagny	Product name	Cat nb
anti DHPR • 1 (from goat)	1:1000	Santa Cruz	L-type Ca++CP• 1S (N-19)	sc-8160
anti DHPR • 1 (from goat)	1:300	Santa Cruz	L-type Ca++CP• 1 (D-15)	sc-32079
Anti Ryr (from mouse)	1:5000	Thermo Scientific	Anti-Ryanodine Receptor mAB	MA3-925
anti SERCA1 (from goat)	1:500	Santa Cruz	SERCA1 (N-19)	sc-8093
anti SERCA2 (from goat)	1:6000	Santa Cruz	SERCA1 (N-19)	sc-8095
anti Sarcalumenine (from mouse)	1:1000	Thermo Scientific	Anti sarcalumenin monoclonal AB	MA3-932
anti Calreticuline (from goat)	Final conc 1.5µg/ml	Santa Cruz	Calregulin (C-17)	sc-6467
anti albumine	1:70000	Bethyl laboratories.inc	Mouse albumine AB HRP conjugated	A90-134P
2^{nd} AB				
Prot G	1 :250000	Sigma	Protein G-peroxidase strepticoccus sp.	P8170
Anti mouse HRP Conj.	1 :200000	Sigma	Anti-mouse IgG (Fab specific) peroxidase conjugate	A2304
Anti chicken HRP conj.	1 :130000	Sigma	Anti-chicken IgY (IgG)peroxidase conjugate	A9046

3.9. ESPERIMENTI QUANTITATIVI DI BINDING IN VESCICOLE MICROSOMALI DI RETICOLO SARCOPLASMATICO

Gli esperimenti di Binding sui recettori della Ryanodina (RyR-1) sono stati effettuati utilizzando il radioligando [^{3}H]-ryanodina (Perkin Elmer). Le vescicole di reticolo sarcoplasmatico (1µg) sono state incubate con rianodina fredda (Calbiochem) e concentrazioni crescenti di [^{3}H]-ryanodina (2-10 nM) over night a temperatura ambiente

al buio in un buffer di binding contenente 2 M NaCl, 40 mM Hepes pH=7,4, 40 µM $CaCl_2$, 10 mM AMP ed un mix 2x di inibitori delle proteasi (Protease Inhibitor Cocktail, Roche Applied Science). La misura del binding non specifico è stata effettuata in presenza di Ryanodina non radio marcata alla concentrazione finale di 500 µM. Il giorno successivo la miscela di binding contenente le vescicole (4,5 µl=4,5 ug) è stata filtrata attraverso filtri Whatman GF/B, i quali sono stati lavati 3 volte con 5 ml di una soluzione fredda di lavaggio (200 mM Choline Chloride, 20 mM Tris HCL pH=7.5) ed asciugati. Tramite uno scintillatore è stata effettuata la misura del legame di [^{3}H]-ryanodina alle vescicole sui filtri immersi nel liquido di scintillazione Pico-Fluor 15 (Perkin Elmer).

Per il binding di 3H-PN200-110 abbiamo preso dai 20-200 µg di vescicole calcolando una quantità di DHPR simile alla K_d. Abbiamo considerato che le vescicole contengono DHPR pari a 5-10 pmol/mg di proteina assumendo una K_d 0,5 nM (Damiani E. Tobaldin Margreth BBRC tra 1992-1995). Le vescicole sono state incubate 2 ore a RT nel binding Buffer (50 mM Tris HCl-pH 7.5 10 • M Ca^{2+} Protease inhibitors 0.05-10 nM (+)-[Methyl-^{3}H]PN200-110) ed al buio over night. La miscela è stata filtrata attraverso filtri Whatman GF/B e lavata 3 volte con la soluzione di lavaggio 200 mM Choline Chloride, 20 mM Tris HCl pH=7,5 ed è stata fatta la conta delle molecole marcate tramite il liquido di scintillazione.

3.10. MISURA DELLA DENSITA' DELLE PROTEINE DEL RETICOLO SARCOPLASMATICO

Le vescicole microsomali di Topi DKO e WT sono state caricate in gel di agarosio. In seguito alla corsa elettroforetica di 20 minuti a temperatura ambiente a 100 V sono state colorate con Bromuro di Etidio e controllate al Gel Doc (BioRad). La densità delle proteine è stata calcolata tramite il software Gel Doc from Biorad.

3.11. TEST DELLA CORSA "RUNNING WHEEL"

Per questo test sono stati scelti dai 5 ai 10 topi transgenici e controllo di 4-6 settimane di età. I topi sono stati rinchiusi all'interno di gabbie singole munite di ruote girevoli attrezzate con un magnete ed un sensore capace di leggere i giri effettuati e di

trasmetterli ad un computer. I giri delle ruote sono stati convertiti in metri totali percorsi da ciascun topo sono stati registrati tramite il programma Santhera (CH). Sono state registrate le attività motorie spontanee, in quanto ogni animale aveva libero accesso alle ruote ad ogni ora del giorno, per una durata di 22 giorni circa.

3.12. PREPARAZIONE DI FIBRE DISSOCIATE DI MUSCOLO FLEXOR DIGITORUM BREVIS (FDB)

I muscoli FDB sono stati estratti dalle zampe posteriori di topi JP45/CSQ-1 DKO, JP45 KO, CSQ-1 KO e WT di 4-6 settimane di età, sacrificati in seguito a dislocazione cervicale, e continuamente bagnati da un Tyrode's Buffer contenente in mM: 137 NaCl, 5.4 KCl, 0.5 $MgCl_2$, 1.8 $CaCl_2$, 11.8 Hepes-NaOH pH= 7.4 e 0,1 % Glucosio. I muscoli sono stati poi incubati 1 ora a 37 °C 5 % CO_2 con 0,20 % Collagenasi di Clostridium Hystolyticum Type I 0,27 units/mg (Invitrogen) sciolto in Tyrode's buffer, per permettere la digestione delle pellicole connettivali varie che avvolgono il muscolo ed i fasci di fibre. Al termine i muscoli sono stati sciacquati con terreno DMEM arricchito con 10 % FBS (Fetal Bovis Serum) capace di inibire l'enzima collagenasi. I muscoli sono stati poi trasferiti in una piastra multiwell contenente vetrini trattati precedentemente con 1,5 µl di Laminina Natural Mouse (1mg/ml Invitrogen) diluita con acqua microfiltrata, per almeno 1 ora e poi aspirata e con 2 ml di terreno DMEM base. Con l'aiuto di pipette di vetro è stata applicata una leggera pressione tra i tendini delle dita dei muscoli a partire con pipette dal diametro grande fino ad arrivare a diametri più sottili per cercare di dissociare i muscoli in singole fibre che depositandosi sono state intrappolate dal velo di laminina steso sui vetrini di 13 mm di diametro. Dopo aver dissociato un numero sufficiente di fibre, sono stati aggiunti 200 µl di FBS in ogni pozzetto e lasciate depositare ulteriormente per circa un'ora in incubatore a 37°C, 5% CO_2. Al termine ciascun vetrino è stato sottoposto a 3 lavaggi con terreno DMEM 10 % FBS e 1% Pennicillin/ Streptomicin (P/S), per togliere le fibre non vitali e non adese, e lasciate over night in incubatore per permetterne la completa adesione ai vetri e ridurre così i movimenti artefatti durante le acquisizioni.

3.13. MISURAZIONE DEL CALCIO BASALE, DEI TRANSIENTI E MANGANESE QUENCHING

Per misurare il livello di calcio basale nelle fibre FDB, le cellule sono state incubate 40 minuti a 20 °C in Tyrode's buffer 1,8 mM $CaCl_2$ in presenza di 10 µM Indo-1,AM, 50 µM BTS (4-Methyl-N-(phenylmethyl) benzenesulfonamide; un inibitore selettivo della attività ATPasica della miosina tipo II del muscolo scheletrico) e 5% Pluronic, un detergente capace di favorire la diffusione del colorante all'interno delle fibre (Hollingworth et al., 2009). Al termine le cellule sono state sciacquate con Tyrode's buffer 1,8 mM $CaCl_2$ fresco e misurate.

Per la misura dei transienti calcio le fibre sono state incubate 15 minuti a 20 °C in Tyrode's buffer 1,8 mM $CaCl_2$ in presenza di 10 µM Mag-Fluo-4,AM, 50 µM BTS e 5% Pluronic. Al termine le cellule sono state sciacquate con Tyrode's buffer 1,8 mM $CaCl_2$ fresco e misurate (Hollingworth et al., 2009; Calderon et al., 2010). Per le acquisizioni in lantanio, l'incubazione con il colorante è stata fatta nel medesimo modo, ma per la misura dei flussi del calcio il Buffer esterno è stato sostituito con lo stesso Tyrode's buffer ma 0 mM $CaCl_2$ e con 100 µM $LaCl_3$.

Per la tecnica di Manganese Quenching le fibre sono state incubate 30 minuti a 37 °C, 5% CO_2 in Tyrode 1,8 mM $MgCl_2$, 5 mM EGTA. Successivamente sono stati aggiunti 50 µM BTS e 50 µM del bloccante rianodina ed incubate per 50 minuti sempre in incubatore. Al termine le fibre sono state sciacquate con Tyrode 1,8 mM $CaCl_2$ ed incubate in quest'ultimo buffer con 5 µM Fura-2AM, 50 µM BTS, 50 µM rianodina , 5% pluronic, a 20°C per 25 minuti. Le acquisizioni sono state eseguite in Tyrode buffer senza calcio e contenente 0,5 mM $MgCl_2$; 1.8 mM $MnCl_2$; 10 µM EGTA, 50 µM rianodina (Clementi et al., 1992; Cherednichenko et al., 2008).

I vetrini sono stati montati in una cameretta e misurati in camera termostatata a 20 °C. I transienti sono stati misurati selezionando un'area sulle fibre di 1 mm di diametro, tramite un microscopio Nikon eclipse TE/2000 adattato per la microfluorescenza, dotato di: una lampada a mercurio, un sistema di fototubi (tubi elettronici in cui l'emissione degli elettroni è provocata dalla luce e da altre radiazioni elettromagnetiche), di fotomoltiplicatori (strumento capace di trasformare gli impulsi deboli luminosi in corrente elettrica amplificandoli) ed una CCD camera per le immagini. Gli stimoli del potenziale di membrana sono stati applicati tramite uno stimolatore elettrico che ci ha permesso di impostare l'intensità e la durata della depolarizzazione sia per gli impulsi singoli (twitch

pari a 0.5 ms 40 V), che per la stimolazione prolungata (stimolazione tetanica 100Hz della durata di 300 ms). La stimolazione locale è stata eseguita tramite un micromanipolatore idraulico ed un capillare di vetro borosilicato (World Precise Instruments), avente una sezione simile al diametro delle fibre, e contenente un filo d'argento (polo +) e la stessa soluzione di acquisizione come conduttori. Un filo d'argento è stato posizionato all' esterno come polo negativo. I fotomoltiplicatori sono stati impostati in base alla lunghezza d'onda di eccitazione dei coloranti fluorescenti ed il microscopio è stato dotato di filtri dicroici che rispettano le lunghezze d'onda di emissione degli stessi (Indo-1AM ex 365 nm, em 405/480 nm; Mag-Fluo-4 ex 480 nm, em 510 nm; Fura-2 AM ex 360 nm, em 510 nm). I fitri dicroici riflettono la luce fino a una certa e fanno passare luce con superiore e sono utilizzati per impedire che la luce di eccitamento influenzi la luce di emissione. I dati sono stati poi registrati tramite un computer grazie ad un programma AUTOLAB RCS, ed analizzati con test statistici GraphPad4 ed Origin.6.

3.14. PROPRIETA' MECCANICHE DEL SOLEO E DELL'EDL

I muscoli Solei ed EDL di topi DKO e WT di 4-6 settimane di età sono stati estratti e tramite i tendini sono stati legati ad uno strumento composto da un trasduttore ed un amplificatore collegati ad un cumputer dotato di un programma capace di misurare la massima forza tetanica. I muscoli sono stati immersi in una soluzione Tyrode 1,8 mM $CaCl_2$ e sono stati applicati una serie di impulsi singoli "twitch" (100 mN) ed una serie di treni di impulsi ripetitivi 100 Hz della durata di 350 ms a 0,27 Hz (300 mN). Al termine della stimolazione, la soluzione è stata scambiata con un Tyrode's buffer senza calcio, ma con 100 µM del bloccante Lantanio e dopo aver atteso 10 minuti per permettere la completa diffusione della soluzione nei muscoli è stato applicato lo stesso protocollo di stimolazione precedente. Successivamente il Tyrode è stato sostituito con quello iniziale con calcio ed è stato ripetuto l'esperimento.

3.15. PATCH-CLAMP

I muscoli FDB di topi JP45/CSQ-1 DKO e WT di 4-6 settimane di età sono stati dissociati enzimaticamente in singole fibre come descritto da Saito el al., 1984. Al termine le fibre sono state messe 3 ore a 4°C per irrigidire le membrane e favorire un migliore sigillo tra la pipetta e la sezione di membrana durante il metodo whole-cell di Patch-clamp. L'whole-cell è stato ottenuto tramite pipette aventi 1 M• di resistenza di accesso. Le fibre sono state caricate in una cameretta per microscopio ed immerse in una soluzione esterna contenente in mM: TEA-methanesulfonate 150, $MgCl_2$ 1, $CaCl_2$ 2, HEPES 10, 4-AP 0.5, BTS 0.025, TTX 0.001, pH aggiustato a 7.4 con TEA-OH; mentre la soluzione interna conteneva in mM: Cs-methanesulfonate 150, EGTA 10, HEPES 10, ATPK 4, $MgCl_2$ 2, GTP-Na 0.4, CP 10, Leupeptine 0.01, pH aggiustato a 7.4 con Cs-OH (Hernandez-Ochoa EO, Schneider MF, 2012). La corrente cationica è stata stimolata da depolarizzazioni della durata di 400 ms da potenziali di -80 mV fino a voltaggi da -60 mV a +60 mV suddivisi in 10 mV. La corrente Calcio è stata isolata con soluzioni che hanno minimizzato le altre correnti cationiche e sottraendo la traccia ottenuta in soluzione esterna di controllo alla traccia ottenuta aggiungendo alla soluzione esterna 50 µM di Nifedipina, bloccante della subunità Ca_v 1.1(• 1s) del DHPR.

3.16. ANALISI STATISTICA

Per l'analisi statistica sono stati utilizzati Mann Whitney test a due code e Dunnett's multiple comparisons test tramite il programma Graph Pad Prism4. Per l'elaborazione dati è stato utilizzato il programma Chart5 for Windows e per la realizzazione delle figure il programma Origin6.

4.RIASSUNTO DEI RISULTATI OTTENUTI

4.1.CARATTERIZZAZIONE DEL MODELLO MURINO JP45 KO E CSQ-1 KO E DI JP45/CSQ-1 DOPPIO KNOCK OUT.

Successivamente allo sviluppo della colonia murina ottenuta incrociando un topo JP45 KO con una femmina ingegnerizzata CSQ-1 KO, per ogni generazione di topi è stato estratto il DNA ed è stata eseguita la genotipizzazione. Abbiamo condotto esperimenti di tipo quantitativo di binding di radioligandi, sugli omogenati totali delle vescicole microsomali di topi DKO e WT, per le proteine principali coinvolte nei flussi di calcio. Abbiamo osservato un incremento del contenuto della subunità •1a del recettore DHPR e della proteina Calreticulina nei topi DKO.

Abbiamo deciso di sottoporre gli animali al test della corsa "Running Wheel", allo scopo di valutarne la durata della forza muscolare nell'esercizio spontaneo. Dall'analisi dei dati statistici è emerso che non vi sono differenze significative tra i topi JP45/CSQ-1 DKO e WT, ma una riduzione di circa 40 Km dei topi JP45 KO e CSQ-1 KO (Distanza totale in Km: DKO e WT 175,3 ± 2,96; JP45 KO 139,7 ± 2,90; CSQ-1 KO 118,1 ± 2,35, i dati sono espressi come media ± sem n= 10-13 topi, Dunnett's multiple comparison test $P<0,05$*). Il nostro gruppo ha deciso di sottoporre gli animali transgenici al test dell'attrito "GRIP TEST" e di confrontarli con topi controllo. Per osservare la forza di attrito, intesa come forza esplosiva. E' emersa una diminuzione della forza di attrito muscolare dei topi DKO e CSQ-1 rispetto ai topi WT.

In seguito abbiamo deciso di valutare i parametri cinetici del calcio in fibre FDB. Dai dati è emerso che i topi JP45/CSQ-1 DKO presentano un livello maggiore e significativo della concentrazione di calcio basale rispetto ai topi controllo (DKO 1,15 ± 0,23* n=41; WT 0,91 ± 0,10 n=40; JP45 KO 1,03 ± 0,18 n=40; CSQ-1 0,95 ± 0,11 n=41; i valori sono espressi come media ± sd, Mann Whitney test a due code $P<0,05$*). Successivamente abbiamo deciso di misurare i transienti calcio. Dall'analisi dei dati è stata fatta una prima classificazione della tipologia "Slow/Fast-Twitch" e una valutazione dei parametri della cinetica del calcio delle fibre come proposto da precedenti lavori (Calderon et al., 2009). Dalla classificazione dei tetani nelle fibre è stata notata una maggior presenza di fibre di tipo lento con transienti che non si inattivano al termine della stimolazione nei topi DKO rispetto al controllo, ed una tipologia diversa nelle fibre

CSQ-1 KO, caratterizzata da un primo picco veloce che si inattiva immediatamente fino al livello basale. Dall'analisi della cinetica dei Twitch è emersa una diminuzione significativa dell'ampiezza dei picchi in presenza di calcio nei topi transgenici rispetto ai WT (Peak Amplitude in V: DKO 0,67 ± 0,16* n=47; WT 1,009 ± 0,18 n=49; JP45 KO 0,80 ± 0,25 n=40; CSQ-1 0,82 ± 0,25 n=47; i valori sono espressi come media ± sd, Mann Whitney test a due code P<0,05*) ed un aumento del tempo di recupero del calcio all'interno dei depositi, nei topi DKO rispetto ai WT (Half Relaxation Time in ms: DKO 4,8 ± 1,9* n=49; WT 3,7 ± 0,7 n=49; JP45 KO 3,7 ± 1,1 n=40; CSQ-1 KO 4,7 ± 2,6 n=47; i valori sono espressi come media ± sd, Mann Whitney test a due code P<0,05*). Le differenze nella cinetica degli impulsi singoli sono scomparse in presenza di Tyrode's Buffer 0 mM Ca^{2+} e con 100 µM La^{3+} e l'effetto del bloccante è stato maggiormente identificato nella stimolazione tetanica 100Hz. Il fatto che nei tetani delle fibre JP45/CSQ-1 DKO in presenza di calcio ci sia una fase di plateau che si prolunga al termine dell'impulso elettrico, la quale scompare in presenza di La^{3+}, ci ha fatto ipotizzare che nei topi DKO ci fosse una corrente esterna entrante durante la stimolazione tetanica. Poiché dai dati in letteratura sappiamo che esistono due vie distinte di entrata del calcio dall'esterno, SOCE (Store-Operated Calcium Entry) ed ECCE (Exitation-Coupled Calcium Entry), quest'ultima coincide con il recettore delle Diidropiridine, indipendente dal calcio dei depositi e attivato nella depolarizzazione di membrana consistente e prolungata, abbiamo deciso di analizzare la corrente ionica del Manganese (Mn^{2+}), in quanto i canali di tipo L possono condurlo in assenza di calcio esterno. Le fibre sono state pretrattate ed acquisite in presenza dell'alcaloide ryanodina (50 µM) per inibire il recettore della Ryanodina-1 ed evitare che la corrente del calcio rilasciata dal reticolo sarcoplasmatico potesse inquinare la corrente ionica del manganese. Dall'analisi dei dati è emerso che nelle fibre DKO vi è un aumento di 3 volte (DKO -0,11 ± 0,039*; WT -0,034 ± 0,021; JP45 KO -0,034 ± 0,011; CSQ-1 -0,027 ± 0,019, i valori sono espressi come media ± sd, Mann Whitney test a due code P<0,05*) della corrente ionica del Mn^{2+} entrante dal recettore canale DHPR, influsso abolito con l'aggiunta di Nifedipina 50 µM, un bloccante specifico della subunità Cav 1.1 (• 1s) del DHPR. L'analisi quantitativa delle proteine ottenuta tramite RT-PCR non ha messo in luce differenze significative nel livello di espressione di altre proteine canale in topi DKO, abbiamo perciò escluso l'intervento di meccanismi compensatori.

Abbiamo successivamente condotto esperimenti di patch-clamp in fibre FDB di topi JP45/CSQ-1 DKO e WT. Dall'analisi statistica dei dati è emerso che a parità di

capacitanza a 0 mV nei topi DKO l'ampiezza della corrente calcio proveniente dall'esterno raddoppia la corrente dei WT (DKO -2,7 ± 1,2 nA/nF n=9; WT -0,8 ± 0,2 nA/nF n=9, medie ± sd. Per di più nei DKO a voltaggi maggiori di -10 mV, la densità di carica degli ioni calcio entranti per unità di area è il doppio rispetto ai WT.

Per escludere che il miglioramento della durata muscolare che è emersa nei DKO fosse dipesa da una diversa composizione biochimica delle fibre, abbiamo estratto muscoli di Soleo (lenti) ed EDL (veloci) e sono state svolte tecniche di immunoistochimica con anticorpi anti-laminina e anti-MCHI. Dall'analisi è emerso che i muscoli EDL dei topi DKO presentano una riduzione del 20% del volume delle fibre di tipo "Fast-twitch" (in µm: DKO 30 ± 3,50; WT 38 ± 5,23, medie ± sd, Mann Whitney test P<0,05*), ma non vi sono differenze nella distribuzione delle fibre all'interno del muscolo, sia per i solei che per gli EDL. Abbiamo inoltre misurato la forza muscolare specifica (forza tetanica massima normalizzata per la sezione trasversale della fibra) di muscoli Solei ed EDL di topi DKO e WT. I dati statistici dell'analisi di oltre 1000 fibre per tipo di muscolo e per pool di topi non mettono in evidenza nessun aspetto importante nei muscoli lenti Solei. Per quanto riguarda i muscoli EDL è emerso che la forza massima normalizzata per la sezione trasversale del muscolo (CSA) è simile tra DKO e WT (in mN: DKO 364,64 ± 76,22; WT 327,86 ± 117,53 n=9, media ± sd, Mann Whitney test a due code P<0,05*), tuttavia gli EDL dei topi DKO nella prima stimolazione tetanica hanno evidenziato un calo del 20% della tensione isometrica che aumenta del 300% rispetto agli EDL WT in seguito a treni di tetani successivi. Differenze che sono state abolite esponendo i muscoli ad una soluzione contenete il bloccante Lantanio. VEDI ARTICOLO 1 a pp. 85.

4.2. ESPERIMENTI SULLA PROTEINA JP45 IN COLLABORAZIONE CON ALTRI COLLEGHI.

Da anni JP45 è oggetto dei nostri studi. Si tratta di una proteina molto importante identificata proprio nel nostro laboratorio, coivolta nello sviluppo e nel mantenimento della forza muscolare. E' stato dimostrato precedentemente che JP45 fa parte delle proteine che si trovano nella triade muscolare e forma una interazione con la subunità cav 1.1 del recettore delle Diidropiridine (DHPR) e con calsequestrina. In lavori precedenti è emerso che il complesso che JP45 forma con cav 1.1 viene sottoregolato durante l'invecchiamento, contribuendo al decadimento della forza muscolare e

favorendo la disabilità fisica tipica dell'anzianità. In passato è stato dimostrato che inattivando il gene (JSPR1) per abolire l'espressione della proteina JP45 (JP45 KO) si ha un decremento della forza muscolare dovuto alla diminuzione dell'espressione del canale calcio voltaggio dipendente Ca_v 1.1, come se venisse alterato il segnale che mette in collegamento queste due molecole. Si è quindi deciso di condurre esperimenti su modelli murini maschi JP45 Knock Out di 3-4 mesi di età hanno confermato un'alterazione del meccanismo di eccitazione-contrazione muscolare determinando debolezza muscolare rispetto ai topi controllo WT. Questo risultato ci ha fatto ipotizzare che tale fenomeno potesse esser più pronunciato in topi JP45 KO di 12-18 mesi di età. Dagli ultimi esperimenti testando la performance muscolare di topi JP45 KO in vitro ed in vivo è emerso che la forza specifica e assoluta tetanica, che era significativamente diversa in topi di 3-4 mesi, non differiva più significativamente nei muscoli Solei ed EDL di topi di 12-18 mesi di età rispetto ai WT. Altri esperimenti hanno rivelato che il ridotto rilascio di calcio dal reticolo sarcoplasmatico e che la diminuzione della densità della subunità cav 1.1 osservata non solo nei muscoli di 3-4 ma anche di 12 mesi, non si presenta a 18 mesi di età. E' stato infatti dimostrato che il livello di mRNA per Ca_v 1.1 non decresce significativamente con l'invecchiamento. Sono stati condotti esperimenti per valutare il livello di espressione di altre proteine che partecipano al meccanismo eccitazione–contrazione, ma non sono state trovate differenze significative tra muscoli JP45 e WT. Abbiamo escluso anche l'intervento di altri meccanismi compensatori che partecipano all'omeostasi del calcio, quali store-operated Ca^{2+} entry (SOCE) ed Excitation Coupled Ca^{2+} Entry (ECCE). Da lavori precedenti è noto che con l'invecchiamento si ha una conversione delle fibre muscolari veloci di tipo II in fibre di tipo lento I come sorta di adattamento e tramite i nostri studi di immunoistochimica abbiamo trovato un aumento delle fibre di tipo lento nei solei di topi JP45 KO di 18 mesi, che unito al meccanismo di eccitazione-contrazione inalterato a questa età, ha permesso agli animali di sostenere l'esercizio fisico e di incrementare il tempo di corsa rispetto ai fratelli controlli. Analizzando sezioni di muscoli di 18 mesi è stata inoltre trovata atrofia delle fibre di soleo a 18 mesi di età ad indicare che la sezione trasversale della fibra non partecipa al mantenimento e al miglioramento della prestazione fisica nell'invecchiamento. Nel nostro studio inoltre abbiamo cercato di trovare una correlazione tra dieta e forza muscolare mettendo a disposizione degli animali una dieta ricca di grassi. Ciò che è emerso è che i topi JP45 KO in generale presentano un diminuito apporto di cibo pari al 20-25% rispetto ai WT ed una minore tendenza a

sviluppare obesità. Sorprendentemente si è visto che in seguito alla dieta, i livelli di espressione di cav 1.1 in topi anziani (18 mesi) erano maggiori rispetto ai controlli, portando alla conclusione che la riduzione delle calorie non solo evita il decremento dell'espressione della subunità cav1.1, ma previene anche il declino della forza muscolare che avvengono con l'età. VEDI ARTICOLO 2 a pp. 94.

4.3. ESPERIMENTI SUL COATTIVATORE PGC-1• IN COLLABORAZIONE CON ALTRI COLLEGHI.

Una caratteristica del tessuto muscolare scheletrico è la plasticità, inoltre per le sue caratteristiche fisiologiche viene classificato dal punto di vista del colore (bianco/rosso), dell'attività metabolica (ossidativa/gli colitica) e per le proprietà contrattili (fibre veloci di tipo II/ fibre lente di tipo I). Il muscolo scheletrico viene inoltre classificato in base ai parametri cinetici del calcio, quali clearance, velocità di rilascio e ampiezza del picco di calcio che determina la forma del Twitch. La plasticità muscolare si presenta anche negli adulti in seguito a fattori ambientali o come adattamento all'esercizio fisico cronico convertendo le fibre veloci di tipo II in fibre lente di tipo I ossidative e perciò capaci di sostenere una attività fisica intensa e prolungata nel tempo. L'intreccio molecolare che determina questa conversione è complicato e deve ancora esser chiarito completamente. Abbiamo collaborato anche con un gruppo di colleghi che studiano PGC-1• (peroxisome proliferator-activated receptor •-coactivator 1•), un coattivatore trascrizionale ed abbiamo osservato che PGC-1• partecipa attivamente alla plasticità muscolare anche in assenza di attività fisica. Come modello dei nostri studi abbiamo analizzato il muscolo scheletrico di topi in cui il coattivatore è stato sovraespresso ed è emerso che PGC-1• conferisce al muscolo un colore rosso dovuto all'incremento della miosina a catena pesante ed aumenta il metabolismo di tipo ossidativo. Nei topi iperesprimenti tale coattivatore si è inoltre notato un livello ridotto di proteine che fanno parte del reticolo sarcoplasmatico quali Ryanodina-1, Triadina e Giuntina, causando di conseguenza una riduzione dei rilasci di calcio dal reticolo, fattori che insieme comportano debolezza muscolare. E' noto che PGC-1• regola l'espressione di geni post sinaptici nel muscolo, mentre nella cellula modula quasi autonomamente i transienti calcio. Dai nostri esperimenti è emerso che in seguito a stimolazione elettrica ex vivo in assenza del motoneurone si osservano transienti calcio alterati, mentre

l'espressione del recettore DHPR, che connette l'attività motoneurale ai flussi di calcio provenienti dal reticolo, rimane invariata nei topi transgenici. Ne deriva che PGC-1• è capace di modulare autonomamente il rilascio di calcio dalle cisterne di stoccaggio del muscolo scheletrico. Tramite esperimenti di microscopia elettronica abbiamo dimostrato che PGC-1• aumenta la biogenesi dei mitocondri nel muscolo ed in altri tessuti. Abbiamo dimostrato anche una distribuzione elevata dei mitocondri a livello subsarcolemmale e interfibrillare. Spesso i mitocondri sono distribuiti nelle vicinanze o adesi alla unità rilascianti calcio CRUs. Tale distribuzione oltre a mettere in comunicazione i mitocondri con il reticolo, permette ai mitocondri di esercitare un'azione inibitoria sui transienti calcio provenienti dal reticolo. Studi su fibre di tipo lento ricche di mitocondri hanno rivelato una diminuzione di calcio rispetto a fibre veloci povere di tali organelli, suggerendo che i mitocondri esercitano un effetto inibitorio sul calcio rilasciato probabilmente controllando l'ambiente redox delle CRUs. Inoltre oltre a incrementare indirettamente la capacità ossidativa promuovendo la biogenesi mitocondriale, PGC-1• favorisce la richiesta di ossigeno nel muscolo promuovendo l'angiogenesi ed incrementa il consumo di ossigeno, l'ossidazione dei lipidi ed il rifornimento energetico. Abbiamo visto che PGC-1• prolunga il tempo di permanenza del calcio nel citosol agendo sull'espressione e sull'attivita della pompa Ca^{2+}-ATPasi SERCA, deputata alla rimozione del calcio dal mioplasma al reticolo sarcoplasmatico. PGC-1• esercita una inibizione doppia sulla pompa poiché diminuisce i livelli dell'ormone tiroideo che regolano la trascrizione di SERCA ed aumenta la trascrizione della proteina Sarcolipina che inibisce la attività di SERCA. Il risultato è un ritardo della rimozione del calcio dal mioplasma nei topi transgenici che determina maggior resistenza alla fatica ma debolezza muscolare. Abbiamo inoltre trovato un aumento del livelli di Phospholamban, una proteina maggiormente espressa nei muscoli lenti (slow twitch) che esercita un ulteriore effetto inibitorio sulla pompa in quanto interagendo con SERCA-2 ritarda il recupero del calcio nelle cisterne di stoccaggio. Tutti questi effetti portano alla conclusione che PGC-1• esercita un effetto modulatorio sui flussi del calcio. VEDI ARTICOLO 3 a pp. 107.

4.4. ESPERIMENTI SULLA PROTEINA SRP-35

Nel tentativo di studiare a fondo le proteine che fanno parte della struttura specializzata da cui ha origine la contrazione muscolare, nel nostro laboratorio è stata identificata una nuova proteina denominata SRP-35 (Sarcoplasmic Reticulum Protein di 35 KDa). Tramite esperimenti di proteomica si è scoperto che appartiene alla famiglia delle proteine DHRS7C, deidrogenasi/reduttasi a catena corta, sottofamiglia 7C, che prendono parte alla via glicolitica. Queste proteine sono enzimi capaci di ridurre molti substrati quali steroli, alcoli, zuccheri, composti aromatici, xenobiotici ed anche il retinolo (vitamina A) precursore dell'acido retinoico, tramite una reazione reversibile che prevede come intermedio la formazione di retinaldeide e la contemporanea riduzione di NAD^+ a NADH. Gli effettori dell'acido retinoico si trovano a livello nucleare e si dividono in due famiglie di recettori: RARs (retinoic acid receptor) RAR •/•/• e RXRs (retinoic x receptor) RXR •/•/• e nel momento in cui l'acido retinoico si attacca a RAR, il recettore dimerizza con RXRs e trasloca nel nucleo dove si attacca a sequenze specifiche di DNA note come elementi risposta dell'acido retinoico, promuovendo così la trascrizione di diversi geni coinvolti nella crescita, sviluppo, differenziamento, produzione di citochine e metabolismo. Analizzando la struttura della proteina si è visto che è composta da una corta sequenza idrofobica all'N-terminale che si trova legata alla membrana del reticolo sarcoplasmatico, ed una sequenza C-terminale contenente il sito attivo che si affaccia sul mioplasma. SRP-35 contiene nel sito attivo residui di tirosina adiacenti a lisine e serine, inoltre contiene come tutte le altre famiglie di SDRs un ripiegamento Rossmann e siti di legame per NAD(P), ma si differenzia dalle altre proteine della stessa famiglia in quanto è lunga 311 residui, invece di 250, tanto da definirla un membro esteso della superfamiglia SDRs. Tramite esperimenti per identificare la localizzazione, abbiamo visto che è presente sul reticolo sarcoplasmatico (SR) e colocalizza con Ca^{2+}- ATPasi SERCA, anche se non interagiscono, ed è quindi posizionata sulle cisterne terminali e sul reticolo longitudinale (LSR). Tramite esperimenti di Western Blot si è visto che è una proteina presente in diversi tessuti quali fegato, reni e nel muscolo scheletrico, in particolare è molto abbondante nei muscoli EDL (Extensor Digitorum Longus) in quanto contengono un volume maggiore di SR. Si tratta di una proteina ubiquitaria, infatti esperimenti su frazioni microsomali hanno rivelato la sua presenza nel citoplasma, nei mitocondri e nel reticolo endoplasmatico (ER) e nei perossisomi. Per scoprire se la sovraespressione di SRP-35 ha effetti sul meccanismo eccitazione-contrazione, sono stati misurati i transienti calcio su miotubi

trasfettati con SRP-35-EYFP e con pEYFP vuoto, utilizzando come impulso depolarizzante quantità crescenti di KCl (mima la depolarizzazione) e 4-chloro-m-cresolo (attiva direttamente RyR-1). I risultati hanno messo in luce in generale un decremento del calcio rilasciato dal canale della Ryanodina-1 ed una riduzione dell' attivazione di quest'ultimo pari al 40%, anche se attivato direttamente da KCl e da 4-chloro-m-cresolo. Stesso risultato è stato ottenuto aggiungendo acido retinoico alle colture cellulari di miotubi C2C12. Risultati simili si sono osservati in colture cellulari ottenute da pazienti affetti da Central Core Disease (CCD) e Multiminicore Disease (MMD) malattie che presentano difetti nel recettore della Ryanodina-1 con conseguente decremento del rilascio di calcio indotto farmacologicamente, un aumento o normali livelli di calcio basale dipendente dal grado di mutazione del canale e ridotta espressione del recettore RyR-1. Esperimenti in cui SRP-35 viene sovraespressa hanno rivelato una diminuzione del rilascio di calcio, ma livelli di calcio basale e di calcio stoccato nelle cisterne inalterati. L'analisi tramite RT-PCR ed Immunoblotting hanno rivelato però una riduzione del 50% del recettore RyR-1 e di Inositolo 1-4,5-trifosfato. Dal passato sappiamo che il trasportatore NADH regola l'attività del recettore della Ryanodina-1 nel cuore ed il fatto che SRP-35 sia localizzata sul SR, organello deputato alla omeostasi del calcio, fa pensare che la proteina sia importante per la mobilizzazione del calcio nel muscolo scheletrico. Inoltre essendo SRP-35 un enzima deidrogenasi può ridurre il NAD^+ generato dall'enzima lattato deidrogenasi in seguito ad attività fisica sostenuta. Tale attività è anche resa possibile dalla localizzazione di SRP-35 nel reticolo sarcoplasmatico, al quale aderiscono altri enzimi che prendono parte alla via glicolitica. La riduzione di NAD+ è accoppiata dalla conversione di all-trans-retinaldeide ad acido retinoico, il quale oltre ad essere un importante attivatore di GLUT4 (glucose transporter 4) è un regolatore dell'espressione di RyR1. VEDI ARTICOLO 4 a pp. 119

5. CONCLUSIONI

Da anni il nostro gruppo studia il muscolo scheletrico, tessuto molto importante che costituisce il 40% circa del nostro corpo. La contrazione muscolare, prevede la trasformazione di un segnale elettrico (potenziale d'azione), in segnale chimico rappresentato da un aumento transiente della [Ca^{2+}] che attiva le proteine contrattili, tramite un meccanismo definito accoppiamento Eccitazione-Contrazione (EC-coupling).

I principali componenti del meccanismo EC-coupling sono il recettore delle diidropiridine subunità Cav 1.1 (DHPR) sui tubuli T, il recettore della Ryanodina-1 sul reticolo sarcoplasmatico e Calsequestrina-1, i quali funzionano come canale e sensore del voltaggio, canale di rilascio del calcio e principale proteina tampone del calcio rispettivamente. L'EC-coupling è attivato da una interazione bidirezionale che prevede: un segnale ortogrado rappresentato da un cambio conformazionale del recettore sensibile al voltaggio DHPR Ca_v 1.1 che stimola l'apertura del canale RyR-1 ed il rilascio del calcio dal reticolo; potenziamento dell'attività di Ca_v 1.1 tramite un segnale retrogrado inviato dal recettore RyR-1.

A questo sofisticato meccanismo partecipano altri componenti minoritari, ma non trascurabili, infatti dai dati in letteratura sappiamo che difetti nelle proteine coinvolte nel meccanismo EC-coupling, comportano malattie degenerative neuromuscolari, debolezza muscolare nell'anzianità e cachessia nel cancro. Il comune denominatore è un'alterazione dell'omeostasi del calcio ed il fatto che le vie di trasduzione dei segnali calcio in alcune miopatie non siano ancora stati chiariti completamente, ha spinto il nostro gruppo a studiare il ruolo delle proteine minoritarie nel meccanismo EC-coupling.

5.1.EFFETTO DEL COMPLESSO JP45/CSQ-1 SULLE CORRENTI CALCIO:

Nei dati ottenuti dagli esperimenti svolti in fibre di muscolo FDB JP45/CSQ-1 Double Knock-out (DKO) *in vitro* è emerso sostanzialmente che, durante potenziali ripetitivi e sostenuti viene innescata una corrente calcio dall'esterno che si unisce alle correnti calcio provenienti dal reticolo sarcoplasmatico. Escludendo l'intervento di meccanismi compensatori ad opera di altre proteine canale quali Orai1, TRPC3 e la isoforma

neonatale di Ca_v 1.1, l'influsso massivo di calcio, coincide con l'attività di canale della subunità Ca_v 1.1 del recettore delle Diidropiridine, in quanto oltre ad essere bloccata tramite l'aggiunta di nifedipina, bloccante di Ca_v 1.1, vi è un aumento pari al 45% della densità di corrente calcio attraverso Ca_v 1.1. Abbiamo mostrato che l'influsso massivo di calcio attraverso Ca_v 1.1 ripristina la forza muscolare in seguito a stimolazioni tetaniche ripetitive di muscoli EDL DKO *in vitro* e sostiene la forza muscolare durante l'esercizio fisico sostenuto e prolungato *in vivo*.

Sulla base di questi dati siamo giunti a conclusione che il complesso JP45/CSQ-1 modula direttamente l'attività del canale sensibile al voltaggio DHPR Ca_v 1.1, in quanto inattivando il complesso, l'influsso di calcio via Ca_v 1.1 (Excitation-Coupled Ca^{2+} Entry, ECCE) considerato fino ad ora irrilevante al fine del meccanismo dell'EC coupling, è importante a migliorare e sostenere la forza muscolare *in vivo* ed è utile a contrastare gli effetti invalidanti della debolezza muscolare tipici dell'anzianità e dei disordini muscolari.

5.2.EFFETTO DI JP45 NEL MANTENIMENTO DELLA FORZA MUSCOLARE:

Dagli esperimenti condotti su muscoli JP45KO in collaborazione con altri gruppi di ricerca è emerso sostanzialmente che il decremento dell'espressione del sensore voltaggio Ca_v 1.1, il disaccoppiamento eccitazione-contrazione (ECU) e la perdita della forza muscolare osservata in topi di 3-4 mesi, non si aggravano nei topi JP45KO di 12 e 18 mesi. Inoltre è emerso che i topi maschi JPKO presentano una riduzione dell'apporto di cibo ed un decremento del peso corporeo rispetto ai fratelli controllo associato ad una stabilizzazione dell'espressione di Ca_v 1.1, anche se il meccanismo di regolazione non è noto. Per tutti questi risultati possiamo sostenere che JP45 è coinvolta nello sviluppo e nel mantenimento della forza muscolare scheletrica nella vita.

5.3.EFFETTO DI PGC-1• (Peroxisome proliferator-activated receptor-• coactivator-1•) NEI SEGNALI CALCIO:

I dati che abbiamo ottenuto sugli studi effettuati sulcoattivatore trascrizionale PGC-1• sovraespresso hanno rivelato una riduzione dei rilasci di calcio accompagnata da un decremento delle proteine che formano il complesso Ryanodina, Triadina, Giuntina che

partecipa al meccanismo dell'EC coupling ed un decremento di alcune proteine contrattili. PGC-1• prolunga i tempi di rimozione del calcio dal mioplasma regolando indirettamente l'attività della pompa SERCA, in quanto abbassa il livello degli ormoni tiroidei che modulano l'attività di SERCA. Inoltre PGC-1• diminuisce i livelli di Parvalbumina, proteina tampone del calcio. Inoltre è emerso che PGC-1• aumenta i livelli di espressione della miosina a catena pesante e promuove un fenotipo ossidativo, favorendo la conversione delle fibre di tipo veloce in tipo lento, anche in assenza di esercizio fisico. Abbiamo inoltre dimostrato che PGC1• favorisce la biogenesi dei mitocondri, organelli che esercitano a loro volta un'azione inibitrice sui rilasci di calcio dal reticolo. Per tutti questi dati possiamo sostenere che PGC-1• influenza l'affaticabilità e la forza muscolare ed è anch'esso un modulatore dei segnali calcio, infatti rimodella i transienti calcio stimolando la conversione del metabolismo glicolitico verso quello ossidativo.

5.4.RUOLO DI SRP-35 NEL METABOLISMO DEL MUSCOLO SCHELETRICO:

I dati ottenuti dagli esperimenti sulla proteina SRP-35 hanno messo in luce in sintesi che per la struttura e sequenza aminoacidica, SRP-35 è un enzima deidrogenasi/reduttasi a catena corta (SDR) coinvolto nella trasduzione dei segnali dell'acido retinoico (Vitamina A) nel muscolo scheletrico. Per la sua localizzazione sul reticolo sarcoplasmatico e per il suo sito attivo che si affaccia sul mioplasma in vicinanza di altri enzimi glicolitici, si è visto che la riduzione di molti substrati è accompagnata dalla formazione di NAD+. I nostri esperimenti di sovraespressione di SRP-35 hanno mostrato una riduzione dei rilasci di calcio causato da un decremento pari al 50% dell'espressione di RyR-1, stessi effetti ottenuti aggiungendo acido retinoico in colture cellulari ed una riduzione dell' inositolo 1,4,5-trifosfato. Per tutti questi dati, anche se non è ancora chiaro il ruolo di SRP-35 *in vivo*, possiamo sostenere che questa nuova proteina ha un ruolo nelle funzioni metaboliche del muscolo scheletrico, poiché producendo acido retinoico è coinvolta nella trascrizione di diversi geni, inclusi alcuni coinvolti nella crescita, sviluppo, differenziamento, produzione di citochine e metabolismo. Inoltre, regolando indirettamente il recettore RyR-1 attraverso i prodotti NAD+, che agisce direttamente sul recettore, ed acido retinoico che oltre ad attivare

GLUT4, regola l'espressione di RyR-1, SRP-35 può essere coinvolta nella mobilitazione del calcio dal reticolo. Per quest'ultima attività SRP-35 potrebbe avere un ruolo nell'ipertermia maligna.

Capire i meccanismi che sono alla base delle alterazioni dell'omeostasi del calcio, è utile non solo per progredire le nostre conoscenze in campo medico scientifico, ma anche per cercare strategie terapeutiche per contrastare la perdita della forza muscolare nell'anzianità e nelle malattie muscolari degenerative.

RINGRAZIAMENTI

Desidero ringraziare il Professor Francesco Zorzato e Susan Treves per avermi dato la possibilità di svolgere questa tesi di dottorato e per tutti i preziosi insegnamenti come pure tutti i consigli e suggerimenti lungo tutto il mio percorso di ricerca. Ci tengo a ringraziare Mirko Vukcevic e Anne-Sylvie Monnet dell'università di Basilea per i loro insegnamenti e la loro disponibilità. Ringrazio inoltre il gruppo di Giorgio Rispoli di Ferrara per il loro importante contributo agli esperimenti. Voglio inoltre ringraziare il gruppo del professor Osvaldo Delbono di Wake Forest a Winston-Salem per la loro solerte supervisione del lavoro, e tutti gli altri componenti che hanno partecipato alla realizzazione della mia tesi. Voglio anche ringraziare la mia collega Leda Bergamelli per tutti i consigli e per il supporto psicologico. Ringrazio i miei genitori per avermi sostenuto ed incoraggiato in questo percorso di vita, il mio compagno Roberto per la disponibilità, la pazienza ed il supporto psicologico ed infine la mia bimba Sara che ho lasciato piangere più volte per definire gli ultimi dettagli nella stesura della tesi.

6.BIBLIOGRAFIA

- Anderson A.A., Treves S, Biral D, Betto R, Sandonà D, Ronjat M & Zorzato F. The novel skeletal muscle sarcoplasmic reticulum JP-45 protein. Molecular cloning tissue distribution, developmental expression, and interaction with alpha 1.1 subunit of the voltage-gated calcium channel. *J Biol Chem* 278: 39987-39992, 2003.

- Ambudkar I.S, Bandyopadhyay B.C, Liu X, Lockwich T.P, Paria B & Ong H.L. Functional organization of TRPC-Ca2+ channels and regulation of calcium microdomains. *Cell Calcium* 40, 495-504, 2006.

- Ambudkar IS. TRPC: a core component of Store-operated calcium channel. *Biochem Soc Trans* 35: 96-100,2007.

- Arai M, Otsu K, MacLennan D.H & Periasamy M. Regulation of Sarcoplasmic reticulum gene expression during cardiac and skeletal muscle development. *Am J Physiol* 262, C614-20, 1992.

- Armstrong CM, Bezanilla FM & Horowicz P. Twitches in the presence of Ethylene glycol bis(-aminoethylether)-N,N-tetracetic acid. *Biochim Biophys Acta* 267, 605-608, 1972.

- Avila G, Dirksen RT. Functional impact of the ryanodine receptor on the skeletal muscle L-type ca2+ channel. *J Gen Physiol* 115, 467-480.

- Bannister RA. Bridging the myoplasmic gap: recent developments in skeletal muscle excitation-contraction coupling. *Journal of Muscle research and Cell Motility* 28, 275-283, 2007.

- Bannister RA, Pessah IN & beam KG. The skeletal L type Ca2+ current is a major contributor to excitation-coupled Ca2+ entry. *J gen Physiol* 50, 2177-2195, 2009.

- Bastianutto C, Clementi E, Codazzi F, Podini P, De Giorgi F, Rizzuto R, Meldolesi J & Pozzan T. Overexpression of calreticulin increases the Ca2+

capacity of rapidly exchanging Ca2+ stores and reveals aspects of their lumenal microenvironment and funcion. *J Cell Biol* 130, 847-855, 1995.

- Beard N.A, Laver D.R & Dulhunty A.F. Regulation of skeletal muscle ryanodine receptors by calsequestrin. *Proc Aust Physiol Pharmacol Soc* 201, 30-43, 1999.

- Beard N.A, Magdalena M, Sakowska, A.F Dulhunty & Derek R.L. calsequestrin is an inhibitor of skeletal muscle Ryanodine Receptor calcium release Channel. *Biophys J* 82, 310-320, 2002.

- Beech DJ, Xu SZ, McHugh D, Flemming R., TRPC store-operated cationic channel subunit. *Cell Calcium* 33: 433-440, 2003.

- Bers DM. Excitation-Contraction Coupling and Cardiac Contractile Force. *Kluwer Academic Publishers, The* Netherlands (2001).

- Bers D.M. Macromolecular complexes regulating cardiac ryanodine receptor function. *J Mol Cell Cardiol* 37, 417-429, 2004.

- Biral D, Volpe P, Damiani E & Margreth A. Coexistence of two calsequestrin isoforms in rabbit slow-twitch skeletal muscle fibers. *FEBS Lett* 299, 175-178, 1992.

- Bleunven C, Treves S, Jinyu X, Leo E, Ronjat M, De Waard M, Kern G, Flucher BE & Zorzato F. SRP-27 is a novel component of the supramolecular signaling complex involved in skeletal muscle excitation- contraction coupling. *Biochem J* 411, 343-349, 2008.

- Block BA, Imagawa T, Campbell KP, Franzini-Armstrong C. Structural evidence for direct interaction between the molecular components of the transverse tubule/sarcoplasmic reticulum junction in skeletal muscle. *J Cell Biol* 107, 2587-2600, 1988.

- Calderon J.C., Pura Bolanos, Torres S.H. Rodriguez-Arroyo G., Caputo C. Different fibre population distinguished by thei calcium transient characteristics in enzimatically dissociated murine flexor digitorum brevis and soleus muscles. *J Muscle res Cell Motil* 30, 125-137, 2009.

- Calderon J.C., Bolanos O., Caputo C. Myosin heavy chainisoform composition and Ca2+ transients in fibres from enzymatically dissociated murine soleus and extensor digitorum longus muscles. *J Physiol* 588: 267-279, 2010.

- Callen D.F, Lane S.A, Kozman H, Kremmidiotis G, Whitmore S.A, Lowenstein M, Dogget N.A, Kenmochi N, Page D.C, & Maglott D.R. Integration of transcript and genetic maps of chromosome 16 at near-1-mb resolution: demonstration of a “hot Spot” for recombination at 16p12. *Genomics* 29, 503-511, 1995.

- Campbell KP, Franzini-Armstrong C & Shamoo AE. Further characterization of light and heavy Sarcoplasmic Reticulum vescicles. Identification of the Sarcoplasmic Reticulum feet associated with heavy sarcoplasmic reticulum vescicles. *Biochim Biophys Acta* 602, 97-116, 1980.

- Campbell KP, MacLennan DH & Jorgensen AO. Sraining of the Ca^{2+}- binding proteins, calsequestrin, calmodulin, troponin C, and S-100, with the cationic carbocyanine dye “stains-all”. *J Biol Chem* 258, 11267-11273, 1983a.

- Caswell A.H, Brandt N.R, Brunschwig J.P & Purkerson S. Localization and partial characterization of the oligomeric disulfide-linked molecular weight 95,000 protein (triadin) which binds the ryanodine and dihydropyridine receptors in skeletal muscle triadic vescicles. *Biochemistry* 30, 7507-7513, 1991.

- Catterall W.A. Structure and regulation of voltage-gated Ca2+ channels. *Annu Rev Cell Dev Biol* 16, 521-555, 2000a.

- Cheng W, Altafaj X, ronjat M, Coronado R. Interaction between the dihydropyridine receptor Ca2+ channel • -subunit and ryanodine receptor type 1 strengthens excitation-contraction coupling. *Proc Natl Acad Sci* USA 102, 19225-19230, 2005.

- Cherednichenko G, Hurne AM, Fessenden JD, Lee EH, Allen PD, Beam KG & Pessah IN. Conformational activation of Ca2+ entry by depolarization of skeletal myotubes. *Proc Natl Acad Sci* USA 101, 15793-15798, 2004.

- Cherednichenko G, Ward CW, Feng W, Cabrales E, Michaelson L, Samso M, López JR, AllenPD, Pessah IN. Enhanced excitation-coupled calcium entry in

myotubes expressing malignant hyperthermia mutation R163C is attenuated by dantrolene. *Mol Pharmacol.* 73:1203-1212 (2008).

- Clapham D.E. TRP channels as cellular sensors. *Nature* 426, 517-524, 2003.

- Clementi E, scheer H, Zacchetti D, Fasolato C, Pozzan T, Meldolesi J. Receptor-activated Ca2+ influx. Two indipendently mechanisms of influx stimulation coexist in neurosecretory PC12 cells. *J Biol Chem* 267: 2164-2172, 1992.

- Copello J.A, Barg S, Onoue H & Fleischer S. Heterogeneity of Ca2+ gating of skeletal muscle and cardiac ryanodine receptors. *Biophys J* 73, 141-156, 1997.

- Damiani E & Margreth A. Characterization study of the ryanodine receptor and of calsequestrin isoforms of mammalian skeletal muscle in relation to fibre types. *J Muscle Res Cell Motil* 15, 86-101, 1994.

- DeHaven WI, Jones BF, Petranka JG, Smyth JT, Tomita T, Bird GS, Putney JW. TRPC channels function independently of STIM1 and Orai1. *J Physiol* 587: 2275-2298, 2009.

- Delbono O, Xia J, Treves S, wang Z. M., Jimenez-Moreno R, Payne A.M., Messi M.L., Briguet A, Schaerer F, Nishi M, Takeshima H, Zorzato F. Loss of skeletal muscle strength by ablation of the sarcoplasmic reticulum protein JP45. *Proc. Natl. Acad. Sci*., 104, 20108-20113, 2007.

- Delbono O, Messi ML, Wang ZM, Treves S, Mosca B, Bergamelli L, Nishi M, Takeshima H, Shi H, Xue B, Zorzato F. Endogenously determined restriction of food intake overcomes excitationcontraction uncoupling in JP45KO mice with aging. *Exp. Gerontol.* 47:304-316. (2012).
- Dode L, Wuytack F, Kools P.F, Baba-Aissa F, Raeymaekers L, Brike F, Van der Ven W.J & Casteels R. cDNA cloning, expression and chromosomal localization of the human sarco/endoplasmic reticulum Ca2+-ATPase 3 gene. *Biochem J* 318 (Pt2), 689-699, 1996.
- Eldar M, Pras E & Lahat H. A missense mutation in the CSQ2 gene is associated with autosomal-recessive catecholamine-induced polymorphic ventricular tachicardia. *Trends Cardiovasc Med* 13, 148-151, 2003.

- Ertel E.A. Campbell K.P. Harpold M.M. Hofmann F, Mori Y, Perez-Reyes E, Schwartz A, Snutch T.P, Tanabe T, Birnbaumer L. Nomenclature of voltage-gated calcium channels. *Neurons* 25, 533-535, 2000.
- Fabiato A. Appraisal of the physiological relevance of two hypothesis for the mechanism of calcium release from the mammalian cardiac sarcoplasmic reticulum: calcium-induced release versus charge-coupled release. *Mol Cell Biochem* 89, 135-140, 1989.
- Fessenden J.D, Perez C.F, Goth S, Pessah IN & Allen P,D. Identification of a key determinant of ryanodine receptor type I required for activation by 4-chloro-m-cresol. *J Biol Chem* 278, 28727-28735, 2003.
- Franzini-Armstrong C & Jorgensen A.O. Structure and development of e-c coupling units in skeletal muscle. *Annu Rev Physiol* 56, 509-534, 1994.
- Fresu L, Dehpuor A, Genazzani A.A, Carafoli E & Guerini D. Plasma membrane calcium ATPase isoforms in astrocytes Glia 28, 150-155, 1999.

- Gauthier G.F. On the relationship of ultrastructural and cytochemical features of color in mammalian skeletal muscle. *Z Zellforsch Mikrosk Anat* 95, 462-482, 1969.

- Gonzales-Serratos H, Valle-Aguilera R, Lathrop DA & Garcia MC. Slow inward calcium currents have no obvious role in muscle excitation-contraction coupling. *Nature* 298, 292-294, 1982.

- Guo W, Jorgensen AO & Kampbell KP. Characterization and ultrastructural localization of a novel 90 KDa protein unique to skeletal muscle junctional sarcoplasmic reticulum. *J Biol Chem* 269, 28359-28365, 1994.

- Gyorke S & Terentyev D. Modulation of ryanodine receptor by luminal calcium and accessory proteins in health and cardiac disease. *Cardiovasc Res* 77, 245-255, 2008.

- Handschin C, Spiegelmann B.M. The role of exercise and PGC1• in inflammation and chronic disease. *Nature* 454, 463-469, 2008.

- Hardie R.C, Raghu P, Moore S, Juusola M, Baines R.A & Sweeney S.T. Calcium influx via TRP channels is required to maintain pip2 levels in drosophila photoreceptors. *Neurons* 30, 149-159, 2001.

- Hernández-Ochoa EO, Schneider MF Voltage clamp methods for the study of membrane currents and SR Ca(2+) release in adult skeletal muscle fibres. *Prog Biophys Mol Biol*. 108: 98-118.(2012)

- Hollingworth S, Gee KR, Baylor SM Low-affinity Ca2+ indicators compared in measurements of skeletal muscle Ca2+ transients. *Biophys J.* 97: 1864-1872. (2009).

- Hurne AM, O'Brien JJ, Wingrove D, Cherednichenko G, Allen PD, Beam KG & Pessah IN. Ryanodine recetor type 1 (RyR1) mutations C4958S and C4961S reveal excitation-coupled calcium entry (ECCE) is independent of Sarcoplasmic reticulum store depletion. *J Biol Chem 280*, 36994-37004, 2005.

- Inesi G, Chen L, Sumbilla C, Lewis D & Kirtley M.E. Ca2+ binding and translocation by the sarcoplasmic reticulum ATPase: functional and structural considerations. *Biosci Rep* 15, 327-339, 1995.

- Jiang Q, Thrower E.C, Chester D.W, Ehrlich B.E & Sigworth F.J. Three-dimensional structure of the type 1 inositol 1,4,5-triphosphate receptor at 24 a resolution. *EMBO J* 21, 3575-3581, 2002.

- Johnson M.A., Polgar J, Weightman D & Appleton D. Data on the distribution of fibre types in thirty-six human muscles. An autopsy study *J Neurol Sci* 18, 111-129, 1973.

- Jones L.R, Zhang L, Sanborn K, Jorgensen A.O & Kelley J. Purification, primary structure and immunological characterization of the 26-KDa calsequestrin binding protein (junction) from cardiac junctional sarcoplasmic reticulum. *J Biol Chem* 270, 30787-30796, 1995.

- Kawasaki T & Kasai M. regulation of calcium channel in sarcoplasmic reticulum by calsequestrin. Biochem Biophys Res Commun 199, 1120-1127, 1994.

- Kim MS, Zeng W, Yuan JP, Shin DM, Worley PF, Muallem S. Native store-operated Ca2+ influx requires the channel function of Orai1 and TRPC1. *J Biol Chem* 284: 9733-9741,2009.

- Knollmann BC, Chopra N, Hlaing T, Akin B, Yang T, Ettensohn K, Knollmann BE, Horton KD, Weissman NJ, Holinstadt I, Zhang W, Roden DM, Jones LR, Franzini-Armstrong C & Pfeifer K. Casq2 deletion causes sarsoplasmic reticulum volume increase, premature Ca2+ release and catecholaminergic polymorphic ventricular tachycardia. *J Clin Invest* 116, 2510-2520, 2006.

- Knollmann BC. New roles of calsequestrin and triadin in cardiac muscle. *J Physiol* 587, 3081-3087, 2009.

- Knudson C.M, Stang K.K, Moomaw C.R, Slaughter C.A & Campbell K.P. Primary structure and topological analysis of a skeletal muscle-specific junctional sarcoplasmic reticulum glycoprotein (triadin). *J Biol Chem* 268, 12646-12654, 1993a.

- Knudson C.M, Stang K.K, Jorgensen A.O. & Campbell K.P. Biochemical characterization of ultrastructural localization of a major junctional sarcoplasmic reticulum glycoprotein (triadin). *J Biol Chem* 268, 12637-12645, 1993b.

- Lamb G.D. Excitation-contraction coupling in skeletal muscle: comparisons with cardiac muscle. *Clin Exp Pharmacol Physiol* 27, 216-224, 2000.

- Leberer E, Timms BG, Campbell KP & McLennan DH. Purification, calcium binding properties and ultrastructural localization of the 53,000 and 160,000 (Sarcalumenin)- Dalton glycoproteins of the Sarcoplasmic Reticulum. *J Biol Chem* 265, 10118-10124, 1990.

- Lee A.G. Ca^{2+}-ATPase structure in the e1 and e2 conformations: mechanism, helix-helix and helix-lipid interactions. *Biochim Biophys Acta* 1565, 246-266, 2002.

- Liao Y, Erxleben C, Abramowitz J, Flockerzi V, Zhu MX, Armstrong DL, Birnbaumer L. Functional interaction among Orai1, TRPCs and STIM1 suggest a STIM-regulated heteromeric Orai/TRPC model of SOCE/Icrac channels. *Proc Natl Acad Sci* USA 105: 2895-2900, 2008.

- Liou J, Fivaz M, Inoue T & Meyer T. Live-cell imaging reveals sequential oligomerization and local plasma membrane targeting of stromal interaction molecule 1 after ca2+ store depletion. *Proc natl Acad Sci USA* 104, 9301-9306, 2007.

- Lyfenko AD, Dirksen RT. Differential dependence of store-operated and excitation-coupled Ca2+ entry in skeletal muscle on STIM1 and Orai1. *J Physiol* 586: 4815-4824, 2008.

- MacLennan D.H & Toyofoku T. Structure-function relationship in the Ca2+ pump of the sarcoplasmic reticulum. *Bioche Soc Trans* 20, 559-562, 1992.

- Marshall I.C & Taylor C.W. Two calcium-binding sites mediate the interconversion of liver inositol 1,4,5-triphosphate receptors between three conformational states. *Biochem J* 301 (Pt2), 591-598, 1994.

- Martonosi A.N & Pikula S. The structure of the Ca2+-ATPase of sarcoplasmic reticulum. *Acta Biochim Pol* 50, 337-365, 2003.

- Meissner G, Conner GE & Fliescher S. Isolation of sarcoplasmatic reticulum by zonal centrifugation and purification of Ca2+ pump and Ca2+ binding proteins. *Biochim Biophys Acta* 298, 246- 269, 1973.

- Meissner G. Ryanodine activation and inhibition of the Ca2+ release channel of sarcoplasmic reticulum. *J Biol Chem* 261, 6300-6306, 1986.

- Meissner G. Ryanodine receptor/Ca2+ release channel and their regulation by andogenous effectors. *Annu Rev Physiol* 56, 485-504, 1994.

- Meissner G. Molecular regulation of cardiac ryanodine receptor ion channel. *Cell Calcium* 35, 621-628, 2004.

- Meissner G, Wang Y, Xu L & Eu JP. Silencing genes of sarcoplasmic reticulum proteins clarifies their roles in excitation-contraction coupling. *J Physiol* 587, 3089-3090, 2009.

- Melzer W, Herrmann-Frank A & Luttgau HC. The role of Ca2+ ions in excitation-contraction coupling of skeletal muscle fibres. Biochimica et Biophysica Acta 1241,59,116, 1995.

- Mery L, Mesaeli N, Michalak M, Opas M, Lew D.P & Krause K.H. Overexpression of calreticulin increasea intracellular Ca2+ storage and decreases store-operated Ca2+ influx. *J Biol Chem* 271, 9332-9339, 1996.

- Minke B & Selinger Z. The inositol-lipid pathway is necessary for light excitation in fly photoreceprors. *Soc Gen Physiol Ser* 47, 201-217, 1992.

- Mitchell R.D, Volpe P, Palade P & Fleischer S. Biochemical characterization, integrity and sideness of purified skeletal muscle triads. *J Biol Chem* 258, 9867-9877, 1983.

- Moller J.V, Nissen O, Sorensen T.L & Le Maire M. Transport mechanism of the sarcoplasmic reticulum Ca^{2+}-ATPase pump. *Curr Opin Struct Biol* 15, 387-393, 2005.

- Muik M, Fahrner m, Derler I, Schindl R, Bergsmann J, Frischauf I, Groschner K & Romanin C. A cytosolic homomerization and a modulatory domain within STIM1 C-terminus determine coupling to Orai1 channels. *J Biol Chem* 284,8421-8426, 2009.

- Nakai J, Dirksen RT, Nguyen HT, Pessah IN, Beam KG & Allen PD. Enhanced dihydropiridine receptor channel activity in the presence of ryanodine receptor. *Nature* 380, 72-75, 1996.

- Nakai J, tanabe T, Konno T, Adams B, Beam KG. Localization in the II-III loop of the dihydropyridine receptor of a sequence critical for excitation-contraction coupling. *J Biol Chem* 273, 24983-24986, 1998b.

- Nakamura K, Zuppini A, Arnaudeau S, Lynch J, Ahsan I, Krause R, Papp S, De Smedt H, Parys J.B, Muller-Esterl W. Functional specialization of calreticulin domains. *J cell Biol* 154, 961-972, 2001.

- Neuhuber B, Gerster U, Doring F, Glossmann H, tanabe T, Flucher BE. Association of calcium channel • 1s and • 1a subunits is required for the targeting of • 1a but • 1s into skeletal muscle triads. *Proc Natl Acad Sci* USA 95, 5015-5020, 1998.

- Ohkura M.T, Ide k, Furukawa T, Kawasaki M, Kasai & Ohizumi Y. calsequestrin is essential for the ca2+ release induced by myotoxin alpha in skeletal muscle sarcoplasmic reticulum. *Can J Physiol Pharmacol* 73, 1181-1185, 1995.

- Otsu K, Fujii J, Periasamy M, Difilippantonio M, Uppender M, Ward D.C & MacLennan D.H. Chromosome mapping of five human cardiac and skeletal muscle sarcoplasmic reticulum protein genes. *Genomics* 17, 507-509, 1993.

- Pan Z, Hirata Y, Nagaraj RY, Zhao J, Nishi M, Hayek SM, Bhat MB, Takeshima H & Maj. Co-ezpression of MG29 and Ryanodine receptor leads to apoptotic cell death: effect mediated by intracellulare Ca2+ release. *J Biol Chem* 279: 19380-19390, 2004.

- Paolini C, Fessenden JD, Pessah IN, Franzini- Armstrong C. Evidence for conformational coupling between two calcium channels. *Proc Natl Acad Sci* USA 101, 12748-12752, 2004a.

- Paolini C, Protasi F, Franzini-Armstrong C. The relative position of RyR feet and DHPR tetrads in skeletal muscle. *J Mol Biol* 342, 145-153, 2004b.

- Paolini C, Quarta M, Nori A, Boncompagni S, canato M, Volpe P, Allen PD, Reggiani C & protasi F. Reorganized stores and impaired calcium handling in skeletal muscle of mice lacking calsequestrin-1. *J Physiol* 583, 767-784, 2007.

- Park K.W, Goo J.H, Chung H.S, Kim H, Kim D.H & Park W.J. Cloning of the genes encoding muose cardiac and skeletal calsequestrins: expression pattern during ombryogenesis. *Gene* 217, 25-30, 1998.

- Pette D & Spamer C. Metabolic properties of muscle fibers. *Fed Proc* 45, 2910-2914, 1986.

- Pette D & Staron R.S. Molecular basis of the Phenotypic characteristics of mammalian muscle fibres. *Ciba Found Synp* 138, 22-34, 1988.

- Postma AV, Denjoy I, Hoorntje TM, Lupoglazoff JM, Da Costa A, Sebillon P, Mannens MM, Wilde AA & Guicheney P. Absence of calsequestrin 2 causes severe forms of catecholaminergic polymorphic ventricular tachycardia. *Circ Res* 91, e21-e26, 2002.

- Protasi F, Paolini C, Nakai J, Beam KG, Franzini-Armstrong C, Allen PD. Multiple regions of RyR1 mediate functional and structural interactions with • 1s-dihydropyridine receptors in skeletal muscle. *Biophys J* 83, 3230-3244, 2002.

- Qin J, Valle G, Nani A, Nori A, Rizzi N, Priori SG, Volpe P & Fill M. Lumunal Ca2+ regulation of single cardiac ryanodine receptors: insights provided by calsequestrin and its mutants. *J Gen Physiol* 131, 325-334, 2008.

- Reeves J.P, Sutko J.L. “Sodium-calcium ion exchange in cardiac membrane vescicles”. *Proc Nat Acad Sci* USA 76, 590-594, 1979.

- Rios E, and Pizarro G. Voltage sensor of excitation-contraction coupling in skeletal muscle. *Physiol* rev 71, 849-908, 1991.

- Sacchetto R, Volpe P, Damiani E & Margreth A. Postnatal development of rabbit fast-twitch skeletal muscle: accumulation, isoform transitino and fibre distribution of calsequestri. *J Muscle res Cell Motil* 14, 646-653, 1993.

- Saito A, Seiler S, Chu A & Fleischer S. Preparation and morphology of Sarcoplasmic Reticulum terminal cisternae from rabbit skeletal muscle. *J Cell Biol* 99, 875-885, 1984.

- Saymi Y & Kung C. Calmodulin as an ion channel subunit. *Annu Rev Physiol* 64, 289-311, 2002.

- Schredelseker J, Di Biase V, Obermaier GJ, Felder ET, Flucher BE, Franzini-Armstrong C, Grabner M. The • 1a subunit is essential for the assembly of dihydropyridine-receptor arrays in skeletal muscle tetrad formation. *Proc Natl Acad Sci* USA 102, 17219-17224, 2005.

- Schumacher M.A, Rivard A.F, Bachinger H.P & Adelman J.P. Structure of the gating domain of a ca2+- activated K+ channel complexed with Ca2+/Calmoduline. *Nature* 410, 1120-1124, 2001.

- Serysheva I.I, Bare D.J, Ludtke S.J, Kettlun C.S, Chiu W & Mignery G.A. Structure of the type 1 inositol 1,4,5-triphosphate receptor revealed by electron cryomicroscopy. *J Biol Chem* 278, 21319-21322, 2003.

- Song L, Alcalai R, Arad M, Wolf CM, Toka O, Conner DA, Berul CI, Eldar M, Seidman CE & Seidman JG. Calsequestrin 2 (CSQ2) mutations increase expression of calreticulin and ryanodine receptor, causing catecholaminergic polymorphic ventricular tachicardia. J Clin Invest 117, 1814-1823, 2007.

- Stathopulos PB, Li GY, Plevin MJ, Ames JB & Ikura M. Stored Ca2+ depletion-induced oligomerization of stomal interaction molecule 1 (STIM1) via the EF-SAM region: An initiation mechanism for capacitative Ca2+ entry. *J Biol Chem* 281, 35855-35862, 2006.

- Strehler E.E & Zacharias D.A. Role of alternative splicing in generating isoform diversity among plasma membrane calcium pumps. *Physiol Rev* 81, 21-50, 2001.

- Strube C, Beurg M, Sukhareva C, Ahern CA, Powell JA, Gregg RG, Coronado R. Reduced ca2+ current, charge movements and absence of Ca2+ transients in skeletal muscle deficient in dihydropyridine receptor • 1 subunit. *Biophys J* 75, 2531-2543, 1996.

- Sun J, Xu L, Eu J.P, Stamler J.S & Meissnei G. Nitric oxide, noc-12 and s-nitrosoglutathione modulate the skeletal muscle calcium release channel/ryanodine receptor by different mechanisms. An allosteric function for O2 in s-nitrosylation of the channel. *J Biol Chem* 278, 8184-8189, 2003.

- Tanabe T, Takeshima H, Mikami A, Flockerzi V, Takahashi H, Kangawa K, Kojiima M, Matsuo H, Hirose T & Numa S. Primary structure of the receptor for calcium channel blockers from skeletal muscle. *Nature* 328, 313-318, 1987.

- Tanabe T, Beam KG, Adams BA, Niidome T, Numa S. regions of skeletal muscle dihydropyridine receptor critical for excitation-contraction coupling. *Nature* 346, 567-569, 1990a.

- Tanabe T, Adams B.A, Numa S & Beam K.G. Repeat I of the dihydropyridine receptor is critical in determining calcium channel activation kinetics. *Nature* 352, 800-803, 1991.

- Takeshima H, Komazaki S, Nish M, Ino M & Kangawa K. Junctophilins: a novel family of junctional membrane complex proteins. *Mol Cell 6*, 11-22, 2000.

- Taylor C.W & Laude A,J. IP3 receptors and their regulation by calmodulin and cytosolic Ca2+. *Cell Calcium* 32, 321-334, 2002.

- Toyoshima C, Nakasako M, Nomura H & Ogawa h. Crystal structure of the calcium pump of sarcoplasmic reticulum at 2,6 a resolution. *Nature* 405, 647-655, 2002.

- Toyoshima C & Nomura H. Structural changes in the calcium pump accompanying the dissociation of calcium. *Nature* 418, 605-611, 2002

- Treves S, Feriotto G, Moccagatta L, Gambari R & Zorzato F. Molecular cloning, expression, functional characterization, chromosomal localization and gene structure of Junctate, a novel integral calcium binding protein of sarco(endo)plasmic reticulum membrane. *J Biol Chem* 275, 39555-39568, 2000.

- Treves s, Vuckcevic M, Maj M Thurnheer R, Mosca B, Zorzato F. Minor sarcoplasmic Reticulum membrane components that modulate excitation-contraction coupling in striated muscle. *J Physiol* 587, 3071-3079, 2009.

- Venkatachalam K, Van Rossum D.B, Patterson R.L, Ma H & Gill D.L. The cellular and molecular basis of store-operated calcium entry. *Nat cell Biol* 4, E263-72, 2002.

- Vukcevic M, Spagnoli GC, Iezzi G, Zorzato F, Treves S. Ryanodine receptor activation by Ca v 1.2 is involved in dendritic cell major histocompatibility complex class II surface expression. *J Biol Chem.* 283: 34913-3422. (2008).

- Wang J.N, Maertz A, Lokua A.J, Kranias E.G & Valdivia H.H. regulation of cardiac ryanodine receptors activity by calsequestrin. *Biophys J* 80: 590, 2001.

- Wang Y, Xu L, Duan H, pasek DA, Eu JP & Meissner G. Knocking down type 2 but not type 1 calsequestrin reduces calcium sequestration and release in C2C12 skeletal muscle myotubes. *J Biol Chem* 281, 15572-15581, 2006.

- William RS & Rosenberg P. Calcium-dependent gene regulation in myocite hypertrophy and remodeling. *Cold Spring Harb Symp Quant Biol* 67, 339-344, 2002.

- Wu MM, Buchanan J, Luik RM % Lewis RS. Ca2+ store depletion causes STIM1 to accumulate in ER regions closely associated with the plasma membrane. *J Cell Biol* 174, 803-813, 2006.

- Xu W, Longo F.J, Wintermantel M.R, Jiang X, Clark R.A & deLisle S. Calreticulin modulates capacitative Ca2+ influx by controlling the extent of inositol 1,4,5-triphosphate-induced Ca2+ store depletion. *J Biol Chem* 275, 36676-36682, 2000.

- Yazawa M, ferrante c, feng J, Mio K, Ogura T, Zhang M, Lin PH, Pan Z, Komazaki S, Kato K, Nishi M, Zhao X, Weisleder N, Sato C, Ma J & Takeshima H. Tric channels are essential for Ca2+ handling in intracellular stores. *Nature* 448, 78-82, 2007.

- Yoshida M, Minamisawa S, Shimura M, Komazaki S, Kume H, Zhang M, Matsumura K, Nishi M, Saito M, Saeki Y, Ishikawa Y, Yanagisawa T & Takeshima H. Impaired Ca2+ store function in skeletal and cardiac muscle cell from Sarcalumenin-deficient mice. *J Biol Chem* 280, 3500-3506, 2005.

- Zhang L, Kelley , Schmeisser G, Kobayashi YM & Jones LR. Complex formation between Junctin, triadin, calsequestrin and the ryanodine receptor. Proteins of the cardiac junctional sarcoplasmic reticulum membrane. *J Biol Chem* 272, 23389-23397, 1997.

- Zanuo N, Shapovalov G, Louis M, Tajeddine N, Gallo C, Van Schoor M, Anguish I, Cao M.L., Schakman O, Dietrich A, Lebacq J, Ruegg U, Roulet E, Birnbaumer L, Gailly P. Role of TRPC1 channel in scheletal muscle function. *Am J Physiol Cell Physiol* C149-C162, 2009.

- Zorzato F, Anderson A.a., Ohlendieck K, Froemming G, Guerrini R, Treves S. Identification of a novel 45 KDa protein (JP-45) from rabbit sarcoplasmic reticulum junctional-face membrane. *Biochem J* 351, 537-543, 2000.

7. ELENCO ARTICOLI INERENTI ALL'ARGOMENTO DELLA TESI:

1) Enhanced dihydropyridine receptor calcium channel activity restores muscle strength in JP45/CASQ1 double knockout mice.
Mosca B, Delbono O, Laura Messi M, Bergamelli L, Wang ZM, Vukcevic M, Lopez R, Treves S, Nishi M, Takeshima H, Paolini C, Martini M, Rispoli G, Protasi F, Zorzato F.

2)Endogenously determined restriction of food intake overcomes excitation-contraction uncoupling in JP45KO mice with aging.
Delbono O, Messi ML, Wang ZM, Treves S, **Mosca B**, Bergamelli L, Nishi M, Takeshima H, Shi H, Xue B, Zorzato F.

3)Remodeling of calcium handling in skeletal muscle through PGC-1• : impact on force, fatigability, and fiber type.
Summermatter S, Thurnheer R, Santos G, **Mosca B**, Baum O, Treves S, Hoppeler H, Zorzato F, Handschin C.

4)SRP-35, a newly identified protein of the skeletal muscle sarcoplasmic reticulum, is a retinol dehydrogenase.
Treves S, Thurnheer R, **Mosca B**, Vukcevic M, Bergamelli L, Voltan R, Oberhauser V, Ronjat M, Csernoch L, Szentesi P, Zorzato F.

5)Minor sarcoplasmic reticulum membrane components that modulate excitation-contraction coupling in striated muscles.
Treves S, Vukcevic M, Maj M, Thurnheer R, **Mosca B**, Zorzato F.

nature COMMUNICATIONS

ARTICLE

Received 9 Jul 2012 | Accepted 14 Jan 2013 | Published xx xxx 2013

DOI: 10.1038/ncomms2496

Enhanced dihydropyridine receptor calcium channel activity restores muscle strength in JP45/CASQ1 double knockout mice

Barbara Mosca[1], Osvaldo Delbono[2], Maria Laura Messi[2], Leda Bergamelli[1], Zhong-Min Wang[2], Mirko Vukcevic[3], Ruben Lopez[3], Susan Treves[1,3], Miyuki Nishi[4], Hiroshi Takeshima[4], Cecilia Paolini[5], Marta Martini[6], Giorgio Rispoli[6], Feliciano Protasi[5] & Francesco Zorzato[1,3]

Muscle strength declines with age in part due to a decline of Ca^{2+} release from sarcoplasmic reticulum calcium stores. Skeletal muscle dihydropyridine receptors ($Ca_v1.1$) initiate muscle contraction by activating ryanodine receptors in the sarcoplasmic reticulum. $Ca_v1.1$ channel activity is enhanced by a retrograde stimulatory signal delivered by the ryanodine receptor. JP45 is a membrane protein interacting with $Ca_v1.1$ and the sarcoplasmic reticulum Ca^{2+} storage protein calsequestrin (CASQ1). Here we show that JP45 and CASQ1 strengthen skeletal muscle contraction by modulating $Ca_v1.1$ channel activity. Using muscle fibres from JP45 and CASQ1 double knockout mice, we demonstrate that Ca^{2+} transients evoked by tetanic stimulation are the result of massive Ca^{2+} influx due to enhanced $Ca_v1.1$ channel activity, which restores muscle strength in JP45/CASQ1 double knockout mice. We envision that JP45 and CASQ1 may be candidate targets for the development of new therapeutic strategies against decay of skeletal muscle strength caused by a decrease in sarcoplasmic reticulum Ca^{2+} content.

[1] Department of Experimental and Diagnostic Medicine, General Pathology section, University of Ferrara, Via Borsari 46, Ferrara 44121, Italy. [2] Department of Physiology and Pharmacology, Wake Forest University School of Medicine, Winston-Salem, North Carolina 27157, USA. [3] Department of Biomedicine and Anesthesiology, Basel University Hospital, Hebelstrasse 20, Basel 4031, Switzerland. [4] Department of Biological Chemistry, Graduate School of Pharmacological Sciences, Kyoto University, Kyoto 606-8501, Japan. [5] CeSI & DNI, University of G. d'Annunzio, Chieti, Italy. [6] Department of Biology and Evolution, Physiology and Biophysics University of Ferrara, Via Borsari 46, Ferrara 44121, Italy. Correspondence and requests for materials should be addressed to F.Z. (email: fzorzato@uhbs.ch).

Activation of skeletal muscle contraction is initiated by the propagation of the action potential deep into the muscle fibre by means of the transverse tubular system (T system)[1–3]. T tubule depolarization causes massive release of Ca^{2+} from the sarcoplasmic reticulum (SR) throughout the entire length of the muscle fibre by a process called excitation-contraction coupling[1,2]. Loss of muscle function has been recognized as a debilitating and life-threatening condition not only in the elderly, but also in cachexia in cancer patients and in all those clinical conditions associated with prolonged bed rest[4,5]. The decay of muscle strength is caused by several factors, including a decrease of releasable calcium from the skeletal muscle SR calcium store[6,7].

EC coupling is operated by a macromolecular complex comprising the α_1-subunit of the voltage-dependent L-type Ca^{2+} channel (dihydropyridine receptor, DHPR, $Ca_v1.1$), the ryanodine receptor (RyR) and calsequestrin (CASQ1)[8], in the contact region between the T system and the SR membrane[3]. $Ca_v1.1$ acts as a voltage sensor and generates orthograde signals that cause opening of the RyR whereby Ca^{2+} is released from the SR into the myoplasm, leading to activation of the contractile proteins[1]. Analysis of voltage-dependent calcium currents in RyR1 knockout (KO) muscle cells was fundamental to clarify the signalling mechanisms between the RyR and $Ca_v1.1$. It is now accepted that the RyR1 not only receives an orthograde signal from $Ca_v1.1$, but also generates a retrograde signal which is important for the activation of $Ca_v1.1$ channel activity[9,10]. The mechanism by which the retrograde Ca^{2+} current enhancement is modulated and its exact physiological role remain elusive. Although calcium influx across the sarcolemma is thought to be non relevant for muscle contraction[11], it has been proposed that it may have a role in replenishing the SR during sustained muscle contractions[12]. Two different modes of calcium influx in skeletal muscle have been described: (i) calcium influx via $Ca_v1.1$ associated with prolonged membrane depolarization is referred to as excitation-coupled calcium entry (ECCE)[10], (ii) calcium influx via STIM1 and Ora1 stimulated by internal store depletion is referred to as store-operated calcium entry (SOCE)[13–15]. However, the analysis of macroscopic calcium currents in adult muscle fibres recorded under voltage clamp condition[16] suggests that both voltage-dependent calcium release and/or SR calcium depletion are not sufficient to activate inward calcium currents and thus challenged the physiological relevance of ECCE and SOCE in adult mammalian fibres. Nevertheless, calcium influx in muscle cells deserves further investigation, because of the potential impact of calcium influx in determining releasable SR calcium content[17], a crucial factor for proper sustained muscle force development [6,7,18].

Calcium influx in skeletal muscle is affected by drugs[19,20] and by accessory proteins such as junctophyllin and mitsugumin-29, two proteins localized in the membrane compartment which form the junction between T tubules and SR[12,21]. T tubules-SR junction membranes encompasses also JP45, a developmentally regulated 45-kDa transmembrane protein that interacts *via* its luminal carboxy-terminal domain with CASQ1, the major calcium storage protein of SR, and with its amino terminal domain with $Ca_v1.1$[22]. Ablation of calsequestrin 1 in skeletal muscle fibres results in a decrease of total calcium

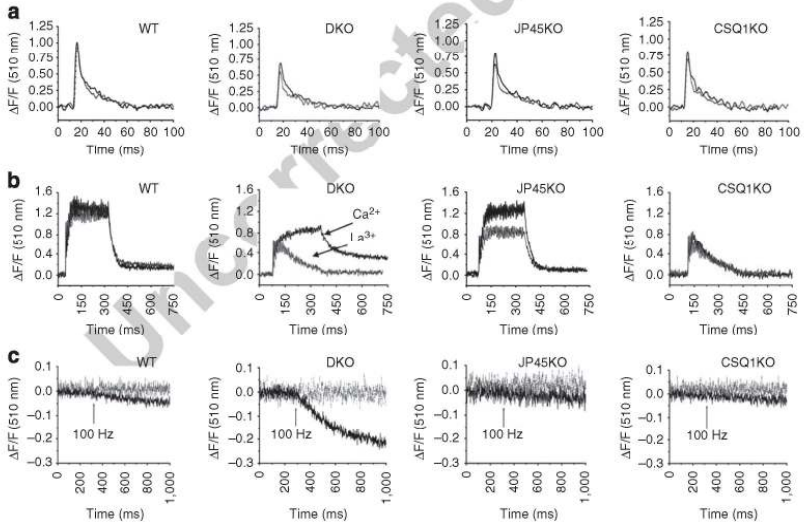

Figure 1 | Ca^{2+} transients and Mn^{2+} quenching in FDB fibres from single and DKO mice. FDB fibres were loaded with the fast low-affinity Ca^{2+} dye Mag-Fluo-4AM [21,22]. (**a**) Ca^{2+} transients were triggered by supramaximal field stimulation with single pulses of 0.5 ms duration. Continuous lines: Ca^{2+} transients recordings in an external solution containing 1.8 mM $CaCl_2$. Overall ANOVA *P*-value < 0.0001; multicomparison Dunnet's ANOVA post test shows difference between of the peak calcium values: WT versus DKO $P<0.01$, WT versus JP45 KO $P<0.01$; WT versus CASQ1 KO $P<0.01$; dotted grey lines: Ca^{2+} transients recordings in an external solution containing 100 μM La^{3+}. Overall ANOVA *P*-value < 0.0001; multicomparison Dunnet's ANOVA post test shows difference between of the peak calcium values: WT versus DKO $P<0.01$, WT versus JP45 KO $P<0.01$, WT versus CASQ1 KO $P<0.01$. (**b**) Recording of Ca^{2+} transients upon stimulation with repetitive pulses at 100 Hz for 300 ms duration. Black and grey lines show recordings in the presence of 1.8 mM Ca^{2+} and 100 μM La^{3+} in the external solution, respectively. In the presence of La^{3+}, the overall ANOVA *P*-value is < 0.0001: multicomparison Dunnet's ANOVA post test shows differences: WT versus DKO $P<0.01$, WT versus JP45 KO $P<0.05$, WT versus CASQ1 KO $P<0.01$. (**c**) Mn^{2+} quenching of Fura-2 fluorescence. Black lines: Mn^{2+} influx was triggered by repetitive pulses at 100 Hz (arrow) for 300 ms duration. Overall ANOVA *P*-value < 0.0001; multicomparison Dunnet's ANOVA post test shows differences: WT versus DKO $P<0.01$. Dotted grey lines: Mn^{2+} quenching recordings in the presence of 50 μM nifedipine in the external solution.

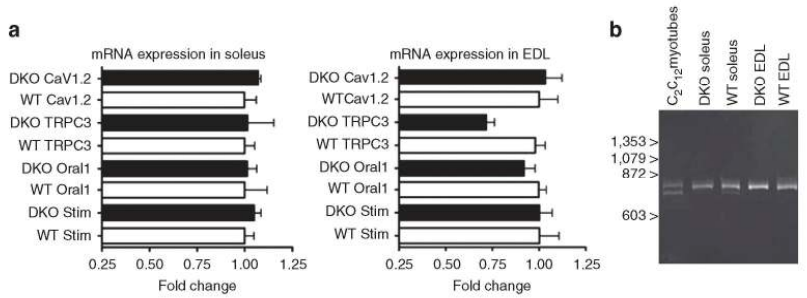

Figure 2 | Expression of calcium entry proteins in fast and slow muscles from DKO mice. (**a**) Real-time reverse transcription (RT) PCR from soleus and EDL of wild-type and DKO mice. Real-time RT PCR was carried out as previously described[41]. Briefly, total RNA was extracted using TRIzol reagent from Soleus or EDL muscles after frozen tissue homogenization, and Cav1.2, TRPC3, Orai1 and STIM1 gene expression was evaluated by quantitative real-time PCR. Boxes represent the mean (±s.e.m.) fold change compared with values obtained from WT for each gene of interest. Gene expression levels were normalized to the expression of the Tata box-binding protein (TBP) and desmin, whose expression was equal between wild-type and KO animals. Pooled data are results carried out on muscles from 5 to 7 different mice. (**b**) Expression of Δ29 $Ca_v1.1$ isoform mRNA in EDL and Soleus from 1-month-old WT and DKO mice. The expression of neonatal Δ29 Cav1.1 isoforms allele (lower band) is present in mRNA from C2C12 myotubes. The Δ29 $Ca_v1.1$ isoforms could be absent or below the detection limit of PCR in EDL. Soleus displays a faint band corresponding to the Δ29 exon $Ca_v1.1$ transcript.

release from the SR, which leads to impaired muscle performance and contractile activation[23–26]. Chronic depletion of JP45 induces a decrease of muscle strength in 3-month-old JP45 KO mice[27]. The decay in strength is apparently not linked to atrophy, but to defects in the EC-coupling machinery caused by alteration of the functional expression of DHPR $Ca_v1.1$ in the T-tubular network.

In the present study, we tested the hypothesis that the skeletal muscle $Ca_v1.1$ channel activity is not only regulated by the RyR, but additionally by the JP45/CASQ1 complex. We generated double JP45 and CASQ1 KO (DKO) and compared their $Ca_v1.1$-mediated Ca^{2+} signals to those observed in WT and each single JP45 and CASQ1 KO mice. Our results show that in DKO mice, tetanic stimulation of skeletal muscle fibres causes massive Ca^{2+} influx due to enhanced $Ca_v1.1$ channel activity and this Ca^{2+} influx restores muscle strength. By using this animal model, we have unveiled a signalling pathway which may be an important target for drugs against the loss of skeletal muscle strength caused by decrease of the SR calcium content.

Results

Calcium transient in flexor digitorum brevis fibres. We compared Ca^{2+} homoeostasis in WT, single JP45 and CSQ1 KO and DKO using the ratiometric Ca^{2+} indicator Indo-1 and found that the resting calcium concentration was increased in DKO $1.15 \pm 0.23^*$ ($n=48$) fibres compared with WT (0.92 ± 0.10, $n=40$), JP45 null (1.03 ± 0.18, $n=42$) and CASQ1 null (0.95 ± 0.11) fibres (F_{405}/F_{480} indo-1 ratio values are mean ± s.d.; *WT versus DKO $P<0.001$ two tailed Mann–Whitney). In the presence of 1.8 mM Ca^{2+} in the extracellular solution, the peak intracellular Ca^{2+} transients measured with the low-affinity calcium indicator MagFluo4 were 1.009 ± 0.18 ($n=47$), 0.67 ± 0.16 ($n-49$), 0.80 ± 0.25 ($n-40$) and 0.82 ± 0.25 ($n-47$) for WT, DKO, JP45 KO and CASQ1 KO, respectively ($\Delta F/F_o$ values are expressed as mean ± s.d., Fig. 1 top panels). The significant decrease of the peak Ca^{2+} transient in DKO fibres is not due to a lower membrane density of RyRs (Supplementary Fig. S1). The half-time of the decay of the Ca^{2+} transients in flexor digitorum brevis (FDB) fibres from DKO mice was significantly slower compared with WT (3.7 ± 0.7, $n=47$ and 4.8 ± 1.9 ms, $n=49$ in WT and DKO fibres, respectively. Analysis of variance (ANOVA) P-values <0.0001; multicomparison Dunnet's post test WT versus DKO $P<0.01$).

Enhanced ECCE in FDB fibres from DKO mice. The slower decay of the calcium transients in FBD fibres from DKO mice is not due to a decrease of calcium uptake in to the SR by the Ca^{2+} pump because we did not observe a reduction of the SERCA1 and SERCA2 expression in DKO mice (Supplementary Fig. S1). The increase of the half-time of the decay of the calcium transient is rather linked to an influx of extracellular Ca^{2+}, as in the presence of La^{3+}, a non-specific calcium channel blocker[11], the difference in the half-time for the decay of calcium transient between WT and DKO fibres disappears (3.1 ± 0.7 and 3.3 ± 1.1 ms for WT and DKO, respectively). The effect of La^{3+} was much more evident upon stimulation of FDB fibres with repetitive action potentials. In the presence of La^{3+}, the Ca^{2+} transient amplitude of tetanic stimulation was highest in WT fibres (1.31 ± 0.28; $n=37$) compared with that of DKO ($0.62 \pm 0.14^*$, $n=34$), JP45 KO ($1.05 \pm 0.30^§$, $n=26$) and CASQ1 ($0.70 \pm 0.15^* n=24$) ($\Delta F/F_o$ values are mean ± s.d., $^*P<0.01$, $^§P<0.05$, (multicomparison Dunnet's ANOVA post test, Fig. 1). In CASQ1 null fibres, the summation of Ca^{2+} transient peaks was dramatically different compared with WT, JP45 null and DKO fibres. After the few initial peaks, which display an amplitude 50% lower compared with WT, the fused Ca^{2+} transients in CASQ1 KO fibres rapidly decayed to basal levels. This event reflects depletion of Ca^{2+} stores due to the ablation of the Ca^{2+} storage protein[23–25]. However, at variance with CASQ1 null fibres, the double KO (DKO) fibres exhibit a sustained Ca^{2+} transient which persisted for the entire duration of the repetitive stimulation in the presence of calcium in the extracellular solution (Fig. 1 middle panels, arrow Ca^{2+}).

Depolarization of DKO fibres causes massive Ca^{2+} influx. The sustained calcium transients evoked by tetanic stimulation in DKO fibres is caused by massive Ca^{2+} influx, as in the presence of 100 μM La^{3+} in the external solution (Fig. 1 middle panel, arrow La^{3+}), the Ca^{2+} transient curve overlapped with that of CASQ1 KO fibres. These data unambiguously demonstrate that ablation of JP45 in a CASQ1 null background unveils a robust Ca^{2+} influx component coupled to membrane depolarization.

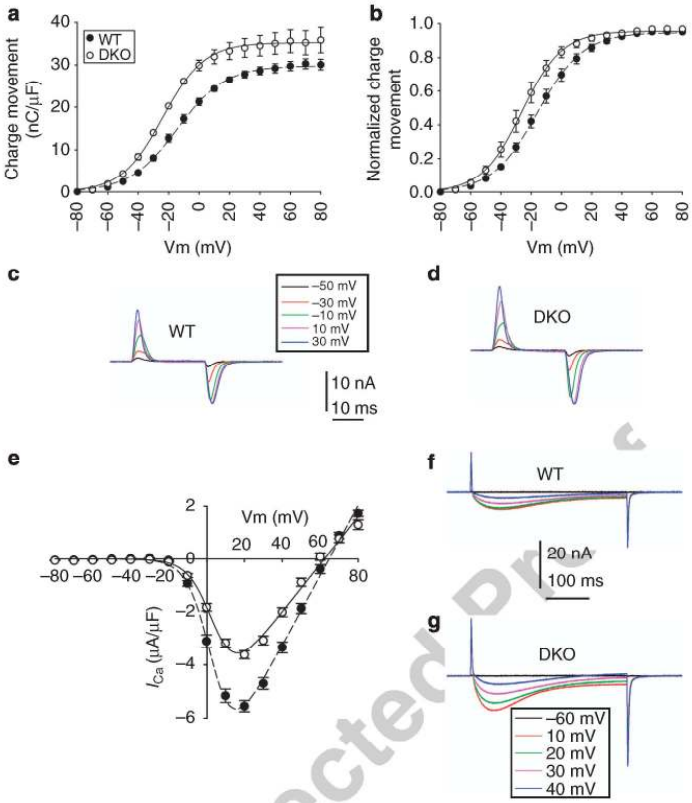

Figure 3 | Voltage dependence of charge movements and Ca^{2+} currents. (**a**) Charge movement–membrane potential relationship for WT ($n=13$) and DKO ($n=15$) muscle fibres. Values are mean ± s.e.m. (**b**) Normalized values to maximal charge movement. Values are mean ± s.e.m (**c**–**d**) Representative charge movement traces recorded in FDB fibres voltage-clamped in the whole-cell configuration of the patch clamp. Holding potential: −80 mV. Command pulses of 25 ms duration evoked currents from −80 to 80 mV. Selected traces correspond to the steepest part of the curve. Notice the larger amplitude and 10 mV shift of the curve toward more negative potentials in DKO compared with WT mice. (**e**) Calcium current–membrane voltage relationship. Command pulses of 400 ms duration evoked currents from −80 to 80 mV. Notice the larger current amplitude for DKO ($n=19$) compared with WT ($n=29$) mice. Values are mean ± s.e.m. (**f**–**g**) Representative calcium currents recorded at the indicated membrane voltages. Fitting curves, their respective equations and best fitting parameter values are described in Tables 1 and 2.

This conclusion is also supported by fura-2 manganese quenching experiments performed in FDB fibres (Fig. 1 lower panels). At an excitation wavelength of 360 nm, the Ca^{2+} independent isosbestic wavelength of fura-2, Mn^{2+} entry quenches fura-2 fluorescence[28]. We measured the extent of the fluorescence quenching at the end of a 300-ms-long train of pulses at 100 Hz. We found that manganese quenching of fura-2 fluorescence was -0.11 ± 0.039 ($n=16$), -0.034 ± 0.021 ($n=17$), -0.034 ± 0.011 ($n=19$), -0.027 ± 0.019 ($n=35$) for DKO, WT, JP45 KO and CASQ1 KO fibres, respectively ($\Delta F/F_o$ values are mean ± s.d.). The threefold increase of fura-2 fluorescence quenching by Mn^{2+} in DKO fibres was abolished by the addition of 50 μM nifedipine (Fig. 1 lower panels grey line), a specific inhibitor of $Ca_v1.1$[11]. Skeletal muscle membrane encompasses several molecules that can mediate calcium influx, including the neonatal splice variant (Δ29) of $Ca_v1.1$[29], TRPC3[15] and Ora1/Stim1[14], $Ca_v1.2$. We investigated the expression levels of other known calcium influx channels, and we found no changes both in fast and slow DKO fibres (Fig. 2). Altogether, these data support the conclusion that the increase of excitation-coupled Mn^{2+} entry is mediated by an enhancement of calcium currents through adult form $Ca_v1.1$[10]. The next set of experiments was designed to evaluate the changes in the functional properties of the $Ca_v1.1$.

Increase of Cav1.1 channel activity in DKO fibres. The T-tubular system is the membrane compartment richest in $Ca_v1.1$[30] and high-resolution electron microscopy shows that volume and surface of the T-tubular system in FDB fibres from 1-month-old DKO and WT mice is not different (Supplementary Fig. S2). Thus, the threefold increase of excitation-coupled Mn^{2+} entry is not fully explained by changes of T-tubular membrane extensions or by a small increase of the $Ca_v1.1$ membrane density (Supplementary Fig. S1), but rather could be consistent with a modification of the channel activity of $Ca_v1.1$. To examine this possibility, we investigated the capacitive and Ca^{2+} currents of $Ca_v1.1$ in FDB fibres from DKO and WT mice by using the whole-cell configuration of the patch-clamp technique. Intact FDB fibres from DKO mice show 10 mV shift to more negative

Table 1 | Best-fitting parameters describing the voltage-dependence of charge movement.

	Qmax (nC μF^{-1})	$V_{Q1/2}$ (mV)	K
WT (n=13)	30 ± 8	−14 ± 2.2	16 ± 1.5
DKO	35 ± 11	−24 ± 1.7	14 ± 1.9
(n=15)	(P=0.724)	(P=0.001)	(P=0.426)

Data points were fitted to a Boltzmann equation of the form: Qon = Qmax/[1 + exp($V_{Q1/2}$ − Vm)/K], where Qmax is the maximum charge, Vm is the membrane potential, $VQ_{1/2}$ is the charge movement half-activation potential and K is the steepness of the curve as described in ref. 27. The number of FDB fibres from three to four mice is between parentheses. Results are expressed as the mean ± s.e.m. Statistical significance was assessed using Student's t-test. The α-level was set at P = 0.05.

Table 2 | Best-fitting parameters describing the voltage-dependence of calcium current.

	Gmax (nS/nF)	$V_{1/2}$ (mV)	Vr (mV)	z
WT (n=29)	90 ± 8	4.7 ± 2.5	62 ± 3.1	3.9 ± 0.6
DKO	132 ± 12	3.8 ± 1.9	64 ± 4.4	4.0 ± 0.8
(n=29)	(P=0.005)	(P=0.775)	(P=0.712)	(P=0.921)

Data points were fitted to the following equation: ICa = Gmax (V − Vm)/{1 + exp[zF($V_{1/2}$ − V)/RT]}, where Gmax is the maximum conductance, V is the membrane potential, Vr is the reversal potential, $V_{1/2}$ is the half activation potential, z is the effective valence, F is the Faraday constant, R is the gas constant and T is the absolute temperature (296 K) as described in ref. 43. The number of FDB fibres from three to four mice is between parentheses. Results are expressed as the mean ± s.e.m. Statistical significance was assessed using Student's t-test. The α-level was set at P = 0.05.

potential of the half maximal gating charge, and small nonsignificant increase (15%) in maximal gating charge, compared with control (Fig. 3b and Table 1). The small increase of maximal gating charges do not account for the ~45% increase of in peak Ca^{2+} current density, which was found in DKO FDB fibres (Fig. 3e). Half-maximal Ca^{2+} currents in wild-type (WT) and DKO mice were observed at very similar membrane potentials (Table 2). These results demonstrate that enhanced calcium influx is accounted for an increase of the $Ca_v1.1$ channel activity.

Skeletal muscle performance is restored in DKO mice. To investigate physiological relevance of the enhanced $Ca_v1.1$ channel activity in DKO mice, we measured *in vivo* muscle performance by assessing spontaneous motor activity (Fig. 4a). Three weeks of training improved skeletal muscle performance in both WT and KO mice, however, the total running distance in JP45 null and CASQ1 null mice was ~40 km lower compared with WT and DKO mice (139.7 ± 2.90 km, 118.1 ± 2.35 km versus 175.3 ± 2.96 km, 175.5 ± 4.23 km, respectively). The enhanced Cav1.1 channel activity restored muscle performance in DKO mice despite a low degree of atrophy of fast fibres (Supplementary Fig. S3), and may be a signature of improved muscle strength[31] mediated by massive Ca^{2+} influx *via* $Ca_v1.1$[12]. To investigate this, we studied the mechanical properties of intact extensor digitorum longus (EDL) (Fig. 4b). EDL from WT and DKO were stimulated with a train of tetani at 0.27 Hz. The onset maximal tetanic force normalized per muscle cross-sectional area of EDL from WT and DKO were not significantly different (327.86 ± 117.53 mN versus 364.64 ± 76.22 mN, respectively; mean ± s.d. n = 9), whereas the time course of force development of EDL from DKO was dramatically different compared to those of WT. In DKO mice, the first train of repetitive pulses of 350 ms duration at 100 Hz caused an initial increase of isometric force and then rapidly decayed to ~20% of the onset value at the end of the repetitive pulses stimulation (Fig. 4b, arrow middle panel 'first'). The reduction of force development during trains of action potentials is most likely indicative of poor calcium buffering capacity of SR caused by the ablation of CASQ1, as a similar inability to sustain muscle contraction has been observed in muscles from CASQ1 KO mice[24] but not in the EDL muscles from **JP45 KO mice[27], which have a normal CASQ1 expression level. Ablation of JP45 in a CASQ1 KO background has a remarkable effect on the peak tension after repetitive tetanic trains at 0.27 Hz. We observed that in the EDL from the DKO mice the isometric tension developed at the end of the last pulse of the train increased up to 300% of the initial value while a modest decrease was evident in WT mice (Fig. 4b arrow middle panel 'last'; lower panels). On the basis of the data reported in Figs. 1 and 3, we reasoned that the ablation of JP45 in the CASQ1 KO background supports a strong calcium influx component mediated by $Ca_v1.1$ channel activity which leads to (i) accumulation of intracellular calcium and to (ii) the improvement of the peak force development after trains of tetanic stimulation. We tested this possibility by examining the effect of La^{3+} on the dynamics of force development of EDL from DKO mice during trains of tetani. As expected incubation of EDL with an external solution containing 100 μM La^{3+} blocked calcium influx, and the increase of isometric force at the end of each train of pulses at 100 Hz in DKO and had no effect on WT muscles (Fig. 4b, lower panels). The effect of La^{3+} in muscles from DKO mice was reversed by re-exposing EDLs to a bathing solution containing 1.8 mM $CaCl_2$ (Fig. 5).

Discussion

Here we investigated the role of the JP45/CASQ1 complex on the modulation of $Ca_v1.1$ function by analysing the functional properties of skeletal muscle fibres from JP45/CASQ1 DKO mice. Our results show that in DKO mice, calcium transients induced by repetitive action potential are supported by massive calcium influx from the extracellular environment. The massive increase of calcium influx is consistent with an enhancement of the $Ca_v1.1$ channel activity because: (1) it is inhibited by nifidipine, a blocker of $Ca_v1.1$; (2) it does not correlate with an increase in the expression of other know calcium influx channels such as Ora1, TRPC3 and the neonatal isoform of $Ca_v1.1$; (3) is associated with a 45% increase of the $Ca_v1.1$ peak calcium current density in intact single FDB fibres. This massive calcium influx via $Ca_v1.1$ restores the development of *in vitro* muscle force of EDL from DKO mice. The maintenance of muscle force *in vitro* is paralleled by the recovery of muscle performance of DKO mice *in vivo*. The characterization of the JP45/CASQ1 DKO animal model supports the conclusion that JP45/CASQ1 complex may be a genetically encoded modulator of the $Ca_v1.1$ channel activity.

The $Ca_v1.1$ complex has a dual function: it acts as (i) voltage sensor which activates, *via* a mechanical coupling, the RyR, and as (ii) a slow activating voltage-dependent calcium channel. Calcium influx via $Ca_v1.1$ channel activity was considered not important for skeletal muscle EC coupling, as it was shown that skeletal muscles can contract for hours in extracellular medium containing very low (sub nM) calcium concentrations[11]. The idea that skeletal muscle EC coupling is independent from the influx of extracellular calcium was confirmed later by pharmacological and genetic manipulation of $Ca_v1.1$ function[32–35]. However, in evaluating the functional significance of the $Ca_v1.1$ channel activity, one can not dismiss results showing that the influx of extracellular calcium in involved in the development of muscle contraction in amphibian and mammalian muscle fibres[36,37]. This apparent discrepancy might be ascribed to different experimental models and conditions that were used to probe the importance of $Ca_v1.1$ channel activity in EC coupling. In this study we exploited the JP45/CASQ1 DKO mouse model to

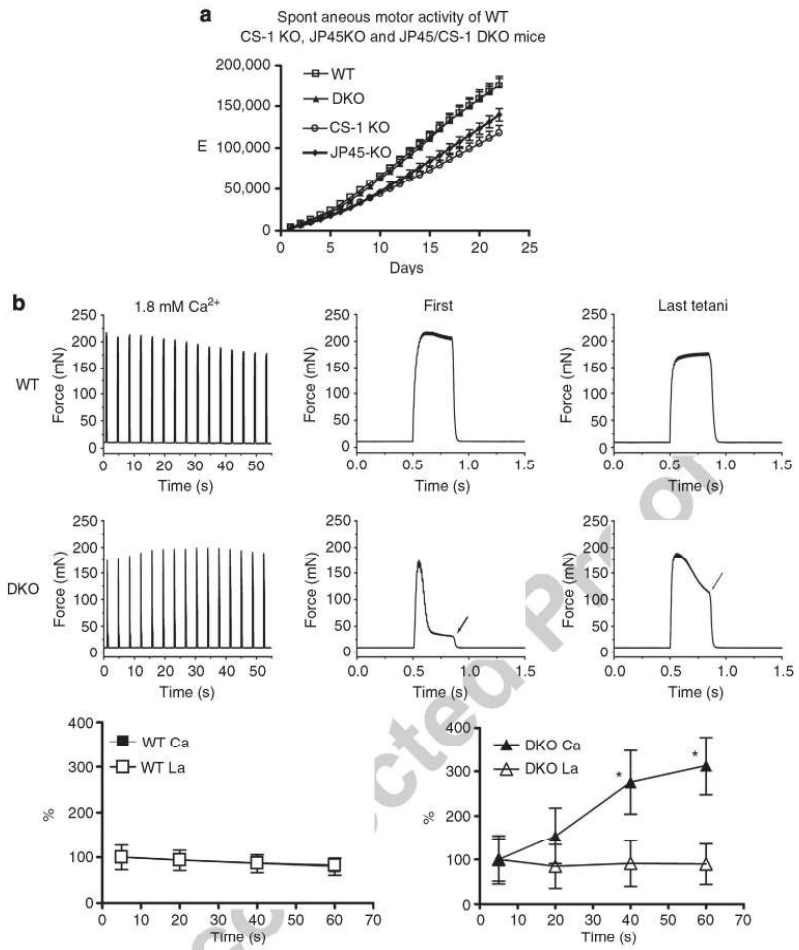

Figure 4 | Skeletal muscle performance of WT and DKO mice. (**a**) *In vivo* evaluation of muscle strength. Spontaneous activity in 4–6 week-old WT, DKO, JP45 KO and CASQ1 KO mice individually housed in cages equipped with a running wheel. Data points are expressed as mean ± s.e.m.; $n=10$ to 13 mice. Overall ANOVA P-value <0.0001; multicomparison Dunnet's ANOVA post test shows difference: WT versus DKO $P>0.05$; WT versus JP45 KO $P<0.05$; WT versus CASQ1 KO $P<0.01$. (**b**) Evaluation of tetanic force of intact EDL. Top and middle row of panels: EDLs were triggered by field stimulation in bathing solution containing 1.8 mM $CaCl_2$ with a train of repetitive pulses (100 Hz, 350 ms duration) at 0.27 Hz (left panels). Time course of force development of the first and last tetani of the trace displayed in the left panels (middle and right panels). Lower row of panels: after repetitive train stimulation the EDL muscles from control (left panel) and DKO (right panel) mice were incubated for 10 min in a bathing solution containing 100 μM La^{3+} and were then stimulated with repetitive trains of pulses at 0.27 Hz. Data point represents the force developed at the end of 350 ms duration repetitive pulse stimulation (values are mean ± s.d. $n=8$, * $P<0.05$ Mann–Whitney). The increase the force developed at the end of tetanic stimulation in EDL from KO mice was abolished by 100 μM La^{3+} a blocker of the calcium influx into muscle fibres (compare DKO Ca^{2+} versus DKO La^{3+}).

investigate to role of $Ca_v1.1$ channel activity during EC coupling and its modulation by JP45/CASQ1 complex. Although we are aware that the JP45/CASQ1 KO mouse model may not recapitulate the physiological setting present in mammalian muscle fibres expressing normal levels of both JP45 and CASQ1, our data provide a strong case as to the potential physiological significance of the $Ca_v1.1$ channel activity during EC coupling, at least in mutant muscle fibres. The robust calcium influx via $Ca_v1.1$ channel activity which was observed during repetitive action potential in JP45/CASQ1 DKO mice results in better contractile function *in vitro* and, most importantly, *in vivo*. Such an effect on muscle contractile function could reflect (i) an indirect global adaptive cellular response to the chronic ablation of two important SR proteins, or (ii) result from the lack of specific regulatory mechanism operated by the JP45/CASQ1 complex on the $Ca_v1.1$ channel activity. Although we cannot exclude any of the two possibilities, we are confident that our results clearly indicate the physiological importance of the dual activity of $Ca_v1.1$ during EC coupling of the DKO muscle fibres. In this mouse model $Ca_v1.1$ clearly operates not only as the voltage sensor that activates RyR (Fig. 2), (ii) but also as calcium influx channel which contribute to maintain an adequate level of

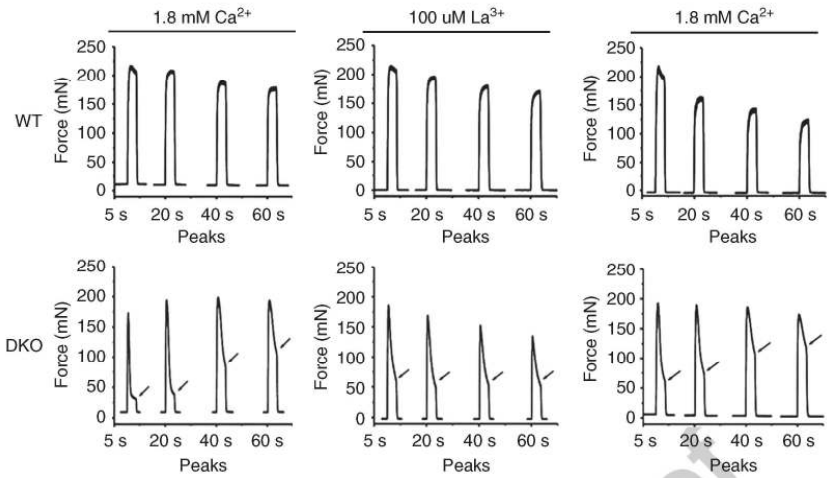

Figure 5 | Tetanic contraction of EDL from WT and JP45/CASQ1 double KO mice. EDL from wild-type and DKO were first incubated in a Tyrode's solution containing 1.8 mM CaCl2. Maximal tetanic force was triggered by field stimulation 28 with a train of repetitive pulses (100 Hz of 350 ms duration) at 0.27 Hz. Tetani at 5, 20, 40 and 60 s are shown. The same stimulation protocols was applied to muscle which were incubated for 10 min in a bathing solution containing 100 μM La3+ (traces WT La3+ and DKO La3+). The increase the force developed at the end of tetanic stimulation in EDL from KO mice was abolished by 100 μM La3+ a blocker of the calcium influx into muscle fibres (compare DKO left panel with middle panel). The effect of La3+ was reversed by 10 min long exposure of EDL muscles to a bathing solution containing Ca2+ (right panels).

releasable SR calcium content during sustained muscle activity evoked by tetanic stimulation (Fig. 3). These data imply that the JP45/CASQ1 complex modulate $Ca_v1.1$ channel activity also in normal fibres, in particular, it may operate in those conditions which causes a deficit SR calcium load.

On the basis of these data we propose that JP45/CASQ1 complex is genetically encoded modulator of the $Ca_v1.1$. channel activity, and that it constitutes a potential target to devise novel therapeutic strategies against the decline of skeletal muscle strength linked to decreased SR calcium content[6,7,12].

Methods

Generation JP45 CASQ1 DKO mice. JP45 KO was obtained as described by Delbono *et al.*[27]. CASQ1 KO mice were obtained as described by Paolini *et al.*[26]. DKO mice were generated by crossing to each other established JP45 KO and CASQ1 KO lines backcrossed in C57BL6J (Supplementary Fig. S4).

Morphology. Immunohistochemistry of EDL and Soleus was carried out as described by Delbono *et al.*[38]. EDL and soleus muscles were embedded in OCT, snap-frozen in isopentane, cryosectioned at the mid-belly region (10 μm) and mounted on coverslips for immunostaining. For staining mounted sections were air dried, treated with PBS containing 1% bovine serum albumin (BSA) and 2% horse serum for 30 min and incubated overnight at 4–8 °C with a PBS solution containing 0.01% Triton X100, 1% BSA, 2% horse serum, 0.5% $\mu g\,ml^{-1}$ anti-mouse slow myosin heavy chain (MAB 1628, Millipore, Billerica, MA), 2 $\mu g\,ml^{-1}$ anti rat α-laminin (MAB1914, Millipore). Sections were then washed with PBS for 15 min four times, and incubated at room temperature for 40 min with a PBS containing Alexa Fluor 488 anti-mouse IgG Ab (2 $\mu g\,ml^{-1}$) and Cy3 anti rat IgG Ab (0.5 $\mu g\,ml^{-1}$). After incubating in the secondary Ab, sections were washed with PBS for 15 min four times, dehydrated with ethanol and mounted using a glycerol medium. Fluorescence images were imaged using a Leica DM5000B fluorescence microscope and analysed with Analysis software package from Soft Imaging System, Muenster, Germany. Image analysis of muscle sections was performed in four steps: (1) determination of the muscle fibre boundaries, (2) determination of the muscle fibre cross-sectional area, (3) calculation of the per cent of muscle fibres positive for anti MHC I Ab and (4) determination of the per cent of muscle fibres negative for anti MHC I Ab staining. The muscle fibre cross-sectional area was determined using the minimal 'Feret's diameter' (the minimum distance of parallel tangents at opposing borders of the muscle fibre). High-resolution electron microscopy was carried out as described by Paolini *et al.*[26] Volume and surface of the transverse tubule (TT) network (see Table in Supplementary. Fig. 4) were determined using the well-established stereology point and intersection counting techniques[39,40] in EM micrographs taken at ×14,000 of magnification. (a) Measurement of relative fibre volume occupied by TT. After covering the images with an orthogonal array of dots at a spacing of 0.20 μm, the ratio between numbers of dots falling in the TT lumen and the total number of dots covering the whole image represent the relative volume of fibre occupied by the TT. (b) Measurement of TT surface area to volume. The images were covered with two sets of grid lines separated by a distance of 0.24 μm and intersecting at right angles. The frequency of intersections between the membrane of interest (TT profiles) and the grid lines was counted. The ratio of TT surface area to volume was obtained from the formula $C/2dP$ test, where C is the number of intersections, d is the spacing between the grid lines, and P test is the number of grid intersections in the test area.

Gene expression analysis. Expression of neonatal Δ29 isoform of $Ca_v1.1$ was detected by semiquantitative RT-PCR[41]. Total RNA was extracted from homogenized mouse muscle tissues EDL and SOL, and cultured C2C12 myotubes using TRIzol reagent. Eight hundred nanograms of RNA were first reverse transcribed into cDNA; the Cav1.1 cDNA was amplified by PCR using primers[29], which span exons 27–34: forward 5′-AGTCGGAGCAGATGAACCAC-3′ and reverse 5′ ATGGCCTTGAACTCATCCAG 3′. The PCR amplification conditions were 95 °C for 5 min, followed by 37 cycles of 94 °C for 40 s, 51 °C for 40 s and 70 °C for 1 min, followed by a 5-min extension at 72 °C. The RT-PCR products encoding the adult and neonatal($Ca_v1.1\Delta29$) isoforms are 790-bp long (upper band) and (lower band) 733 bp long, respectively.

Analysis of total SR and muscle strength assessment. Total SR membranes were prepared[42] starting from a 20% skeletal muscle total homogenate; this was sedimented at $3{,}000_{gmax}$ for 10 min and the resulting supernatant was centrifuged at $15{,}000_{gmax}$ for 20 min to remove the myofibrillar protein components. The $15{,}000_{gmax}$ supernatant was then centrifuged for 60 min at $100{,}000_{gmax}$ to isolate the total SR (microsomal) pellet. SDS-polyacrylamide electrophoresis and western blot of total SR proteins were carried out as described by Anderson *et al.*[22] Blots were probed with a polyclonal primary Ab followed by peroxidase-conjugated secondary antibodies. The immunopositive bands were visualized by chemiluminescence using the Super Signal West Dura kit from Thermo Scientific. Densitometry of the immunopositive bands was carried out by using BioRad GelDoc 2000. [^{3}H]-PN200-110 and [^{3}H]-Ryanodine binding was carried out according to Anderson *et al.*[43] Briefly, total SR membranes were incubated for 1 h in the dark in a solution containing 50 mM Tris–HCl pH 7.5, 10 mM $CaCl_2$ plus

protease inhibitor cocktail (ROCHE cat. no. 05892953001), 0.05–5 nM PN200-100 and (+)-[5-methyl-^{3}H]. The samples were then filtered through Whatman glass microfibre GF/B filters by Millipore manifold filtering apparatus, rinsed three times with 5 ml of solution containing 200 mM choline chloride, 20 mM Tris-HCl pH 7.5, and the radioactivity retained on the filters was determined by liquid scintillation counting. [^{3}H]-ryanodine binding was carried out by incubating total SR membranes for 12–16 h at room temperature with 20 mM HEPES pH 7.4, 1 M NaCl, 5 mM AMP, 20 μM $CaCl_2$, 0.05–10 nM [^{3}H]-ryanodine and protease inhibitor cocktail (ROCHE cat. no. 05892953001). Membrane bound [^{3}H]-ryanodine was determined by scintillation counting as described above. Non-specific binding was evaluated in the presence of 1 μM unlabelled nifedipine and 10 μM unlabelled ryanodine, respectively.Curve fitting was performed using Graph Pad Prism 4 software package. Skeletal muscle performance and mechanical properties of EDL were analysed as described by Debono *et al.*[27] Briefly, animals were individually housed in cages equipped with a running wheel carrying a magnet. Wheel revolutions were registered by a reed sensor connected to an I-7053D Digital-Input module (Spectra AG, Egg, Switzerland), and the revolution counters were read by a standard laptop computer via an I-7520 RS-485—to—RS-232 interface converter (Spectra AG, Egg, Switzerland). Digitized signals were processed by the 'mouse running' software developed at Santhera Pharmaceuticals, Liestal, Switzerland. To test force *in vitro*, EDL muscles were dissected and mounted into a muscle testing set-up (Heidelberg-Scientific Instruments, Heidelberg, Germany). Muscle force was digitized at 4 kHz using an AD Instruments converter and stimulated with 15 V pulses for 0.5 ms. EDL tetanus was recorded in response to 400 ms pulses at 10–120 Hz. Specific force was normalized to the muscle cross-sectional area (CSA) = wet weight (mg)/length (mm) × 1.06 (density mg mm^{-3}).

Cell electrophysiology recordings and optical recording. FDB fibres from WT and DKO mice were enzymatically dissociated, plated and recorded following published procedures[44,45]. The composition of the pipette solution was (mM): 140 Cs-aspartate; 5 Mg-aspartate$_2$, 10 Cs_2EGTA (ethylene glycol-bis(α-aminoethyl ether)-*N,N,N′N′*-tetraacetic acid), 10 HEPES (*N*-[2-hydroxyethyl]piperazine-*N′*-[2-ethanesulfonic acid]), pH was adjusted to 7.4 with CsOH. The external solution contained (mM): 145 TEA (tetraethylammonium hydroxide)-Cl, 10 CaCl2, 10 HEPES and 0.001 tetrodotoxin. Solution pH was adjusted to 7.4 with TEA.OH. For charge movement recording, calcium current was blocked with the addition of 0.5 Cd^{2+} plus 0.3 La^{3+} to the external solution[43,45]. Peak Ca^{2+} currents were normalized to membrane capacitance and expressed as Amperes per Farad, whereas intramembrane charge movements were calculated as the integral of the current in response to depolarizing pulses and expressed per membrane capacitance as Coulombs per Farad. Fura-2 Mn^{2+} quenching in intact FDB fibres was carried out as previoulsy described[19,28]. Calcium transients were measured by using the low-affinity fuorescent calcium indicator MagFluo4[46,47]. Briefly, changes in the $[Ca^{2+}]_i$ induced by supramaximal field stimulation were monitored in FDB fibres loaded with Mag-Fluo-4/AM in Tyrode's buffer[48]. All experiments were carried out at room temperature (20–22 °C) in the presence of 50 μM N-benzyl-p-toluensulfonamide (BTS) (Tocris) to minimize movement artefacts. Measurements were carried out with a Nikon ECLIPSE TE2000-U inverted fluorescent microscope equipped with a ×20 magnification objective. Fluorescent signals were capture by a photomultiplier connected to a Nikon Photometer P101 amplifier. Calcium transients were analysed by ADinstrument Chart5 and Origin.6 programs. Changes in fluorescence were calculated as $\Delta F/F = (Fmax - Frest)/(Frest)$. Resting calcium was measured with Indo1 loaded FDB fibres[46].

Statistical analysis. We used GraphPad Prims 4.0 software package to perform curve fitting and statistical analysis.

References

1. Rios, E. & Pizarro, G. Voltage sensor of excitation-contraction coupling in skeletal muscle. *Physiol. Rev.* **71,** 849–908 (1991).
2. Tanabe, T., Beam, K. G., Powell, J. A. & Numa, S. Restoration of excitation-contraction coupling and slow calcium current in dysgenic muscle by dihydropyridine receptor complementary DNA. *Nature* **336,** 134–139 (1990).
3. Franzini-Armstrong, C. & Jorgensen, A. O. Structure and development of E-C coupling units in skeletal muscle. *Annu. Rev. Physiol.* **56,** 509–534 (1994).
4. Manini, T. M. & Clark, B. C. Dynapenia and aging: an update. *J. Gerontol. A Biol. Sci. Med. Sci.* **67,** 28–40 (2012).
5. Dodson, S. *et al.* Muscle wasting in cancer cachexia: clinical implications, diagnosis, and emerging treatment strategies. *Annu. Rev. Med.* **62,** 265–279 (2011).
6. Kabbara, A. A. & Allen, D. G. The role of calcium stores in fatigue of isolated single muscle fibres from the cane toad. *J. Physiol.* **519,** 169–176 (1999).
7. Andersson, D. C. *et al.* Ryanodine receptor oxidation causes intracellular calcium leak and muscle weakness in aging. *Cell Metab.* **14,** 196–207 (2011).
8. Treves, S. *et al.* Minor sarcoplasmic reticulum membrane components that modulate excitation-contraction coupling in striated muscles. *J. Physiol.* **587,** 3071–3079 (2009).
9. Nakai, J. *et al.* Enhanced dihydropyridine receptor channel activity in the presence of ryanodine receptor. *Nature* **380,** 72–75 (1996).
10. Bannister, R. A., Pessah, I. N. & Beam, K. G. The skeletal L-type Ca2+ current is a major contributor to excitation-coupled Ca2+ entry. *J. Gen. Physiol.* **133,** 79–91 (2008).
11. Armstrong, C. M., Bezanilla, F. M. & Horowicz, P. Twitches in the presence of ethylene glycol bis(-aminoethyl ether)-N,N'-tetracetic acid. *Biochim. Biophys. Acta.* **267,** 605–608 (1972).
12. Pan, Z. *et al.* Dysfunction of store-operated calcium channel in muscle cells lacking mg29. *Nat. Cell Biol.* **4,** 379–383 (2002).
13. Kurebayashi, N. & Ogawa, Y. Depletion of Ca2+ in the sarcoplasmic reticulum stimulates Ca2+ entry into mouse skeletal muscle fibres. *J. Physiol.* **533,** 185–199 (2001).
14. Yarotskyy, V. & Dirksen, R. T. Temperature and RyR1 regulate the activation rate of store-operated Ca^{2+} entry current in myotubes. *Biophys. J* **103,** 202–211 (2012).
15. Launikonis, S. & Rios, S. Store-operated Ca2+ entry during intracellular Ca2+ release in mammalian skeletal muscle. *J. Physiol.* **583,** 81–97 (2007).
16. Allard, B., Couchoux, H., Pouvreau, S. & Jacquemond, V. Sarcoplasmic reticulum Ca2+ release and depletion fail to affect sarcolemmal ion channel activity in mouse skeletal muscle. *J. Physiol.* **575,** 69–81 (2006).
17. Rios, E. The cell boundary theorem: a simple law of the control of cytosolic calcium concentration. *J. Physiol. Sci.* **60,** 81–84 (2010).
18. Allen, D. G., Lamb, G. D. & Westerblad., H. Impaired calcium release during fatigue. *J. Appl. Physiol.* **104,** 296–330 (2008).
19. Cherednichenko, G. *et al.* Enhanced excitation-coupled calcium entry in myotubes expressing malignant hyperthermia mutation R163C is attenuated by dantrolene. *Mol. Pharmacol.* **73,** 1203–1212 (2008).
20. Zhao, X. *et al.* Azumolene inhibits a component of store-operated calcium entry coupled to the skeletal muscle ryanodine receptor. *J. Biol. Chem.* **281,** 33477–33486 (2006).
21. Hirata, Y. *et al.* Uncoupling store-operated Ca2+ entry and altered Ca2+ release from sarcoplasmic reticulum through silencing of junctophilin genes. *Biophys. J.* **90,** 4418–4427 (2006).
22. Anderson, A. A. *et al.* The junctional SR protein JP-45 affects the functional expression of the voltage-dependent Ca2+ channel Cav1.1. *J. Cell Sci.* **19,** 2145–2155 (2006).
23. Canato, M. *et al.* Massive alterations of sarcoplasmic reticulum free calcium in skeletal muscle fibers lacking calsequestrin revealed by a genetically encoded probe. *Proc. Natl Acad. Sci. USA* **107,** 22326–22331 (2010).
24. Olojo, R. O. *et al.* Mice null for calsequestrin 1 exhibit deficits in functional performance and sarcoplasmic reticulum calcium handling. *PLoS One* **6,** e27036 (2012).
25. Sztretye, M. *et al.* Measurement of RyR permeability reveals a role of calsequestrin in termination of SR Ca(2+) release in skeletal muscle. *J. Gen. Physiol.* **138,** 231–247 (2011).
26. Paolini, C. *et al.* Reorganized stores and impaired calcium handling in skeletal muscle of mice lacking calsequestrin-1. *J. Physiol.* **583,** 767–784 (2007).
27. Delbono, O. *et al.* Loss of skeletal muscle strength by ablation of the sarcoplasmic reticulum protein JP45. *Proc. Natl Acad. Sci. USA* **104,** 20108–20113 (2007).
28. Clementi, E. *et al.* Receptor-activated Ca2+ influx. Two independently regulated mechanisms of influx stimulation coexist in neurosecretory PC12 cells. *J. Biol. Chem.* **267,** 2164–2172 (1992).
29. Tuluc, P. *et al.* A Cav1.1 Ca2+ channel splice variant with high conductance and voltage-sensitivity alters EC coupling in developing skeletal muscle. *Biophys. J.* **96,** 35–44 (2009).
30. Fosset, M., Jaimovich, E., Delpont, E. & Lazdunski, M. [^{3}H]nitrendipine receptors in skeletal muscle. *J. Biol. Chem.* **258,** 6086–6092 (1983).
31. Brooks, S. V. & Faulkner, J. A. Skeletal muscle weakness in old age: underlying mechanisms. *Med. Sci. Sports Exerc.* **26,** 432–439 (1994).
32. Gonzales-Serratos, H., Valle-Aguilera, R., Lathrop, D. A. & Garcia, M. C. Slow inward calcium currents have no obvious role in muscle excitation-contraction coupling. *Nature* **298,** 292–41982 (1982).
33. Miledi, R., Parker, I. & Zhu, P. H. Extracellular ions and excitation-contraction coupling in frog twitch muscle fibres. *J. Physiol.* **351,** 687–710 (1984).
34. Melzer, W., Herrmann-Frank, A. & Lüttgau, H. C. The role of Ca2+ ions in excitation-contraction coupling of skeletal muscle fibres. *Biochim. Biophys. Acta.* **1241,** 59–116 (1995).
35. Dirksen, R. T. & Beam, K. G. Role of calcium permeation in dihydropyridine receptor function. Insights into channel gating and excitation-contraction coupling. *J. Gen. Physiol.* **114,** 393–403 (1999).
36. Ildefonse, M., Jacquemond, V., Rougier, O., Renaud, J. F., Fosset, M. & Lazdunski, M. Excitation contraction coupling in skeletal muscle: evidence for a role of slow Ca2+ channels using Ca2+ channel activators and inhibitors in the dihydropyridine series. *Biochem. Biophys. Res. Commun.* **129,** 904–909 (1985).

37. Lamb, G. D. Asymmetric charge movement in contracting muscle fibres in the rabbit. *J. Physiol.* **376,** 63–83 (1986).
38. Delbono, O. *et al.* Endogenously determined restriction of food intake overcomes excitation-contraction uncoupling in JP45KO mice with aging. *Exp. Gerontol.* **47,** 304–316 (2012).
39. Loud, A. V., Barany, W. C. & Pack, B. A. Quantitative Evaluation of Cytoplasmic *Structures in Electron Micrographs. Lab. Invest.* **14,** 996–1008 (1965).
40. Mobley, B. A. & Eisenberg, B. R. Sizes of components in frog skeletal muscle measured by methods of stereology. *J. Gen. Physiol.* **66,** 31–45 (1975).
41. Vukcevic, M., Spagnoli, G. C., Iezzi, G., Zorzato, F. & Treves, S. Ryanodine receptor activation by Ca v 1.2 is involved in dendritic cell major histocompatibility complex class II surface expression. *J. Biol. Chem.* **283,** 34913–3422 (2008).
42. Franzini-Armstrong, C. & Protasi, F. Ryanodine receptors of striated muscles: a complex channel capable of multiple interactions. *Physiol. Rev.* **77,** 699–729 (1997).
43. Anderson, K., Cohn, A. H. & Meissner, G. High-affinity [^{3}H]PN200-110 and [^{3}H]ryanodine binding to rabbit and frog skeletal muscle. *Am. J. Physiol.* **266,** C462–C466 (1994).
44. Wang, Z. M., Messi, M. L. & Delbono, O. Patch-clamp recording of charge movement, Ca2 + current and Ca2 + transients in adult skeletal muscle fibers. *Biophys. J.* **77,** 2709–2716 (1999).
45. Hernández-Ochoa, E. O. & Schneider, M. F. Voltage clamp methods for the study of membrane currents and SR Ca(2 +) release in adult skeletal muscle fibres. *Prog. Biophys. Mol. Biol.* **108,** 98–118 (2012).
46. Hollingworth, S., Gee, K. R. & Baylor, S. M. Low-affinity Ca2 + indicators compared in measurements of skeletal muscle Ca2 + transients. *Biophys. J.* **97,** 1864–1872 (2009).
47. Calderón, J. C., Bolaños, P. & Caputo, C. Myosin heavy chain isoform composition and Ca(2 +) transients in fibres from enzymatically dissociated murine soleus and extensor digitorum longus muscles. *J. Physiol.* **588,** 267–279 (2010).
48. Tomasi, M. *et al.* Calsequestrin (CASQ1) rescues function and structure of calcium release units in skeletal muscles of CASQ1-null mice. *Am. J. Physiol. Cell Physiol.* **302,** C575–C586 (2012).

Acknowledgements

This work was supported by funds from Swiss Muscle foundation, A.F.M., S.N.F and Department of Biomedicine University Hospital Basel. This study was also supported by Research Grant no. GGP08153 from the Italian Telethon ONLUS Foundation to F.P. and grants from the NIH/NIA (AG13934 and AG15820) to O.D.

Author contributions

B.M. and L.B. developed and monitored mouse colony, collected and analysed calcium measurements data; M.V. collected and analysed expression data; R.L. collected and analysed force measurements data; M.T. and H.T. generated mice model; C.P. and F.P provided CASQ1 KO mice and performed structural analysis; O.D., M.L.M., Z-.M.W., M.M. and G.R. collected and analysed electrophysiological data; S.T. collected and analysed biochemical data; and F.Z. took care of conception and design of the experiments, collection and analysis of biochemical, histochemistry and physiological data, and drafting of the manuscript.

Additional information

Supplementary Information accompanies this paper on http://www.nature.com/naturecommunications

Competing financial interests: The authors declare no competing financial interests.

Reprints and permission information is available online at http://npg.nature.com/reprintsandpermissions/

How to cite this article: Mosca, B. *et al.* Enhanced dihydropyridine receptor calcium channel activity restores muscle strength in JP45/CASQ1 double knockout mice. *Nat. Commun.* x:x doi: 10.1038/ncomms2496 (2013).

ARTICLE IN PRESS
EXG-08969; No of Pages 13
Experimental Gerontology xxx (2012) xxx–xxx
Contents lists available at SciVerse ScienceDirect
Experimental Gerontology
journal homepage: www.elsevier.com/locate/expgero

Endogenously determined restriction of food intake overcomes excitation–contraction uncoupling in JP45KO mice with aging

Osvaldo Delbono [a,*], Maria Laura Messi [a], Zhong-Min Wang [a], Susan Treves [d,e], Barbara Mosca [g], Leda Bergamelli [g], Miyuki Nishi [f], Hiroshi Takeshima [f], Hang Shi [a,c], Bingzhong Xue [b,c], Francesco Zorzato [d,e,f]

[a] Department of Internal Medicine, Section on Gerontology and Geriatric Medicine, Wake Forest University School of Medicine, Winston-Salem, NC 27157, United States
[b] Section on Endocrinology and Metabolism, Wake Forest University School of Medicine, Winston-Salem, NC 27157, United States
[c] Center of Diabetes Research, Wake Forest University School of Medicine, Winston-Salem, NC 27157, United States
[d] Department of Anaesthesia, Basel University Hospital, Hebelstrasse 20, 4031 Basel, Switzerland
[e] Department of Research, Basel University Hospital, Hebelstrasse 20, 4031 Basel, Switzerland
[f] Department of Biological Chemistry, Graduate School of Pharmaceutical Sciences, Kyoto University, Kyoto 606-8501, Japan
[g] Department of Experimental and Diagnostic Medicine, General Pathology Section, University of Ferrara, Via Borsari 46, 44100 Ferrara, Italy

ARTICLE INFO

Article history:
Received 25 November 2011
Received in revised form 30 December 2011
Accepted 16 January 2012
Available online xxxx

Section Editor: Christiaan Leeuwenburgh

Keywords:
Skeletal muscle
Aging
JP45
Excitation–contraction uncoupling
Food intake
Caloric restriction

ABSTRACT

The decline in muscular strength with age is disproportionate to the loss in total muscle mass that causes it. Knocking out JP45, an integral protein of the junctional face membrane of the skeletal muscle sarcoplasmic reticulum (SR), results in decreased expression of the voltage-gated Ca^{2+} channel, $Ca_v1.1$; excitation–contraction uncoupling (ECU); and loss of muscle force (Delbono et al., 2007). Here, we show that $Ca_v1.1$ expression, charge movement, SR Ca^{2+} release, in vitro contractile force, and sustained forced running remain stable in male JP45KO mice at 12 and 18 months. They also exhibit the level of ECU reported for 3–4-month mice (Delbono et al., 2007). No further decline at later ages was recorded. Preserved ECC was not related to increased expression of any protein that directly or indirectly interacts with JP45 at the triad junction. However, maintained muscle force and physical performance were associated with ablation of JP45 expression in the brain, spontaneous and significantly diminished food intake and less tendency toward obesity when exposed to a high-fat diet compared to WT. We propose that (1) endogenously generated restriction in food intake overcomes the deleterious effects of JP45 ablation on ECC and skeletal muscle force mainly through downregulation of neuropeptide-Y expression in the hypothalamic arcuate nucleus; and (2) the JP45KO mouse constitutes an invaluable model to examine the mechanisms controlling food intake as well as skeletal muscle function with aging.

1. Introduction

Skeletal muscle contraction in response to muscle fiber excitation (sarcolemmal depolarization), termed *excitation–contraction coupling* (ECC), is mediated by a transient elevation in intracellular Ca^{2+} concentration (Melzer et al., 1995). ECC starts at the triad junction, a structure where the transverse (T) tubule and the sarcoplasmic reticulum (SR) terminal cisternae intimately interact via the two major Ca^{2+} channel macromolecular complexes interact, the voltage-gated Ca^{2+} channel $Ca_v1.1$, previously known as $DHPR\alpha_{1S}$ (Catterall et al., 2005), containing both the Ca^{2+}-conducting pore and the voltage-sensing S4 domain, which is localized in the transverse (T) tubule membranes, and the ryanodine receptor (RyR) Ca^{2+}-release channel localized in the SR terminal cisternae. The Ca_v1 is a hetero-oligomeric complex made up of at least four subunits: $Ca_v1.1$, ß1a, α2-δ and γ (Catterall, 1995) and the pore-forming $Ca_v1.1$ subunit is an integral membrane protein and essential for ECC (Melzer et al., 1995). The close proximity of the $Ca_v1.1$ and RyR1 allows sarcolemmal depolarization to rapidly (within ms) translate into SR Ca^{2+} release, prompting formation of contractile myofilament cross-bridges and generating force.

The decline in muscular strength with age is disproportionate to the loss in total muscle mass that largely causes it. This loss of specific force (total force/cross- sectional area) in old age (Gonzalez et al., 2000a) is characterized, in part, by a deficit in Ca^{2+} release following depolarization, a phenomenon known as *excitation–contraction uncoupling (ECU)* (Jimenez-Moreno et al., 2008). We have proposed

Abbreviations: ECU, excitation-contraction uncoupling; JP45, 45kDa junctional protein; $Ca_v1.1$, voltage-gated calcium channel-skeletal muscle isoform; ER, endoplasmic reticulum; SR, sarcoplasmic reticulum; DHPR, dihydropyridine receptor; RyR, ryanodine receptor; NPY, neuropeptide-Y; AgRP, agouti-related peptide; POMC, proopiomelanocortin; TRH, thyrotropin-releasing hormone; CRH, corticotropin-releasing hormone; PVN, paraventricular nucleus; EDL, extensor digitorum longus; FDB, flexor digitorum brevis; Q, charge movement.

* Corresponding author at: Wake Forest University School of Medicine, 1 Medical Center Boulevard, Winston-Salem, NC 27157, United States. Tel.: +1 336 716 9802; fax: +1 336 716 2273.
E-mail address: odelbono@wfubmc.edu (O. Delbono).

0531-5565/$ – see front matter © 2012 Elsevier Inc. All rights reserved.
doi:10.1016/j.exger.2012.01.004

that ECU is not a result of decreased Ca^{2+} stores or RyR1-mediated release function (Jimenez-Moreno et al., 2008) but may be caused by alterations in the functionality and expression of Ca_v1 and its subunits with aging (Renganathan et al., 1997a; Taylor et al., 2009).

A variety of proteins with a putative role in ECC are found at the triad. Our previous studies demonstrated that JP45, a protein integral to the skeletal muscle SR junctional face membrane, interacts with $Ca_v1.1$ and the luminal Ca^{2+}-binding protein, calsequestrin (Anderson et al., 2006; Delbono et al., 2007). $Ca_v1.1$ and JP45 form a complex that is downregulated during aging and may contribute to decayed muscle strength and physical disability in the elderly (Anderson et al., 2006; Wang et al., 2000). Deleting the gene that encodes JP45 results in decreased muscle strength in young mice due to decreased functional expression of the voltage-dependent Ca^{2+} channel $Ca_v1.1$ (Delbono et al., 2007).

These results underscore the importance of JP45 as a molecule involved in the development and maintenance of skeletal muscle strength throughout life. To test this concept, we examined ECC in 12- and 18-month-old JP45 knockout (KO) and wild-type (WT) mice. We hypothesized that ablation of JP45 expression together with diminished $Ca_v1.1$ expression would result in more marked muscle weakness in JP45KO than WT mice with aging. Surprisingly, aging male JP45KO mice exhibit less food intake and significantly lower trend to develop obesity than WT mice when exposed to high-fat diet. As caloric restriction is a powerful antiaging intervention (Mayhew et al., 1998; Marzetti et al., 2008; Sakuma and Yamaguchi, 2010), we reasoned that it mediates protective effects on skeletal muscle protein expression and function in JP45KO mice with aging. Here, we postulate that self-imposed or endogenously developed restriction of food intake accounts for their sustained muscle force, response to highly demanding exercise, and $Ca_v1.1$ expression. We also found that the JP45KO mouse is a model of endogenous, moderate, sustained restriction of food intake, not associated with disease or hibernation. We propose that an imbalance in orexigenic and anorexigenic hypothalamic neuropeptide secretion leads to reduced food consumption and a lean phenotype. This mouse model may prove invaluable in examining the mechanisms controlling food intake and preserving skeletal muscle function with aging.

2. Material and methods

2.1. Flexor digitorum brevis, soleus and flexor digitorum brevis muscle fibers

Extensor digitorum longus (EDL) and *soleus* muscles and single *flexor digitorum brevis* (FDB) fibers were obtained from 12- and 18-month male JP45KO and C57BL6 (WT) mice raised in the Wake Forest University School of Medicine (WFUSM) Animal Research Program. Mice subjected to activity recording and/or training did not participate in more than one experiment. They were killed by cervical dislocation and thoroughly inspected for gross pathology. Animal handling followed a protocol approved by the WFUSM Animal Care and Use Committee.

2.2. Generation of JP45KO mice

JP45KO mice were generated as previously described (27). Briefly, a mouse genomic library (Stratagene) was screened with a cDNA probe to isolate genomic clones encompassing the 5′ end of the JP45 gene. A targeting vector was constructed using a 5′-end JP45 genomic clone, neo-resistance, and the diphtheria toxin gene DT-A as positive and negative selection cassettes, respectively. A SalI-linearized vector was used to transfect J1 mouse embryonic stem (ES) cells, and 140 ES clones carrying a homologous recombination were identified by Southern blot screening. JP45−/− mice were backcrossed three times in a C57BL6 background and then intercrossed to obtain JP45−/− mice. Genotyping was carried out by PCR using the following primers: JP45F2, 5′-TAA AGA CAG AGA CCA CAT CCT CCC-3′; JP45R4, 5′-GAC AAG GGG TGT GGG GTA TGA GGC-3′ (Delbono et al., 2007).

2.3. In vitro muscle force assessment

EDL and soleus muscles were stimulated directly by an electrical field generated between two parallel platinum electrodes connected to a stimulator (Heidelberg Scientific Instruments, Heidelberg, Germany or Grass S48, Warwick, RI). Muscle length was adjusted to the estimate of sarcomere length eliciting maximal twitch and tetanic force (L_o). Rectangular supramaximal pulses (1.5× threshold and 0.5 ms duration) were applied to elicit brief contractions. Trains of pulses of variable frequency, ranging from 10 to 150 Hz, were applied for 400 ms (EDL) or 1100 ms (soleus) to elicit unfused or fused contractions. All the experiments were performed at room temperature (21–23 °C). The solution used for contraction recording contained (mM): NaCl 121, KCl 5, $CaCl_2$ 1.8, $MgCl_2$ 0.5, NaH_2PO_4 0.4, $NaHCO_3$ 24.0, glucose 5.5, and EDTA 0.1. It was permanently bubbled with a mixture of 5% CO_2 and 95% O_2 to attain pH 7.4 in the recording chamber. The interval between trains of pulses was constant (5 min). Force recordings were digitized using an A/D converter (AD Instruments) at 4 kHz. Stimulation pulse waveform was acquired and digitized together with the contraction signal and stored for analysis off-line. Specific force was normalized to the muscle cross-sectional area (CSA = wet weight [mg]/length [mm] × 1.06 [density mg/mm^3]). Muscle length was measured in the recording chamber at L_o by stereoscopic visualization at 30× magnification.

2.4. Charge-movement recordings

FDB fibers from JP45KO and WT mice were enzymatically dissociated, plated, and recorded as previously described (Wang et al., 1999a). For the whole-cell patch clamp, the pipette solution was 140 mM Cs-aspartate, 5 mM Mg-aspartate$_2$, 10 mM Cs2EGTA [ethylene glycol-bis(α-aminoethyl ether)-*N,N,N′N′*-tetraacetic acid], and 10 mM Hepes [*N*-(2-hydroxyethyl)piperazine-*N′*-(2-ethanesulfonic acid)]. The pH was adjusted to 7.4 with CsOH. The external solution contained (mM): 145 tetraethylammonium hydroxide (TEA).Cl, 10 $CaCl_2$, 10 Hepes, and 0.001 tetrodotoxin. Solution pH was adjusted to 7.4 with TEA.OH. For charge-movement recording, Ca^{2+} current was blocked by adding 0.5 Cd^{2+} plus 0.3 La^{3+} to the external solution (Adams et al., 1990; Wang et al., 2000). We recorded $Ca_v1.1$ channel charge movement using a protocol consisting of a 2-s prepulse to −30 mV and a subsequent 5-ms repolarization to a pedestal potential of −50 mV followed by a 25-ms depolarization from −50 mV to 50 mV with 10-mV intervals (Anderson et al., 2006). Intramembrane charge movements were calculated as the integral of the current in response to depolarizing pulses and expressed per membrane capacitance (coulombs per farad). To analyze the relationship between charge movement and membrane voltage, data points were fitted to Eq. (1).

2.5. Sarcoplasmic reticulum Ca^{2+} release

Enzymatically dissociated fibers were transferred to a small, flow-through Lucite chamber positioned on a microscope stage and continuously perfused with the external solution (see below) using a push-pull syringe pump (WPI). Only fibers exhibiting a clean surface and no contracture were used for electrophysiological recordings. Muscle fibers were voltage-clamped using an Axopatch-200B amplifier (Molecular Devices) in the whole-cell configuration of the patch-clamp technique (Hamill et al., 1981). Patch pipettes were pulled from borosilicate glass (Boralex; WPI, Sarasota, FL) using a Flaming Brown micropipette puller (P97, Sutter Instrument Co., Novato, CA) then

Please cite this article as: Delbono, O., et al., Endogenously determined restriction of food intake overcomes excitation–contraction uncoupling in JP45KO mice with aging, Exp. Gerontol. (2012), doi:10.1016/j.exger.2012.01.004

fire-polished to obtain electrode resistances ranging from 450 to 650 kΩ. In the cell-attached configuration, the seal resistance was in the range of 1–4.5 GΩ, and in the whole-cell configuration, values ranged from 75 to 120 MΩ (Wang et al., 1999a).

The pipette was filled with the following solution (mM): 140 Cs-aspartate, 5 Mg-aspartate$_2$, 20 Cs_2EGTA (ethylene glycol tetraacetic acid), 10 HEPES (N-[2-hydroxyethyl]piperazine-N′-[2-ethanesulfonic acid]), and 500 OGB-5N (Invitrogen, Carlsbad, CA), and pH was adjusted to 7.4 with CsOH (Adams et al., 1990; Wang et al., 1999a). The external solution contained (mM): 150 TEA-CH_3SO_3, 2 $MgCl_2$, 2 $CaCl_2$, 10 Na-HEPES, 0.05 N-benzyl-p-toluene sulphonamide (BTS), and 0.001 tetrodotoxin (Delbono et al., 1997). Solution pH was adjusted to 7.4 with CsOH. All the experiments were conducted at room temperature (21–22 °C).

We used OGB-5N for these experiments due to its high quantum yield and suitability for cell imaging with laser confocal microscopy. The fibers were loaded with it via the patch pipette, and it was allowed to diffuse for 20 to 30 min before fiber stimulation and after attaining the whole-cell voltage-clamp configuration. Intracellular OGB-5N transients were recorded using a Bio-Rad Radiance 2100 laser scanning confocal microscope (Zeiss, Oberkochen, Germany). Confocal microscopy allowed us to improve the signal-noise ratio under experimental conditions in which myoplasmic Ca^{2+} concentration was strongly buffered by 20 mM EGTA to ensure a resting myoplasmic Ca^{2+} concentration value that approached the 60 nM in the pipette (Woods et al., 2004). This experimental manipulation also ensured more accurate estimation of the Ca^{2+} release flux.

Fibers were imaged through a C-Apochromat x 40 water-immersion objective (NA 1.2, Zeiss) or a x20 Fluar (NA 0.75) using a krypton-argon laser at 488-nm excitation wavelength. Fluorescence emission was measured at 528 ± 25 nm wavelength. For most experiments, the laser was attenuated to 6–12% with a neutral density filter. Fibers were imaged in line-scan (*x*-*t*) mode, always oriented parallel to the *x* scan direction. Linescan images were acquired with 256 pixels (0.236 μm per pixel) in the *x*- and 512 pixels (0.833 ms per pixel) in the *t*-direction. For image acquisition and intensity profile analysis, we used LaserSharp 2000 (Bio-Rad, Zeiss) and Image-J (NIH), respectively.

2.6. In vivo mouse spontaneous and forced activity

Animals were housed individually in cages equipped with a running wheel carrying a magnet. Wheel revolutions were registered by a reed sensor connected to an I-7053D Digital-Input module (Spectra), and the revolution counters were read by a standard laptop computer via an I-7520 RS-485-to-RS-232 interface converter (Spectra). Digitized signals were processed by the "mouse running" software developed by Santhera Pharmaceuticals.

Forced activity was measured using an Exer 6 lane treadmill (Columbus Instruments, Columbus, OH). Training was as follows. On consecutive days, mice were allowed to run on the treadmill for 5 min at 10 m/min on days 1 and 2 and 5 min at 10 m/min followed by 2 m/min increments until reaching 20 m/min for 2 min each period on day 3. The treadmill was not inclined for the first two days but tilted 5 degrees uphill on the third day. After training, mouse running time was recorded. The initial speed was 10 m/min to a maximum of 5 min, and then we increased the pace by 2 m/min every 2 min to a maximum of 24 m/min or until exhaustion. We considered the mouse exhausted when it remained at least 10 sec in the electric shock area of the treadmill. In all cases, the ramp was tilted 5 degrees uphill. Maximal running time sums all partial times at various paces. For instance, a mouse's maximal running time of 9 min indicates that he ran 5 min at 10 m/min plus 2 min at 12 m/min plus 2 min at 14 m/min and did not reach 16, 18, 20, 22, and 24 m/min. If he reached the highest speed (24 m/min), he was allowed to run with no time limit until exhaustion.

2.7. Microsomal preparation, SR protein composition, and [^{3}H]PN200-110 radioligand binding assay

SR membrane fraction isolation (Saito et al., 1984) and SDS/PAGE analysis were carried out as described (Anderson et al., 2006). [^{3}H]PN200-110 and [^{3}H]ryanodine binding was carried out as described (Delbono et al., 2007). Densitometry of the immunopositive bands used BioRad GelDoc 2000. Curve fitting used Prism4 software (GraphPad). Densitometry was analyzed with NIH ImageJ software. For Western blot analysis of SR proteins, we used anti-SERCA1 and -SERCA2 Abs (Santa Cruz Biotechnology, Santa Cruz, CA), anti-RyR1, antisarcalumenin, and anticalreticulin Abs (Thermo Scientific, Waltham, MA). The anticalsequestrin1 and antiJP45 Abs were developed by our group (Anderson et al., 2003). Protein levels were normalized and expressed as percent of albumin, which was immunodetected using the specific antibody A90-134P (Bethyl Laboratories, Montgomery, TX).

2.8. Fiber-type composition and fiber measurement

EDL and soleus muscles were embedded in OCT, snap-frozen in isopentane, cryosectioned at the midbelly region (10 μm), and mounted on coverslips for immunostaining. Mounted sections were air-dried, treated with PBS containing 1% BSA and 2% horse serum for 30 min, and incubated overnight at 4–8 °C with a PBS solution containing 0.01% Triton X100, 1% BSA, 2% horse serum, 0.5% μg/ml antimouse slow myosin heavy chain (MAB 1628, Millipore, Billerica, MA), and 2 μg/ml antirat α-laminin (MAB1914, Millipore). Sections were then washed with PBS four times for 15 min each and incubated at room temperature for 40 min with a PBS-containing Alexa Fluor 488 antimouse IgG Ab (2 μg/ml) and Cy3 antirat IgG Ab (0.5 μg/ml). After incubation in the secondary Ab, sections were washed with PBS four times for 15 min each, dehydrated with ethanol, and mounted using a glycerol medium at room temperature. They were then imaged using a Leica DM5000B fluorescence microscope. Muscle fiber analysis (Soft Imaging System, Muenster, Germany) determined: (1) boundaries, using laminin immunofluorescence; (2) diameter, using the minimal Feret's diameter (distance between parallel tangents at opposing borders); (3) percent positive to anti-MHC IAb; and (4) percent negative to anti-MHC I Ab staining.

2.9. Insulin and leptin determinations

Serum insulin and leptin levels were measured using rat insulin enzyme-linked immunosorbent assay (ELISA) and mouse leptin ELISA kits (Crystal Chem, Downers Grove, IL), respectively (Shi et al., 2006).

2.10. Mouse brain immunocytochemistry

JP45 and WT mice were deeply anesthetized with ketamine (200 mg/kg weight) and xylazine (10 mg/kg) and perfused first with 15 ml normal saline and then 10 ml 4% PFA in 0.1 M sodium phosphate buffer (PB) at pH: 7.4 through left ventricle, following published procedures (Hu et al., 2009). The brain was dissected and immersed in the 4% PFA buffer for 24 h at 4 °C and then exchanged with fresh PFA and left for another 24 h. The brain was rinsed in 10% sucrose in 0.1 M PB for 24 h and then in 20% for another day. It was then positioned in an embedding mold, covered with tissue freezing medium TBS (Triangle Biomedical Sciences, Durham, NC), and frozen in dry ice. Coronal sections (40 μm) were obtained using a Leica (Bannockburn, IL) cryostat. Brain sections were dried at room temperature and stored at −80 °C. Slides containing various brain slices were rinsed in 4% PFA for 15 min at room temperature and washed three times with PBS, permeabilized in 0.5% triton and 1% goat serum in PBS for 15 min at room temperature, followed by three washes with PBS and blocked in 10% goat serum at 4 °C

Please cite this article as: Delbono, O., et al., Endogenously determined restriction of food intake overcomes excitation–contraction uncoupling in JP45KO mice with aging, Exp. Gerontol. (2012), doi:10.1016/j.exger.2012.01.004

overnight. Slides were rinsed with PBS and incubated in JP45 antibody for 4 h and then exposed to the secondary goat anti-rabbit Alexa Fluor 594 antibody (Invitrogen). Preparations were mounted using Dako (Carpinteria, CA) mounting medium and examined with an IX81 Olympus microscope controlled by Olympus MetaMorph.

2.11. Dissection of hypothalamic regions

Hypothalamic regions were dissected as previously described (Xue et al., 2009). Briefly, each hypothalamic region was dissected from 1-mm-thick sagittal sections of fresh mouse brain. Arcuate (ARH) and paraventricular (PVN) hypothalamus were dissected from the first sections from the midline of the brain. Coordinates for each hypothalamic region were described previously (Xue et al., 2009).

2.12. Quantitative real-time RT-PCR

Total RNA was isolated from hypothalamus using Tri-Reagent according to the manufacturer's instructions (Molecular Research Center, Cincinnati, OH). Messenger RNAs of specific genes were quantified by real-time RT-PCR using TaqMan One-step RT-PCR Master Mix (Applied Biosystems) and a Stratagene Mx3000P system (Stratagene, La Jolla, CA). The sequences for each primer/probe set are included in Table 1.

2.13. Statistical analysis

Data are presented as means ± S.E.M. and were analyzed with *Student t*-test, Mann–Whitney rank sum test, or one- or two-way repeated measures ANOVA when appropriate. An alpha value of $P<0.05$ was considered significant.

3. Results

3.1. Mechanical properties of EDL and soleus muscles from 12- and 18-month JP45KO and WT mice

Previous work from our laboratory demonstrated that ablating the SR protein JP45 leads to loss of absolute and specific skeletal muscle force in young (3–4-month) mice (Delbono et al., 2007) (Fig. 1A). Here, we report that the difference in tetanic force between 12-month JP45KO and WT mice is significant only for extensor digitorum longus (EDL), and that all mechanical properties recorded at 18-month JP45KO and WT mice do not differ significantly (Fig. 1A). Changes in the force–frequency curve do not account for their similar force response to brief and tetanic stimulation; a wide range of frequencies were tested per muscle (10, 20, 40, 100, 120, and 150 Hz), and the maximal force output was recorded at the same frequency, 150 and 100 Hz for EDL and soleus muscles, respectively, regardless of genetic background or age.

Muscle weight between JP45KO and WT mice at 12 and 18 months of age did not differ significantly. Values expressed in mg, as mean ± SD, were: EDL WT 12 months = 14 ± 1.5; EDL WT 18 = 13 ± 1.2; soleus WT 12 = 10 ± 1.7; soleus WT 18 = 11 ± 1.5; EDL JP45KO 12 = 14 ± 1.7; EDL JP45KO 18 = 13 ± 1.3; soleus JP45KO 12 = 10 ± 1.3; and soleus JP45KO 18 = 11 ± 1.4.

These results support the concept that the difference in muscle force between 3-4-month JP45KO and WT disappears with aging.

Table 1
Primer sequences for real-time PCR.

Neurotransmitter	Primers
Agouti related protein (AGRP)	5′-GCGGAGGTGCTAGATCCA-3′ (forward) 5′-AGGACTCGTGCAGCCTTA-3′ (reverse) 5′-CGAGTCTCGTTCTCCGCG-3′ (probe)
Neuropeptide-Y (NPY)	5′-CTCCGCTCTGCGACACTAC-3′ (f) 5′-AATCAGTGTCTCAGGGCT-3′ (r) 5′-CAATCTCATCACCAGACAG-3′ (p)
Pro-opiomelanocortin (POMC)	5′-ACCTCACCACGGAGAGCA-3′ (f) 5′-GCGAGAGGTCGAGTTTGC-3′ (r) 5′-TGCTGGCTTGCATCCGGG-3′ (p)
Thyrotropin-releasing factor (TRH)	5′-CTCTTCTCTCTGACAGCCC-3′ (f) 5′-AGGCGTGGAAGAACCGTC-3′ (r) 5′-TCTCTCGCCCCTTCGACAC-3′ (p)
Corticotropin-releasing hormone (CRH)	5′-GGAGCCGCCCATCTCTCT-3′ (f) 5′-CCGGGCCATTTCCAAGAC-3′ (r) 5′-ATCTCACCTTCCACCTTCTGCGGGA-3′ (p)
Ribosomal 18S	5′-AGTCCCTGCCCTTTGTACACA-3′ (f) 5′-GATCCGAGGGCCTCACTAAAC-3′ (r) 5′-CGCCCGTCGCTACTACCGATTGG-3′ (p)

Since deleting the gene encoding JP45 decreases muscle strength in young mice by diminishing functional expression of the voltage-dependent Ca^{2+} channel $Ca_v1.1$ (Delbono et al., 2007), we examined the functional and biochemical expression of this subunit in 12- and 18-month JP45KO and WT mice.

3.2. $Ca_v1.1$ charge movement and content in total SR membrane from JP45 KO and WT mice

Charge movement, which represents functional expression of $Ca_v1.1$ in the T tubule, was recorded in flexor digitorum brevis (FDB) fibers in the whole-cell configuration of patch-clamp (Hamill et al., 1981; Wang et al., 2000). Although in vitro muscle force was recorded in EDL and soleus muscles, charge movement was recorded in FDB muscle because its short fibers allow voltage-clamping in the whole-cell configuration and undergo age-dependent changes similar to those described for longer hindlimb muscles (Gonzalez et al., 2000a).

The current recorded after blocking the Ca^{2+} current is the intramembrane charge movement. Saturated at both extremes of the voltage range, the amount of charge moved during depolarization (Q_{on}) is equal to the charge that returns during repolarization (Q_{off}), which has been demonstrated for adult skeletal muscle fibers recorded in the whole-cell configuration of the patch-clamp technique (Wang et al., 1999a). We used a protocol consisting of a 2-s prepulse to −30 mV and a subsequent 5-ms repolarization to a pedestal potential of −50-mV, followed by a 25-ms depolarization from −50 to 50-mV with 10-mV intervals (Adams et al., 1990). The membrane potential was held at −80 mV between pulses. The optimal duration of the prepulse is defined as the value at which charge immobilization ceases, or 2 s after testing a range of prepulses from 1 to 6-s. Fig. 1B shows $Ca_v1.1$ charge movement for 3-, 12- and 18-month JP45KO and WT mice. To analyze the voltage-dependence of the charge, data points were fitted to a Boltzmann equation of the form:

$$Q_{on} = Q_{max} / \left[1 + \exp\left(V_{1/2Q} - V_m\right)/K\right], \quad (1)$$

Fig. 1. Skeletal muscle force, $Ca_v1.1$ charge movement and content in total SR membrane from JP45 KO and WT mice. A. Twitch, tetanic force, and specific force recorded in WT and JP45KO EDL and soleus muscles. The number of muscles tested was: EDL WT 3 [months] = 17; EWT12 = 14; EWT18 = 12; soleus [S] WT 3 = 15; SWT 12 = 13; SWT18 = 9; EDL JP45KO [KO] 3 = 16; EKO12 = 14; EKO18 = 16; SKO3 = 14; SKO12 = 15; and SKO18 = 11. Data points are expressed as mean ± SD. *ANOVA test $P<0.05$. Data for 3-month-old WT and JP45KO mice are from (Delbono et al., 2007). B. $Ca_v1.1$ charge movement recorded after blocking the inward Ca^{2+} current. Data points were fitted to Eq. (1). Table 2 shows best-fitting parameters. C. [^{3}H]-PN200-110 binding assay. R1 fraction proteins from 18-month JP45KO and WT mice were separated by 7.5% PAGE, blotted, and stained with a peroxidase-conjugated antibody against albumin (see Material and methods). Albumin content was measured by densitometry of the protein band. Data of 20–24 determinations carried out in three different total SR fraction preparations. Data for 3-month-old mice are from (Delbono et al., 2007). Data points represent mean ± S.E.M.

Please cite this article as: Delbono, O., et al., Endogenously determined restriction of food intake overcomes excitation–contraction uncoupling in JP45KO mice with aging, Exp. Gerontol. (2012), doi:10.1016/j.exger.2012.01.004

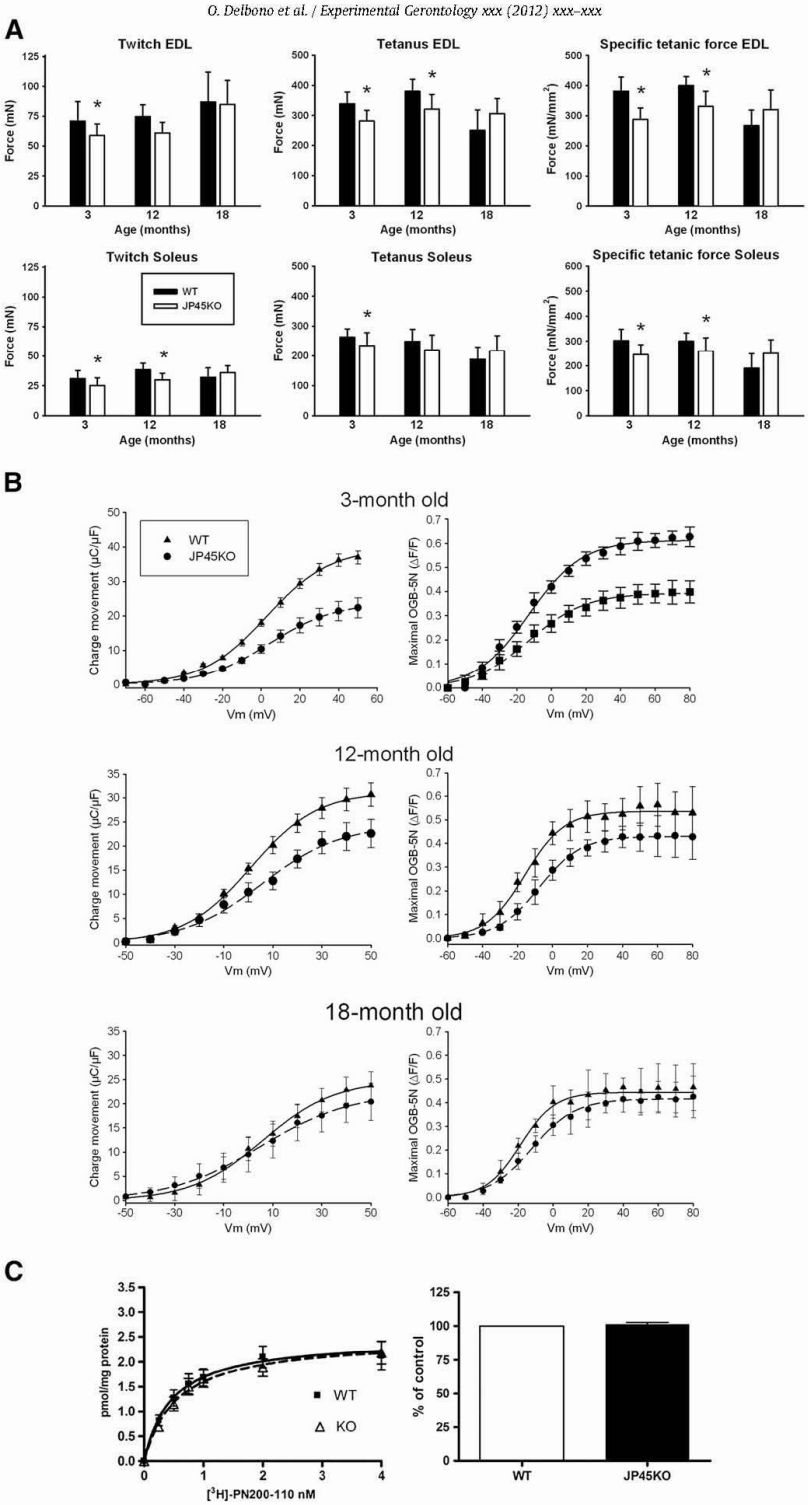

Please cite this article as: Delbono, O., et al., Endogenously determined restriction of food intake overcomes excitation–contraction uncoupling in JP45KO mice with aging, Exp. Gerontol. (2012), doi:10.1016/j.exger.2012.01.004

where Q_{max} is the maximal charge; V_m is the membrane potential; $V_{1/2Q}$ is the charge movement half-activation potential; and K is the steepness of the curve. Table 2 includes the best-fitting parameters for Q_{max}, $V_{1/2Q}$, and K. Values significantly differed for 3- and 12- but not 18-month mice, consistent with the in vitro contraction results reported above.

To determine whether the lack of difference in charge movement results in similar intracellular Ca^{2+} mobilization, we recorded SR Ca^{2+} release. Single FDB fibers were loaded with Oregon-green-bapta-5N (OGB-5N) via the patch pipette, and intracellular Ca^{2+} was recorded using a confocal microscope in the line-scan mode.

To determine the voltage-dependence of intracellular Ca^{2+} release, we applied 40-ms depolarizing voltage steps from the holding potential (−80 mV) to command potentials ranging from −60 to 80 mV. Data points were fitted to a Boltzmann equation of the form:

$$F = F_{max}/\left[1 + \exp\left(V_{1/2F} - V_m\right)/K\right], \quad (2)$$

where F_{max} is the maximum charge; and $V_{1/2F}$ is the Ca^{2+} fluorescence half-activation potential. Table 2 shows the best fitting parameters for F_{max},$V_{1/2F}$, and K recorded in muscle fibers from 3-, 12- and 18-month JP45KO and WT mice. No statistically significant difference in SR Ca^{2+} release was recorded between 12-month JP45KO and WT mice, indicating that the significantly different charge movement recorded is not sufficient to compromise intracellular Ca^{2+} mobilization and its voltage-dependent activation. The lack of difference in SR Ca^{2+} release correlates with the similar charge movement recorded in 18-month mice (Fig. 1B).

$Ca_v1.1$ content was assessed by radioligand-binding assay and normalized to albumin content in muscle SR fraction (Fig. 1C). Maximal [^{3}H]-PN200-110 binding number did not differ significantly between 18-month JP45KO and WT mice. Albumin was measured by densitometry of the protein band detected with an albumin antibody and used as a specific protein marker for T-tubule membranes. Data points represent the mean ± S.E.M. of 20–24 determinations carried out in three different SR fraction preparations. Results are consistent with the lack of difference in charge movement and intracellular Ca^{2+} release between JP45KO and WT mice at 18 months.

3.3. Age-dependent JP45 expression in WT and SR protein composition in JPKO mice

We examined JP45 expression in 3–18 month-old WT mice. Adding a third time point (6 months) helped us to define a steady decline in protein expression from the early to late ages (Fig. 2A and B). We also analyzed the levels of specific molecules expressed in the SR membrane and lumen to determine whether an increase in any of them compensates for the lack of JP45 expression in JP45KO mice with aging. Fig. 2C-D shows expression of the SR Ca^{2+} release channel RyR and sarcoplasmic/endoplasmic reticulum Ca^{2+} pump-1 and -2 (SERCA1/2). Protein expression was normalized to albumin levels. Albumin was selected as a reference because we did not observe a significant difference in its content in the isolated sarcotubular membrane fractions from JP45KO and WT mice (Delbono et al., 2007). We also examined sarcalumenin, a major luminal Ca^{2+}-binding protein that mediates ion shuttling in the longitudinal SR; calreticulin, a low-affinity, high-capacity Ca^{2+}-binding protein; and calsequestrin, an SR terminal cisternae Ca^{2+}-binding protein with significant influence on SR Ca^{2+} release. None of these proteins differed significantly in 12- (C) or 18- (D) month JP45KO mice. Thus, compensatory overexpression of the major triadic proteins as a result of JP45KO is unlikely, but we cannot rule out a role for minor triadic proteins (see Discussion).

3.4. Spontaneous and forced activity in JP45KO and WT mice

To determine whether sustained skeletal muscle contraction force in JP45KO mice improves whole body performance, we tested their spontaneous and forced activity compared with that of age-matched WT littermates. Fig. 3A shows running distance over 10 s. recorded from 5 P.M. to 5 A.M in JP45KO (triangles) and WT (squares) mice. In contrast to 3–4 months (Delbono et al., 2007) (A), total spontaneous running distance decreased approximately 70% in 12- (B) and 18- (C) month mice, with a negligible difference between types.

To measure physical performance and endurance independent of motivation, we examined forced mechanical activity in JP45KO and WT mice (Fig. 3D). After a training period, mice were subjected to the experimental running program described below (Material and methods). Young (2–3 month) WT mice tend to run longer than JP45KO, consistent with the weaker in vitro muscle contraction recorded in JP45KO. This trend is no longer apparent at 12–14 months and reversed at 18 months, when JP45KO mice run longer (15.9 ± 0.9 m/min) than WT mice (11.8 ± 0.6) ($P<0.01$); while WT mice reach a pace of 18 m/min, JP45KO mice average 22 m/min. We conclude that the sustained charge movement, $Ca_v1.1$ expression, and in vitro contraction force recorded in JP45KO mice sustains their physical performance across ages.

3.5. Body weight, food intake, and high-fat diet

Similar spontaneous activity and age-dependent forced activity, maintained in JP45KO but declining in WT mice, prompted us to examine their body weight and food intake because calorie restriction has been reported to preserve skeletal muscle function in rodents (Mayhew et al., 1998). Fig. 3E shows body weight recorded in JP45KO and WT mice at 3, 4, 12 and 18 months. JP45KO mice weigh significantly less than WT mice at all ages. Reduced food intake is explained by the fact that JP45KO mice ate significantly less than WT mice during 20 days of observation at 12 months (Fig. 3F) and 18 months (Fig. 3G) of age. The significant decrease in body weight in JP45KO compared with WT indicates that decreased food intake in the former starts at early ages.

A linear regression analysis examined the relationship between ECC measurements and food intake in 18-month-old JP45KO mice.

Table 2
Best-fitting parameters describing the voltage dependence of charge movement and intracellular Ca^{2+} release in FDB fibers from WT and JP45KO mice.

Charge movement				Intracellular Ca^{2+}		
Mice	Q_{max}, μC/μF	$V_{1/2Q}$, mV	K	$\Delta F/F_{max}$	$V_{1/2F}$, mV	K
3-M WT[a] (n = 15–17)	30.5 ± 3.4	7.6 ± 0.92	14.2 ± 1.8	0.61 ± 0.08	12.9 ± 0.19	15.4 ± 1.8
3-M JP45KO[a] (n = 16–20)	17.8 ± 2.6#	6.4 ± 0.75	12.0 ± 1.5	0.39 ± 0.06#	13.0 ± 0.15	16.3 ± 1.9
12-M JP45KO (n = 10)	24.4 ± 0.8	5.6 ± 1.7	16 ± 1.2	0.43 ± 0.03	7.5 ± 0.51	11.9 ± 0.44
12-M WT (n = 11)	31.2 ± 0.5#	1.1 ± 1.8	13.6 ± 1.6	0.54 ± 0.06	15.7 ± 0.9	11.3 ± 0.75
18-M JP45KO (n = 12)	24.9 ± 0.6	5.9 ± 1.1	14.7 ± 0.8	0.42 ± 0.05	6.9 ± 0.9	12.3 ± 0.74
18-M WT (n = 14)	22.4 ± 0.5	5.1 ± 1.3	8.6 ± 0.8	0.44 ± 0.07	7.6 ± 1.2	9.8 ± 1.0

Values are mean ± SEM. "n" indicates the number of fibers.
[a] Data from ref. (Delbono et al., 2007).
# $P<0.05$ statistically significant difference between WT and JP45KO mice.

Please cite this article as: Delbono, O., et al., Endogenously determined restriction of food intake overcomes excitation–contraction uncoupling in JP45KO mice with aging, Exp. Gerontol. (2012), doi:10.1016/j.exger.2012.01.004

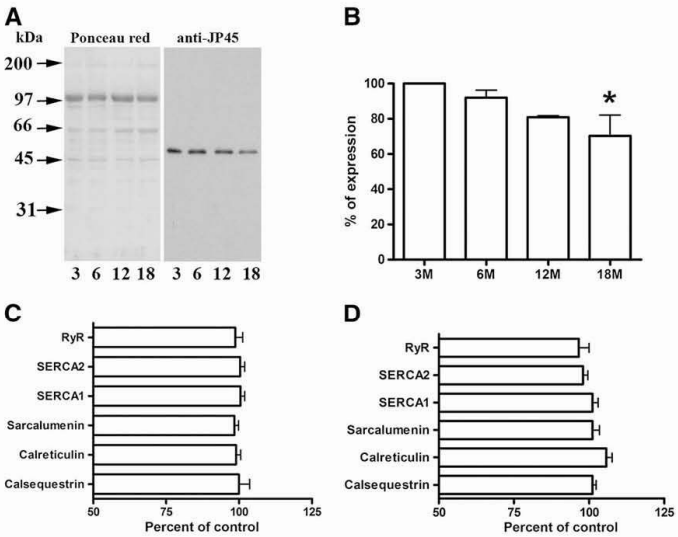

Fig. 2. Age-dependent JP45 expression in WT and SR protein composition in JPKO mice. A. Western blot analysis of JP45 expression in microsomes from 3, 6, 12, and 18 month-old WT mice. B. JP45 expression at 6–18 months is represented as a percent at 3 months ($n=3$). The asterisk indicates a statistically significant difference at 18 compared with 3 month-old mice ($p<0.05$). Immunoblot analysis of SR fraction protein expression in 12- (C) and 18- (D) month JP45KO mice. Total SR (15 μg) was separated on SDS gel and transferred to nitrocellulose membrane ($n=12$–14 determinations in 2–3 SR membrane preparations). Data are expressed as a percent of albumin expression. Data for 3-month-old mice are from (Delbono et al., 2007). Values represent mean ± S.E.M.

A negative relationship was observed between specific tetanic force (Pearson correlation coefficient, $r=-0.443$) or maximal charge movement ($r=-0.563$) and foot intake, which further supports the concepts that endogenously determined restriction in food intake enhances specific force and $Ca_v1.1$ expression.

To further examine their eating habits, we exposed 5-week JP45KO and WT mice to a high-fat diet (D12492 rodent diet with 60 kcal% fat; Research Diets, New Brunswick, NJ) for 33 weeks. Initially, the increase in body weight was similar but differed significantly at week 15, indicating that JP45KO mice are less susceptible than WT to obesity, even when challenged by a high-fat diet (Fig. 3H). We applied the diet at this early age, rather than when JP45KO consume significantly less food than WT (12- or 18-month), based on previous observations that very young mice are more prone to develop obesity when offered a high-fat diet (Shi et al., 2004). This indicates that JP45KO exhibits less tendency to develop obesity than WT mice.

3.6. Muscle fiber-type composition

To determine whether sustained force in JP45KO mice results from changes in muscle fiber-type composition, we examined MHC isoforms in EDL and soleus muscles from 12- and 18-month JP45KO and WT mice (Fig. 4). All EDL fibers are type-II, and our immunostaining technique found no type-I fibers (Fig. 4A, B). Soleus muscles showed more fast- than slow-twitch fibers at both ages. We found no significant difference in MHC I or MHC II between JP45KO and WT mice at 12 months (Fig. 4A, C), but at 18 months, fiber-type profile analysis showed increased slow- and decreased fast-twitch fibers (Fig. 4B, D). These results indicate that JP45KO does not prevent the typical switch in fiber-type profile reported for aging skeletal muscle (Larsson, 1995).

3.7. EDL and soleus muscle fiber size from JP45KO and WT mice

To examine whether age-dependent changes in fiber size influence muscle performance in vivo and in vitro, we analyzed the distribution in EDL and soleus fibers from 12- and 18-month JP45KO and WT mice (Fig. 4). EDL (E) and soleus (F) fiber diameter ranged from 15 to 75 μm and 25 to 75 μm, respectively, with more fibers at 55 μm for both muscles from 12-month mice. JP45KO and WT mice did not differ (G); the range of fiber diameters at both ages was similar. The higher percent of EDL (H) and soleus (I) fibers from 18-month mice was 40 and 45 μm, respectively. We detected no significant difference between 18-month JP45KO and WT mice (J). These results indicate that JP45KO does not affect age-related changes in fiber size distribution.

Fig. 4 also shows soleus muscle fiber diameter distribution based on MHC composition in the mice at both ages. MHC I fibers ranged from 35 to 75 μm, with a maximum of 55 μm for WT and 40 μm for JP45KO mice at 12 months ($P<0.05$) (K). This shift toward smaller fibers is also apparent at 12 months for MHCII (K), though not statistically significant. Similarly, type I (L) and II (N) fibers peak at 45 μm for 18-month JP45KO and WT mice, and no significant difference was observed at 12 months (N). At 18 months, for type II fibers in soleus muscle, the percent of 45 μm increased and 50 μm decreased. These results are unlikely to explain the sustained fiber force and endurance in aging JP45KO mice.

3.8. Insulin and leptin determinations

Insulin and leptin concentrations were determined in 4–24 month mice. Fig. 5 shows individual determinations of leptin (A, C) or insulin (B, D) as a function of age (A, B) and mouse weight (C, D). Serum leptin but not insulin increases as a function of age and body weight. Leptin concentration, expressed as mean ± SEM, for all mice 11-month or older was: 11.7 ± 2.2 ng/ml ($n=8$) and 13.6 ± 2.4 ($n=10$) for WT and JP45KO mice, respectively, while insulin was 2.8 ± 0.9 ng/ml ($n=10$) and 3.2 ± 1.2 ($n=12$). No statistically significant differences between JP45KO and WT were found. These results indicate that JP45 ablation does not modify leptin or insulin secretion with aging.

Please cite this article as: Delbono, O., et al., Endogenously determined restriction of food intake overcomes excitation–contraction uncoupling in JP45KO mice with aging, Exp. Gerontol. (2012), doi:10.1016/j.exger.2012.01.004

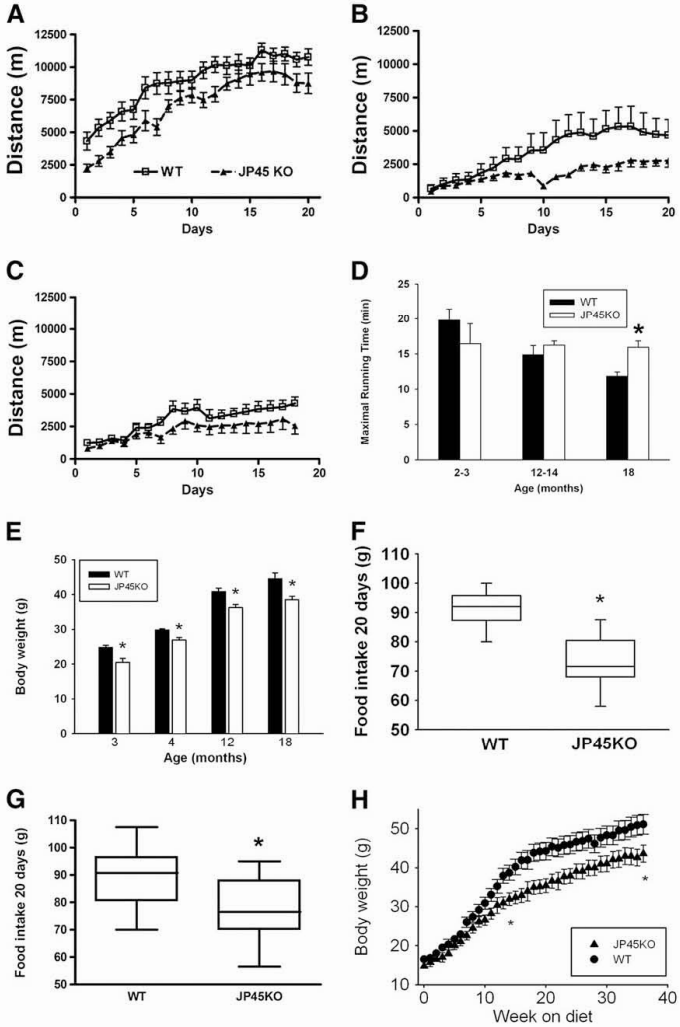

Fig. 3. Spontaneous and forced activity, body weight and food intake in JP45KO and WT mice. Dark phase (5 P.M.–5 A.M.) running distance assessed in 3- (A), 12- (B) and 18- (C) month JP45KO (triangles) and WT (squares) mice, housed and equipped individually. Speed events represent the running distance over 10 s. Data points from 3 (n = 12–14), 12 (n = 7–8) and 18 (n = 9–10) month-old mice. D. Maximal running time was measured using a forced treadmill. Data are compared with the 2–3-month-old mouse cohort. Data are mean ± S.E.M. for 2–3 (n = 6), 12–14 (n = 6), and 18 (n = 5) month-old mice. E. Body weight recorded in 3-month WT (n = 11) and JP45KO (n = 12); 4-month WT (n = 13) and JP45KO (n = 15); 12-month WT (n = 30) and JP45KO (n = 11) mice; and 18-month WT (n = 9) and JP45KO (n = 16) mice. *ANOVA test $P<0.05$. F. Food consumed over a 20-day period by 13 JP45KO and 14 WT mice at 12 months of age. * $p<0.05$. G. Food consumed over a 20-day period by 10 JP45KO and 10 WT mice at 18 months of age. * $p<0.05$. H. Mouse body weight recorded at 5 weeks and for the next 33 weeks. Data points represent mean ± S.E.M of 6 JP45KO and 5 WT mice. Differences between asterisks are statistically significant.

3.9. JP45 expression in the hippocampus and proposed model for hypothalamic neuropeptide network operation

A previous report supports the lack of JP45 expression in total microsomal and mRNA from the mouse brain (Anderson et al., 2003), however, we re-examined this tenet using immunocytochemistry based on the possibility JP45 expression may be restricted to small areas and/or below the level of immunodetection in the whole brain. Fig. 6 illustrates JP45 expression in the hyppocampal nuclei of 3–4-month WT (A) and JP45KO (B) mice in brain coronal sections

Fig. 4. Fiber-type composition and fiber size in EDL and soleus muscle, and MHC fiber size distribution in soleus muscle from JP45 KO and WT mice. Myosin-heavy chain I (MHCI) composition in EDL and soleus muscles from (A, C) 12- and (B, D) 18-month-old mice. Fiber-type composition determined by myosin-heavy chain (MHC) immunocytochemistry in E[DL] WT 12 [months] = 4; EWT18 = 4; S[oleus]WT12 = 4; SWT18 = 4; E[JP45]KO12 = 4; EKO18 = 4; SKO12 = 4; and SKO18 = 4. Asterisks indicate statistically significant differences between JP45KO and WT mice ($P<0.05$). EDL (E) and soleus (F) fiber size distribution and average minimal fiber Feret (G) in 12-month JP45KO and WT mice. EDL (H) and soleus (I) fiber size distribution and average minimal fiber Feret (J) in 18- month JP45KO and WT mice. The number of fibers analyzed was: EWT12 = 1026; EKO12 = 1213; SWT12 = 869; SKO12 = 844; EWT18 = 1372; EKO18 = 1460; SWT18 = 1171; and SKO18 = 1377. MHC I distribution in (K) 12- and (C) 18-month JP45KO and WT mice and MHC II distribution in (L) 12- and (D) 18-month JP45KO and WT mice. For 12-month WT and JP45KO mice, the number of MHC I fibers studied was 376 and 220, respectively (A); MHC II fibers, 493 and 319, respectively (B). For 18-month WT and JP45KO mice, the number of MHC I fibers was 417 and 594, respectively (M); MHC II, 759 and 778, respectively (N). Values represent mean ± S.E.M.

Please cite this article as: Delbono, O., et al., Endogenously determined restriction of food intake overcomes excitation–contraction uncoupling in JP45KO mice with aging, Exp. Gerontol. (2012), doi:10.1016/j.exger.2012.01.004

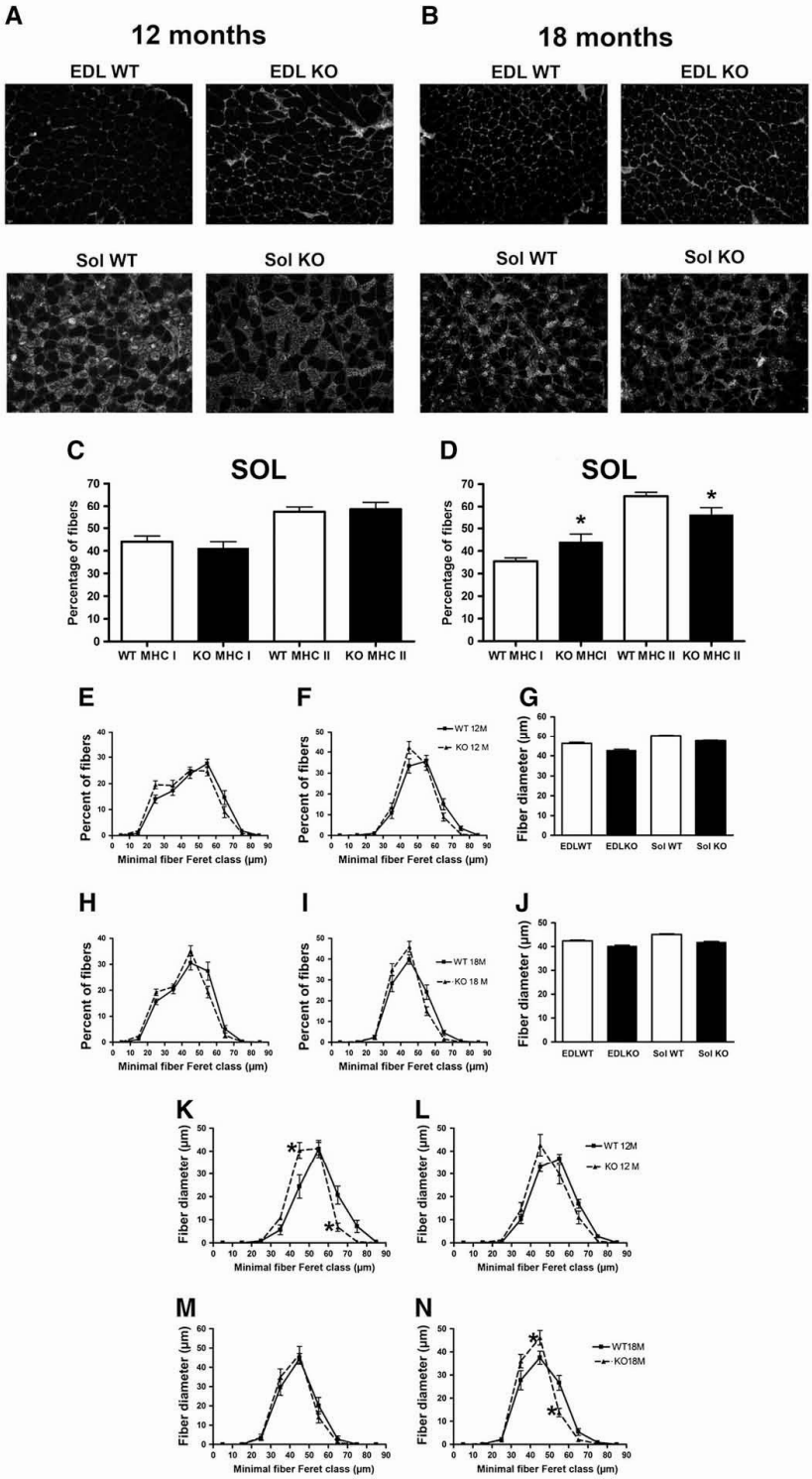

Please cite this article as: Delbono, O., et al., Endogenously determined restriction of food intake overcomes excitation–contraction uncoupling in JP45KO mice with aging, Exp. Gerontol. (2012), doi:10.1016/j.exger.2012.01.004

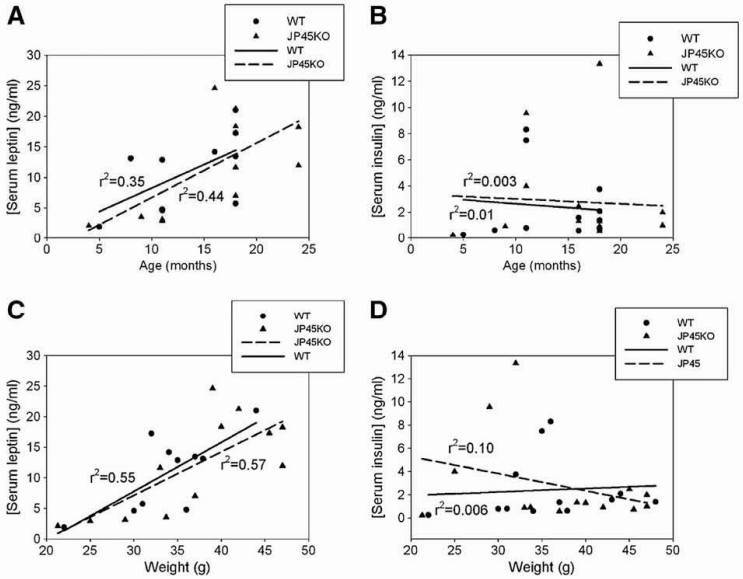

Fig. 5. Serum leptin and insulin concentration in JP45KO and WT mice. Individual serum leptin concentration determination as a function of age (4–24 months) (A) or mouse weight (C). Serum insulin concentration as a function of age (B) or weight (D). Linear regression lines for JP45KO and WT mice are superimposed.

near the third ventricle. The dotted JP45 fluorescence pattern indicates intracellular and probably organelle-associated expression. The specificity of the signal was tested by omitting the JP45 primary antibody (C) or replacing it with rabbit IgG (D). These results support the concept that JP45 is expressed in the brain and may be associated with the food intake central circuitry. To examine whether JP45 ablation alters neuropeptide expression, we performed quantitative real-time PCR for neuropeptide-Y (NPY), agouti-related peptide (AgRP), pro-opiomelanocortin (POMC) (E), thyrotropin-releasing hormone (TRH), and corticotropin-releasing hormone (CRH) (F) in isolated arcuate (ARH) and paraventricular (PVN) hypothalamic nuclei and measured their transcript. Significantly decreased neuropeptide-Y (NPY) and possibly agouti-related peptide (AgRP) but not pro-opiomelanocortin (POMC), were associated with increased thyrotropin-releasing hormone (TRH), and corticotropin-releasing hormone (CRH). We propose a model in which JP45 ablation reduces endoplasmic reticulum (ER) Ca^{2+} release and Ca^{2+} influx through voltage-gated Ca^{2+} channels, resulting in reduced NPY and AgRP but not POMC expression in ARH neurons, leading to increased TRH and CRH in PVN neurons, reduced food intake, and the lean JP45KO mouse phenotype (G).

4. Discussion

This work's main conclusion is that at 12 and 18 months, in contrast to WT mice, forced running and in vitro contractility in JP45KO mice was similar to 3–4 month mice. This maintained in vivo and in vitro muscle performance was associated with stable $Ca_V1.1$ expression, charge movement, and SR Ca^{2+} release. JP45KO mice at 12 and 18 months exhibited the same level of ECU reported for 3-4-month mice (Delbono et al., 2007). Moreover, their preserved ECC was associated with significantly diminished food intake, body weight, less tendency to develop obesity when exposed to a high-fat diet, and ablation of JP45 expression in the brain. We propose that JP45 ablation impairs intracellular Ca^{2+}, resulting in selective NPY and AgRP expression in ARH neurons, reduced food intake, and the lean JP45KO mouse phenotype.

4.1. Sustained skeletal muscle performance with aging recorded in vivo and in vitro in JP45KO mice

Aging is characterized by reduced skeletal muscle mass and specific force in mammalian species, including humans (Delbono, 2011; Gonzalez et al., 2000a). EDL and soleus muscle twitch and absolute tetanic force are significantly reduced in 12-month JP45KO compared to WT mice. However, tetanic absolute and specific force in both EDL and soleus muscle, which differ significantly between JP45KO and WT mice at 3–4 months (Delbono et al., 2007), do not differ significantly at 12 and 18 months. Previous work from our and other laboratories showed a decrease in EDL, soleus (Gonzalez et al., 2000b), and FDB (González et al., 2003) muscle fiber specific force with aging and proposed ECU as the underlying mechanism. Other theories include contraction-induced injury and posttranslational modifications of contractile proteins. Although contraction-induced injury after lengthening contractions has been reported in humans and reproduced in animal models (Faulkner and Brooks, 1995), diminished specific force has been recorded in the absence of this stress (Gonzalez et al., 2000a; González et al., 2003), suggesting that other mechanisms must be operating as well. The lack of change in specific force in manually skinned mouse EDL fibers, where activation of $Ca_V1.1$/RyR coupling was bypassed, argues against the proposal that posttranslational modifications in aging muscle switch contractile proteins from strongly to weakly bound actomyosin (for a review see (Delbono, 2011).

The data reported here support the conclusion that contraction efficiency depends on ECC. $Ca_V1.1$ expression, which is significantly lower in muscles from JP45KO mice at 3–4 months, is no lower at 18 months. Intramembrane $Ca_V1.1$ charge movement and SR Ca^{2+} release do not differ significantly. The notion that $Ca_V1.1$ expression declines during old age is supported by several studies (Ryan et al., 2000; O'Connell et al., 2008). Note that $Ca_V1.1$ mRNA does not decrease

Please cite this article as: Delbono, O., et al., Endogenously determined restriction of food intake overcomes excitation–contraction uncoupling in JP45KO mice with aging, Exp. Gerontol. (2012), doi:10.1016/j.exger.2012.01.004

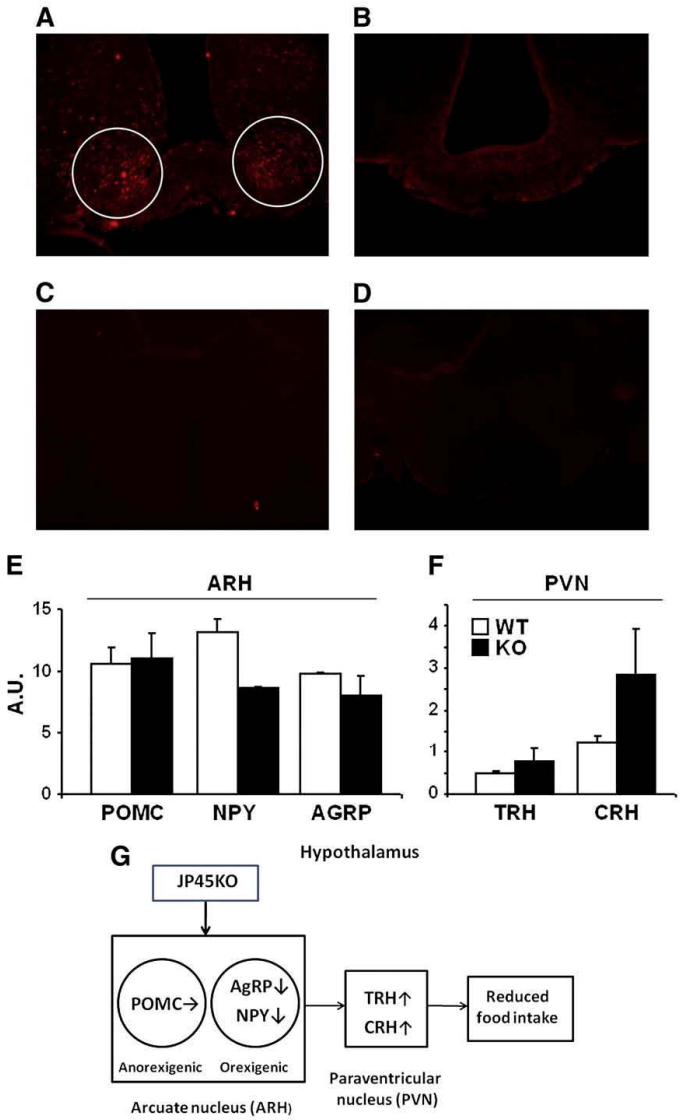

Fig. 6. JP45 expression in hipothalamus, effect of JP45 ablation on hypothalamic neuropeptide expression and proposed model for neuropeptide network operation in JP45KO mice. Brain coronal sections showing JP45 expression in the arcuate nucleus of the hypothalamus of a WT mouse (A) and JP45KO mouse (B). Whole WT brain coronal sections in which the JP45 primary antibody was omitted (C) or replaced by rabbit IgG (D). Images are representative of brains from JP45KO ($n=3$) and WT ($n=3$) mice. (E) Expression of POMC, NPY and AGRP in arcuate hypothalamus (ARH). (F) Expression of TRH and CRH in paraventricular hypothalamus (PVN). Dissection of hypothalamic regions and measurement of gene expression have been described in Material and methods. Gene expression was normalized to 18S ribosomal RNA level. Data are expressed as mean ± S.E.M. G. JP45KO leads to decreased neuropeptide-Y (NPY) and agouti-related peptide (AgRP) but not proopiomelanocortin (POMC) secretion, which results in increased thyrotropin-releasing hormone (TRH) and corticotropin-releasing hormone (CRH) secretion in the paraventricular nucleus and reduced food intake.

significantly with age (Zheng et al., 2001), implicating some other mechanism in the decline in its protein level. Previous work demonstrated that $Ca_V1.1$ expression also declines following endogenous overexpression of $Ca_V\beta_{1a}$ with aging (Taylor et al., 2009). Future studies should determine whether JP45KO alters β1a expression.

JP45 expression in wild-type mice with aging does not reduce food intake and body mass probably because it is reduced only 20% compared to complete protein ablation in the JP45KO mouse. Progressive decrease in $Ca_V1.1$ expression in wild-type mice leads to reduced contraction force at 18 months, not before, probably due to a $Ca_V1.1$ and SR calcium release safety margin; that is, both must decline below certain critical values to result in depressed mechanical output.

Lack of changes in triadic proteins in 12- and 18-month JP45KO mice rules out a compensatory effect of major triadic protein overexpression with aging but not the contribution of other mechanisms involved in myofiber Ca^{2+} homeostasis, such as store-operated Ca^{2+} entry (SOCE) and excitation-coupled Ca^{2+} entry (ECCE) (Lyfenko and

Please cite this article as: Delbono, O., et al., Endogenously determined restriction of food intake overcomes excitation–contraction uncoupling in JP45KO mice with aging, Exp. Gerontol. (2012), doi:10.1016/j.exger.2012.01.004

Dirksen, 2008). The role of other minor SR membrane components that modulate ECC in striated muscles, such as mitsugumin-29, SRP-27/TRIC-A, and junctate/humbug, in sustained muscle performance with age has not been investigated.

Sustained exercise on a treadmill requires the activation of a complex biological mechanism, including appropriate neural drive and preserved nerve-muscle integrity and transmission. Maintaining skeletal muscle strength is crucial to the sustained response to a forced exercise regime seen here. Resistance to fatigue in aging animals has been attributed to a switch from fast to slow fiber type (Larsson and Ansved, 1995). We found more type-I and fewer type-II fibers in the soleus muscle of JP45KO compared to WT mice at 18 months, which, together with sustained ECC, probably accounts for their more prolonged running time.

Finally, myofiber number and cross-sectional area are major determinants of skeletal muscle force. We recorded atrophy in soleus muscle fiber, which indicates that fiber cross-sectional area did not contribute to the sustained in vitro force measures and treadmill running distance recorded in aging JP45KO mice.

4.2. Endogenously determined restriction in food intake offsets JP45KO-dependent ECU

In this work, both JP45KO and WT mice had access to food and water ad libitum. Unexpectedly, compared to WT mice, the JP45KO mice ate less when exposed to Prolab RMH 3000 and tended significantly less toward obesity when exposed to a high-fat diet. We propose that calorie restriction accounts for their sustained muscle force and response to highly demanding treadmill exercise by modulating $Ca_v1.1$ expression. Previous reports on skeletal muscle from aging rodents and rabbits show a marked decline in $Ca_v1.1$ expression (Renganathan et al., 1997a,b; Ryan et al., 2002). Here, we recorded more sustained $Ca_v1.1$ expression in aging JP45KO than WT mice. Maximal binding capacity in both at 18 months was remarkably lower than in 3–4 month-old mice (Delbono et al., 2007); however, the decline was more marked for WT mice, leading to a nonsignificant difference in $Ca_v1.1$ expression compared with JP45KO mice. Calorie restriction prevents age-dependent decrease in skeletal muscle force (Mayhew et al., 1998) and $Ca_v1.1$ expression (Renganathan and Delbono, 1998), in addition to increase life span (Barzilai and Bartke, 2009). While the magnitude of restriction here (~20–25%) and in our previous work (40%) (Mayhew et al., 1998) differs, levels in this range have been reported to prevent age-associated tissue function decline and disease in the mouse and other species (for a review, see (Yu, 1999). Development was unaffected, as JP45KO mice did not seem to reduce their intake in the first weeks of life; no significant differences in body weight were detected.

Many calorie restriction regimes have been applied to rodents and monkeys (Yu, 1999). Human subjects are participating or have participated in approximately 84 clinical trials of dietary interventions (*ClinicalTrials.gov*). To our knowledge, this model of "endogenously determined" restriction of food intake is the first reported in the literature. Since spontaneous activity in JP45KO and WT mice is similar, energy expenditure does not account for differences in body weight.

4.3. The central nervous system and food intake in JP45KO mice

To explain calorie restriction in JP45KO mice, we looked for JP45 expression in areas of the brain associated with central regulation of food intake (Roche et al., 2008) in WT mice using a specific JP45 antibody (Anderson et al., 2006). We found that JP45 is expressed in periventricular hippocampus nuclei in WT but not JP45KO. These results are consistent with the detection of the JP45 transcript in 55-day-old C57BL/6J male mouse brain by situ hybridization (ISH) (Allen Institute for Brain Science; http://mouse.brain-map.org) (Lein et al., 2007).

To examine whether JP45KO alters neuropeptide expression, we analyzed their gene expression in the hypothalamus. Our model proposes that JP45 ablation results in reduced ER Ca^{2+} release and probably Ca^{2+} influx through voltage-gated Ca^{2+} channels (Yamamori et al., 2004), leading to reduced NPY and AgRP but not POMC expression in ARH neurons and increased TRH and CRH in PVN and reduced food intake. The mechanism by which JP45 differentially modulates neuropeptide gene expression may depend on the set of Ca^{2+} channels expressed in specific NPY or POMC-secreting neurons (Sun and Miller, 1999) or the distinct leptin-dependent modulation of intracellular signaling involved in gene expression (Wang et al., 2008).

We examined only male JP45KO and WT mice. To our knowledge, no gender difference in the response to various exogenous calorie restriction regimens has been reported; however, future studies on females and the effect of menopause are needed.

How restricted food intake regulates $Ca_v1.1$ expression is unknown. It has been associated with decreased growth hormone/insulin-like growth factor 1 (IGF-1 axis; (Chiba et al., 2007), but whether calorie restriction modifies IGF-1 concentration in skeletal muscle is unknown. The strong influence of IGF-1 auto/paracrine secretion on muscle protein synthesis and function has been shown (Florini et al., 1996). We reported that IGF-1 prevents age-dependent decline in $Ca_v1.1$ (Renganathan et al., 1998) by activating gene transcription (Wang et al., 1999b) and specifically regulates $Ca_v1.1$ transcription in muscle cells by acting on the cAMP-response element-binding (CREB) protein of the promoter (Zheng et al., 2002).

In conclusion, male JP45KO, in contrast to WT mice, sustains in vivo and in vitro skeletal muscle force as they age. At 3–4 months, perhaps earlier, they restrict their food intake even when offered a high-fat diet, resulting in significantly lower body weight than WT, which may account for their functional advantage. JP45 is involved in NPY and AgRP expression in the nucleus arcuate of the hypothalamus, which regulates food intake by means of regulating neuropeptides expressed in paraventricular and lateral nuclei neurons (Fig. 7).

Acknowledgments

This study was supported by grants from the National Institutes of Health/National Institute on Aging (AG07157 and AG15820) to Osvaldo Delbono and the Wake Forest University Claude D. Pepper Older Americans Independence Center (P30-AG21332). Grants from the Association Française Contre les Myopathie AFM and Progetti di Ricerca di Interesse Nazionale PRIN to Francesco Zorzato also funded this project. We thank Jackson Taylor for performing brain and spinal cord immunoblots and Alexander Birbrair for helping with mouse perfusion.

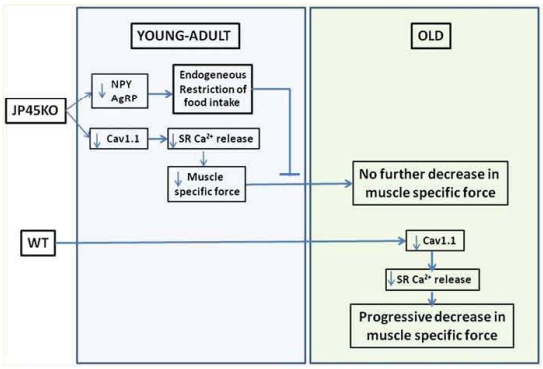

Fig. 7. Time course of excitation–contraction uncoupling and endogenous caloric restriction in JP45KO and WT mice.

Please cite this article as: Delbono, O., et al., Endogenously determined restriction of food intake overcomes excitation–contraction uncoupling in JP45KO mice with aging, Exp. Gerontol. (2012), doi:10.1016/j.exger.2012.01.004

References

Adams, B.A., Tanabe, T., Mikami, A., Numa, S., Beam, K.G., 1990. Intramembrane charge movement restored in dysgenic skeletal muscle by injection of dihydropyridine receptor cDNAs. Nature 346, 569–572.

Anderson, A.A., Treves, S., Biral, D., Betto, R., Sandona, D., Ronjat, M., Zorzato, F., 2003. The novel skeletal muscle sarcoplasmic reticulum JP-45 protein. Molecular cloning, tissue distribution, developmental expression, and interaction with alpha 1.1 subunit of the voltage-gated calcium channel. J. Biol. Chem. 278, 39987–39992.

Anderson, A.A., Altafaj, X., Zheng, Z., Wang, Z.M., Delbono, O., Ronjat, M., Treves, S., Zorzato, F., 2006. The junctional SR protein JP-45 affects the functional expression of the voltage-dependent Ca2+ channel Cav1.1. J. Cell Sci. 119, 2145–2155.

Barzilai, N., Bartke, A., 2009. Biological approaches to mechanistically understand the healthy life span extension achieved by calorie restriction and modulation of hormones. J. Gerontol. A Biol. Sci. Med. Sci. 64, 187–191.

Catterall, W.A., 1995. Structure and function of voltage-gated ion channels. Annu. Rev. Biochem. 64, 493–531.

Catterall, W.A., Goldin, A.L., Waxman, S.G., 2005. International Union of Pharmacology. XLVII. Nomenclature and structure–function relationships of voltage-gated sodium channels. Pharmacol. Rev. 57, 397–409.

Chiba, T., Yamaza, H., Shimokawa, I., 2007. Role of insulin and growth hormone/insulin-like growth factor-I signaling in lifespan extension: rodent longevity models for studying aging and calorie restriction. Curr. Genomics 8, 423–428.

Delbono, O., 2011. Excitation–contraction coupling regulation in aging skeletal muscle. In: Lynch, G.S. (Ed.), Sarcopenia-Age-Related Muscle Wasting and Weakness. Mechanisms and Treatment. Springer, Victoria, pp. 113–134.

Delbono, O., Renganathan, M., Messi, M.L., 1997. Regulation of mouse skeletal muscle L-type Ca2+ channel by activation of the insulin-like growth factor-1 receptor. J. Neurosci. 17, 6918–6928.

Delbono, O., Xia, J., Treves, S., Wang, Z.M., Jimenez-Moreno, R., Payne, A.M., Messi, M.L., Briguet, A., Schaerer, F., Nishi, M., Takeshima, H., Zorzato, F., 2007. Loss of skeletal muscle strength by ablation of the sarcoplasmic reticulum protein JP45. Proc. Natl. Acad. Sci. U. S. A. 104, 20108–20113.

Faulkner, J.A., Brooks, S.V., 1995. Muscle fatigue in old animals. Unique aspects of fatigue in elderly humans. Adv. Exp. Med. Biol. 384, 471–480.

Florini, J.R., Ewton, D.Z., Coolican, S.A., 1996. Growth hormone and insulin growth factor system in myogenesis. Endocr. Rev. 17, 481–517.

Gonzalez, E., Messi, M.L., Delbono, O., 2000a. The specific force of single intact extensor digitorum longus and soleus mouse muscle fibers declines with aging. J. Membr. Biol. 178, 175–183.

Gonzalez, A., Kirsch, W.G., Shirokova, N., Pizarro, G., Brum, G., Pessah, I.N., Stern, M.D., Cheng, H., Rios, E., 2000b. Involvement of multiple intracellular release channels in calcium sparks of skeletal muscle. Proc. Natl. Acad. Sci. U. S. A. 97, 4380–4385.

González, E., Messi, M.L., Zheng, Z., Delbono, O., 2003. Insulin-like growth factor-1 prevents age-related decrease in specific force and intracellular Ca2+ in single intact muscle fibres from transgenic mice. J. Physiol. 552, 833–844.

Hamill, O.P., Marty, A., Neher, E., Sakmann, B., Sigworth, F.J., 1981. Improved patch-clamp techniques for high-resolution current recording from cells and cell-free patches. Pflugers Arch. 391, 85–100.

Hu, W., Tian, C., Li, T., Yang, M., Hou, H., Shu, Y., 2009. Distinct contributions of Nav1.6 and Nav1.2 in action potential initiation and backpropagation. Nat. Neurosci. 12, 996–1002.

Jimenez-Moreno, R., Wang, Z.M., Gerring, R., Delbono, O., 2008. Sarcoplasmic reticulum Ca2+ release declines in muscle fibers from aging mice. Biophys. J. 94, 3178–3188.

Larsson, L., 1995. Motor units: remodeling in aged animals. J. Gerontol. A Biol. Sci. Med. Sci. 50, 91–95.

Larsson, L., Ansved, T., 1995. Effects of ageing on the motor unit. Prog. Neurobiol. 45, 397–458.

Lein, E.S., Hawrylycz, M.J., Ao, N., Ayres, M., Bensinger, A., Bernard, A., Boe, A.F., Boguski, M.S., Brockway, K.S., Byrnes, E.J., Chen, L., Chen, L., Chen, T.-M., Chi Chin, M., Chong, J., Crook, B.E., Czaplinska, A., Dang, C.N., Datta, S., Dee, N.R., Desaki, A.L., Desta, T., Diep, E., Dolbeare, T.A., Donelan, M.J., Dong, H.-W., Dougherty, J.G., Duncan, B.J., Ebbert, A.J., Eichele, G., Estin, L.K., Faber, C., Facer, B.A., Fields, R., Fischer, S.R., Fliss, T.P., Frensley, C., Gates, S.N., Glattfelder, K.J., Halverson, K.R., Hart, M.R., Hohmann, J.G., Howell, M.P., Jeung, D.P., Johnson, R.A., Karr, P.T., Kawal, R., Kidney, J.M., Knapik, R.H., Kuan, C.L., Lake, J.H., Laramee, A.R., Larsen, K.D., Lau, C., Lemon, T.A., Liang, A.J., Liu, Y., Luong, L.T., Michaels, J., Morgan, J.J., Morgan, R.J., Mortrud, M.T., Mosqueda, N.F., Ng, L.L., Ng, R., Orta, G.J., Overly, C.C., Pak, T.H., Parry, S.E., Pathak, S.D., Pearson, O.C., Puchalski, R.B., Riley, Z.L., Rockett, H.R., Rowland, S.A., Royall, J.J., Ruiz, M.J., Sarno, N.R., Schaffnit, K., Shapovalova, N.V., Sivisay, T., Slaughterbeck, C.R., Smith, S.C., Smith, K.A., Smith, B.I., Sodt, A.J., Stewart, N.N., Stumpf, K.-R., Sunkin, S.M., Sutram, M., Tam, A., Teemer, C.D., Thaller, C., Thompson, C.L., Varnam, L.R., Visel, A., Whitlock, R.M., Wohnoutka, P.E., Wolkey, C.K., Wong, V.Y., Wood, M., Yaylaoglu, M.B., Young, R.C., Youngstrom, B.L., Feng Yuan, X., Zhang, B., Zwingman, T.A., Jones, A.R., 2007. Genome-wide atlas of gene expression in the adult mouse brain. Nature 445, 168–176.

Lyfenko, A.D., Dirksen, R.T., 2008. Differential dependence of store-operated and excitation-coupled Ca2+ entry in skeletal muscle on STIM1 and Orai1. J. Physiol. doi:10.1113/jphysiol.2008.160481

Marzetti, E., Lawler, J.M., Hiona, A., Manini, T., Seo, A.Y., Leeuwenburgh, C., 2008. Modulation of age-induced apoptotic signaling and cellular remodeling by exercise and calorie restriction in skeletal muscle. Free Radic. Biol. Med. 44, 160–168.

Mayhew, M., Renganathan, M., Delbono, O., 1998. Effectiveness of caloric restriction in preventing age-related changes in rat skeletal muscle. Biochem. Biophys. Res. Commun. 251, 95–99.

Melzer, W., Herrmann-Frank, A., Luttgau, H.C., 1995. The role of Ca2+ ions in excitation–contraction coupling of skeletal muscle fibres. Biochim. Biophys. Acta 1241, 59–116.

O'Connell, K., Gannon, J., Doran, P., Ohlendieck, K., 2008. Reduced expression of sarcalumenin and related Ca2+ −regulatory proteins in aged rat skeletal muscle. Exp. Gerontol. 43, 958–961.

Renganathan, M., Delbono, O., 1998. Caloric restriction prevents age-related decline in skeletal muscle dihydropyridine receptor and ryanodine receptor expression. FEBS Lett. 434, 346–350.

Renganathan, M., Messi, M.L., Delbono, O., 1997a. Dihydropyridine receptor-ryanodine receptor uncoupling in aged skeletal muscle. J. Membr. Biol. 157, 247–253.

Renganathan, M., Messi, M.L., Schwartz, R., Delbono, O., 1997b. Overexpression of hIGF-1 exclusively in skeletal muscle increases the number of dihydropyridine receptors in adult transgenic mice. FEBS Lett. 417, 13–16.

Renganathan, M., Messi, M.L., Delbono, O., 1998. Overexpression of IGF-1 exclusively in skeletal muscle prevents age-related decline in the number of dihydropyridine receptors. J. Biol. Chem. 273, 28845–28851.

Roche, J.R., Blache, D., Kay, J.K., Miller, D.R., Sheahan, A.J., Miller, D.W., 2008. Neuroendocrine and physiological regulation of intake with particular reference to domesticated ruminant animals. Nutr. Res. Rev. 21, 207–234.

Ryan, M., Carlson, B.M., Ohlendieck, K., 2000. Oligomeric status of the dihydropyridine receptor in aged skeletal muscle. Mol. Cell Biol. Res. Commun. 4, 224–229.

Ryan, A.S., Dobrovolny, C.L., Smith, G.V., Silver, K.H., Macko, R.F., 2002. Hemiparetic muscle atrophy and increased intramuscular fat in stroke patients. Arch. Phys. Med. Rehabil. 83, 1703–1707.

Saito, A., Seiler, S., Chu, A., Fleischer, S., 1984. Preparation and morphology of sarcoplasmic reticulum terminal cisternae from rabbit skeletal muscle. J. Cell Biol. 99, 875–885.

Sakuma, K., Yamaguchi, A., 2010. Molecular mechanisms in aging and current strategies to counteract sarcopenia. Curr. Aging Sci. 3, 90–101.

Shi, H., Tzameli, I., Bjorbaek, C., Flier, J.S., 2004. Suppressor of cytokine signaling 3 is a physiological regulator of adipocyte insulin signaling. J. Biol. Chem. 279, 34733–34740.

Shi, H., Cave, B., Inouye, K., Bjorbaek, C., Flier, J.S., 2006. Overexpression of suppressor of cytokine signaling 3 in adipose tissue causes local but not systemic insulin resistance. Diabetes 55, 699–707.

Sun, L., Miller, R.J., 1999. Multiple neuropeptide Y receptors regulate K+ and Ca2+ channels in acutely isolated neurons from the rat arcuate nucleus. J. Neurophysiol. 81, 1391–1403.

Taylor, J.R., Zheng, Z., Wang, Z.M., Payne, A.M., Messi, M.L., Delbono, O., 2009. Increased CaVbeta1A expression with aging contributes to skeletal muscle weakness. Aging Cell 8, 584–594.

Wang, Z.M., Messi, M.L., Delbono, O., 1999a. Patch-clamp recording of charge movement, Ca2+ current and Ca2+ transients in adult skeletal muscle fibers. Biophys. J. 77, 2709–2716.

Wang, Z.-M., Messi, M.L., Renganathan, M., Delbono, O., 1999b. Insulin-like growth factor-1 enhances rat skeletal muscle L-type Ca^{2+} channel function by activating gene expression. J. Physiol. 516, 331–341.

Wang, Z.-M., Messi, M.L., Delbono, O., 2000. L-type Ca2+ channel charge movement and intracellular Ca2+ in skeletal muscle fibers from aging mice. Biophys. J. 78, 1947–1954.

Wang, J.H., Wang, F., Yang, M.J., Yu, D.F., Wu, W.N., Liu, J., Ma, L.Q., Cai, F., Chen, J.G., 2008. Leptin regulated calcium channels of neuropeptide Y and proopiomelanocortin neurons by activation of different signal pathways. Neuroscience 156, 89–98.

Woods, C.E., Novo, D., DiFranco, M., Vergara, J.L., 2004. The action potential-evoked sarcoplasmic reticulum calcium release is impaired in mdx mouse muscle fibres. J. Physiol. 557, 59–75.

Xue, B., Pulinilkunnil, T., Murano, I., Bence, K.K., He, H., Minokoshi, Y., Asakura, K., Lee, A., Haj, F., Furukawa, N., Catalano, K.J., Delibegovic, M., Balschi, J.A., Cinti, S., Neel, B.G., Kahn, B.B., 2009. Neuronal protein tyrosine phosphatase 1B deficiency results in inhibition of hypothalamic AMPK and isoform-specific activation of AMPK in peripheral tissues. Mol. Cell. Biol. 29, 4563–4573.

Yamamori, E., Iwasaki, Y., Oki, Y., Yoshida, M., Asai, M., Kambayashii, M., Oiso, Y., Nakashima, N., 2004. Possible involvement of ryanodine receptor-mediated intracellular calcium release in the effect of corticotropin-releasing factor on adrenocorticotropin secretion. Endocrinology 145, 36–38.

Yu, B.P., 1999. Methods in Aging Research, 2nd. ed. CRC Press, New York.

Zheng, Z., Wang, Z.M., Delbono, O., 2002. Insulin-like growth factor-1 increases skeletal muscle DHPR alpha 1S transcriptional activity by acting on the cAMP-response element-binding protein element of the promoter region. J. Biol. Chem. 277, 50535–50542.

Zheng, Z., Messi, M.L., Delbono, O., 2001. Age-dependent IGF-1 regulation of gene transcription of Ca^{2+} channels in skeletal muscle. Mech Ageing Dev. 122 (4), 373–384.

Please cite this article as: Delbono, O., et al., Endogenously determined restriction of food intake overcomes excitation–contraction uncoupling in JP45KO mice with aging, Exp. Gerontol. (2012), doi:10.1016/j.exger.2012.01.004

Am J Physiol Cell Physiol 302: C88–C99, 2012.
First published September 14, 2011; doi:10.1152/ajpcell.00190.2011.

Remodeling of calcium handling in skeletal muscle through PGC-1α: impact on force, fatigability, and fiber type

Serge Summermatter,[1] Raphael Thurnheer,[2] Gesa Santos,[1] Barbara Mosca,[3] Oliver Baum,[4] Susan Treves,[2] Hans Hoppeler,[4] Francesco Zorzato,[2,3] and Christoph Handschin[1]

[1]*Biozentrum, Department of Pharmacology/Neurobiology, University of Basel, Basel, Switzerland;* [2]*Departments of Anesthesia and Biomedicine, Basel University Hospital, Basel, Switzerland;* [3]*Department of Experimental and Diagnostic Medicine, University of Ferrara, Ferrara, Italy; and* [4]*Institute of Anatomy, University of Bern, Bern, Switzerland*

Submitted 14 June 2011; accepted in final form 31 August 2011

Summermatter S, Thurnheer R, Santos G, Mosca B, Baum O, Treves S, Hoppeler H, Zorzato F, Handschin C. Remodeling of calcium handling in skeletal muscle through PGC-1α: impact on force, fatigability, and fiber type. *Am J Physiol Cell Physiol* 302: C88–C99, 2012. First published September 14, 2011; doi:10.1152/ajpcell.00190.2011.—Regular endurance exercise remodels skeletal muscle, largely through the peroxisome proliferator-activated receptor-γ coactivator-1α (PGC-1α). PGC-1α promotes fiber type switching and resistance to fatigue. Intracellular calcium levels might play a role in both adaptive phenomena, yet a role for PGC-1α in the adaptation of calcium handling in skeletal muscle remains unknown. Using mice with transgenic overexpression of PGC-1α, we now investigated the effect of PGC-1α on calcium handling in skeletal muscle. We demonstrate that PGC-1α induces a quantitative reduction in calcium release from the sarcoplasmic reticulum by diminishing the expression of calcium-releasing molecules. Concomitantly, maximal muscle force is reduced in vivo and ex vivo. In addition, PGC-1α overexpression delays calcium clearance from the myoplasm by interfering with multiple mechanisms involved in calcium removal, leading to higher myoplasmic calcium levels following contraction. During prolonged muscle activity, the delayed calcium clearance might facilitate force production in mice overexpressing PGC-1α. Our results reveal a novel role of PGC-1α in altering the contractile properties of skeletal muscle by modulating calcium handling. Importantly, our findings indicate PGC-1α to be both down- as well as upstream of calcium signaling in this tissue. Overall, our findings suggest that in the adaptation to chronic exercise, PGC-1α reduces maximal force, increases resistance to fatigue, and drives fiber type switching partly through remodeling of calcium transients, in addition to promoting slow-type myofibrillar protein expression and adequate energy supply.

muscle plasticity

MORE THAN 600 DIFFERENT MUSCLES are present in the human body, and every skeletal muscle is composed of a distinct set of heterogeneous muscle fibers with various contractile properties (10, 43). On the basis of their twitch characteristic, muscle fibers are broadly classified into two major groups: fast-twitch fibers, which are capable of strong, explosive contractions, and slow-twitch fibers, which are suitable for prolonged physical activities (54).

A cardinal difference between different fiber types is their respective peak amplitude and rate of calcium transients (5). Compared with slow-twitch fibers, fast-twitch fibers express higher amounts of proteins involved in calcium release. The voltage sensor DHPR (1,4-dihydropyridine receptor) and the calcium channel ryanodine receptor 1 (RyR1) are both abundant in fast-twitch muscles (17). Thus, more calcium can be released in response to motor neuron activation (5). Once released from the sarcoplasmic reticulum (SR), calcium binds to troponin, thereby pulling away tropomyosin, exposing the myosin-binding sites and allowing contraction. A direct quantitative relationship exists between calcium concentration and force generation (35, 36). Moreover, fast-twitch fibers are endowed with a high amount of sarcoplasmic/endoplasmic reticulum calcium-ATPase 1 (SERCA1), a protein that pumps calcium back into the SR, and with parvalbumin, a protein that sequesters calcium and enhances calcium reuptake (17, 30). The interplay of these proteins allows rapid muscle relaxation. With respect to their amplitude and dynamics of calcium handling, the respective muscle fibers thus clearly differ, with fast-twitch fibers displaying much higher peak amplitudes and faster rates of calcium turnover compared with slow-twitch fibers.

The fiber type composition of muscle displays considerable plasticity even in the adult, differentiated state. In response to certain environmental demands (e.g exercise), skeletal muscle remodels accordingly to adapt its functional capacity (4, 16). A prominent hallmark of adaptation to chronic endurance exercise is the fiber type switching towards an increased proportion of slow-twitch fibers. The underlying molecular networks are complex and only partially elucidated. An interplay of various, independent signaling pathways mediate exercise adaptation, many of which seem to converge ultimately on common key molecules where these signals are integrated (4, 15). The peroxisome proliferator-activated receptor-γ coactivator-1α (PGC-1α) represents such a systemic hub in muscle plasticity (4, 21, 22, 33).

The central importance of PGC-1α in exercise adaptation is impressively exemplified by studies using PGC-1α transgenic mice. Muscle-specific overexpression of PGC-1α, even in the absence of physical activity, is sufficient to drive changes that are typical of endurance training. PGC-1α increases the oxidative capacity by promoting mitochondrial biogenesis (32), improves oxygen supply to muscle by promoting angiogenesis (1), and increases peak oxygen consumption (12), lipid oxidation, and energy refueling (44, 47). Most importantly, PGC-1α has been shown to drive fiber type switching from fast, glycolytic towards slow, oxidative fibers as defined by changes in myosin heavy chain (MHC) composition and metabolic parameters (33). Intriguingly, muscle-specific PGC-1α transgenic mice (MPGC-1α TG) exhibit an increased endurance capacity in treadmill exercise tests (12), which is associated with an

Address for reprint requests and other correspondence: C. Handschin, Division of Pharmacology/Neurobiology, Biozentrum, Univ. of Basel, Klingelbergstrasse 50-70, CH-4056 Basel, Switzerland (e-mail: christoph.handschin@unibas.ch).

Table 1. *Primer list*

Gene Symbol	Forward Primer (5′–3′)	Reverse Primer (5′–3′)
mRyR1	GCACACAGTCGTATGTACCTG	CCTCCCCTGTTGCGTCTTC
mTBP	ATATAATCCCAAGCGATTTGC	GTCCGTGGCTCTCTTATTCTC
mDHPR	TCAGCATCGTGGAATGGAAAC	GTTCAGAGTGTTGTTGTCATCCT
mTdn	ATGACTGAGATCACTGCTGAAGG	ATGTTGTCACAATGTCTTCGGT
mJnc	CAGCTCTGACAAGAGTTCCAAG	CTGGCAGCCACTTTACTAGAAA
mCalsequestrin1	ACTCAGAGAAGGATGCAGCT	CTCTACAGGGTCTTCTAGGA
mCalsequestrin2	AGCTTGTGGAGTTTGTGAAG	GGATTGTCAGTGTTGTCCC
mSERCA1	AGCCAGTGATGGAGAACTCG	CACCACCAACCAGATGTCAG
mSERCA2	GAGAACGCTCACACAAAGACC	CAATTCGTTGGAGCCCCAT
mParvalbumin	ATCAAGAAGGCGATAGGAGCC	GGCCAGAAGCGTCTTTGTT
mMICU1	ACACCCTCAAGTCTGGCTTAT	TTCCCATCTTTGAAGTGCTTCTT
mNCX	CTTCCCTGTTTGTGCTCCTGT	AGAAGCCCTTTATGTGGCAGTA
mTRα	TTCTCTCCTTCCTCCCATCCTT	GGCTGGAGGGTCTGAGGG
mSLN	TGTGCCCCTGCTCCTCTTC	TGATTGCACACCAAGGCTTG
mPLB	ATGACGACGATTCAAATCTCTTGG	TGGGTTTGCAAAGTTAGGCATAA

elevated content of slow-type fibers. However, a modulation of calcium handling in MPGC-1α TG mice to meet the specific demands of slow-type, high-endurance fiber contractions has not yet been investigated. Thus, it is unknown whether PGC-1α changes calcium handling cell-autonomously in skeletal muscle, although this would be a prerequisite to permit slow-type contractions. Thus, we investigated whether PGC-1α modulates calcium levels, whether it quantitatively and/or qualitatively affects force generation in skeletal muscle, and which mechanisms might underlie such changes. To address these issues, we used a mouse model with physiological overexpression of PGC-1α that is limited to skeletal muscle (33).

MATERIALS AND METHODS

Ethical approval. All studies were performed according to criteria outlined for the care and use of laboratory animals and with approval of the Swiss authorities. MPGC-1α TG mice (33) and control littermates were maintained according to institutional guidelines in a conventional facility with a fixed 12:12-h light-dark cycle on a commercial pellet chow diet and free access to tap water. All experiments were performed in 8-wk-old male mice.

In vivo and ex vivo muscle strength assessment. Maximal force was tested in vivo using a grip strength meter (Chatillon, DFE Series Digital Force Gauge). In brief, mice were held by their tail and gently lowered towards the apparatus. They were allowed to grip the grid with their front or hindlimbs and were then slowly pulled backwards in a horizontal plane. Each measurement was repeated three times per mouse, and the average was taken as maximal strength. To test force ex vivo, extensor digitorum longus (EDL) muscles were dissected and mounted into a muscle testing setup (Heidelberg Scientific Instruments). Muscle force was digitized at 4 kHz by using an AD Instruments converter. EDL tetanus was recorded in response to 350-ms pulses at 100 Hz as previously described (13). Specific force was normalized to the muscle cross-sectional area [CSA = wet weight

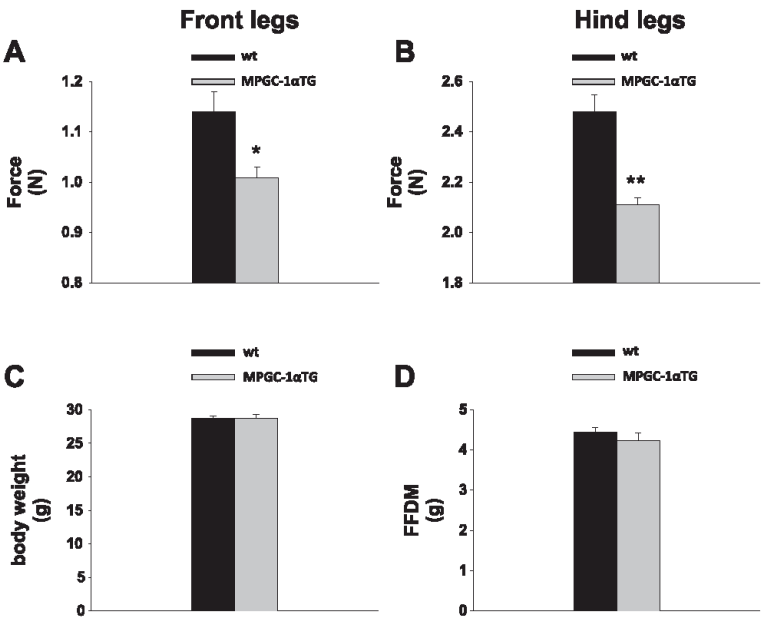

Fig. 1. Reduced maximal force in muscle-specific peroxisome proliferator-activated receptor-γ coactivator-1α (PGC-1α) transgenic (MPGC-1α TG) animals. *A* and *B*: maximal force of front legs (*A*) and hind legs (*B*) in MPGC-1α TG and control mice. *C* and *D*: total body weight (*C*) and fat-free dry mass (FFDM) (*D*) in MPGC-1α TG and control mice. WT, wild type. All values are expressed as means ± SE (n = 7 per group); *$P < 0.05$; **$P < 0.01$.

(mg)/length (mm) × 1.06 (density mg/mm^3)] (13). To test resistance to fatigue, repeated tetani were recorded in response to 350-ms pulses at 100 Hz with intervals of 3.65 s (18).

Electron microscopy and morphometry. Electron microscopy and morphometry to determine muscle composition was performed as described previously (25). In brief, EDL muscles of control and transgenic mice were fixed in 6.5% (vol/vol) glutaraldehyde diluted in 0.1 M sodium cacodylate buffer, pH 7.4, at 4–8°C for several days and then subdivided into ~20 tissue blocks (1 mm^3 in size). These blocks were used to prepare ultrathin sections of 50–70 nm thickness which were stained with lead citrate and uranyl acetate before viewing in a Philips EM-400 electron microscope. Transversely or slightly obliquely oriented sections from randomly selected blocks of each EDL muscle were subjected to morphometry. To this end, 20 micrographs obtained by systematic sampling were recorded at a magnification of ×6,000. These microphotographs were overlaid with a quadratic grid of 12 × 12 lines in distance of 0.916 μm. In accordance with standard stereological rules, the interceptions were counted to determine the volume density of individual muscle components (53).

RNA extraction and RT-PCR. Frozen tissues were homogenized under liquid nitrogen, and total RNA was isolated using TRIzol reagent (Invitrogen). RNA concentrations were adjusted and reverse transcription was carried out using random hexamer primers (Promega). Real-time PCR analysis (Power SYBR Green Master Mix, Applied Biosystems) was performed using the ABI Prism 7000 Sequence Detector. Relative expression levels for each gene of interest were calculated with the $\Delta\Delta C_t$ method (where C_t is the threshold cycle number) and normalized to the expression of the Tata box-binding protein (TBP), whose expression was equal between wild-type and transgenic animals. The amplification efficiency of all investigated genes was similar to TBP. Primer sequences are listed in Table 1.

Body composition. Body composition was determined with an EchoMRI qNMR (Echo Medical Systems).

Calcium transients. Flexor digitorum brevis (FDB) muscles were enzymatically dissociated at 37°C for 60 min in an incubator for cell culture in Tyrode's solution containing 0.20% collagenase I (Sigma C0130-16). The muscles were rinsed in DMEM-10% FCS, transferred to DMEM and mechanically dissociated with fire-polished pasteur pipettes. The dissociated fibers were placed on glass coverslips previously coated with laminin (Invitrogen catalog no. 23017-015). FDB fibers were loaded for 20 min at 20°C in Tyrode's solution (137 mM NaCl, 5.4 mM KCl, 0.5 mM $MgCl_2$, 1.8 mM $CaCl_2$, 11.8 mM HEPES-NaOH, pH 7,4, 0.1% glucose) containing 10 μM Mag-Fluo-4-AM and 50 μM BTS [4 methyl-*N*-(phenylmethyl)benzenesulfonamide], and calcium transients were triggered by field stimulation with a 40-V pulse of 0.5 ms duration (11, 24). Fluorescent signals were recorded with a Nikon EclipseTE2000-U fluorescent microscope equipped with a P101 photomultiplier and digitized at 10 kHz. Calcium transients were calculated as $(F_{max} - F_{rest})/F_{rest}$.

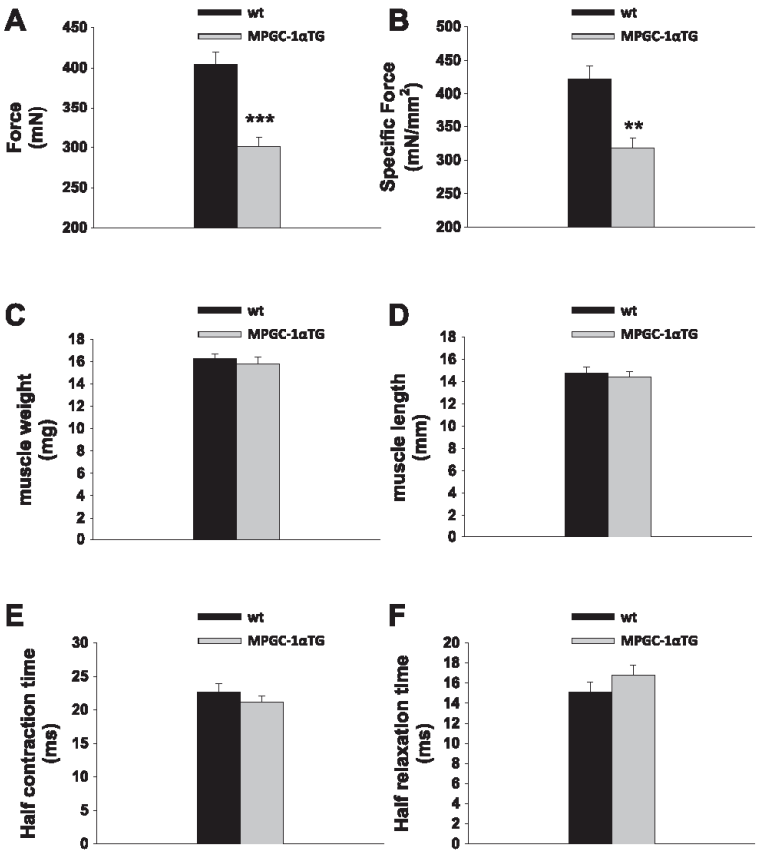

Fig. 2. Reduced tetanic force, but unaltered kinetics of force generation in extensor digitorum longus (EDL) muscle of MPGC-1α TG animals. *A* and *B*: absolute (*A*) and relative (*B*) tetanic force in EDL muscle of MPGC-1α TG and control mice in response to 100 Hz stimulation ex vivo. *C* and *D*: muscle weight (*C*) and length (*D*) of EDL muscle of MPGC-1α TG and control mice. *E* and *F*: half-contraction time (*E*) and half-relaxation time (*F*) of EDL muscle of MPGC-1α TG and control mice following tetanic stimulation at 100 Hz. All values are expressed as means ± SE (n = 8 per group); $^{**}P < 0.01$; $^{***}P < 0.001$.

Calcium transients in myotubes, grown on glass coverslips, were performed 24 h after adenoviral infection. In brief, myotubes were loaded with 5 μM fura-red at 37°C for 30 min, after which the coverslips were mounted onto a 37°C thermostatically controlled chamber which was continuously perfused with Krebs-Ringer medium. Myotubes were first visualized by epifluorescence. Calcium transients were elicited by addition of 600 μM 4-chloro-*m*-cresol in 100 μM La^{3+}, and measurements were made on a Nikon Eclipse TE2000- E inverted microscope. Fura-red was excited with a 405 nm laser, and the changes in fura-red fluorescence were followed at 625 nm using a brightline HC 625/26 cut-off filter (AHF Analysentechnir). Images were acquired every 100 ms through an oil immersion CFI Plan Apochromat 60 TIRF objective (1.49 numerical aperture) as previously described (49). Changes in fluorescence were analyzed with Metamorph imaging software.

SERCA activity. SERCA activity was determined as described by Simonides and van Hardeveld (41). In brief, fresh muscle homogenates were incubated in 1 mM EGTA, 10 mM phosphoenolpyruvate, 18 U/ml each of pyruvate kinase and lactate dehydrogenase, 0.2 mM NADH, 20 mM HEPES, pH 7.5, supplemented with 200 mM KCl, 15 mM $MgCl_2$, 200 mM NaN_3, and Triton X-100 (0.005%). The assay was started by addition of 4 mM MgATP followed by calcium at various concentrations.

Calcineurin activity. Calcineurin activity was assayed using a commercially available kit from Enzo Life Sciences. In brief, muscles were lysed in lysis buffer containing protease inhibitors and passed through 18-gauge needles to loosely break up the tissue. After centrifugation at 100 *g* at 4°C for 45 min, the supernatant was desalted by gel filtration. Calcineurin activity was determined colorimetrically according to the manufacturer's instructions.

Western blot analysis. Protein extraction was performed as described previously (45, 46). In brief, frozen tissues were crushed under liquid nitrogen, homogenized in lysis buffer [20 mM Tris·HCl, 138 mM NaCl, 2.7 mM KCl, 5% (vol/vol) glycerol, 1% (vol/vol) NP-40, and various hydrolase inhibitors] and incubated for 60 min. After centrifugation at 15,294 *g* for 15 min, protein concentration in the supernatant was quantified and equal amounts of protein extracts were separated by SDS-PAGE. The gels were then blotted on PVDF membranes and analyzed with the following antibodies: calsequestrin 1 [molecular mass (MM): 60 kDa] and 2 (MM: 55 kDa) (Sigma), SERCA 1 (MM: 100 kDa), 2 (MM: 114 kDa) and tubulin (MM: 55 kDa) (Cell Signaling), thyroid hormone receptor-α (MM: 47 kDa) (Abcam), sarcolipin (MM: 4 kDa), phospholamban and phosphorylated phospholamban (MM: 6 kDa) (Santa Cruz Biotechnology). Tubulin was used as loading control and for normalization. Bands within the linear range were quantified densitometrically.

Data analysis and statistics. All data are presented as means ± SE. The data were analyzed by two-tailed, unpaired Student's *t*-test or Mann-Whitney test when the difference between the two SDs was significantly different. Statistical significance was set at $P < 0.05$.

RESULTS

Reduced muscle strength, but unchanged muscle mass in MPGC-1α TG mice. PGC-1α drives the formation of slow-twitch, oxidative fibers (33). However, it is unresolved whether characteristic features of fast-twitch fibers are lost upon PGC-1α-induced fiber type transition. We thus first tested whether PGC-1α-induced fiber type switching affects muscle strength in vivo. MPGC-1α TG mice generated less force [forelimbs, −12%, $P < 0.05$ (Fig. 1*A*); hindlimbs, −15%, $P < 0.01$ (Fig. 1*B*)] than control animals in the absence of alterations in body weight (Fig. 1*C*) or fat-free dry mass (Fig. 1*D*).

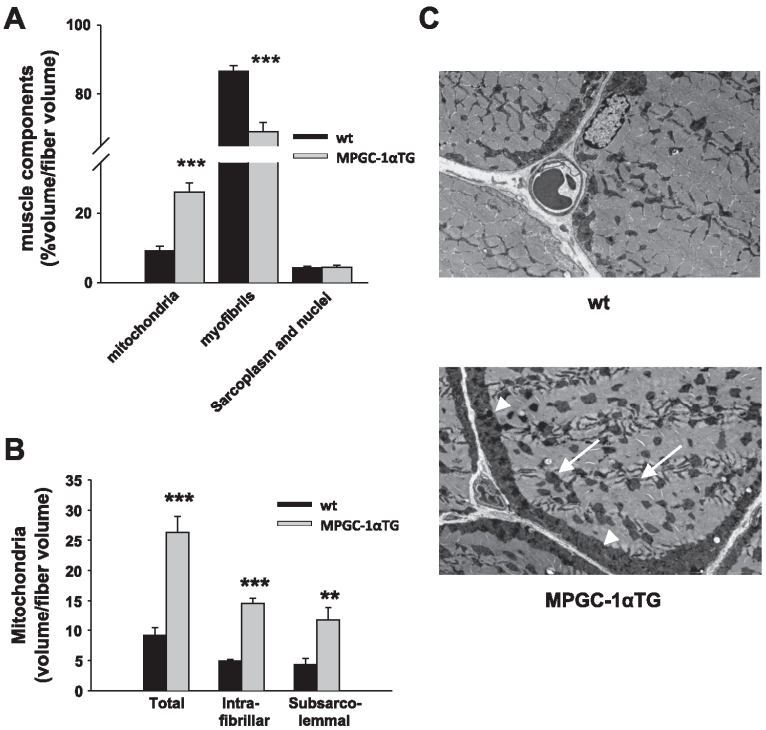

Fig. 3. Elevated subsarcolemmal and intermyofibrillar mitochondria, but diminished myofibrillar structures, in EDL muscle of MPGC-1α TG animals. *A*: quantification of morphometrical analysis of EDL muscle of MPGC-1α TG and control mice. *B*: detailed quantification of different mitochondrial subpopulations. *C*: representative micrographs from electron microscopy of EDL muscle of MPGC-1α TG and control mice. Arrows indicate intermyofibrillar mitochondria and arrowheads indicate subsarcolemmal mitochondria. All values are expressed as means ± SE ($n = 8$ per group); $^{**}P < 0.01$; $^{***}P < 0.001$.

To scrutinize further the nature of the reduced muscle force generation, the experiments were extended to intact muscle preparations ex vivo. Isolated EDL muscle of MPGC-1α TG mice showed reduced absolute (−25%, $P < 0.001$) (Fig. 2*A*) and specific (−25%, $P < 0.01$) (Fig. 2*B*) tetanic force compared with their control littermates. EDL weight (Fig. 2*C*) and length (Fig. 2*D*) were not different between control and transgenic animals, indicating that the reduced force was not due to loss in muscle mass. Despite the lower force in MPGC-1α TG mice, kinetics of muscle force contraction (Fig. 2*E*) and relaxation (Fig. 2*F*) in response to tetanic stimulation remained similar in both groups.

Altered muscle morphology in EDL of MPGC-1α TG mice. Since muscle mass was equal between transgenic and control mice, we speculated that the reduced force generation could conceivably result from altered muscle morphology. To test whether structural changes account for the reduced force, the composition of EDL muscle was determined by electron microscopy. Because of the overexpression of PGC-1α, transgenic mice showed elevated mitochondrial mass (+187%, $P < 0.001$), at the expense of total myofibrillar structures, which were reduced by 20% ($P < 0.001$) (Fig. 3*A*).

Detailed quantitative analyses revealed that both mitochondrial subpopulations were elevated to a similar extent, the centrally located intramyofibrillar mitochondria, which are in close contact to the SR, by +198% ($P < 0.001$) and the subsarcolemmal mitochondria by +175% ($P < 0.01$) (Fig. 3*B*).

Capacity for calcium release is diminished in EDL of MPGC-1α TG mice. Calcium release from the sarcoplasmic reticulum is an important determinant of muscle force generation. The skeletal muscle L-type Ca^{2+} channel (DHPR) serves

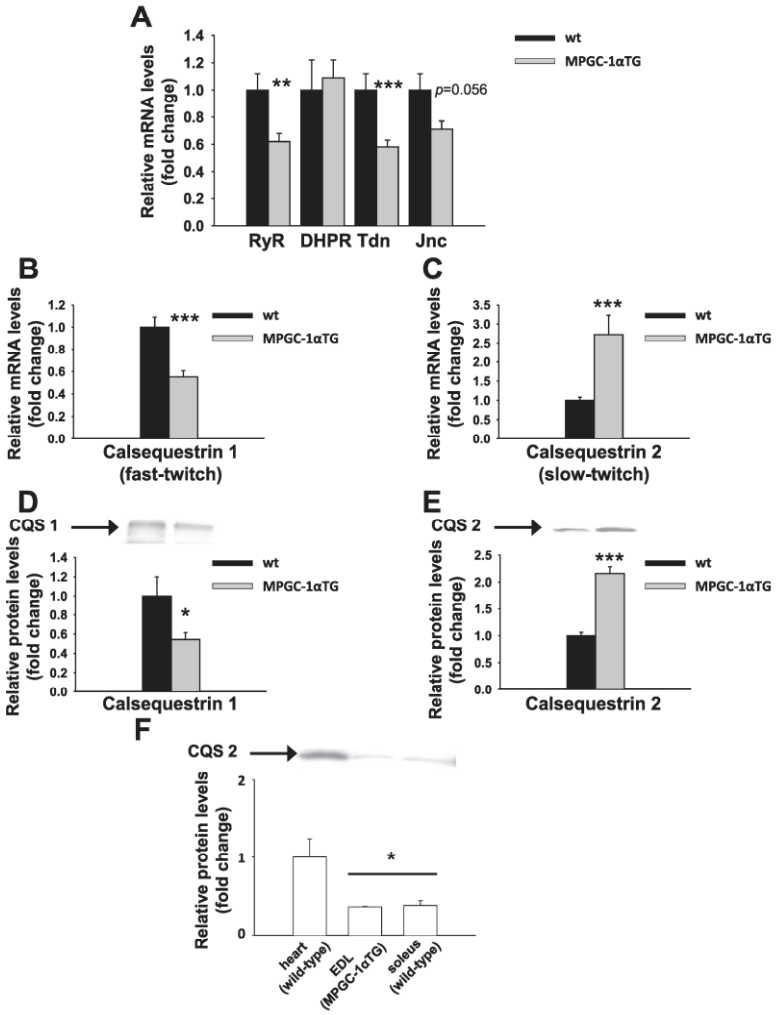

Fig. 4. Decreased capacity for calcium release and fiber type switching in muscle of MPGC-1α TG animals. *A*: relative expression of genes involved in calcium release from the sarcoplasmic reticulum in muscle of MPGC-1α TG and control mice. RyR, ryanodine receptor 1; DHPR, 1,4-dihydropyridine receptor; Tdn, triadin; Jnc, junctin. *B* and *C*: relative mRNA expression of fast-twitch specific calsequestrin 1 (*B*) and slow-twitch specific calsequestrin 2 (*C*). *D* and *E*: protein levels of calsequestrin 1 (CQS 1; *D*) and calsequestrin 2 (CQS 2; *E*). *F*: comparison of calsequestrin 2 protein levels across different muscle tissues. All values are expressed as means ± SE ($n = 6–8$ per group); $*P < 0.05$; $**P < 0.01$; $***P < 0.001$.

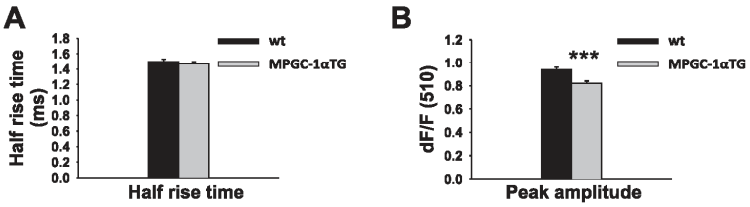

Fig. 5. Decreased calcium release in muscle of MPGC-1α TG animals. *A*: half-rise time of myoplasmic calcium in response to a single twitch. *B*: peak amplitude of calcium in muscle of MPGC-1α TG and control mice following a single twitch. All values are expressed as means ± SE (n = 6–8 per group); ***$P < 0.001$.

as the voltage sensor for excitation-contraction (EC) coupling and activates Ca^{2+} release from the sarcoplasmic reticulum via RyR1 (40). RyR1 entertains a complex network with regulatory proteins, such as calsequestrin, triadin, and junctin (6).

While the mRNA expression of DHPRα1s was similar between wild-type and transgenic animals, the mRNA expression levels of RyR1, triadin, and junctin were reduced in EDL muscles of transgenic animals (Fig. 4*A*).

In addition, the mRNA expression of calsequestrin 1 was reduced, while calsequestrin 2 was elevated (Fig. 4, *B* and *C*, respectively). The same pattern was observed at the protein level (Fig. 4, *D* and *E*, respectively). This is in line with the fiber type switching towards oxidative fibers in the MPGC-1α TG animals, as calsequestrin 1 and 2 are specific for fast-twitch and slow-twitch fibers, respectively (6). A comparison of calsequestrin 2 across different muscle tissues was then performed to determine the extent of fiber type transition. Calsequestrin 2 levels in EDL muscles of transgenic animals were lower than in hearts but similar to levels in soleus of wild-type animals as assessed by ANOVA and Tukey's post hoc test (Fig. *4F*).

To test functionally whether reduced expression of the calcium release machinery impairs calcium release from the SR, single fibers were isolated from FDB muscle and stimulated electrically. The kinetics of the calcium rise was unaltered in the transgenic animals (Fig. 5*A*). However, quantitatively less calcium was released into the myoplasm in transgenic animals compared with controls (Figs. 5*B* and 6*A*).

To demonstrate that the reduced calcium release was not primarily due to altered neuronal activity during development or changes at the neuromuscular junction, calcium release was determined in cultured myotubes following adenoviral infection with green fluorescent protein (GFP) or bicistronic PGC-1α-GFP. To this end, the ryanodine receptor was directly stimulated by 4-chloro-*m*-cresol. Calcium release was reduced following adenoviral overexpression of PGC-1α (Fig. 6*B*). Quantification of the traces showed reduced calcium release following overexpression of PGC-1α (GFP: 0.23 ± 0.013 vs. PGC-1α-GFP: 0.14 ± 0.003; n = 12–15; $P < 0.001$).

Improved resistance to fatigue in EDL of MPGC-1α TG mice. Interestingly, when muscles of MPGC-1α TG mice and control littermates were repeatedly stimulated, they showed different temporal development of force generation. The first tetanic stimulation generated less force in transgenic animals than in their control littermates. However, following repeated tetanic stimulation, transgenic animals displayed higher force generation than wild type animals over time (Fig. 6*C*) and were therefore more resistant to fatigue, similar to previously pub-

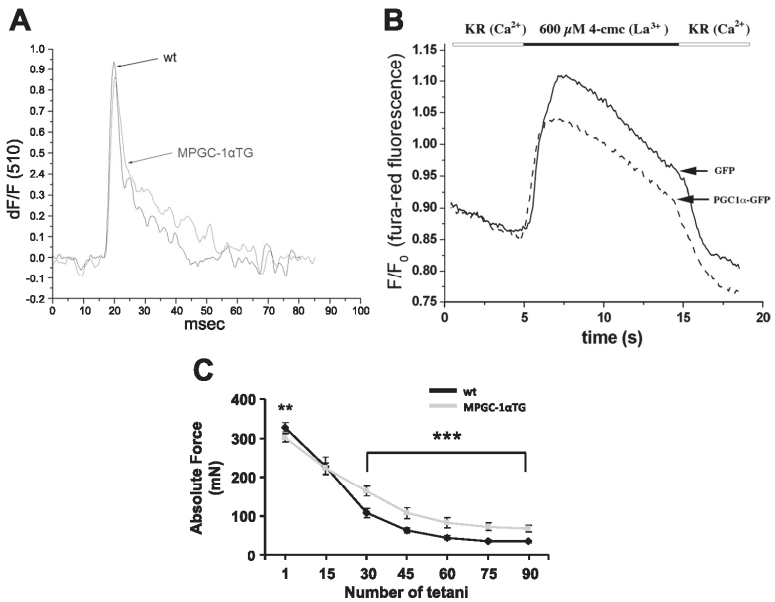

Fig. 6. Calcium trace in isolated flexor digitorum brevis (FDB) fibers and resistance to fatigue in EDL muscle of MPGC-1α TG animals. *A*: representative calcium trace in FDB fibers isolated from WT and MPGC-1α TG animals in response to a single twitch. *B*: representative calcium trace in myotubes transfected with green fluorescent protein (GFP) or bicistronic PGC1α-GFP in response to direct ryanodine receptor stimulation by 4-chloro-*m*-cresol (4-cmc). KR, Krebs-Ringer. *C*: absolute force of EDL muscle from MPGC-1α TG and control mice in response to repeated tetanic stimulation at 100 Hz. All values are expressed as means ± SE (n = 8 per group); **$P < 0.01$; ***$P < 0.001$.

lished data that demonstrated an increased time of stimulation in muscles of MPGC-1α TG animals until force generation dropped to 30% (33).

Calcium reuptake capacity is diminished in EDL of MPGC-1α TG mice. A possible explanation for the relative higher tetanic force in transgenic animals in response to repeated tetani could reside within a delayed decay of the calcium transient. Reduced calcium reuptake into the SR has been demonstrated in fatigue-resistant endurance-trained athletes (31). SERCAs are largely responsible for postcontraction calcium clearance. In adult skeletal muscle, two major isoforms of SERCA exist: SERCA1, which is very abundant in glycolytic muscle, and SERCA2, which has generally a low expression in all muscles, but which is the predominant isoform in slow oxidative fibers (6).

EDL muscle overexpressing PGC-1α showed reduced mRNA levels of SERCA1 (Fig. 7*A*), but unaltered levels of SERCA2 (Fig. 7*B*). These results were confirmed at the protein level (Fig. 7, *C* and *D*). Total SERCA activity was significantly reduced in transgenic animals (Fig. 7*E*). In line with this finding, the half-relaxation time of the calcium transient was increased in transgenic animals (Fig. 7*F*).

Besides calcium reuptake by the sarcoplasmic reticulum, calcium binding to the buffering molecule parvalbumin (30), mitochondrial calcium uptake regulated by mitochondrial calcium uptake 1 (MICU1) (39), and calcium export by sodium-calcium exchangers (NCX) (7) might contribute to muscle relaxation. Parvalbumin expression was significantly reduced in PGC-1 transgenic animals (Fig. 7*G*), while MICU1 was unaltered (Fig. 7*G*). Moreover, NCX levels were significantly reduced in MPGC-1α TG mice (Fig. 7*G*).

Potential inhibitory mechanisms of SERCA in MPGC-1α TG mice. The expression of SERCA is regulated by thyroid hormones (42). We thus tested whether thyroid hormone receptor expression is altered in skeletal muscle of PGC-1 transgenic mice. We observed a significant reduction in thyroid hormone receptor mRNA expression in transgenic mice (Fig. 8*A*). Moreover, protein levels of the thyroid hormone receptor were reduced (Fig. 8*B*). Finally, we tested the expression of inhibitors of SERCA activity. Relative mRNA and protein levels of

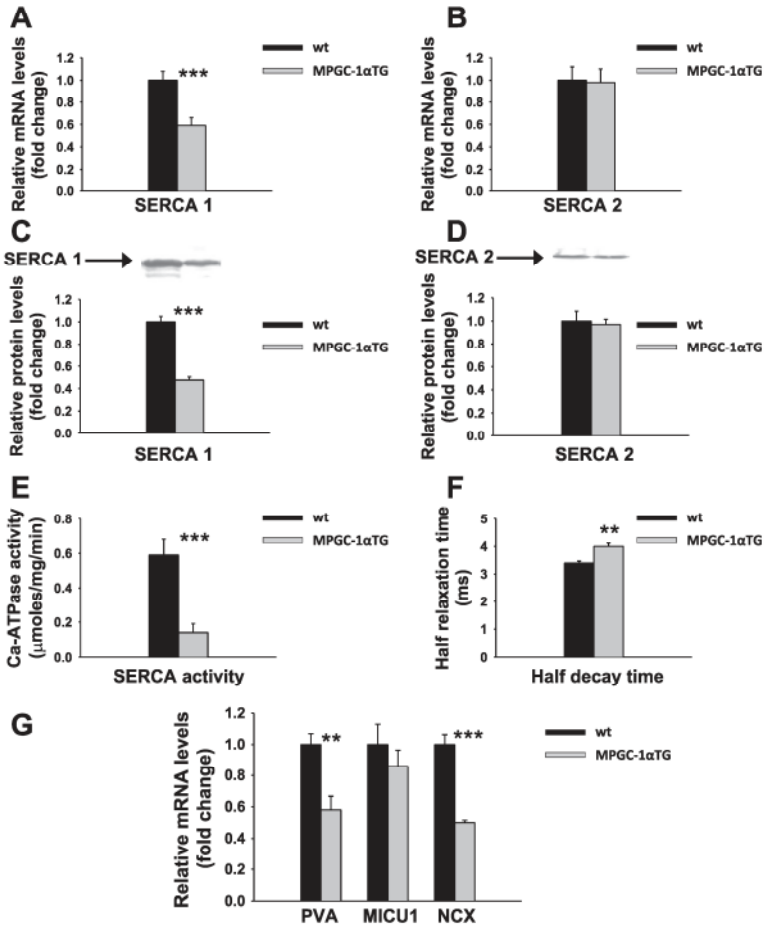

Fig. 7. Diminished calcium removal in muscle of MPGC-1α TG animals. *A* and *B*: relative mRNA expression of sarcoplasmic/endoplasmic reticulum calcium-ATPase 1 (SERCA1; *A*) and SERCA2 (*B*) in muscle of MPGC-1α TG and control mice. *C* and *D*: protein levels of SERCA1 (*C*) and SERCA2 (*D*) in muscle of MPGC-1α TG and control mice. *E*: total SERCA activity in skeletal muscle of MPGC-1α TG and control mice. *F*: half-decay time of calcium following single-pulse electrical stimulation ex vivo. *G*: relative expression of genes involved in calcium removal in muscle of MPGC-1α TG and control mice. PVA, parvalbumin; MICU1, mitochondrial calcium uptake 1; NCX, sodium-calcium exchanger. All values are expressed as means ± SE (n = 6–8 per group); $^{**}P < 0.01$; $^{***}P < 0.001$.

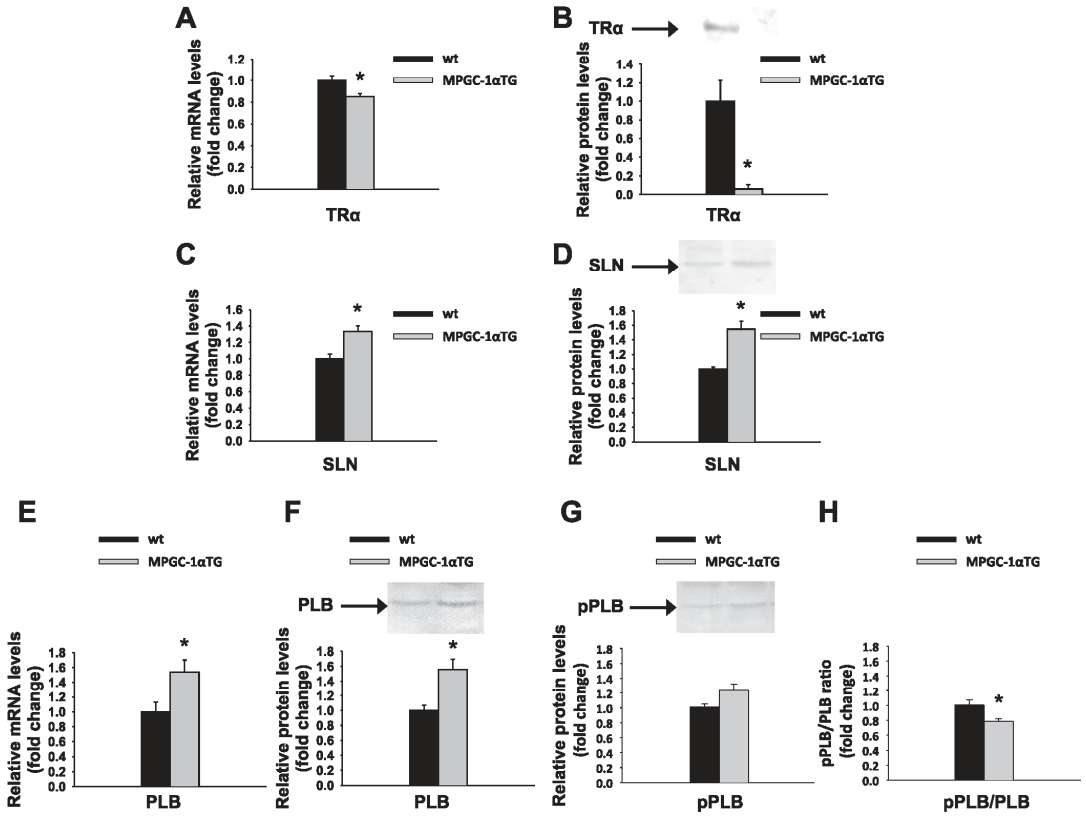

Fig. 8. Mechanisms of SERCA inhibition. *A* and *B*: relative mRNA expression (*A*) and protein levels (*B*) of thyroid hormone receptor-α (TRα) in muscle of MPGC-1α TG and control mice. *C* and *D*: relative mRNA expression (*C*) and protein levels (*D*) of sarcolipin (SLN) in muscle of MPGC-1α TG and control mice. *E–H*: relative mRNA expression (*E*) and protein levels of phospholamban (PLB) (*F*), phosphorylated phospholamban (pPLB) (*G*), as well as the ratio between phosphorylated and total phospholamban (*H*) in muscle of MPGC-1α TG and control mice. All values are expressed as means ± SE (n = 6–10 per group); *$P < 0.05$.

sarcolipin were elevated in MPGC-1α TG mice (Fig. 8*C* and *D*, respectively). Furthermore, we found elevated mRNA and protein levels of phospholamban in MPGC-1α TG mice (Fig. 8*E* and *F*, respectively). However, the inhibition of SERCA through phospholamban can be relieved by phosphorylation of phospholamban. MPGC-1α TG mice had a tendency to display higher levels of phosphorylated phospholamban ($P = 0.066$) (Fig. 8*G*), yet the ratio of phosphorylated phospholamban to total phospholamban was lower in the transgenic mice (Fig. 8*H*).

Elevated calcineurin activity in MPGC-1α TG mice. Sustained elevated calcium levels can activate calcineurin, which is involved in the establishment and maintenance of a slow fiber type-specific gene program (38, 55). We thus tested whether the prolonged calcium transients in MPGC-1α TG mice would affect calcium-dependent calcineurin activity. In the transgenic animals, altered calcium handling was associated with increased activity of calcineurin in skeletal muscle (Fig. 9).

DISCUSSION

Muscle fibers are distinguished on the basis of their physiological features, such as appearance (red vs. white), predominant MHC isoform (MHC I and IIA vs. MHC IIB and X), metabolic parameters (oxidative vs. glycolytic), or contractile properties (slow- vs. fast-twitching) (3, 4, 9, 23, 43). The latter concept is inextricably linked to calcium handling. The speed of calcium release, clearance, and its peak amplitude determine the characteristic of the twitch (5, 50).

Interconversion of different fiber types can occur because of the high plasticity of skeletal muscle. PGC-1α confers a reddish appearance to skeletal muscle, increases slow MHC isoform expression, and metabolically promotes a more oxidative phenotype (33). We have now shown that the transcriptional coactivator PGC-1α remodels calcium release by reducing the mRNA expression of several components of the sarcoplasmic reticulum calcium channel complex (namely, RyR1, triadin, and junctin). The ensuing lower myoplasmic concentration of calcium in combination with a decrease in contractile

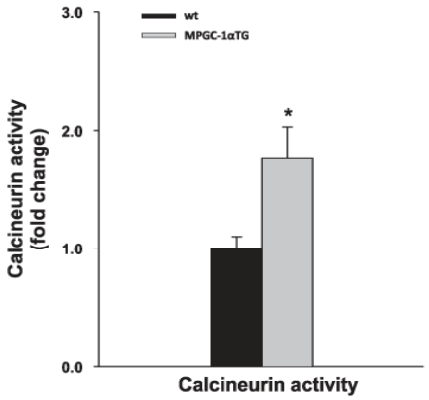

Fig. 9. Elevated calcineurin activity in muscle of MPGC-1α TG animals. Calcineurin activity in skeletal muscle of MPGC-1α TG and control mice. All values are expressed as means ± SE (n = 6 per group); *$P < 0.05$.

elements (myofibrils), possibly as a result from increased mitochondrial biogenesis, culminates in a diminished maximal force generation. Furthermore, PGC-1α prolongs myoplasmic calcium transients by impairing SERCA mRNA and protein expression, as well as activity, thereby inhibiting calcium reuptake into the SR, by decreasing the mRNA levels of the cytosolic calcium buffer parvalbumin, and by reducing NCX mRNA levels and hence the potential to export calcium from the muscle fiber.

In contrast, the mRNA level of MICU1, a molecule that regulates mitochondrial calcium import, remains unaltered. Given the increase in mitochondrial mass, relatively lower levels of MICU1 per mitochondria occur in MPGC-1α TG mice.

Taken together, our findings demonstrate that PGC-1α slows down calcium handling in skeletal muscle. Altered calcium transients secondarily influence force generation, fatigability, and fiber type switching (Fig. 10).

Importantly, while PGC-1α regulates the expression of postsynaptic genes in skeletal muscle (19), the modulation of calcium signaling by PGC-1α is at least in part exerted in a cell autonomous manner. Thus, we observed altered calcium transients following electrical stimulation ex vivo in the absence of a motor neuron. Moreover, our experiments on muscle cells in vitro demonstrate that overexpression of PGC-1α is sufficient to alter calcium transients (Fig. 5*B*). This is further underlined by the finding that PGC-1α diminishes the mRNA levels of both the ryanodine receptor (calcium release) and SERCA1 (calcium reuptake) in myotubes following adenoviral overexpression of PGC-1α (Fig. 11). Thus, muscle PGC-1α per se is able to change calcium handling in skeletal muscle.

PGC-1α strongly promotes mitochondrial biogenesis in skeletal muscle and other tissues (33). We now demonstrate that subsarcolemmal and intermyofibrillar mitochondria are both elevated to a similar extent. Intermyofibrillar mitochondria are often positioned adjacent to calcium release units (CRUs) and are even tethered to them (8, 52). This proximity facilitates the communication between mitochondria and sarcoplasmic reticulum (14). Emerging evidence suggests that mitochondria exert an inhibitory action on local SR calcium release presumably by controlling the local redox environment of CRUs (26, 27, 34). Support for this hypothesis derives from studies on isolated slow- and fast-twitch fibers. Mitochondria-rich slow-twitch fibers display diminished local SR calcium

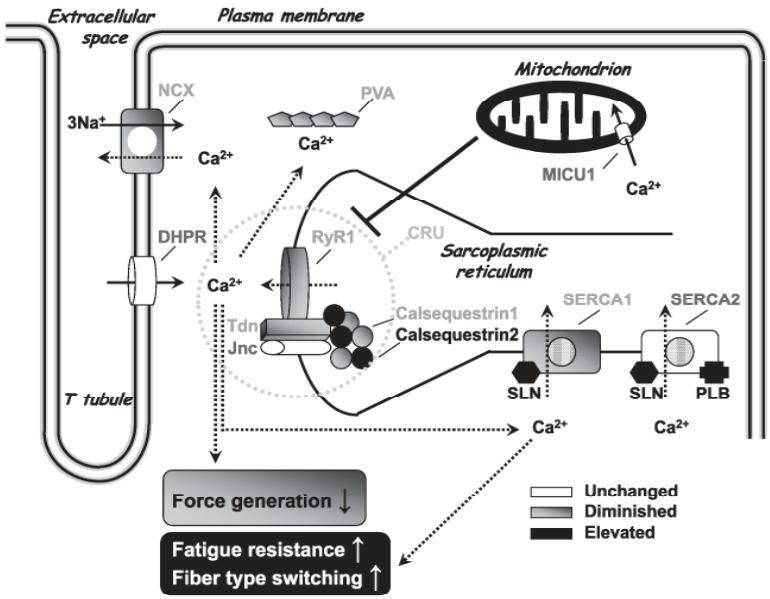

Fig. 10. PGC-1α slows down calcium handling in skeletal muscle. This model integrates the findings of the present study. PGC-1α promotes mitochondrial biogenesis and downregulates the calcium releasing unit (CRU), which consists of RyR1, Tdn, Jnc, and calsequestrin. Subsequently, lower levels of calcium are released from the sarcoplasmic reticulum and force generation is altered. Moreover, NCX, PVA, and SERCA1, which are responsible for postcontraction calcium removal, are reduced in MPGC-1α TG mice. Concomitantly, the levels of SERCA inhibitors (SLN and PLB) are elevated. Thus calcium transients in the cytoplasm are slowed down and can influence muscle fatigability and fiber type switching.

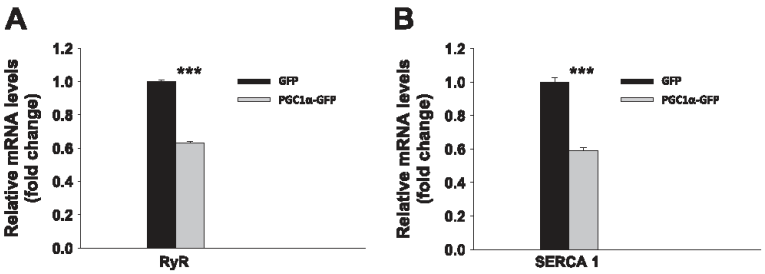

Fig. 11. Reduced RyR and SERCA1 in myotubes with adenoviral expression of PGC-1α. *A* and *B*: relative mRNA expression of RyR (*A*) and SERCA1 (*B*) in myotubes following adenoviral overexpression of GFP or bicistronic PGC-1α-GFP. All values are expressed as means ± SE (n = 9–12/group); ***P < 0.001.

release compared with mitochondria-poor fast-twitch fibers (26, 27).

SERCA accounts for the majority of calcium removal in skeletal muscle, and its expression is regulated by thyroid hormones (42). We now show that PGC-1α diminishes the levels of thyroid hormone receptor in skeletal muscle. Diminished levels of thyroid hormone receptor are associated with reduced SERCA transcription (28). Moreover, it has been demonstrated that calcium represses thyroid hormone-dependent transcription of SERCA1 (48). The coordinated effect of reduced thyroid hormone receptor and sustained elevated myoplasmic calcium levels through PGC-1α thus explains the transcriptional reduction in SERCA1. In addition, we observed elevated mRNA and protein levels of sarcolipin in MPGC-1α TG mice. Sarcolipin inhibits SERCA activity, and mice that overexpress sarcolipin in muscle are resistant to fatigue but have weaker muscles compared with their control littermates (51), a phenotype that is remarkably similar to the PGC-1α muscle-specific transgenic animals in that regard.

Similarly, we found elevated mRNA and protein levels of the SERCA inhibitor phospholamban. Phospholamban is mainly expressed in slow-twitch muscle, where it interacts with SERCA2 and thereby inhibits calcium reuptake into the sarcoplasmic reticulum. Interestingly, the inhibitory effect of phospholamban can be amplified by sarcolipin (2). Although the quantitative contribution of the different inhibitors remains unclear, their interplay clearly results in inhibition of total SERCA activity and delayed calcium removal from the myoplasm.

Taken together, PGC-1α interferes with multiple mechanisms that can lower myoplasmic calcium levels postcontraction, but it mainly affects SERCA expression and activity. Overall, PGC-1α slows down calcium removal and thus induces features of calcium handling in fast-twitch fibers that are reminiscent of fatigue-resistant slow-twitch fibers. How PGC-1α reduces the expression of these genes mechanistically remains unclear.

Beyond its key role in excitation-contraction coupling, calcium could be implicated in fiber type switching. Inhibition of the calcium release channel is crucial for fiber type transformation since RyR activity in fast muscle fibers contributes to the repression of slow muscle-specific genes (29). Furthermore, calcium is involved in transcriptional regulation through calcium-dependent enzymes such as calcineurin and calmodulin-dependent kinases. In adult mouse skeletal muscle fibers, the concerted action of the two pathways is required to accomplish a fast-to-slow fiber type transformation (37). Our results suggest that modified calcium handling in PGC-1α muscle-specific transgenic animals could relieve the repression on slow muscle-specific genes and support sustained activation of calcium-dependent enzymes that drive fiber type switching. Interestingly, PGC-1α thus appears to be downstream and upstream of calcium signaling in muscle: the induction of PGC-1α gene expression in endurance exercise is mediated to a large extent by calcium signaling (20), and, in turn, PGC-1α promotes a slow fiber type-specific calcium handling in muscle. Thereby, PGC-1a promotes all three prerequisites for high-endurance contractions: availability of calcium, slow-type myofibrillar proteins, and adequate supply of energy.

In conclusion, we have provided the first evidence that PGC-1α drives changes in muscular calcium handling by reducing calcium release and clearance. Decreased calcium release accounts for reduced maximal force and relieves the inhibition of slow muscle-specific genes, while diminished calcium clearance promotes resistance to fatigue and fiber type switching. Our data suggest that elevated PGC-1α levels, in combination with muscle contraction, promote fiber type switching. PGC-1α alters calcium handling capacity, and elevated myoplasmic calcium levels, which support fiber type switching, are achieved in response to contraction. Our findings provide new physiological insights into the role of PGC-1α in skeletal muscle adaptation.

ACKNOWLEDGMENTS

We thank Urs A. Meyer (Biozentrum, Basel) and Mirko Vukcevic (University Hospital Basel) and our colleagues in the laboratory for discussions and comments on the manuscript and acknowledge Franziska Graber and Adolfo Odriozola (Institute of Anatomy, University of Bern) for excellent technical assistance.

GRANTS

This project was funded by the Swiss National Science Foundation (SNF PP00A-110746), the Muscular Dystrophy Association USA, the SwissLife "Jubiläumsstiftung für Volksgesundheit und medizinische Forschung," the Swiss Society for Research on Muscle Diseases (SSEM), the Swiss Diabetes Association, the Roche Research Foundation, the United Mitochondrial Disease Foundation, the Association Française contre les Myopathies, and the University of Basel.

DISCLOSURES

No conflicts of interest, financial or otherwise, are declared by the author(s).

AUTHOR CONTRIBUTIONS

Author contributions: S.S., O.B., S.T., H.H., F.Z., and C.H. conception and design of research; S.S., R.T., G.S., B.M., O.B., S.T., and F.Z. performed experiments; S.S., R.T., G.S., B.M., O.B., S.T., F.Z., and C.H. analyzed data; S.S., O.B., S.T., H.H., F.Z., and C.H. interpreted results of experiments; S.S. and S.T. prepared figures; S.S. and C.H. drafted manuscript; S.S., O.B., S.T.,

H.H., F.Z., and C.H. edited and revised manuscript; S.S., R.T., G.S., B.M., O.B., S.T., H.H., F.Z., and C.H. approved final version of manuscript.

REFERENCES

1. **Arany Z, Foo SY, Ma Y, Ruas JL, Bommi-Reddy A, Girnun G, Cooper M, Laznik D, Chinsomboon J, Rangwala SM, Baek KH, Rosenzweig A, Spiegelman BM.** HIF-independent regulation of VEGF and angiogenesis by the transcriptional coactivator PGC-1alpha. *Nature* 451: 1008–1012, 2008.
2. **Asahi M, Kurzydlowski K, Tada M, MacLennan DH.** Sarcolipin inhibits polymerization of phospholamban to induce superinhibition of sarco(endo)plasmic reticulum Ca^{2+}-ATPases (SERCAs). *J Biol Chem* 277: 26725–26728, 2002.
3. **Baar K.** Epigenetic control of skeletal muscle fibre type. *Acta Physiol (Oxf)* 199: 477–487, 2010.
4. **Bassel-Duby R, Olson EN.** Signaling pathways in skeletal muscle remodeling. *Annu Rev Biochem* 75: 19–37, 2006.
5. **Baylor SM, Hollingworth S.** Sarcoplasmic reticulum calcium release compared in slow-twitch and fast-twitch fibres of mouse muscle. *J Physiol* 551: 125–138, 2003.
6. **Beard NA, Wei L, Dulhunty AF.** Ca(2+) signaling in striated muscle: the elusive roles of triadin, junctin, and calsequestrin. *Eur Biophys J* 39: 27–36, 2009.
7. **Bers DM, Bridge JH.** Relaxation of rabbit ventricular muscle by Na-Ca exchange and sarcoplasmic reticulum calcium pump. Ryanodine and voltage sensitivity. *Circ Res* 65: 334–342, 1989.
8. **Boncompagni S, Rossi AE, Micaroni M, Beznoussenko GV, Polishchuk RS, Dirksen RT, Protasi F.** Mitochondria are linked to calcium stores in striated muscle by developmentally regulated tethering structures. *Mol Biol Cell* 20: 1058–1067, 2009.
9. **Booth FW, Laye MJ, Spangenburg EE.** Gold standards for scientists who are conducting animal-based exercise studies. *J Appl Physiol* 108: 219–221, 2010.
10. **Bottinelli R, Reggiani C.** Human skeletal muscle fibres: molecular and functional diversity. *Progr Biophys Mol Biol* 73: 195–262, 2000.
11. **Calderon JC, Bolanos P, Caputo C.** Myosin heavy chain isoform composition and Ca(2+) transients in fibres from enzymatically dissociated murine soleus and extensor digitorum longus muscles. *J Physiol* 588: 267–279, 2010.
12. **Calvo JA, Daniels TG, Wang X, Paul A, Lin J, Spiegelman BM, Stevenson SC, Rangwala SM.** Muscle-specific expression of PPARγ coactivator-1α improves exercise performance and increases peak oxygen uptake. *J Appl Physiol* 104: 1304–1312, 2008.
13. **Delbono O, Xia J, Treves S, Wang ZM, Jimenez-Moreno R, Payne AM, Messi ML, Briguet A, Schaerer F, Nishi M, Takeshima H, Zorzato F.** Loss of skeletal muscle strength by ablation of the sarcoplasmic reticulum protein JP45. *Proc Natl Acad Sci USA* 104: 20108–20113, 2007.
14. **Dirksen RT.** Sarcoplasmic reticulum-mitochondrial through-space coupling in skeletal muscle. *Appl Physiol Nutr Metab* 34: 389–395, 2009.
15. **Finck BN, Kelly DP.** PGC-1 coactivators: inducible regulators of energy metabolism in health and disease. *J Clin Invest* 116: 615–622, 2006.
16. **Fluck M, Hoppeler H.** Molecular basis of skeletal muscle plasticity–from gene to form and function. *Rev Physiol Biochem Pharmacol* 146: 159–216, 2003.
17. **Froemming GR, Murray BE, Harmon S, Pette D, Ohlendieck K.** Comparative analysis of the isoform expression pattern of Ca(2+)-regulatory membrane proteins in fast-twitch, slow-twitch, cardiac, neonatal and chronic low-frequency stimulated muscle fibers. *Biochim Biophys Acta* 1466: 151–168, 2000.
18. **Gonzalez E, Delbono O.** Age-dependent fatigue in single intact fast- and slow fibers from mouse EDL and soleus skeletal muscles. *Mech Ageing Dev* 122: 1019–1032, 2001.
19. **Handschin C, Kobayashi YM, Chin S, Seale P, Campbell KP, Spiegelman BM.** PGC-1alpha regulates the neuromuscular junction program and ameliorates Duchenne muscular dystrophy. *Genes Dev* 21: 770–783, 2007.
20. **Handschin C, Rhee J, Lin J, Tarr PT, Spiegelman BM.** An autoregulatory loop controls peroxisome proliferator-activated receptor gamma coactivator 1alpha expression in muscle. *Proc Natl Acad Sci USA* 100: 7111–7116, 2003.
21. **Handschin C, Spiegelman BM.** Peroxisome proliferator-activated receptor gamma coactivator 1 coactivators, energy homeostasis, and metabolism. *Endocr Rev* 27: 728–735, 2006.
22. **Handschin C, Spiegelman BM.** The role of exercise and PGC1alpha in inflammation and chronic disease. *Nature* 454: 463–469, 2008.
23. **Handschin C, Summermatter S, LeBrasseur NK, Lin J, Spiegelman BM.** For a pragmatic approach to exercise studies. *J Appl Physiol* 108: 223–223; author reply 226, 2010.
24. **Hollingworth S, Gee KR, Baylor SM.** Low-affinity Ca2+ indicators compared in measurements of skeletal muscle Ca^{2+} transients. *Biophys J* 97: 1864–1872, 2009.
25. **Hoppeler H, Howald H, Conley K, Lindstedt SL, Claassen H, Vock P, Weibel ER.** Endurance training in humans: aerobic capacity and structure of skeletal muscle. *J Appl Physiol* 59: 320–327, 1985.
26. **Isaeva EV, Shirokova N.** Metabolic regulation of Ca^{2+} release in permeabilized mammalian skeletal muscle fibres. *J Physiol* 547: 453–462, 2003.
27. **Isaeva EV, Shkryl VM, Shirokova N.** Mitochondrial redox state and Ca^{2+} sparks in permeabilized mammalian skeletal muscle. *J Physiol* 565: 855–872, 2005.
28. **Johansson C, Lannergren J, Lunde PK, Vennstrom B, Thoren P, Westerblad H.** Isometric force and endurance in soleus muscle of thyroid hormone receptor-α_1- or -β-deficient mice. *Am J Physiol Regul Integr Comp Physiol* 278: R598–R603, 2000.
29. **Jordan T, Jiang H, Li H, DiMario JX.** Inhibition of ryanodine receptor 1 in fast skeletal muscle fibers induces a fast-to-slow muscle fiber type transition. *J Cell Sci* 117: 6175–6183, 2004.
30. **Leberer E, Pette D.** Immunochemical quantification of sarcoplasmic reticulum Ca-ATPase, of calsequestrin and of parvalbumin in rabbit skeletal muscles of defined fiber composition. *Eur J Biochem* 156: 489–496, 1986.
31. **Li JL, Wang XN, Fraser SF, Carey MF, Wrigley TV, McKenna MJ.** Effects of fatigue and training on sarcoplasmic reticulum Ca^{2+} regulation in human skeletal muscle. *J Appl Physiol* 92: 912–922, 2002.
32. **Lin J, Handschin C, Spiegelman BM.** Metabolic control through the PGC-1 family of transcription coactivators. *Cell Metab* 1: 361–370, 2005.
33. **Lin J, Wu H, Tarr PT, Zhang CY, Wu Z, Boss O, Michael LF, Puigserver P, Isotani E, Olson EN, Lowell BB, Bassel-Duby R, Spiegelman BM.** Transcriptional co-activator PGC-1 alpha drives the formation of slow-twitch muscle fibres. *Nature* 418: 797–801, 2002.
34. **Martins AS, Shkryl VM, Nowycky MC, Shirokova N.** Reactive oxygen species contribute to Ca^{2+} signals produced by osmotic stress in mouse skeletal muscle fibres. *J Physiol* 586: 197–210, 2008.
35. **Metzger JM, Moss RL.** Effects of tension and stiffness due to reduced pH in mammalian fast- and slow-twitch skinned skeletal muscle fibres. *J Physiol* 428: 737–750, 1990.
36. **Moss RL, Giulian GG, Greaser ML.** The effects of partial extraction of TnC upon the tension-pCa relationship in rabbit skinned skeletal muscle fibers. *J Gen Physiol* 86: 585–600, 1985.
37. **Mu X, Brown LD, Liu Y, Schneider MF.** Roles of the calcineurin and CaMK signaling pathways in fast-to-slow fiber type transformation of cultured adult mouse skeletal muscle fibers. *Physiol Genomics* 30: 300–312, 2007.
38. **Oh M, Rybkin II, Copeland V, Czubryt MP, Shelton JM, van Rooij E, Richardson JA, Hill JA, De Windt LJ, Bassel-Duby R, Olson EN, Rothermel BA.** Calcineurin is necessary for the maintenance but not embryonic development of slow muscle fibers. *Mol Cell Biol* 25: 6629–6638, 2005.
39. **Perocchi F, Gohil VM, Girgis HS, Bao XR, McCombs JE, Palmer AE, Mootha VK.** MICU1 encodes a mitochondrial EF hand protein required for Ca(2+) uptake. *Nature* 467: 291–296, 2010.
40. **Sheridan DC, Takekura H, Franzini-Armstrong C, Beam KG, Allen PD, Perez CF.** Bidirectional signaling between calcium channels of skeletal muscle requires multiple direct and indirect interactions. *Proc Natl Acad Sci USA* 103: 19760–19765, 2006.
41. **Simonides WS, van Hardeveld C.** An assay for sarcoplasmic reticulum Ca2(+)-ATPase activity in muscle homogenates. *Anal Biochem* 191: 321–331, 1990.
42. **Simonides WS, van Hardeveld C.** Thyroid hormone as a determinant of metabolic and contractile phenotype of skeletal muscle. *Thyroid* 18: 205–216, 2008.
43. **Spangenburg EE, Booth FW.** Molecular regulation of individual skeletal muscle fibre types. *Acta Physiol Scand* 178: 413–424, 2003.
44. **Summermatter S, Baum O, Santos G, Hoppeler H, Handschin C.** Peroxisome proliferator-activated receptor gamma coactivator 1alpha (PGC-1alpha) promotes skeletal muscle lipid refueling in vivo by activat-

ing de novo lipogenesis and the pentose phosphate pathway. *J Biol Chem* 285: 32793–32800, 2010.

45. **Summermatter S, Mainieri D, Russell AP, Seydoux J, Montani JP, Buchala A, Solinas G, Dulloo AG.** Thrifty metabolism that favors fat storage after caloric restriction: a role for skeletal muscle phosphatidylinositol-3-kinase activity and AMP-activated protein kinase. *FASEB J* 22: 774–785, 2008.
46. **Summermatter S, Marcelino H, Arsenijevic D, Buchala A, Aprikian O, Assimacopoulos-Jeannet F, Seydoux J, Montani JP, Solinas G, Dulloo AG.** Adipose tissue plasticity during catch-up fat driven by thrifty metabolism: relevance for muscle-adipose glucose redistribution during catch-up growth. *Diabetes* 58: 2228–2237, 2009.
47. **Summermatter S, Troxler H, Santos G, Handschin C.** Coordinated balancing of muscle oxidative metabolism through PGC-1alpha increases metabolic flexibility and preserves insulin sensitivity. *Biochem Biophys Res Commun* 408: 180–185, 2011.
48. **Thelen MH, Simonides WS, van Hardeveld C.** Electrical stimulation of C2C12 myotubes induces contractions and represses thyroid-hormone-dependent transcription of the fast-type sarcoplasmic-reticulum Ca^{2+}-ATPase gene. *Biochem J* 321: 845–848, 1997.
49. **Treves S, Vukcevic M, Griesser J, Armstrong CF, Zhu MX, Zorzato F.** Agonist-activated Ca^{2+} influx occurs at stable plasma membrane and endoplasmic reticulum junctions. *J Cell Sci* 123: 4170–4181, 2010.
50. **Trinh HH, Lamb GD.** Matching of sarcoplasmic reticulum and contractile properties in rat fast- and slow-twitch muscle fibres. *Clin Exp Pharmacol Physiol* 33: 591–600, 2006.
51. **Tupling AR, Asahi M, MacLennan DH.** Sarcolipin overexpression in rat slow twitch muscle inhibits sarcoplasmic reticulum Ca^{2+} uptake and impairs contractile function. *J Biol Chem* 277: 44740–44746, 2002.
52. **Vendelin M, Beraud N, Guerrero K, Andrienko T, Kuznetsov AV, Olivares J, Kay L, Saks VA.** Mitochondrial regular arrangement in muscle cells: a "crystal-like" pattern. *Am J Physiol Cell Physiol* 288: C757–C767, 2005.
53. **Weibel ER.** Stereological principles for morphometry in electron microscopic cytology. *Int Rev Cytol* 26: 235–302, 1969.
54. **Westerblad H, Bruton JD, Katz A.** Skeletal muscle: energy metabolism, fiber types, fatigue and adaptability. *Exp Cell Res* 316: 3093–3099, 2010.
55. **Wu H, Naya FJ, McKinsey TA, Mercer B, Shelton JM, Chin ER, Simard AR, Michel RN, Bassel-Duby R, Olson EN, Williams RS.** MEF2 responds to multiple calcium-regulated signals in the control of skeletal muscle fiber type. *EMBO J* 19: 1963–1973, 2000.

BJ www.biochemj.org

Biochem. J. (2012) 441, 731–741 (Printed in Great Britain) doi:10.1042/BJ20111457

SRP-35, a newly identified protein of the skeletal muscle sarcoplasmic reticulum, is a retinol dehydrogenase

Susan TREVES*†, Raphael THURNHEER*, Barbara MOSCA†, Mirko VUKCEVIC*, Leda BERGAMELLI†, Rebecca VOLTAN†, Vitus OBERHAUSER‡, Michel RONJAT§, Laszlo CSERNOCH‖, Peter SZENTESI‖ and Francesco ZORZATO*†[1]

*Departments of Anaesthesia and of Biomedicine, Basel University Hospital, Hebelstrasse 20, 4031 Basel, Switzerland, †Department of Experimental and Diagnostic Medicine, General Pathology Section, University of Ferrara, Via Borsari 46, 44100 Ferrara, Italy, ‡Albert-Ludwigs-Universität Freiburg Institut für Biologie I (Zoologie), Hauptstrasse 1, 79104 Freiburg, Germany, §Unité Inserm U836, Université Joseph Fourier, Grenoble Institute of Neuroscience, Site Santé, 38700 La Tronche, France, and ‖Department of Physiology, University of Debrecen, Nagyerdei krt. 98, 4012 Debrecen, Hungary

In the present study we provide evidence that SRP-35, a protein we identified in rabbit skeletal muscle sarcoplasmic reticulum, is an all-*trans*-retinol dehydrogenase. Analysis of the primary structure and tryptic digestion revealed that its N-terminus encompasses a short hydrophobic sequence bound to the sarcoplasmic reticulum membrane, whereas its C-terminal catalytic domain faces the myoplasm. SRP-35 is also expressed in liver and adipocytes, where it appears in the post-microsomal supernatant; however, in skeletal muscle, SRP-35 is enriched in the longitudinal sarcoplasmic reticulum. Sequence comparison predicts that SRP-35 is a short-chain dehydrogenase/reductase belonging to the DHRS7C [dehydrogenase/reductase (short-chain dehydrogenase/reductase family) member 7C] subfamily. Retinol is the substrate of SRP-35, since its transient overexpression leads to an increased production of all-*trans*-retinaldehyde. Transfection of C2C12 myotubes with a fusion protein encoding SRP-35–EYFP (enhanced yellow fluorescent protein) causes a decrease of the maximal Ca^{2+} released via RyR (ryanodine receptor) activation induced by KCl or 4-chloro-*m*-cresol. The latter result could be mimicked by the addition of retinoic acid to the C2C12 cell tissue culture medium, a treatment which caused a significant reduction of RyR1 expression. We propose that in skeletal muscle SRP-35 is involved in the generation of all-*trans*-retinaldehyde and may play an important role in the generation of intracellular signals linking Ca^{2+} release (i.e. muscle activity) to metabolism.

Key words: calcium release, excitation–contraction coupling, retinoic acid, ryanodine receptor (RyR), skeletal muscle.

INTRODUCTION

The skeletal muscle SR (sarcoplasmic reticulum) is an intracellular membrane compartment highly specialized in calcium homoeostasis. Structurally it can be subdivided into two membrane portions: the terminal cisternae facing the transverse tubules and the LSR (longitudinal SR) that connects two terminal cisternae [1]. Depolarization of the plasma membrane causes the Ca^{2+} stored in the SR to be released, leading to muscle contraction by a process known as excitation–contraction coupling [2,3]; Ca^{2+} is then pumped back into the SR via SERCAs (sarcoplasmic/endoplasmic reticulum Ca^{2+}-ATPases), which are located on the terminal cisternae and LSR, leading to muscle relaxation [4–6]. These highly co-ordinated events occur within milliseconds of each other thanks to the spatial organization of the membrane compartments carrying the different proteins involved in sensing plasma membrane depolarization, Ca^{2+} release and Ca^{2+} uptake [7]. Indeed, excitation–contraction coupling occurs at the triad, a structure made up of the transverse tubules (which are invaginations of the plasma membrane), carrying the voltage-sensing DHPR (dihydropyridine receptor) and two terminal cisternae carrying the RyR (ryanodine receptor) Ca^{2+} release channel [8,9]. Although these two Ca^{2+} channels are the basic unit underlying excitation–contraction coupling, they nevertheless function in co-ordination with a number of accessory proteins and enzymes involved in maintaining the architecture and optimal function of the calcium release unit. Because of their potential roles in regulating excitation–contraction coupling and since they may be targets of mutations causing neuromuscular disorders, several laboratories have focused their research on identifying novel proteins present on these specialized intracellular membrane compartments and a number of minor components, including mitsugumins, junctophilins, junctate, JP-45 and SRP27, have been characterized (for reviews, see [10,11]).

In the present study, we identified a 35 kDa protein using a proteomic approach in skeletal muscle SR, which we called SRP-35, for SR protein of 35 kDa. Sequence motif comparison indicates that this protein belongs to the DHRS7C {dehydrogenase/reductase [SDR (short-chain dehydrogenase/reductase) family] member 7C} subfamily [12] and is likely to catalyse the conversion of all-*trans*-retinol to retinaldehyde by reducing the cofactor NAD^+ to NADH [13]. SDRs are ubiquitously expressed and constitute a large protein family involved in the reduction of a variety of substrates, among which is retinol, the precursor of retinoic acid [14]. In vertebrates, the effectors of retinoic acid signalling belong to the nuclear receptor family that are divided into two subgroups: the nuclear RARs (retinoic acid receptors), RAR$\alpha/\beta/\gamma$, and the RXRs (retinoid

Abbreviations used: CCD, charge-coupled-device; DDM, *N*-dodecyl-β-D-maltoside; DHPC, 1,2-diheptanoyl-*sn*-glycero-3-phosphocholine; DHPR, dihydropyridine receptor; DHRS7C, dehydrogenase/reductase (short-chain dehydrogenase/reductase family) member 7C; DMEM, Dulbecco's modified Eagle's medium; EDL, extensor digitorum longus; EGFP, enhanced green fluorescent protein; ER, endoplasmic reticulum; EYFP, enhanced yellow fluorescent protein; GFP, green fluorescent protein; HEK-293, human embryonic kidney 293; LSR, longitudinal sarcoplasmic reticulum; NA, numerical aperture; NCBI, National Center for Biotechnology Information; RAR, retinoic acid receptor; RT, reverse transcription; RXR, retinoid X receptor; RyR, ryanodine receptor; SDR, short-chain dehydrogenase/reductase; SERCA, sarcoplasmic/endoplasmic reticulum Ca^{2+}-ATPase; SR, sarcoplasmic reticulum; YFP, yellow fluorescent protein.

[1] To whom correspondence should be addressed (email zor@unife.it).

X receptors), RXR$\alpha/\beta/\gamma$ [15–18]. Upon retinoic acid binding to RAR, the receptors undergo hetero-dimerization with RXRs and translocate into the nucleus, where they bind to target DNA sequences known as retinoic-acid-response elements, promoting the transcription of several genes, including some involved in growth, development, differentiation, cytokine production and metabolism [14,19]. Interestingly, treatment of mice with all-*trans*-retinoic acid reduces body weight, adipose tissue content and promotes skeletal muscle fatty acid oxidation [20]. Thus SRP-35 may be part of a signalling pathway linking muscle activity and metabolism; indeed, this polypeptide is enriched in tissues involved in fatty acid metabolism, notably liver, adipose tissue, kidney and skeletal muscle. Interestingly, in the latter tissue it is enriched in the LSR, where a number of glycolytic enzymes, such as pyruvate kinase, aldolase, enolase and glyceraldehyde 3-phosphate dehydrogenase have also been found to compartmentalize [21]. Since SRP-35 oxidizes all-*trans*-retinol to all-*trans*-retinaldehyde at a site directly involved in Ca^{2+} homoeostasis, we hypothesize that SRP-35 might have a dual function: first, reducing NAD^+ linked to lactic acid generation. The NADH would in turn down-regulate Ca^{2+} release by affecting the redox equilibrium adjacent to RyR1 (the skeletal muscle isoform of the RyR). Secondly, SRP may regulate skeletal muscle gene transcription via the RAR pathway.

EXPERIMENTAL

Materials

Anti-calregulin and anti-calnexin antibodies, peroxidase-conjugated protein A, trypsin-EDTA, DMEM (Dulbecco's modified Eagle's medium), MEM (minimal essential medium) plus Earls salts, L-glutamine, penicillin/streptomycin, horse serum, fetal bovine serum, deoxyribonuclease I, Alexa Fluor® 488 chicken anti-rabbit IgG and Alexa Fluor® 568 donkey anti-mouse IgG were from Invitrogen. All-*trans*-retinol and all-*trans*-retinaldehyde, Protein A–Sepharose, ESCORT IV, peroxidase-conjugated Protein G, peroxidase-conjugated anti-mouse IgG and rabbit anti-DHRS7C anitbodies were from Sigma–Aldrich. Mouse anti-RyR1 (MA3-925) and anti-SERCA (MA3-910) monoclonal antibodies were from Thermo Scientific. The pGEX-5X-3 plasmid and HiTrap Blue Sepharose were from GE Healthcare. The UNI-ZAP XR cDNA library, pEYFP-C1 [where EYFP is enhanced YFP (yellow fluorescent protein)] and pEGFP-C1 [where EGFP is enhanced GFP (green fluorescent protein)] plasmids were from Clontech. Goat anti-DHPRα1.1 antibody was from Santa Cruz Biotechnology. Anti-albumin antibodies were from Bethyl Laboratories. Oxy-Blot protein oxidation detection kit was from Millipore. Nitrocellulose membrane was from Schleicher & Schuell BioScience. Protein molecular mass markers and the Protein Assay Kit were from Bio-Rad Laboratories. NAD^+, NADH, $NADP^+$, FuGENE™ 6, anti-proteases and Taq polymerase were from Roche Diagnostics. The High Capacity cDNA RT (reverse transcription) kit and fast SYBR Green master mix were from Applied Biosystems. Fura 2 acetoxymethylester was from Calbiochem. Tri-Reagent was from Molecular Research Center. PCR primers were from Microsynth. Paraffin-embedded mouse skeletal muscle sections were from Ciochain Institute (BioCat). All other chemicals were reagents of the highest available grade. Mice were bred in-house and rabbits (New Zealand White) were purchased from Charles Rivers Laboratories. All procedures were performed in accordance with the stipulations of the Helsinki Declarations for care and use of laboratory animals. The experiments were approved by the local Basel Kantonal authorities to use animals as tissue donors and for antibody production.

Protein sequencing

Proteins present in the terminal cisternae and junctional face membrane fractions were separated on SDS/PAGE (10% gels) prepared under ultraclean conditions and allowed to polymerize at room temperature (23°C) for 72 h; the gel was stained with Coomassie Brilliant Blue R250 [0.1% in 50% (v/v) methanol and 0.1% acetic acid] and destained overnight at 4°C in 1% acetic acid and 50% (v/v) methanol; the 35 kDa band was cut out with a clean scalpel blade and the SDS and Coomassie Brilliant Blue were removed by slicing the gel finely in 40% (v/v) propan-1-ol, washing and vortexing the sample and changing the solution several times. After the last propan-1-ol wash, the gel was resuspended in a solution containing 0.2 M NH_4HCO_3 and 40% (v/v) acetonitrile and washed with this solution 5 times. After the final wash, excess liquid was removed and the gel fragments were dried in a speedvac. The sample was then rehydrated in 0.1 M NH_4CO_3 and trypsin (sequencing grade, 25 ng/μl) and incubated at 37°C overnight. The supernatant was then collected and transferred to a clean tube; the pellet was treated with a solution made with 80% (v/v) acetonitrile and 0.1% trifluoroacetic acid to extract the remaining peptides. The two supernantants were combined and dried in a speedvac and then subjected to MS analysis using a Q-TOF (quadrupole–time-of-flight; Micromass) mass spectrometer [22].

SRP-35 cDNA cloning

Total RNA was isolated from mouse skeletal muscles using Tri-Reagent following the instructions provided by the manufacturer (Molecular Research Center). Total RNA was converted to cDNA as described previously [23] and primers were designed based on the peptide sequence obtained from trypsin digestion of rabbit SRP-35. These primers (5′-GGAGAGCCTCTACGCTGCCT-3′ and 5′-ACGCCAACTACTTTGGACCCA-3′ for forward and reverse reactions respectively) were used to amplify a sequence from mouse skeletal muscle cDNA; a band of approximately 220 bp was obtained using the following amplification conditions: 1 cycle at 95°C for 5 min followed by 35 cycles of annealing (55°C for 30 s), extension (72°C for 45 s) and denaturation (95°C for 45 s), followed by a 5 min extension cycle at 72°C. The PCR-amplified cDNA was then used as a probe to screen a mouse skeletal muscle UNI-ZAP XR cDNA library as described previously [23]. A clone of 960 bp, containing the entire ORF (open reading frame), was pulled out and sequenced (Microsynth). The coding sequence of SRP-35 was subcloned into the pGEX-5X-3 bacterial expression plasmid and into pEGFPC1 and pEYFPC1 for expression in mammalian cells.

Cell culture and transfection

C2C12 cells were cultured in growth medium [DMEM plus glutamax, high glucose (4.5 g/l), 20% (v/v) fetal bovine serum, 200 mM L-glutamine and penicillin/streptomycin (50 units/ml and 50 μg/ml final concentration respectively)] and maintained below confluence. For differentiation into myotubes, cells were allowed to reach 70% confluence, then the medium was switched to the differentiation medium [DMEM plus Glutamax and high glucose, 5% (v/v) horse serum, 200 mM L-glutamine and penicillin/streptomycin), until cells had visibly fused into myotubes (approximately 5 days). Transfection of C2C12 cells was carried out using FuGENE™ 6 at a ratio of 1.5 μl of FuGENE™ per μg of plasmid DNA per ml culture media. Cells were transfected on days 1 and 3 following the switch to differentiation medium and harvested on day 4

post-differentiation. In some experiments, C2C12 were incubated for 4 days with retinoic acid (5 μM) during differentiation.

HEK-293 (human embryonic kidney 293) cells were cultured and transfected with the pEGFPC1 and pEGFPC1-SRP-35-plasmids using ESCORT IV as described previously [24].

Subcellular fractionation, trypsin digestion and fluorescence analysis

Total microsomes from different mouse tissues (heart, lung, brain, kidney, skeletal muscle, liver, spleen, stomach and intestine), total homogenates prepared from mouse tissues and from isolated fast [EDL (extensor digitorum longus)] and slow (soleus) fibres, and skeletal muscle SR subfractions enriched in plasma membrane, terminal cisternae and LSR were prepared as described previously [1,23,24]. In order to determine whether SRP-35 is an integral membrane protein, mouse skeletal muscle SR vesicles were treated with Na_2CO_3/KCl as described previously [25]. Mouse skeletal muscle SR (15 μg) were digested with increasing concentrations of trypsin for 2 min at room temperature. The reaction was blocked by the addition of trypsin inhibitor; samples were then loaded on to SDS/PAGE (12.5 % gels), blotted on to nitrocellulose membranes and probed with the indicated antibodies. Localization of GFP-tagged recombinant proteins in transfected C2C12 cells was performed 48 h after transfection. Briefly, myotubes were fixed with 3.7 % paraformaldehyde (in PBS), mounted in glycerol medium and observed under fluorescent light (excitation wavelength 480 nm, emission wavelength 510 nm) with an inverted fluorescent microscope (Axiovert S100 TV, Carl Zeiss) equipped with a 20× water-immersion FLUAR objective [0.75 NA (numerical aperture)] attached to a Cascade 128+ CCD (charge-coupled-device) camera (Photometrics).

Polyclonal antibody production, Western blotting and confocal microscopy

Polyclonal antibodies raised against the recombinant GST–SRP-35 fusion protein were obtained by immunizing rabbits and the IgG fraction was purified as described previously [25]. Alternatively, commercial rabbit anti-DHRS7C antibodies were tested on blotted proteins and indirect immuno-enzymatic staining was carried out as described previously [25]. Confocal microscopy was performed on paraffin-embedded mouse skeletal muscle tissue sections; briefly, sections were re-hydrated by incubating sequentially in Xylene (twice, 2 min), 100 % ethanol (twice, 30 s), 95 % and 80 % ethanol (once, 30 s) followed by water (3 times, 3 min) and equilibration in PBS; membranes were permeabilized for 30 min at room temperature with a solution containing 0.5 % Triton X-100, 2 % (v/v) horse serum and 1 % (v/v) BSA; slides were then incubated with the primary antibody (rabbit anti-DHRS7C and mouse anti-SERCA monoclonal antibody) diluted in 0.01 % Triton X-100, 1 % BSA and 2 % (v/v) horse serum in PBS overnight at 4 °C, followed by 4 washes of 15 min each with PBS and incubation for 40 min at room temperature with Alexa Fluor®-488 chicken anti-rabbit IgG and Alexa Fluor®-568 donkey anti-mouse IgG diluted in 0.01 % Triton X-100, 1 % (v/v) BSA and 2 % (v/v) horse serum in PBS. Slides were mounted and fluorescence was observed by confocal microscopy using a Leica DM1400 confocal microscope equipped with a 100× HCX APO TIRF objective (1.47 NA).

Affinity chromatography

In order to determine whether SRP-35 is a dinucleotide-binding protein, we used the affinity column HiTrap Blue Sepharose; the ligand Cibacron Blue F3G-A shows structural similarities to NAD(H), enabling proteins that bind strongly to this cofactor to attach to the resin [26]. Total SR vesicles (1 mg/ml) were solubilized for 30 min at 4 °C in a solution containing 10 mM Tris/HCl, pH 8.0, 1 % (v/v) DDM (*N*-dodecyl-β-D-maltoside) and 1 M NaCl. The solubilized SR membrane proteins were diluted 10-fold with a solution containing Tris/HCl, pH 8.0, and 1 M NaCl and then incubated with Cibacron Blue F3G-A Sepharose previously equilibrated with 10 mM Tris/HCl, pH 8.0, 0.1 % DDM and 1M NaCl. The resin was washed with 10 bed volumes of buffer containing 10 mM Tris/HCl, pH 8.0, 0.1 % DDM and 1M NaCl, and proteins were eluted by adding 1 mM NADH. In order to verify if some SRP-35 was still bound to the resin, 100 μl of Laemmli loading buffer were added to the Cibacron Blue F3G-A Sepharose, after 5 min of incubation, samples were centrifuged and 30 μl of supernatant were loaded on the gel.

Ca^{2+} release and KCl dose–response curves

C2C12 cells, that were grown on glass cover slips, transfected (with pEYFPC1 or pEYFPC1-SRP-35) and differentiated, were loaded with the ratiometric Ca^{2+} indicator fura 2 acetoxymethylester (5 μM) in Krebs–Ringer solution (140 mM NaCl, 5 mM KCl, 1 mM Mg^{2+}, 20 mM Hepes, 1 mM $NaHPO_4$, 5.5 mM glucose, when indicated, and 2 mM Ca^{2+}, pH 7.4) for 30 min at 37 °C. YFP-positive cells were first identified using a 40× Plan-Neofluar objective (NA 1.3) and filter set N°44 (Carl Zeiss MicroImaging; BP 475/40, FT 500, BP 530/50) as described previously [24]. Transfected cells were then analysed for their response to pharmacological activation with KCl or 4-chloro-*m*-cresol, or for the status of the intracellular Ca^{2+} stores, by treating the cells with 5 μM ionomycin plus 1 μM thapsigargin in Krebs–Ringer solution containing no added Ca^{2+} and 0.5 mM EGTA, by monitoring the changes in fura 2 fluorescence [27]. Images were acquired with a Cascade 128 + CCD camera and analysed using the Metamorph imaging software version 7.7.0.0. Generation of dose–response curves and statistical analysis were performed using GraphPad Prism version 4.00 (GraphPad Software). For some experiments, myotubes were treated with retinoic acid (5 μM) for 4 days, loaded with fura 2 and analysed for their calcium response to KCl and 4-chloro-*m*-cresol as indicated above.

Retinol/retinal enzymatic assays

HEK-293 cells were transfected with pEYFPC1 or pEYFPC1-SRP-35, and 24 h post-transfection either all-*trans*-retinol (10 μM) was added to the cell medium for 6 h, or all-*trans*-retinaldehyde (5 μM) was added to the cell medium for 3 h. After incubation, the cells were washed twice with PBS and the medium was replaced with 1 ml 100 % methanol and 1 ml 2 M hydroxylamine, pH 6.7. Cells were subsequently scraped off from the tissue culture flask, homogenized in a glass potter and after a 10 min incubation at room temperature, the homogenate was stored at − 80 °C until used.

For retinol quantification, all solutions were made diluting a stock solution of all-*trans*-retinol or all-*trans*-retinaldehyde prepared in 100 % ethanol, to an aqueous solution containing 10 μM BSA (when all-*trans*-retinol was added) or 5 μM BSA (when all-*trans*-retinaldehyde was added) followed by sonication (23 °C, 10 min continuous pulse at maximum setting using a Branson sonifier, 2210E-MTH 47 KHz/234 W). The final concentration of ethanol did not exceed 1 % (v/v). This procedure

guarantees a more soluble and stable retinoid substrate solution [28]. To quench the reaction, 1 vol. of 2 M hydroxylamine, pH 6.7, and 1 vol. of 100 % methanol were added, which also stabilized the retinoids. Retinoid extraction from 500 μl of the homogenates was optimized by adding acetone (1 vol.) as a phase-mixing agent followed by three times extraction with petrol ether (0.6 vol.). The organic solvent was evaporated under a stream of nitrogen and the retinoid pellet was dissolved in 100 μl of HPLC mobile phase (99.5:0.5 hexane/ethanol), and injected into the HPLC. The relative amounts of retinaldehyde and retinol are expressed as percentages (the amount of a retinoid species divided by the total amount of all retinoids present).

Real-time PCR

Total RNA was extracted from C2C12 cells and treated with deoxyribonuclease I as described previously [29]. After RT using 1000 ng of RNA, cDNA was amplified by quantitative real-time PCR using SYBR Green technology as described previously [29] and the following primers: RyR1, forward 5′-GCACACAGTCGTATGTACCTG-3′ and reverse 5′-CCTCCCC-TGTTGCGTCTTC-3′; SRP-35, forward 5′-CCCTGGAGCTT-GACAAAAAGA-3′ and reverse 5′-GTTCACTAACACAATCT-GGCCT-3′; and $Ca_v1.1$, forward 5′-TCAGCATCGTGGAATGG-AAAC-3′ and reverse 5′-GTTCAGAGTGTTGTTGTCATCCT-3′. Gene expression was normalized using self-TATA-box binding protein as a reference with the following primers: forward 5′-GCCATAAGGCATCATTGGAC-3′ and reverse 5′-AACAACAGCCTGCCACCTTA-3′.

Software and statistical analysis

BLAST alignments were performed on the NCBI (National Center for Biotechnology Information) web site using BLAST 2.2.8. Multiple sequence alignments were performed using the ClustalW algorithm available from the Swiss node of the European Molecular Biology Network. Statistical analysis was performed using the Student's t test for two populations. Values were considered significant when $P < 0.05$.

RESULTS

Primary structure of SRP-35

The skeletal muscle SR junctional face membrane is enriched in proteins playing a major role in Ca^{2+} homoeostasis. One of the aims of the research of our and other laboratories is to identify all the protein constituents of this membrane fraction [10,11,30]. Results obtained by electrospray MS analysis revealed the presence of a novel polypeptide with an approximate molecular mass of 35 kDa in the SR. On the basis of the amino acid sequence obtained from two peptides of the 35 kDa rabbit skeletal muscle protein (Figure 1, light grey boxes), primers were designed and used to amplify by RT–PCR (from mouse skeletal muscle mRNA) a cDNA sequence of approximately 960 nucleotides, whose primary sequence matched that of a hypothetical mouse protein present in the NCBI database (see Figure 1). The predicted primary sequence of SRP-35 encompasses: (i) the peptide sequences obtained from the rabbit skeletal muscle protein from which primers were designed (light grey boxes); (ii) an N-terminal hydrophobic sequence (dark grey box) which may be a signal sequence or a transmembrane domain; and (iii) an NAD(P)(H)-binding and catalytic site (underlined sequence) - the bold letters indicate perfectly conserved residues within the NAD(P)(H)-binding and catalytic sites. BLAST search analysis of the human genome revealed that the human homologue of the rabbit protein maps to human chromosome 17p13.1 (GenBank® accession number NM_001105571) and specifically to the DRS7C_human locus (dehydrogenase/reductase SDR family member 7C or SDR32C2); polymorphisms/mutations have so far not been associated with any human genetic disorder. Figure 1 also shows that SRP-35 is conserved among mammals (87–95 % identity with the mouse sequence); however, not all vertebrates express the 7C member of the SDR family of dehydrogenase/reductases, and in fact BLAST analysis revealed that the gene encoding SDR7C is less conserved but present in the genomes of *Xenopus* (73 % identity), *Drosophila* (38 % identity) and zebrafish (58 % identity).

Tissue distribution, subcellular localization and membrane topology of SRP-35

In order to gain information concerning its physiological function, we analysed the tissue distribution of SRP-35 by Western blot using two anti-SRP35 polyclonal antibodies (with similar results), one raised against the GST–SRP-35 fusion protein and the other, commercially available, antibody raised against the putative DHRS7C gene product. Figure 2(A) shows that an immunoreactive band of approximately 35 kDa is present in the total homogenate of different mouse tissues, including adipose tissue, liver and skeletal muscle. Interestingly, SRP-35 is not present in the microsomal fraction of the liver, but remains in the 100000 g supernatant (Figure 2B), whereas in skeletal muscle it is highly enriched in the total SR fraction (Figure 2C) and undetectable in the post-microsomal supernatant (results not shown). In all other tissues tested, the 35 kDa immunoreactive protein is undetectable in the microsomal fraction. These results indicate that in muscle, SRP-35 may interact with macromolecules that are exclusively present in skeletal muscle. As we were interested in the functional role of SRP-35 in skeletal muscle, all subsequent experiments were performed on this tissue.

The subcellular distribution of SRP-35 was analysed: (i) in isolated fractions of the SR/ER (endoplasmic reticulum); (ii) by monitoring the expression of GFP-tagged SRP-35 in C2C12 myotubes; and (iii) by confocal microscopy on mature mouse skeletal muscle longitudinal sections. Figure 2(D) shows that SRP-35 is enriched in the skeletal muscle fraction corresponding to the LSR. Quantitative immunoblot analysis revealed that the immunopositive band corresponding to SRP-35 is enriched 6-fold (5.97 ± 0.2, mean $\pm$ S.E.M.; $n = 6$) in LSR compared with total muscle homogenate (see Supplementary Figure S1 at http://www.BiochemJ.org/bj/441/bj4410731add.htm). These results are compatible with the distribution of fluorescence in C2C12 myotubes transfected with GFP-tagged SRP-35 (Figure 2F). As shown, transfection of C2C12 cells with pEGFP results in an even cytoplasmic distribution of GFP fluorescence, whereas when cells expressed the SRP-35–GFP fusion protein, the resulting punctuated fluorescence is compatible with the localization of SRP-35 in membrane-bound organelles. High-resolution confocal analysis on longitudinal sections of mouse skeletal muscle, shows a cross-striated distribution of endogenous SRP-35 with a centre to centre distance between the bands of approximately 1.5 μm. This fluorescent pattern partially overlaps with that of the SERCA pump (see Supplementary Figure S2 at http://www.BiochemJ.org/bj/441/bj4410731add.htm), indicating a common subcellular distribution. A similar expression pattern was observed after *in vivo* transfection of FDB (flexor digitorum brevis) fibres with the SRP-35–EGFP construct (results not shown). Interestingly, and as shown in Figure 2(H), slow twitch fibres contain significantly less SRP-35 than fast twitch fibres (means $\pm$ S.E.M., $n = 6$, percentage intensity

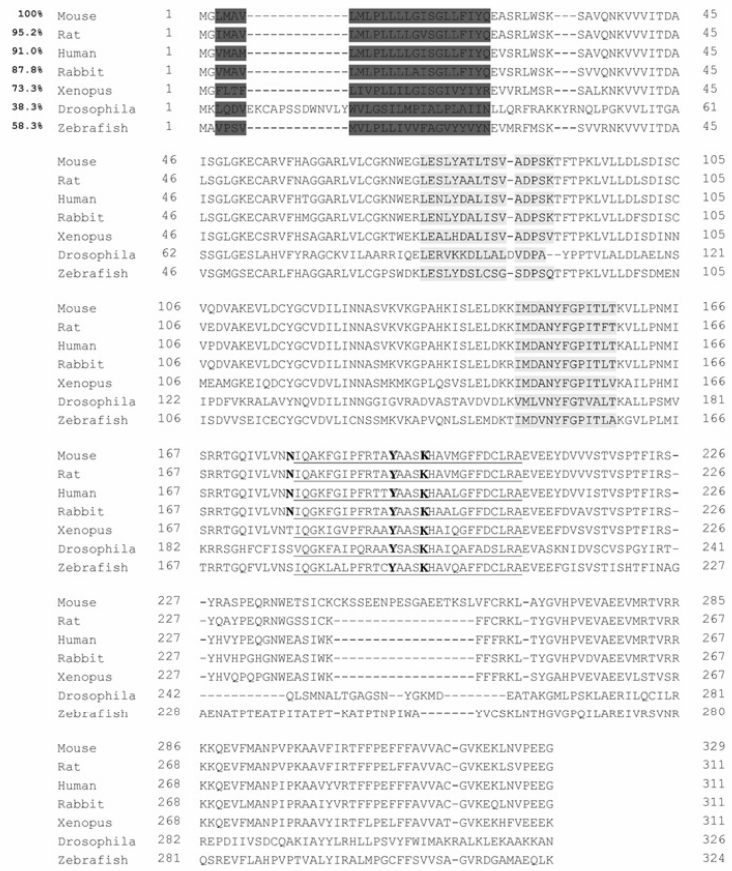

Figure 1 Predicted primary sequence of mouse SRP-35 and comparison with that of other vertebrates

Dark grey boxes indicate hydrophobic residues encoding the putative transmembrane domain. The two light grey boxes indicate the peptide sequences obtained from rabbit skeletal muscle SRP-35 from which primers were designed. Underlined residues indicate the catalytic consensus sequence and the bold letters indicate perfectly conserved residues within the NAD(P)(H)-binding site.

of the immunopositive band in Western blots from soleus was $69.7 \pm 5.6\,\%$ of that from EDL; $P < 0.0001$).

On the basis of its deduced primary sequence, the N-terminal of this protein encompasses a hydrophobic peptide of 24 residues, which could be a signal sequence or may form a trans-membrane α-helical segment. To establish whether in skeletal muscle SRP-35 is an integral membrane protein we: (i) extracted SR vesicles with KCl/Na_2CO_3; and (ii) performed trypsin digestion followed by Western blot analysis. Treatment of mouse total SR membrane fraction with 0.6M KCl, a procedure used to separate loosely bound proteins from the membrane of microsomal vesicles, did not dissociate SRP-35 from the SR vesicles (Figure 3A, left-hand panel). The failure to extract SRP-35 with high-ionic strength wash might be due to the localization of SRP-35 in the lumen of the SR vesicles, similarly to calsequestrin (Figure 3A, right-hand panel), or it might result from its integral association to the SR membrane. To discriminate between these possibilities, we performed an alkaline extraction of the SR fraction with 100 mM Na_2CO_3. As expected, calsequestrin (Figure 3B, right-hand panel), an intra-lumenal SR protein, was found in the Na_2CO_3-solubilized fraction. In contrast, SRP-35 was still associated with the insoluble membrane fraction (Figure 3B, left-hand panel), as was calnexin, a 90 kDa integral membrane protein of the ER (Figure 3B, middle panel). We further tested under what conditions SRP-35 could be solubilized, by treating SR vesicles with different detergents [CHAPS, DHPC (1,2-diheptanoyl-*sn*-glycero-3-phosphocholine) and DDM] under high ionic conditions. As shown, extraction with 1 % (w/v) CHAPS was not efficient, whereas the treatment of SR vesicles with 1 % (w/v) DHPC or DDM in the presence of 1 M NaCl was equally efficient at solubilizing SRP-35 (Figure 3C). Finally, the topological orientation of SRP-35 was assessed by proteolysis of SR vesicles with increasing concentrations of trypsin. Under our experimental conditions, the immunoreactivity of SRP-35 decreased with increasing trypsing concentration even at very low trypsin concentrations (30 and 150 ng), whereas at these concentrations the immunoreactivity of calregulin, which is a luminal SR protein and thus not exposed to trypsin, was unaffected (Figure 3D). These results indicate that the majority of the SRP-35 polypeptide, including its epitope(s), protrudes from the SR vesicles and is exposed towards the myoplasm and only a small portion is bound to the SR membrane.

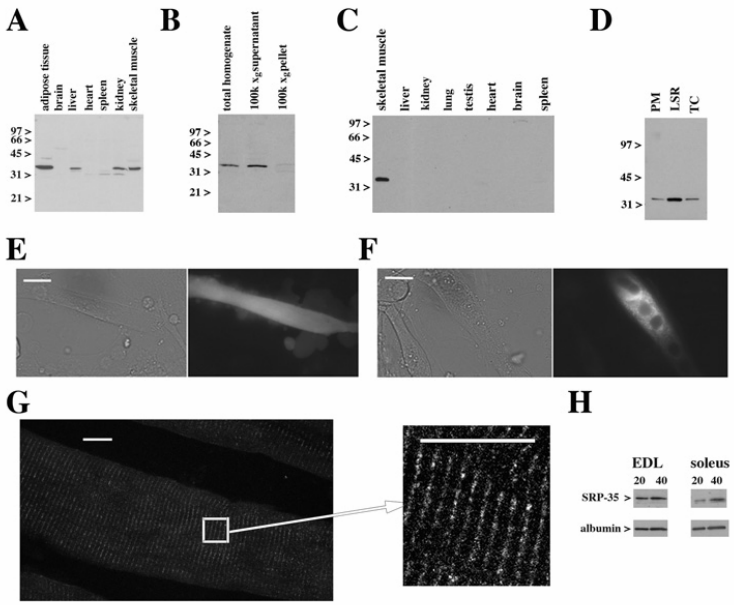

Figure 2 Tissue and subcellular distribution of SRP-35

(**A**) Total homogenates (30 μg/lane) from the indicated mouse tissues were separated on SDS/PAGE (12.5 % gel), blotted on to nitrocellulose membranes and probed with anti-SRP-35 antibody. (**B**) Total liver homogenate, the microsomal fraction (100 000 ***g*** pellet) or post-microsomal supernatant (100 000 ***g*** supernatant) (30 μg/lane) were loaded on to SDS/PAGE (12.5 % gel), blotted on to nitrocellulose membranes and probed with anti-SRP-35 antibody. (**C**) Total SR from mouse skeletal muscle or the microsomal fraction from the indicated tissues (50 μg/lane) were separated on SDS/PAGE (10 % gel), blotted on to nitrocellulose membranes and probed with anti-SRP-35 antibody. (**D**) Total mouse SR was fractionated into light (PM), LSR and terminal cisternae (TC) (30 μg/lane); proteins were separated on SDS/PAGE (10 % gel), blotted on to nitrocellulose and probed with anti-SRP-35 antibody. (**E**) C2C12 myotubes transfected with the plasmid encoding pEGFP were visualized by brightfield (left) or under fluorescent light with a 20$\times$ water-immersion FLUAR objective (0.75 NA). (**F**) C2C12 myotubes transfected with the plasmid encoding SRP-35–EGFP were visualized by brightfield (left) or under fluorescent light. Note that in these cells fluorescence is punctuated and excluded from the nuclei. Scale bar indicates 50 μm. (**G**) Longitudinal sections of mouse skeletal muscle were stained with anti-SRP-35 antibody followed by anti-rabbit-conjugated Alexa-Fluor® 488 antibody. Muscle tissue was visualized with a Leica DM1400 confocal microscope equipped with a HCX APO 100$\times$ oil immersion TIRF objective (1.47 NA). Images (1024$\times$1024) were acquired at 400 Hz through a 1 μm pinhole; note the striated distribution of SRP-35 compatible with a membrane localization. Scale bar indicates 10 μm. (**H**) Total homogenates (20 and 40 μg) of fast (EDL) and slow (soleus) muscles were loaded on to SDS/PAGE (10 % gel), the proteins were blotted on to nitrocellulose membranes and probed with anti-SRP-35 antibody as described above. Immunoreactivity with albumin was used as a control to show that similar amounts of proteins were loaded. Molecular masses in kDa are shown to the left-hand side of the Western blots in (**A**)–(**D**)

SRP-35 binds the dinucleotide NAD(H) and has catalytic activity

In silico comparison analysis of the deduced amino acid sequence of SRP-35 revealed that it shares homology with proteins belonging to the SDR family. In order to determine whether it indeed binds dinucleotides, the affinity column HiTrap Blue Sepharose was used; the ligand Cibacron Blue F3G-A shows structural similarities to NAD(H), enabling proteins strongly binding to this cofactor to attach to the resin [26]. Solubilized SR proteins were incubated with HiTrap Blue Sepahrose, the resin was extensively washed and bound proteins were eluted with 1 M NaCl plus NADH. The fraction(s) enriched in SRP-35 were identified by immunostaining with anti-SRP-35 antibodies. Figure 4 shows a representative result; the left-hand panels of Figures 4(A) and 4(B) are Ponceau-Red-stained membranes, whereas the right-hand panels are the same blots stained with anti-SRP-35 antibodies (Figure 4A) and with anti-calsequestrin antibodies as a control (Figure 4B). An immunoreactive band corresponding to SRP-35 is present in the total SR (lane 1), in the solubilized SR fraction (lane 3) and in the NADH-eluted fraction (lane 6). Not all SRP-35 was eluted with NADH, as demonstrated by the presence of an immunoreactive band of 35 kDa in an aliquot of the Cibacron Blue F3G-A resin (lane 7). On the other hand, when the same experiment was performed by following the distribution of calsequestrin, a major SR protein which should not bind to Cibacron Blue F3G-A, its immunoreactivity is present in the total SR, but not in the NADH eluate nor bound to the resin.

Since SRP-35 shares homology with the catalytic domains of classical SDR family members that convert, among others, retinol substrates to retinaldehyde derivatives, concomitantly reducing NAD, we set up an assay to validate the enzymatic activity of SRP-35 by verifying if its over-expression affects the amount of all-*trans*-retinol converted to all-*trans*-retinaldehyde. As an experimental setup we chose an '*in situ*' whole cell assay in which transiently transfected cells (HEK-293 cells or C2C12 myotubes) were incubated with all-*trans*-retinol or all-*trans*-retinaldehyde, and the amount of product formed was compared with that obtained in cells transiently transfected with the empty pEYFP plasmid. Figures 4(C) and 4(D) show original HPLC chromatograms obtained from lipid extracts of YFP- and SRP-35–YFP-transfected HEK-293 cells, Figures 4(E) and 4(F) show the cumulative results obtained by pooling data from three independent transfection experiments and normalized for the relative amount of all-*trans*-retinaldehyde-oxim (peaks 2 and 5) and retinol (peak 4) divided by the total amount of peaks 1–5, defined as 100 % (the total amount of all intracellular retinoids present in the lipid extracts). As shown, HEK-293 cells overexpressing SRP-35 generate a significantly larger proportion

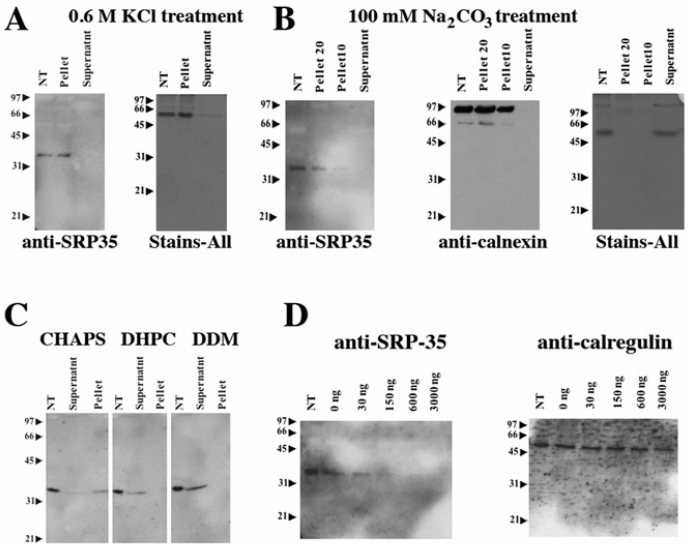

Figure 3 SRP-35 is tightly associated with SR membranes and the majority of the protein faces the myoplasm

Total mouse SR microsomes were incubated for 30 min on ice with either KCl (**A**) or Na_2CO_3 (**B**) and centrifuged at 150 000 ***g*** for 45 min. Proteins present in the supernatant and in the pellet were separated on SDS/PAGE (12.5 % gels) and stained with anti-SRP-35 antibodies or Stains-All (to visualize calsequestrin which stains metachromatically blue). (**C**) Total mouse skeletal muscle SR (1 mg/ml) was treated with the indicated detergent (1 %) in the presence of 1 M NaCl for 30 min at 4 °C. After centrifugation at 135 000 ***g***, pellets and supernatant were collected and proteins (30 μg/lane) were separated by SDS/PAGE (12.5 % gels), blotted on to nitrocellulose membranes and stained with anti-SRP-35 antibody. (**D**) Total SR from mouse skeletal muscles (50 μg of protein) were treated with increasing concentrations of trypsin for 2 min at room temperature. After treatment, the reaction was blocked and proteins were loaded on to SDS/PAGE (12.5 %), blotted on to nitrocellulose membranes and stained with antibodies against SRP-35 (left) and calregulin (as a control for vesicle integrity). NT, no treatment. Molecular masses in kDa are shown to the left-hand side of the Western blots.

of all-*trans*-retinaldehyde (sum of peaks 2 and 5) compared with YFP-transfected controls (Figure 4E). Interestingly, the reaction appears to preferentially proceed in the forward oxidative reaction, since no change in the relative amount of all-*trans*-retinol was obtained in SRP-35 overexpressing cells (Figure 4F). Similar results were obtained in C2C12-transfected myotubes (results not shown). In addition, 13-*cis*-retinol was sometimes detected in the SRP-35-transfected HEK-293 cells (peak 3), but may be an artefactual change of all-*trans*-retinol due to the extraction procedure. We also verified if SRP-35 overexpression affects the overall redox status of cells by performing Oxy-Blot analysis on total extracts of GFP- and SRP-35–GFP-transfected HEK-293 cells; as shown in Supplementary Figure S3 (at http://www.BiochemJ.org/bj/441/bj4410731add.htm), cells transfected with the SRP-35 fusion protein exhibited a significant increase in the quantity of oxidatively modified proteins, confirming that SRP-35 is indeed involved in redox reactions.

Effect of SRP-35 overexpression on excitation–contraction coupling

SRP-35 is located within a subcellular membrane devoted to the regulation of the Ca^{2+} concentration, thus we investigated if its overexpression affects Ca^{2+} homoeostasis. C2C12 mytotubes were transfected with SRP-35–EYFP or with the empty pEYFP vector, loaded with fura 2 and individually stimulated with different concentrations of either KCl (mimicking depolarization) or 4-chloro-*m*-cresol (inducing direct activation of the RyR1). As shown in Figure 5, overexpression of SRP-35 affected neither the resting Ca^{2+} concentration (Figure 5C) nor the EC_{50} for KCl (26.2 ± 0.8 and 27.6 ± 1.8 mM for YFP and SRP-35–YFP overexpressing cells respectively; Figure 5A) and 4-chloro-*m*-cresol (340.6 ± 32.6 and 306.7 ± 16.9 μM for YFP and SRP-35–YFP over-expressing cells respectively; Figure 5B) induced Ca^{2+} release; however, it significantly decreased the peak Ca^{2+} release induced by maximal stimulatory concentrations of KCl by approximately 40 % (Figure 5D; $P < 0.05$) and 4-chloro-*m*-cresol (Figure 5E; $P < 0.008$). This decrease in peak Ca^{2+} release was not due to depletion of intracellular stores, since the peak Ca^{2+} transients elicited by a treatment aimed at depleting intracellular stores (5 μM ionomycin plus 1 μM thapsigargin in 0.5 mM EGTA) were not significantly different (Δ fluorescence ratios were 0.251 ± 0.041 and 0.205 ± 0.048; $P = 0.479$ in YFP- and SRP-35–YFP-expressing cells). Interestingly, addition of retinoic acid to C2C12 myotubes during myotube differentiation mimicked the effect of SRP-35 overexpression by causing a significant decrease in the peak Ca^{2+} concentration induced by KCl (Figure 5D; $P < 0.01$) and 4-chloro-*m*-cresol (Figure 5E; $P < 0.008$). The reduced Ca^{2+} release could be due to allosteric regulation by products deriving from the enzymatic activity of SRP-35, such as NADH and/or to alterations of the level of expression of the proteins involved in excitation–contraction coupling. The latter event may result from the effect of retinoic acid generated from the retinaldehyde produced by SRP-35. In order to investigate this, we performed real-time PCR on mRNA extracted from C2C12 myotubes treated in culture with 5 μM retinoic acid. We chose this approach to avoid the variability linked to the efficiency of transient transfections of C2C12 cells. Figure 5(F) shows that retinoic acid treatment of C2C12 myotubes induces a 2.5-fold induction in the level of expression of SRP-35; no effect was observed on the expression level of the α1.1 subunit of the voltage-sensing DHPR (Figure 5G), but, interestingly,

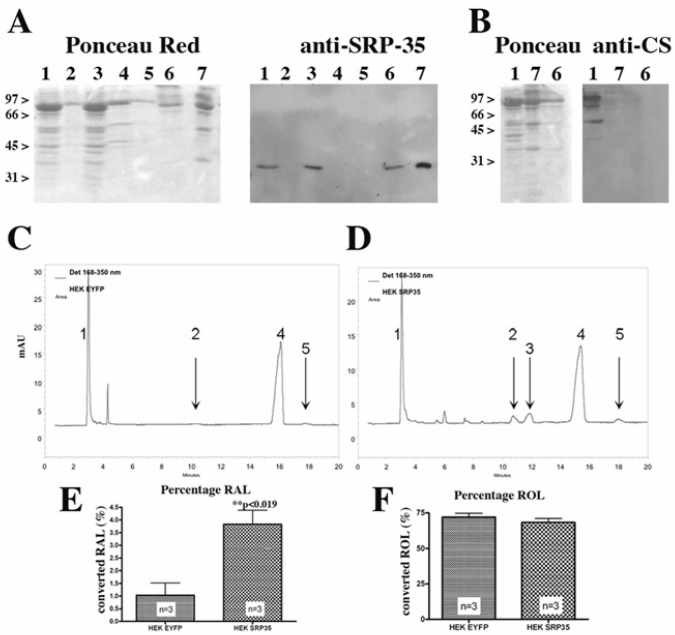

Figure 4 SRP-35 is a dinucleotide-binding protein and its overexpression leads to an increased production of all-*trans*-retinaldehyde

SRP-35 binds Cibacron Blue F3G-A ligand (**A**) 1 mg/ml total SR vesicles were solubilized in a solution containing 1% DDM, 1 M NaCl and subsequently incubated with Cibacron Blue F3G-A resin as described in the Experimental section. Proteins present in the total SR (30 μg, lane 1), the pellet after solubilization with DDM/NaCl (30 μl, lane 2), total SR proteins solubilized with DDM/NaCl (30 μl, lane 3), void (30 μl, lane 4), last wash (30 μl, lane 5), eluted with NADH (30 μl, lane 6) and attached to the resin (30 μl, lane 7). Left-hand panel, Ponceau Red-stained blot; right-hand panel, blot stained with anti-SRP-35 Abs. (**B**) as in (**A**), except that the right-hand blot was stained with anti-calsequestin antibodies. Note that calsequestrin does not bind to Cibacron Blue F3G-A. (**C** and **D**) Chromograms (325 nm) of the homogenates of pEYFPC1- and pEYFPC1-SRP-35-transfected HEK-293 cells. All-*trans*-retinylester (1), all-*trans*-retinaldehyde-oxim (syn: 2; anti: 5) (RAL), 13-*cis*-retinol (3) and all-*trans* retinol (4) (ROL). The peaks were identified by authentic standards. (**E** and **F**) Bar histograms comparing the percentage of retinaldehyde (RAL) and retinol (ROL) present in pEYFPC1- and pEYFPC1-SRP-35-transfected cells. Results are the means $\pm$ S.E.M. of the experiments. The percentage of retinaldehyde in cells overexpressing SRP-35 was significantly higher than in YFP-transfected cells, $P < 0.019$. Molecular masses in kDa are shown to the left-hand side of the Western blots in (**A**) and (**B**).

it caused a significant reduction (Figure 5H; $P < 0.025$) in the expression level of the mRNA encoding RyR1. This decrease in the RyR1 transcript was paralleled by a decrease in the content of the RyR1 protein as confirmed by Western blot analysis (see Supplementary Figure S4 at http://www.BiochemJ.org/bj/441/bj4410731add.htm). The extent of decrease of the mRNA level is similar to the extent of decrease of Ca^{2+} release observed after pharmacological activation of the RyR1 and most likely results from changes in the protein level of the RyR1 induced by retinoic acid production after 6 days of SRP-35 over-expression.

DISCUSSION

The skeletal muscle SR is an organelle that is specialized at regulating calcium homoeostasis, and identifying all its protein components constitutes a major step towards the elucidation of the regulation of calcium under normal and pathological conditions. In the present study we identified SRP-35 and show that this novel component of the skeletal muscle SR belongs to the SDR protein family, an enzyme whose activity may link calcium homoeostasis to activation of metabolism.

The enzyme superfamily of SDRs consits of more than 46000 family members that are ubiquitously expressed and whose transcripts have been found in virtually all genomes investigated [12,31,32]. In the presence of specific co-factors they dehydrogenate numerous substrates, including sterols, 3-hydroxysterols, alcohols, retinols, sugars, aromatic compounds and xenobiotics [33], thus playing critical roles in lipid, amino acid and carbohydrate metabolism; they also regulate many physiological processes by sensing the redox status in metabolism and transcription [13]. Although SDRs share little genetic similarity (15–30%) [32], some sequence motifs in their tertiary structures resemble each other [13] and, importantly, their co-factor-binding domain is highly conserved. In humans and mouse at least 70 distinct SDRs have been identified: they have a highly variable C-terminal substrate-binding domain, but all contain a Rossmann-fold scaffold and bind NAD(P) dinucleotides [13,31]. SRP-35 contains a tyrosine residue with adjacent lysine and serine residues in its active site, but is slightly larger than 'classical' SDR, being 311 rather than the classical 250 residues long; thus it should be classified as an 'extended' member of the SDR superfamily [13]. Among the many functions catalysed by SDR family members, some are involved in retinol/retinladehyde metabolism. Indeed, retinols (such as vitamin A) that are taken in with the diet are transported at high concentrations via the serum bound to retinol-binding protein and can be taken up by any cell for storage or potential conversion into retinoic acid. Once inside the cell they are converted into retinal via a reversible reaction catalysed by SDR (or alcohol dehydrogenases), first to retinaldehyde with the concomitant generation of NADH and subsequently to retinoic

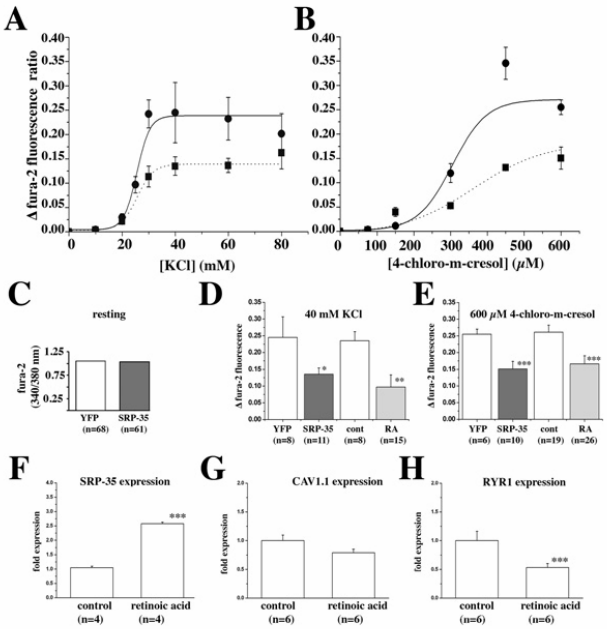

Figure 5 Effect of SRP-35 on calcium fluxes in C2C12 myotubes

(**A** and **B**) KCl- and 4-chloro-*m*-cresol dose–response curves in C2C12 transfected with pEYFPC1 (full line) or pEYFPC1-SRP-35 (dashed line). Data points represent the mean peak fluorescence increase of 6–11 cells. Curves were fitted using a Boltzmann equation; there were no significant differences in the EC_{50} for KCl or 4-chloro-*m*-cresol. (**C**) SRP-35 over-expression does not affect the resting Ca^{2+} concentrations of C2C12 cells. (**D** and **E**) Peak fura-2 Δ fluorescence (means ± S.E.M. of the indicated number of cells) in C2C12 transfected with pEYFPC1 (YFP), pEYFPC1-SRP-35 (SRP-35), untreated (cont) and treated with retinoic acid (RA; 5 μM) for 4 days. $^{*}P < 0.005$; $^{**}P < 0.01$; $^{***}P < 0.008$. (**F–H**) Real-time RT–PCR on control or retinoic acid-treated C2C12 cells. retinoic acid does not affect the relative expression level of $Ca_V1.1$, but it significantly increases the relative expression level of SRP-35 while decreasing that of RyR1. Results are expressed as means ± S.E.M. of the indicated number of experiments. $^{***}P < 0.001$.

acid by cytosolic aldehyde dehydrogenases (Aldh1a1 to Aldh1a3) [34,35].

The results of the present study support a role for SRP-35 in the conversion of retinol to retinaldehyde and thus to its involvement in the retinoic acid signalling pathway in skeletal muscle. Skeletal muscles express RAR and high levels of RXRγ [15,36,37], receptors that can activate the muscle-specific transcription factors myogenin and myoD [38,39], and treatment of muscle cells in culture with retinoic acid has been shown to stimulate myotube differentiation [39,40].

An intriguing aspect of SRP-35 is its particular tissue and subcellular distribution; in fact, Western blot analysis of different tissues revealed that it is abundantly expressed in liver and kidney, where it is absent from the microsomal fraction, but present in the post-microsomal supernatant. Indeed, SDRs have been found in the cytosol, in organelles such as the ER and mitochondria as well as in low-density peroxisomes [41,42], the latter being too light to be pelleted by a 1 h centrifugation at 100 000 *g*. In order to investigate whether SRP-35 is present in 'light' membrane fractions in liver and kidney, a more detailed analysis of rough and smooth ER, peroxisomes and lysosomes should be carried out. Nevertheless, in skeletal muscle, SRP-35 is present in the SR and on the basis of our subcellular fractionation experiments, it is enriched in the LSR, a fraction also enriched in proteins such as the SERCA pump and sarcalumenin (for a review, see [11]). Such a distribution is compatible with the high-resolution confocal immunofluorescence experiments of endogenous SRP-35, which revealed the presence of cross-striated bands, a pattern which is similar and partially overlaps with the distribution of SERCA. We cannot exclude that in skeletal muscle targeting of SRP-35 to the LSR is mediated by its interaction with other proteins. Co-immunoprecipitation experiments did not reveal any interaction with either SERCA1 or SERCA2 (results not shown) and binding to other SR proteins may be of low affinity and thus easily disrupted by the high salt concentration and detergents required to solubilize SRP-35. Interestingly, quantitative analysis of the content of SRP-35 in slow and fast twitch muscles indicates that this protein is enriched in fast twitch muscles; although of potential significance, this may be due to the fact that the relative volume of the SR is almost double in EDL compared with soleus muscles [43–45].

The biochemical characterization of this novel muscle SDR strongly support that it is a membrane-bound protein with its catalytic site facing the cytoplasm; in fact: first, it could not be extracted by treating vesicles with high salt or bicarbonate, methods which have been successfully used to extract loosely bound or soluble proteins from the ER/SR [23,24,46]; and secondly, mild detergents such as CHAPS were not efficient at solubilising SRP-35. Thirdly, trypsin digestion revealed that most of the protein faces the myoplasm; thus both its product (retinaldehyde) and NAD(P)H would be released into the myoplasm. The generation of NADH in the myoplasm may have functional signalling relevance; in fact, lactate dehydrogenase requires NADH as reducing power to generate lactate from pyruvate and, although NADH is available in the mitochondria where it is used to generate ATP, there are no transporters for

NADH and therefore the reduced co-factor must be regenerated in the cellular compartments where it is consumed [47]. It should also be mentioned that cytosolic NADH has been shown to regulate the activity of the RyR, especially in the heart [48,49]. Although we are aware that SRP-35 is a low abundance SR protein and we do not exactly know the stoichiometric ratio between SRP-35 and RyR1, we speculate the NADH generated by SRP-35 in a microdomain adjacent to SR membranes might allosterically modulate RyR1 activity. We also can not exclude the possibility that SRP-35 indirectly modulates Ca^{2+} release by affecting the level of expression of the RyR1 protein.

Our results from the present study show that overexpression of SRP-35 in C2C12 myotubes results in a decrease of RyR1-mediated Ca^{2+} release, a result that could be mimicked by the addition of retinoic acid to the culture medium during differentiation. Indeed, both the Ca^{2+} release induced by KCl (mimicking depolarization) as well as that induced by direct activation of RyR1 were reduced by approximately 40% with no significant change in the EC_{50} for either agonist. Such a result is reminiscent of the effect of mutations in the *RYR1* gene linked to some forms of central core disease and multiminicore disease; in fact, mytubes from such patients have reduced pharmacologically evoked Ca^{2+} release, and, depending on the mutation, increased or normal resting Ca^{2+} concentration and/or reduced expression of RyR1 in muscle [25,50–52]. In the case of SRP-35, the decreased Ca^{2+} release was not accompanied by a change in the resting Ca^{2+} concentration nor in the Ca^{2+} present in intracellular stores, suggesting that the effect was not due to a modification of Ca^{2+} fluxes across surface membranes [53], but probably due to reduced expression of components of the Ca^{2+} release units. Real-time PCR on retinoic acid-treated cells shows that the level of expression of the $Ca_v1.1$ was not affected, but that of the RyR1 was reduced by approximately 50%, a result confirmed by immunoblotting. A similar effect of retinoic acid treatment on the expression of inositol 1,4,5-trisphoshate receptors has been reported [54,55] and is thought to be due to a decrease in the promoter activity in response to retinoic acid.

What is the function of SRP-35 *in vivo* and what is the physiological activator of this SDR? Skeletal muscle constitutes approximately 40% of the total body mass, accounts for more than 30% of energy expenditure and is the major tissue involved in insulin-dependent glucose uptake. Metabolism is largely regulated by nuclear hormone receptors that function as regulators of transcription and it has been demonstrated that in mice retinoic acid treatment favours mobilization of body fat, increases fatty acid oxidation and decreases body weight [20,56]. Alhough at the moment it is difficult to envisage what activates the enzymatic activity of SRP-35, its strategic subcellular localization in a compartment dedicated to Ca^{2+} homoeostasis, and the fact that during the conversion of retinol to retinaldehyde it will concomitantly generate NADH, indicates that it may be an important molecule linking Ca^{2+} mobilization and thus muscle contraction to the activation of metabolic functions. SRP-35 is a dehydrogenase and could reduce the NAD^+ generated by lactate dehydrogenase during sustained muscle activity. In fact, the NAD^+ that is generated during glycolysis remains in the cytoplasm since the inner mitochondrial membrane lacks a specific transport system [47]. Interestingly, many enzymes involved in the glycolytic pathway adhere to the SR membranes [21]. The reduction of NAD^+ by SRP-35 is coupled to the conversion of all-*trans*-retinaldehyde to retinoic acid, an important activator of *GLUT4* (glucose transporter 4) gene transcription [57] and regulator of RyR1 expression (Figure 5). Additionally, a secondary effect of SRP-35 could be mediated by NADH, which has been shown to regulate RyR activity [49]. The development of an experimental model overexpressing SRP-35 in the skeletal muscle will allow us to investigate in greater detail many aspects of this novel SDR, ranging from metabolism to activation of transcription of specific genes.

AUTHOR CONTRIBUTION

Susan Treves devised the experiments, co-wrote the manuscript, performed the calcium measurements and performed confocal microscopy experiments. Raphael Thurnheer performed the retinol/retinal measurements, bioinformatics, transfection of C2C12 cells and HEK-293 cells and helped perform the calcium imaging experiments. Barbara Mosca, Mirko Vukcevic and Leda Bergamelli created the plasmid constructs, and performed the RT–PCR and molecular biology. Rebecca Voltan performed the original PCR to obtain mouse cDNA, Western blotting, proteolysis, vesicle solubilization and Cibachron Blue chromatography. Vitus Oberhauser supervised and helped in the retinol/retinaldehyde quantification. Michel Ronjat performed the original MS and protein sequencing. Lazslo Csenoch and Peter Szentesi performed the GFP–SRP-35 fluorescence measurements in intact fibres. Francesco Zorzato devised the experiments, supervised all the steps and wrote the paper.

ACKNOWLEDGEMENTS

We would like to thank Ms Anne-Sylvie Monnet for her expert technical assistance and Caroline Steiblin for her help with the bioinformatics.

FUNDING

This work was supported by the Department of Anesthesia, Basel University Hospital and by the Association Française contre les Myopathies, Telethon GGP08020, Ministero della Ricerca Scientifica e Tecnologica ex 40% e 60% [grant number HPRN-CT-2002-00331].

REFERENCES

1 Saito, A., Seiler, S., Chu, A. and Fleischer, S. (1984) Preparation and morphology of sarcoplasmic reticulum terminal cisternae from rabbit skeletal muscle. J. Cell. Biol. **99**, 875–885
2 Schneider, M. F. and Chandler, W. K. (1972) Voltage dependent charge movement of skeletal muscle: a possible step in excitation-contraction coupling. Nature **242**, 244–246
3 Melzer, W., Herrmann-Frank, A. and Luttgau, H. C. (1995) The role of Ca^{2+} ions in excitation-contraction coupling of skeletal muscle fibres. Biochim. Biophys. Acta **1241**, 59–116
4 Inesi, G., Canitlina, T., Yu, X., Nikic, D., Sagara, Y. and Kirtley, M. E. (1992) Long-range intramolecular linked functions in activation and inhibition of SERCA ATPases. Ann. N.Y. Acad. Sci. **671**, 32–47
5 MacLennan, D. H. (2000) Ca^{2+} signaling and muscle disease. Eur. J. Biochem. **267**, 5291–5297
6 MacLennan, D. H., Asahi, M. and Tupling, A. R. (2003) The regulation of SERCA-type pumps by phospholamban and sarcolipin. Ann. N.Y. Acad. Sci. **986**, 472–480
7 Franzini-Armstrong, C. and Jorgensen, A. O. (1994) Structure and development of E-C coupling units in skeletal muscle. Annu. Rev. Physiol. **56**, 509–534
8 Mitchell, R. D., Saito, A., Palade, P. and Fleischer, S. (1983) Morphology of isolated triads. J. Cell Biol. **96**, 1017–1029
9 Rios, E. and Pizarro, G. (1991) Voltage sensor of excitation-contraction coupling in skeletal muscle. Physiol. Rev. **71**, 849–908
10 Weisleder, N., Takeshima, H. and Ma, J. (2008) Immuno-proteomic approach to excitation-contraction coupling in skeletal and cardiac muscle: molecular insights revealed by the mitsugumins. Cell Calcium **43**, 1–8
11 Treves, S., Vukcevic, M, Maj, M., Thurnheer, R., Mosca, B. and Zorzato, F. (2009) Minor sarcoplasmic reticulum membrane components that modulate excitation-contraction coupling in striated muscles. J. Physiol. **587**, 3071–3079
12 Persson, B., Kallberg, Y., Bray, J. E., Bruford, E., Dellaporta, S. L., Favia, A. D., Duarte, R. G., Jörnvall, H., Kavanagh, K. L., Kedishvili, N. et al. (2009) The SDR (short-chain dehydrogenase/reductase and related enzymes) nomenclature initiative. Chem. Biol. Interact. **178**, 94–98
13 Kavanagh, K. L., Jörnvall, H., Persson, B. and Oppermann, U. (2008) Medium- and short-chain dehydrogenase/reductase gene and protein families: the SDR superfamily: functional and structural diversity within a family of metabolic and regulatory enzymes. Cell Mol. Life Sci. **65**, 3895–3990

14 Theodosiou, M., Laudet, V. and Schubert, M. (2010) From carrot to clinic: an overview of the retinoic acid signaling pathway. Cell Mol. Life Sci. **67**, 1423–1445
15 Mangelsdorf, D. J., Borgmeyer, U., Heyman, R. A., Zhou, J. Y., Ong, E. S., Oro, A. E., Kakizuka, A. and Evans, R. M. (1992) Characterization of three RXR genes that mediate the action of 9-cis retinoic acid. Genes Dev. **6**, 329–344
16 Petkovich, M., Brand, N. J., Krust, A. and Chambon, P. (1987) A human retinoic acid receptor which belongs to the family of nuclear receptors. Nature **330**, 444–450
17 Germain, P., Chambon, P., Eichele, G., Evans, R. M., Lazar, M. A., Leid, M., De Lera, A. R., Lotan, R., Mangelsdorf, D. J. and Groenmeyer, H. (2006) International Union of Pharmacology. LX. Retinoic acid receptors. Pharmacol. Rev. **58**, 712–725
18 Ziouzenkova, O. and Plutzky, J. (2008) Retinoid metabolism and nuclear receptor responses: new insights into coordinated regulation of the PPAR-RXR complex. FEBS Lett. **582**, 32–38
19 Napoli, J. L. (1996) Biochemical pathways of retinoid transport, metabolism and signal transduction. Clin. Immunol. Immunopathol. **80**, S52–S62
20 Amengual, J., Ribot, J., Bonet, M. L. and Palou, A. (2008) Retinoic acid treatment increases lipid oxidation capacity in skeletal muscle of mice. Obesity **16**, 585–591
21 Xu, K. Y. and Becker, L. C. (1998) Ultrastructural localization of glycolytic enzymes on sarcoplasmic reticulum vesicles. J. Histochem. Cytochem. **46**, 419–427
22 Journet, A., Chapel, A., Kieffer, S., Louwagie, M., Luche, S. and Garin, J. (2000) Towards a human repertoire of monocytic lysosomal proteins. Electrophoresis **21**, 3411–3419
23 Anderson, A. A., Treves, S., Biral, D., Betto, R., Sandonà, D., Ronjat, M. and Zorzato, F. (2003) The novel skeletal muscle sarcoplasmic reticulum JP-45 protein. Molecular cloning, tissue distribution, developmental expression, and interaction with α1.1 subunit of the voltage-gated calcium channel. J. Biol. Chem. **278**, 39987–39992
24 Treves, S., Feriotto, G., Moccagatta, L., Gambari, R. and Zorzato, F. (2000) Molecular cloning, expression, functional characterization, chromosomal localization, and gene structure of junctate, a novel integral calcium binding protein of sarco(endo)plasmic reticulum membrane. J. Biol. Chem. **275**, 39555–39568
25 Zorzato, F., Anderson, A. A., Ohlendieck, K., Froemming, G., Guerrini, R. and Treves, S. (2000) Identification of a novel 45 kDa protein (JP-45) from rabbit sarcoplasmic-reticulum junctional-face membrane. Biochem. J. **351**, 537–543
26 Sharkis, D. H. and Swenson, R. P. (1989) Purification by cibacron blue F3GA dye affinity chromatography and comparison of NAD(P)H: quinone reductase (E.C.1.6.99.2) from rat liver cytosol and microsomes. Biochem. Biophys. Res. Commun. **161**, 434–441
27 Ducreux, S., Zorzato, F., Müller, C., Sewry, C., Muntoni, F., Quinlivan, R., Restagno, G., Girard, T. and Treves, S. (2004) Effect of ryanodine receptor mutations on interleukin-6 release and intracellular calcium homeostasis in human myotubes from malignant hyperthermia-susceptible individuals and patients affected by central core disease. J. Biol. Chem. **279**, 43838–43846
28 Gough, W. H., VanOoteghem, S., Sint, T. and Kedishvill, N. Y. (1998) cDNA cloning and characterization of a new human microsomal NAD+-dependent dehydrogenase that oxidizes all-trans-retinol and 3 α-hydroxysteroids. J. Biol. Chem. **273**, 19778–19785
29 Treves, S., Vukcevic, M., Jeannet, P. Y., Levano, S., Girard, T., Urwyler, A., Fischer, D., Voit, T., Jungbluth, H., Lillis, S. et al. (2011) Enhanced excitation coupled Ca^{2+} entry induces nuclear translocation of NFAT and contributes to IL-6 release from myotubes from patients with Central core disease. Hum. Mol. Genetics **20**, 589–600
30 Takeshima, H., Komazaki, S., Nishi, M., Iino, M. and Kangawa, K. (2002) Junctophilins: a novel family of junctional membrane complex proteins. Mol. Cell **6**, 11–22
31 Persson, B., Krook, M. and Jörnvall, H. (1991) Characteristics of short-chain alcohol dehydrogenases and related enzymes. Eur. J. Biochem. **200**, 537–543
32 Kallberg, Y., Oppermann, U., Jörnvall, H. and Persson, B. (2002) Short-chain dehydrogenase/reductase (SDR) relationships: a large family with eight clusters common to human, animal, and plant genomes. Protein Sci. **11**, 636–641
33 Persson, B., Kallberg, Y., Oppermann, U. and Jörnvall, H. (2003) Coenzyme-based functional assignments of short-chain dehydrogenases/reductases (SDRs). Chem. Biol. Interact. **143**, 271–278
34 Duester, G. (1996) Involvement of alcohol dehydrogenase, short-chain dehydrogenase/reductase, aldehyde dehydrogenase, and cytochrome P450 in the control of retinoid signaling by activation of retinoic acid synthesis. Biochemistry **35**, 12221–12227
35 Parés, X., Farrés, J., Kedishvili, N. and Duester, G. (2009) Medium- and short-chain dehydrogenase/reductase gene and protein families: the SDR superfamily: functional and structural diversity within a family of metabolic and regulatory enzymes. Cell Mol. Life Sci. **65**, 3895–3906
36 Liu, Q. and Linney, E. (1993) The mouse retinoid-X receptor-γ gene: genomc organization and evidence for functional isoforms. Mol. Endocrinol. **7**, 651–658
37 Smith, A. G. and Muscat, G.E.O. (2005) Skeletal muscle and nuclear hormone receptors: implications for cardiovascular and metabolic disease. Int. J. Biochem. Cell Biol. **37**, 2047–2063
38 Muscat, G.E, Mynett-Johnson, L., Dowhan, D., Downes, M. and Griggs, R. (1994) Activation of myoD gene transcription by 3,5,3′-triodo-L-thyronine: a direct role for the thyroid hormone and retinoid X receptors. Nucleic Acids Res. **22**, 583–591
39 Halevy, O. and Lerman, O. (1993) Retinoic acid induces adult muscle cell differentiation mediated by the retinoic acid receptor α. J. Cell Physiol. **154**, 566–572
40 Zhu, G. H., Huang, J., Bi, Y., Su, Y., Tang, Y., He, B. C., He, Y., Luo, J., Wang, Y., Chen, L. et al. (2009) Activation of RXR and RAR signaling promotes myogenic differentiation of myoblastic C2C12 cells. Differentiation **78**, 195–204
41 Filling, C., Wu, X., Shafqat, N., Hult, M., Martensson, E., Shafqat, J. and Oppermann, U.C.T. (2001) Subcellular targeting analysis of SDR-type hydroxysteroid dehydrogenases. Mol. Cell Endocrinol. **171**, 99–101
42 Markus, M., Husen, B. and Adamski, J. (1995) The subcellular localization of 17β-hydroxysteroid dehydrogenase type 4 and its interaction with actin. J. Steroid Biochem. Molec. Biol. **55**, 617–621
43 Luff, A. R. and Atwood, H. L. (1971) Changes in the sarcoplasmic reticulum and transverse tubular system of fast and slow skeletal muscles of the mouse during postnatal development. J. Cell Biol. **51**, 369–383
44 Eisenberg, B. R., Kuda, A. M. and Peter, J. B. (1974) Stereological analysis of mammalian skeletal muscle. I. Soleus muscle of the adult guinea pig. J. Cell Biol. **60**, 732–754
45 Franzini-Armstrong, C. and Peachey, L. D. (1981) Striated muscle contractile and control mechanisms. J. Cell Biol. **91**, 166–186
46 Cala, S. E. and Jones, L. R. (1983) Rapid purification of calsequestrin from cardiac and skeletal muscle sarcoplasmic reticulum vesicles by Ca^{2+}-dependent elution from phenyl-sepharose. J. Biol. Chem. **258**, 11932–11936
47 Voet, D. and Voet, J. G. (2004) Biochemistry, pp. 800–802, John Wiley & Sons, New York
48 Cherednichenko, G., Zima, A. V., Feng, W., Schafer, S., Blatter, L. A. and Pessah, I. N. (2004) NADH oxidase activity of rat cardiac sarcoplasmic reticulum regulates calcium induced calcium-release. Circ. Res. **94**, 478–486
49 Zima, A. V., Copello, J. A. and Blatter, L. A. (2003) Differential modulation of cardiac and skeletal muscle ryanodine receptors by NADH. FEBS Lett. **547**, 32–36
50 Zhou, H., Yamaguchi, N., Xu, L., Wang, Y., Sewry, C., Jungbluth, H., Zorzato, F., Bertini, E., Muntoni, F., Meissner, G. and Treves, S. (2006) Chracterization of recessive RYR1 mutations in core myopathies. Hum. Mol. Genet. **15**, 2791–2803
51 Zhou, H., Jungbluth, H., Sewry, C. A., Feng, L., Bertini, E., Bushby, K., Straub, V., Roper, H., Rose, M. R., Brockington, M. et al. (2007) Molecular mechanisms and phenotypic variation in RYR1 related congenital myopathies. Brain **130**, 2024–2036
52 Ghassemi, F., Vukcevic, M., Xu, L., Zhou, H., Meissner, G., Muntoni, F., Jungbluth, H., Zorzato, F. and Treves, S. (2009) A recessive ryanodine receptor 1 mutation in a CCD patient increases channel activity. Cell Calcium **45**, 192–197
53 Rios, E. (2010) The cell boundary theorem: a simple law of the control of cytosolic calcium concentration. J. Physiol. Sci. **60**, 81–84
54 Stefanik, P., Macejova, D., Mravec, B., Brtko, J. and Krizanova, O. (2005) Distinct modulation of a gene expression of the type 1 and 2 IP_3 receptors by retinoic acid in brain areas. Neurochem. Int. **46**, 559–564
55 Deelman, L. E., Jonk, L.J.C. and Henning, R. H. (1998) The isolation and characterization of the promoter of the human type I inositol 1,4,5-trisphosphate receptor. Gene **207**, 219–225
56 Haugen, B., Jensen, D. R., Sharma, V., Pulawa, L. K., Hays, W. R., Krezel, W., Chambon, P. and Eckel, R. H. (2004) Retinoid X receptor γ-deficient mice have increased skeletal muscle lipoprotein lipase activity and less weight gain when fed a high-fat diet. Endocrinology **145**, 3679–3685
57 Sleeman, M. W., Zhou, H., Rogers, S., Ng, K. W. and Best, J. D. (1995) Retinoic acid stimulates glucose transporter expression in L6 muscle cells. Mol. Cell. Endocrinol. **27**, 161–167

Received 10 August 2011/3 October 2011; accepted 14 October 2011
Published as BJ Immediate Publication 14 October 2011, doi:10.1042/BJ20111457

Biochem. J. (2012) **441**, 731–741 (Printed in Great Britain) doi:10.1042/BJ20111457

SUPPLEMENTARY ONLINE DATA

SRP-35, a newly identified protein of the skeletal muscle sarcoplasmic reticulum, is a retinol dehydrogenase

Susan TREVES*†, Raphael THURNHEER*, Barbara MOSCA†, Mirko VUKCEVIC*, Leda BERGAMELLI†, Rebecca VOLTAN†, Vitus OBERHAUSER‡, Michel RONJAT§, Laszlo CSERNOCH‖, Peter SZENTESI‖ and Francesco ZORZATO*†[1]

*Departments of Anaesthesia and of Biomedicine, Basel University Hospital, Hebelstrasse 20, 4031 Basel, Switzerland, †Department of Experimental and Diagnostic Medicine, General Pathology Section, University of Ferrara, Via Borsari 46, 44100 Ferrara, Italy, ‡Albert-Ludwigs-Universität Freiburg Institut für Biologie I (Zoologie), Hauptstrasse 1, 79104 Freiburg, Germany, §Unité Inserm U836, Université Joseph Fourier, Grenoble Institute of Neuroscience, Site Santé, 38700 La Tronche, France, and ‖Department of Physiology, University of Debrecen, Nagyerdei krt. 98, 4012 Debrecen, Hungary

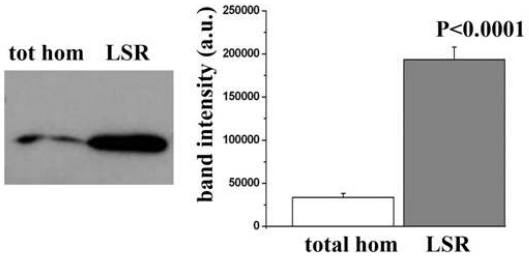

Figure S1 Subcellular distribution of SRP-35 in mouse skeletal muscle

Muscle tissue was extracted from mouse hindlimbs, homogenized (10 %, w/v) in 150 mM NaCl, 100 mM Tris/HCl, pH 8.0, 1 mM EDTA and a cocktail of antiproteases (Roche Applied Science), and spun for 5 s in a Tomy PMC-060 Capsulfuge. The supernatant represents the 'total homogenate' (tot hom). The LSR was isolated by sucrose gradient centrifugation according to the protocol of Saito et al. [1]. Total homogenate and LSR (40 μg) were separated on SDS/PAGE (15 % gel), blotted on to nitrocellulose membranes and probed with anti-SRP-35 antibody (left-hand panel) as described in the Experimental section of the main text. The right-hand panel shows the histogram of the mean ($\pm$ S.E.M.; $n = 6$) intensity of the SRP-35 immunopositive band in the total homogenate and LSR.

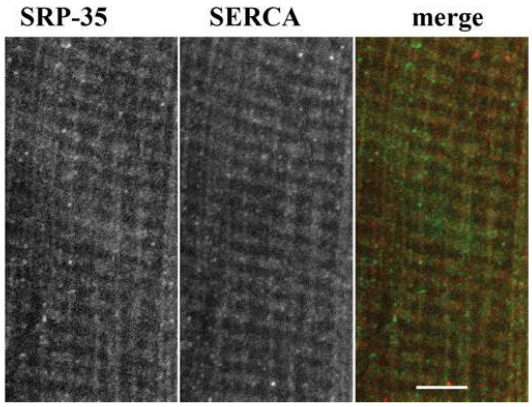

Figure S2 Double immunofluorescence labelling of SRP-35 and SERCA in mouse skeletal muscle tissue sections

Mouse skeletal muscle longitudinal sections were labelled as described in the Experimental section of the main text with rabbit anti-SRP-35 antibody followed by anti-rabbit Alexa Fluor® 488 conjugate and mouse anti-SERCA antibody followed by anti-mouse Alexa Fluor® 568 conjugate. Slides were mounted and visualized by confocal microscopy with a Leica DM1400 confocal microscope equipped with a 100× HCX APO TIRF objective (1.47 NA) at a resolution of 1024×1024 pixels and a pinhole of 1 μm. Scale bar indicates 5 μm. Co-localization of SRP-35 and SERCA was performed using the 'measure colocalization' application included in the Metamorph 5.7.4 software package. Analysis revealed that, within the area positive for SRP-35, 16.8 % was also positive for SERCA and within the area positive for SERCA, 15.2 $\pm$ 1.1 % was also positive for SRP-35.

[1] To whom correspondence should be addressed (email zor@unife.it).

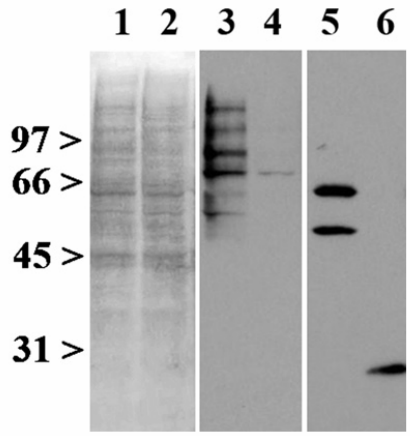

Figure S3 OxyBlot analysis of HEK-293 cells transfected with GFP or SRP-35–GFP

Cells were transfected with pEGFPC1 or pEGFPC1-SP-35; 48 h after transfection cells were harvested, washed 3 times with PBS, lysed in 1 % Nonidet P40, 0.5 % sodium deoxycholate, 150 mM NaCl, 5 mM EDTA and 50 mM Tris/HCl, pH 8.0, and processed as described in the OxyBlot Protein oxidation detection kit (Millipore). Protein (10 μg) (lanes 1, 3 and 5, pEGFPC1-SP-35; lanes 2,4 and 6, pEGFP) was separated on SDS/PAGE (10 % gels), blotted on to nitrocellulose membranes and the oxidatively modified proteins were visualized by chemiluminescence. Lanes 1 and 2: Ponceau Red; lanes 3 and 4: Oxy-Blot; and lanes 5 and 6: anti-GFP. The EGFP–SRP-35 fusion protein appears as a doublet in HEK-293 cells, indicating probable post-translational processing in non-muscle cells. Molecular masses in kDa are shown to the left-hand side.

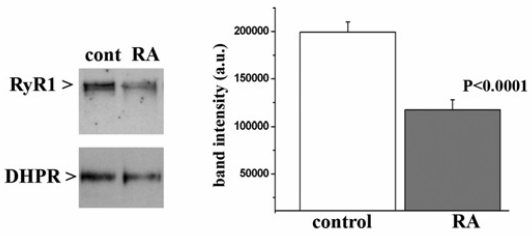

Figure S4 Treatment of C2C12 cells for 4 days with retinoic acid leads to a decrease in RyR1 protein content

Left-hand panel: 30 μg of protein from the microsomal fraction isolated from untreated (cont) or retinoic acid (5 μM, RA) treated C2C12 myotubes were separated on SDS/PAGE (6 % gels), blotted on to nitrocellulose and probed with anti-RyR1 antibody. The blots were then stripped and re-probed with anti-DHPRα1.1 antibody. Right-hand panel: histogram of the mean ($\pm$S.E.M.; $n = 7$) intensity of the RyR1 immunopositive band normalized from the content of the DHPRα1.1 immunopositive band in control and retinoic acid-treated cells.

REFERENCE

1 Saito, A., Seiler, S., Chu, A. and Fleischer, S. (1984) Preparation and morphology of sarcoplasmic reticulum terminal cisternae from rabbit skeletal muscle. J. Cell. Biol. **99**, 875–885

Received 10 August 2011/3 October 2011; accepted 14 October 2011
Published as BJ Immediate Publication 14 October 2011, doi:10.1042/BJ20111457

J Physiol 587.13 (2009) pp 3071–3079

SYMPOSIUM REVIEW

Minor sarcoplasmic reticulum membrane components that modulate excitation–contraction coupling in striated muscles

Susan Treves[1,2], Mirko Vukcevic[1], Marcin Maj[1], Raphael Thurnheer[1], Barbara Mosca[2] and Francesco Zorzato[2]

[1]*Departments of Anesthesia and Biomedicine, Basel University Hospital, Hebelstrasse 20, 4031 Basel, Switzerland*
[2]*Department of Experimental and Diagnostic Medicine, University of Ferrara, Via Borsari 46, 44100 Ferrara, Italy*

In striated muscle, activation of contraction is initiated by membrane depolarisation caused by an action potential, which triggers the release of Ca^{2+} stored in the sarcoplasmic reticulum by a process called excitation–contraction coupling. Excitation–contraction coupling occurs via a highly sophisticated supramolecular signalling complex at the junction between the sarcoplasmic reticulum and the transverse tubules. It is generally accepted that the core components of the excitation–contraction coupling machinery are the dihydropyridine receptors, ryanodine receptors and calsequestrin, which serve as voltage sensor, Ca^{2+} release channel, and Ca^{2+} storage protein, respectively. Nevertheless, a number of additional proteins have been shown to be essential both for the structural formation of the machinery involved in excitation–contraction coupling and for its fine tuning. In this review we discuss the functional role of minor sarcoplasmic reticulum protein components. The definition of their roles in excitation–contraction coupling is important in order to understand how mutations in genes involved in Ca^{2+} signalling cause neuromuscular disorders.

(Received 6 March 2009; accepted after revision 10 April 2009; first published online 29 April 2009)
Corresponding author F. Zorzato: Department of Experimental and Diagnostic Medicine, University of Ferrara, Via Borsari 46, 44100 Ferrara, Italy. Email: zor@unife.it

Abbreviations DHPR, dihydropyridine receptor; EC coupling, excitation–contraction coupling; JFM, junctional face membrane; KO, knock out; LSR, light sarcoplasmic reticulum; RyR, ryanodine receptor; SR, sarcoplasmic reticulum; SERCA, sarcoplasmic reticulum Ca^{2+}-ATPase.

Calcium homeostasis in striated muscles

Over the decades, the role(s) played by Ca^{2+} in skeletal muscle have been unveiled and it is now clearly established that it is the key element underlying muscle contraction. Its importance is given by the fact that movement of the contractile proteins is dependent on the Ca^{2+} released from the sarcoplasmic reticulum (SR), an organelle constituting approximately 10% of the cell's volume and fully dedicated to uptake and release of Ca^{2+} (Peachey, 1965; Volpe & Simon, 1991). The SR can be structurally divided into two distinct portions: the terminal cisternae, which face the transverse tubules (invaginations of the plasma membrane) and the longitudinal sarcoplasmic reticulum, connecting two terminal cisternae. The terminal cisternae can be further divided into junctional face membrane (JFM) (the domain facing the transverse tubules) and non-junctional membrane (Saito *et al.* 1984; Costello *et al.* 1986).

Depolarization of the plasma membrane of skeletal muscle leads to release of Ca^{2+} from the SR resulting in muscle contraction, by a process known as excitation–contraction coupling (Schneider & Chandler, 1972; Melzer *et al.* 1995; Berchtold *et al.* 2000). Excitation–contraction coupling (EC coupling) occurs at the triad, a structure composed of the two membrane

This review was presented at *The Journal of Physiology* Symposium on *Calsequestrin, triadin and more: the proteins that modulate calcium release in cardiac and skeletal muscle*, which took place at the 53rd Biophysical Society Annual Meeting at Boston, MA, USA on 27 February 2009. It was commissioned by the Editorial Board and reflects the views of the authors.

DOI: 10.1113/jphysiol.2009.171876

compartments, transverse tubules containing the voltage sensing dihydropyridine receptor (DHPR, an L-type Ca^{2+} channel) and terminal cisternae on which ryanodine receptor (RyR) Ca^{2+} release channels are localized (Mitchell *et al.* 1983; Rios & Pizarro, 1991). The disposition of DHPRs and RyRs on their respective membranes is highly ordered and each DHPR faces alternate rows of RyR tetramers (Fig. 1) (Block *et al.* 1988; Franzini-Armstrong & Jorgensen, 1994; Paolini *et al.* 2004). These two Ca^{2+} channels are the basic unit underlying excitation–contraction coupling, but they do not function alone – there are a number of accessory proteins involved in their fine regulation.

Major and minor protein components of the sarcoplasmic reticulum

One of the major advances in the field of excitation–contraction coupling was the development of reproducible procedures enabling the fractionation of SR membranes enriched in proteins involved in calcium handling (Meissner *et al.* 1973; Campbell *et al.* 1980; Saito *et al.* 1984). This revealed that protein components of the longitudinal SR (LSR) and terminal cisternae are different, reflecting the functional subspecialization of these membrane fractions, which are, respectively, Ca^{2+} uptake and Ca^{2+} release. Figure 2 shows a 5–15% SDS–polyacrylamide gel stained with Coomassie Brilliant Blue of the protein components of LSR, terminal cisternae and junctional face membrane. The major component of the LSR, constituting approximately 80% of the total proteins present, is the 110 kDa Ca^{2+}-ATPase (SERCA), i.e. the pump responsible for pumping the Ca^{2+} released by the RyR1s back into the SR. The 22 kDa protein band present in the longitudinal SR fraction is phospholamban, a protein involved in regulating the activity of the SERCA pump in heart and slow twitch muscle fibres. When phospholamban is dephosphorylated it inhibits the activity of SERCA, whereas in its phosphorylated state, inhibition is relieved (Slack *et al.* 1997; Liu *et al.* 1997; MacLennan *et al.* 2003). Ablation of phospholamban causes a significant (25%) decrease in the time to half-relaxation of isolated solei with no change in the contraction time (Jay *et al.* 1997), supporting its important role in regulation of SERCA activity.

Two glycoproteins of 160 kDa (sarcalumenin) and 53 kDa (53 kDa glycoprotein) represent minor protein constituents of the LSR membrane fraction and are generated by alternative splicing of the same transcript, which is expressed both in heart and skeletal muscle. The large transcript (sarcalumenin) is a low affinity ($K_D = 0.6$ mM), high capacity (35 mol mol^{-1} protein) Ca^{2+} binding protein, while the shorter product of 53 kDa lacks the NH_2 terminus and thus the Ca^{2+} binding domain. Sarcalumenin is involved in the maintenance of the SERCA protein as illustrated by the fact that sarcalumenin knock-out (KO) animals exhibit significantly decreased SERCA activity and SERCA protein content (Leberer *et al.* 1990; Yoshida *et al.* 2005).

As shown in Fig. 2, the protein composition of the JFM is far more complex than that of the LSR (Costello

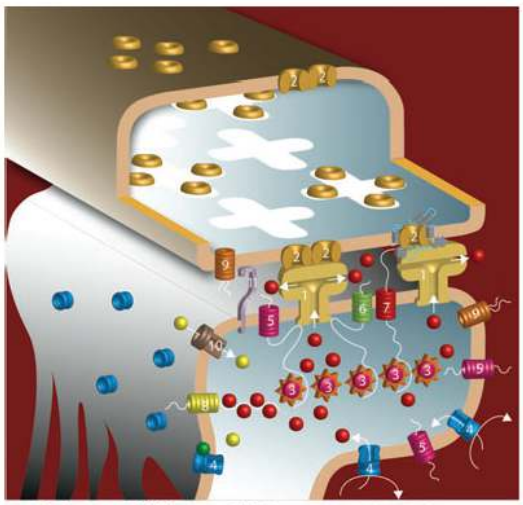

Figure 1. Schematic representation of the protein components of skeletal muscle sarcoplasmic reticulum

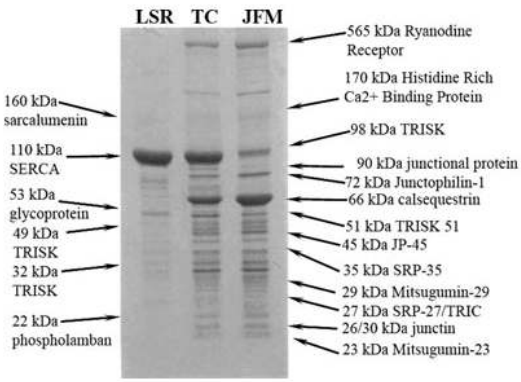

Figure 2. Coomassie Brilliant Blue stained gradient (5–15%) SDS-PAGE of protein components present in the longitudinal sarcoplasmic reticulum (LSR), in terminal cisternae (TC) and in the junctional face membrane (JFM) fractions obtained from rabbit SR
Reproduced from Fig. 2 of Zorzato *et al.* (1986).

et al. 1986); aside from the most abundant components, including the ryanodine receptor (RyR), calsequestrin (CsQ), histidine rich Ca^{2+} binding protein and triadin(s) (TRISK), which will not be discussed in this review, there are a number of other minor protein components whose function has recently been unravelled or that still await functional characterization. Much work has focused on the identification of the full set of protein constituents of the junctional face membrane and on understanding their functional role in excitation–contraction coupling. Two main approaches have been used to characterize the minor membrane protein components at the molecular, cellular and functional level: (i) the immuno-proteomic approach utilized by the group of Takeshima, which combines production of monoclonal antibodies directed against membrane proteins selected on the basis of specific triadic immunostaining of muscle sections, cDNA cloning, expression and biochemical analysis of identified proteins and gene knock-out techniques (Weisleder *et al.* 2008); and (ii) junctional face membrane purification or heparin agarose chromatography and identification of proteins co-eluting with the RyR, combined with Western blotting, mass spectrometry analysis and peptide sequencing (Divet *et al.* 2005). These approaches have been relatively successful and at least five minor membrane protein components, which will be described in the next section, have been identified and characterized.

Mitsugumin-29. This is a 29 kDa membrane protein related to the synaptophysin-family, originally identified in the SR of skeletal muscle and in the endoplasmic reticulum of kidney renal tubules (Shimuta *et al.* 1998). Analysis of its primary sequence, as well as biochemical and ultrastructural evidence, suggests that mitsugumin-29 contains four transmembrane domains and that it is localized in the transverse tubules of mature skeletal muscles where it self-associates as hexamers (Shimuta *et al.* 1998; Brandt *et al.* 2001). Though mitsugumin-29 does not tightly associate with other proteins, experimental evidence suggests that it can functionally interact with the RyR1, whereby it increases RyR1 open probability without affecting channel current amplitude (Pan *et al.* 2004). Muscles isolated from mitsugumin-29 KO mice exhibit swollen transverse tubules, vacuolated SR and misaligned triadic structures. These ultrastructural changes are accompanied by dysfunctional Ca^{2+} handling; specifically, the intracellular Ca^{2+} stores of myotubes from mitsugumin-29 KO mice deplete more rapidly and refill more slowly after depolarization than myotubes from control mice (Pan *et al.* 2002). Such alterations lead to 'global' functional changes, so that muscles from mitsugumin-29 KO mice fatigue more rapidly than their wild-type counterpart (Nagaraj *et al.* 2000). Taken together these results suggest that mitsugumin-29 functions as a tethering structure, forcing the transverse tubules into a conformation, which favours the formation of triadic structures. Lack of integral triads then leads to altered Ca^{2+} handling and defective SOC-dependent Ca^{2+} influx.

Junctophilin-1. Junctophilins are membrane spanning proteins with a large cytoplasmic region containing a 14-amino-acid repeat motif (MORN motif) with selective binding affinity for the plasma membrane and a carboxy-terminal transmembrane segment spanning the ER/SR (Takeshima *et al.* 2000). At least three isoforms encoded by distinct genes, exist: junctophilin-1 is specifically expressed in skeletal muscle, junctophilin-2 is expressed in the heart, in skeletal muscles and in smooth muscles, and junctophilin-3 is expressed in the brain (Nishi *et al.* 2000). In skeletal muscle junctophilin-1 (72 kDa protein) is involved in physically linking the transverse tubules to the SR membrane. Protein overlay and surface plasmon assays suggest that it achieves this by interacting with phospholipids, especially with sphingomyelin and phosphatidylchloine, rather than through protein–protein interactions (Weisleder *et al.* 2008). Ablation of junctophilin-1 severely affects muscle function leading homozygous KO mice to premature death within 20 h after birth. Ultrastructural examination of the skeletal muscles of junctophilin-1 KO mice shows morphological abnormalities, including incomplete formation of the junctional complexes between transverse tubules and the SR, swollen terminal cisternae and reduced numbers of triads. As a consequence muscles develop less contractile force after electrical stimulation and show abnormal sensitivity to extracellular Ca^{2+} (Ito *et al.* 2001; Komazaki *et al.* 2002).

SRP-27/TRIC-A. Mitsugumin-33 or TRIC-A (trimeric intracellular cation-selective channel) (Yazawa *et al.* 2007) also known as SRP-27 (sarcoplasmic reticulum protein of 27 kDa) (Bleunven *et al.* 2008) is expressed in excitable tissues and is particularly enriched in fast twitch skeletal muscles, where its expression level peaks after 2 months of post-natal development. Mice lacking TRIC/SRP-27 are viable and display no overt phenotype. Double-labelling immunocytochemistry experiments of mouse muscle fibres indicate that SRP-27 is localized in the perinuclear endoplasmic reticulum as well as in a SR subcompartment, which is adjacent to, but distinct from, that containing the RyR1 and SERCA (Bleunven *et al.* 2008). Interestingly, SRP-27/TRIC-A could be pulled-down by beads coated with maurocalcine and RyR1, but not with maurocalcine alone, raising the possibility that SRP-27/TRIC-A is part of the RyR1 macromolecular complex (Bleunven *et al.* 2008). Hydrophobicity plots and biochemical analysis also revealed that TRIC-A/SRP-27 is an integral ER/SR

protein containing up to three membrane spanning domains, whose amino terminus is located in the lumen of the ER/SR and whose carboxy terminus is exposed to the cytoplasm. Sequence comparison also predicts the presence of an ion-conducting pore between the first and second transmembrane domains and cross-linking experiments demonstrate that TRIC-A/SRP-27 tends to form homo-oligomers (dimers and trimers). Three-dimensional reconstruction studies of the native protein suggest that it acquires a pyramidal elongated structure, similar to that of bacterial porin channels (Yazawa *et al.* 2007). Interestingly, reconstitution in lipid bilayers suggest that TRIC-A/SRP-27 is a cation channel, with a selectivity of K^+ over Na^+ (permeability ratio $P_K/P_{Na} = 1.5$) (Yazawa *et al.* 2007). To gain more insight into the function of this channel, Yazawa *et al.* (2007) followed changes in the membrane potential of isolated muscle fibres from control and TRIC-A/SRP-27 KO mice. The lack of TRIC-A/SRP-27 reduced the K^+ permeability accompanying thapsigargin-induced Ca^{2+} efflux, without affecting Ca^{2+} permeability, suggesting that this protein may act as a monovalent-cation channel. Such a channel could be activated physiologically during RyR1-mediated Ca^{2+} release to counter-balance the charge movement due to efflux of Ca^{2+} (Somlyo *et al.* 1981), which would otherwise leave the SR lumen with a negative charge. However, the role of TRIC-A/SRP-27 as a monovalent-cation contercurrent channel during Ca^{2+} release has been challenged by data of Gillespie & Fill (2008), which indicates that the RyR1 channel mediates its own potassium countercurrent during SR Ca^{2+} release. This would obviate the need of an additional counter-current carrier during SR Ca^{2+} release, leaving the exact functional role of TRIC-A/SRP-27 controversial.

JP-45. JP-45 is a 45 kDa polypeptide containing a single transmembrane segment, which is highly enriched in skeletal muscle junctional face membrane where its expression is developmentally regulated, reaching maximal levels during the second month of post-natal development (Anderson *et al.* 2003). Originally JP-45 was identified as a protein weakly phosphorylated by cAMP-dependent protein kinase and co-eluting with the RyR1 and DHPR from a heparin-agarose column (Zorzato *et al.* 2000). Surprisingly, however, co-immunoprecipitation experiments revealed that JP-45 is not part of the RyR1 macromolecular complex, but rather it interacts with calsequestrin via its luminal carboxy-terminal domain and with $Ca_v1.1$, through its cytoplasmic amino terminus (Anderson *et al.* 2003). Extensive pulldown and co-immunoprecipitation experiments revealed that JP-45 binds to different regions on the $Ca_v1.1$, namely to its carboxy terminus and to a region within the I–II loop referred to as AID, where the β1a subunit also binds (Anderson *et al.* 2006). The interaction between $Ca_v1.1$ and β1a is thought to be essential for targeting or stabilizing $Ca_v1.1$ on the plasma membrane (Flucher *et al.* 2002).

Several approaches have been exploited to unravel the function of JP-45 in skeletal muscle: (i) acute over-expression and depletion of JP-45 in differentiated C2C12 myotubes (Anderson *et al.* 2006; Gouadon *et al.* 2006), and (ii) chronic depletion in JP-45 knock out mice (Delbono *et al.* 2007). Interestingly both over-expression and ablation of JP-45 result in a decrease of voltage-dependent Ca^{2+} release. This effect could be due to a decrease of functional expression of the $Ca_v1.1$ on the transverse tubules (Anderson *et al.* 2006; Delbono *et al.* 2007). Alternatively, the effect on Ca^{2+} release may be linked to alterations of the interaction of JP-45 with calsequestrin. Gouadon *et al.* (2006) showed that low levels of JP-45 over-expression affect the permeability of the Ca^{2+} release unit by altering excitation–contraction coupling transfer function (Gouadon *et al.* 2006). Given that the lumenal carboxy terminus of JP-45 binds to calsequestrin, it is possible that JP-45 constitutes a key protein for a signalling pathway between calsequestrin and $Ca_v1.1$. Over-expression of JP-45 may result in the accumulation of JP-45 molecules which are not associated with calsequestrin, and this in turn may send an inhibitory signal to the $Ca_v1.1$.

Interestingly the skeletal muscle phenotype of young JP-45 KO mice is reminiscent of that of aged mice. During mouse ageing, the membrane density of the voltage sensor ($Ca_v1.1$), the SR membrane content of JP-45 and the Ca^{2+} currents of muscle membranes are significantly lower compared to those of young animals (Delbono *et al.* 1995; Renganathan *et al.* 1997; Gonzales *et al.* 2003; Anderson *et al.* 2006). These data suggest that both $Ca_v1.1$ and JP-45 may be important for the maintenance of muscle strength, and indicate that JP-45 KO mice may be a useful experimental model to investigate alterations of excitation–contraction coupling linked to ageing.

Junctate/humbug. Junctate is a 33 kDa protein with a single ER/SR membrane spanning domain, expressed in a variety of excitable and non-excitable tissues (Treves *et al.* 2000; Dinchuk *et al.* 2000; Hong *et al.* 2001). Figure 3*A* shows how transcripts deriving from the same gene (*BAH* or AβH-J-J locus) located on human chromosome 8q12.1 can give rise to four distinct classes of proteins via a complex pattern of alternative splicing. Though the complexity of AβH-J-J locus is more the exception than the rule, it illustrates how important it is to precisely establish the number and type of gene products when deciding to create knock out animal models of protein(s) encoded by the *BAH* gene.

Figure 3*B* illustrates schematically how the different polypeptides are assembled to yield: (i) junctin, a structural calsequestrin binding protein present in cardiac and skeletal muscle SR that forms a quaternary complex with triadin, RyR1 and calsequestrin (Jones *et al.* 1995; Kagari *et al.* 1996; Zhang *et al.* 1997); (ii) aspartyl-β-hydroxylase, an enzyme catalysing post-translational hydroxylation of aspartate and asparagine residues within epidermal growth factor-like domains present in receptors and receptor ligands involved in cell growth and differentiation, and extracellular matrix molecules (Stenflo *et al.* 1989; Gronke *et al.* 1989; Monkovic *et al.* 1992); (iii) junctate, a moderate affinity (K_D 217 μM), high capacity (21 mol Ca^{2+}/mol protein) Ca^{2+} binding protein (Treves *et al.* 2000); and (iv) humbug, a truncated version of aspartyl-β-hydroxylase, lacking its catalytic domain, which shares with junctate the high capacity moderate affinity Ca^{2+} binding domain

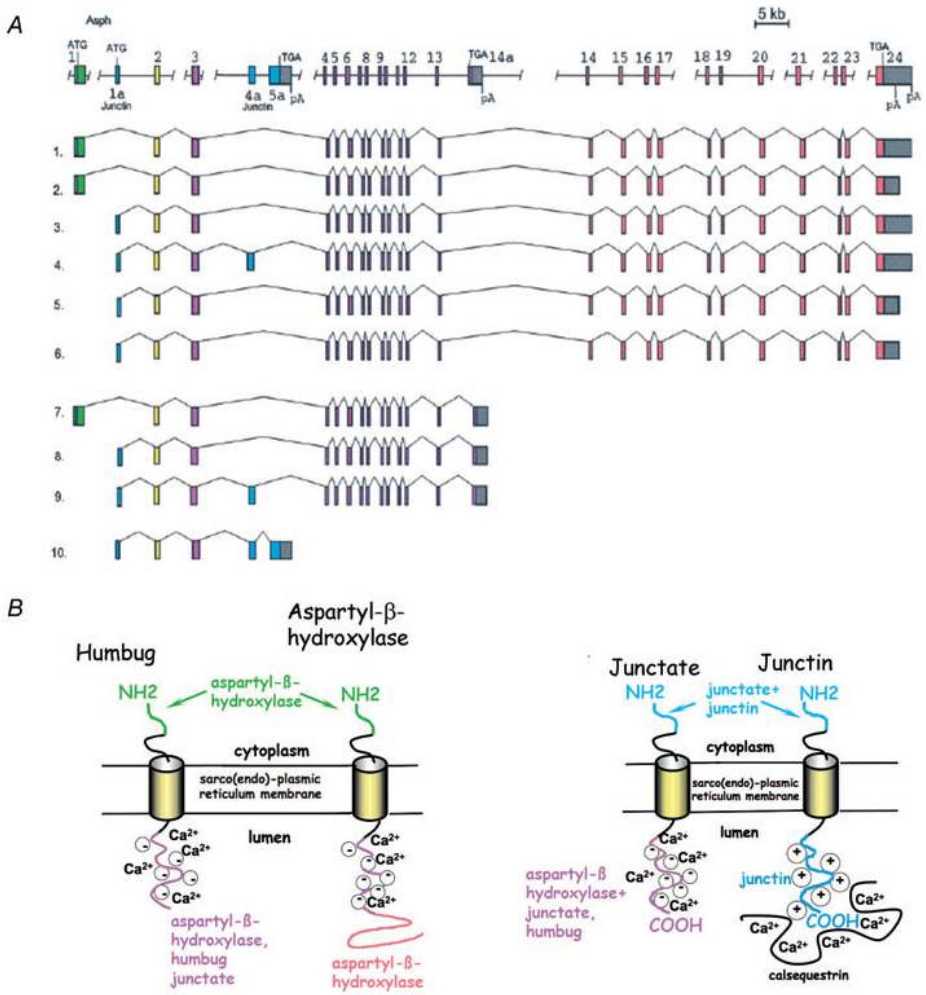

Figure 3. Genomic organization, splicing pattern and main protein products deriving from of the A-β-J-J locus

A, coloured boxes represent different exons. Products deriving from exon 1 (green box) give rise to β-aspartyl-hydroxylase/humbug; products deriving from exon 1b (light blue) give rise to junctin/junctate. Yellow box encodes the transmembrane domain. Reproduced from Fig. 4 of Dinchunk *et al.* 2000. *B*, schematic representation of the 4 main proteins (junctin, junctate, aspartyl-β-hydroxylase and humbug) derived by assembling the different exons (colours of the protein domains match those of the exons from which they are derived).

(Dinchuk *et al.* 2000; Treves *et al.* 2000; Hong *et al.* 2001). Analysis of the genomic organization of the AβH-J-J locus has revealed the presence of two distinct promoters, P1 and P2 (Feriotto *et al.* 2006), which are regulated by specific transcription factors, giving rise to polypeptides with distinct amino termini and tissue distribution. Transcripts starting from exon 1 (green box in Fig. 3*A*), which is under the control of the P1 promoter, are expressed in most tissues and share their NH_2 terminus with aspartyl-β-hydroxylase (Treves *et al.* 2000; Dinchuk *et al.* 2000; Feriotto *et al.* 2007). Exon 1a (blue box in Fig. 3*A*) is approximately 8 kb downstream from exon 1 and is under the control of the P2 promoter, whose induction is controlled by the muscle specific transcription factor MEF-2 (Feriotto *et al.* 2005). Transcripts starting from this exon are expressed in striated muscles and share their NH_2 termini with junctin/junctate (Treves *et al.* 2000; Dinchuk *et al.* 2000). Exon 2 encodes the transmembrane domain (yellow box in Fig. 3*A*) and together with exon 3 is shared by all family members deriving from the AβH-J-J locus. The carboxy-terminal portion of the proteins depends on which exons are transcribed: junctin results from transcription of exons 4a and 5a, while all other products are generated via transcription of exons 4–24 and result in a variety of products of different sizes. The longer transcripts give rise to the enzyme aspartyl-β-hydroxylase with an apparent molecular mass of approximately 120 kDa. The shorter transcripts generate proteins with molecular masses ranging from 40 to 53 kDa which share the acidic Ca^{2+} binding domain (Treves *et al.* 2000; Dinchuk *et al.* 2000; Hong *et al.* 2001). Heart expresses junctin and junctate, as well as humbug and aspartyl-β-hydroxylase (Treves *et al.* 2000; Dinchuk *et al.* 2000; Hong *et al.* 2001). Interestingly, humbug is also highly expressed in a variety of invasive human tumours and its level of expression has been suggested to be useful as a prognostic marker for cancer progression (Wang *et al.* 2007; Lee, 2008).

In the rest of this section, only the functional properties of junctate will be discussed, and the reader is referred to other articles describing the function of aspartyl-β-hydroxylase and junctin (Gronke *et al.* 1989; Jones *et al.* 1995; Kagari *et al.* 1996; Zhang *et al.* 1997; Wang *et al.* 2007). Because of its calcium binding properties, a number of approaches were undertaken to define the potential role of junctate in Ca^{2+} homeostasis: (i) acute over-expression and depletion of junctate from cultured cells (Treves *et al.* 2000, 2004), and (ii) chronic over-expression of junctate in skeletal muscles (Divet *et al.* 2007) and heart (Hong *et al.* 2008). Acute over-expression of junctate in COS-7 and HEK293 cells is accompanied by significant functional and structural changes of the ER membrane. Specifically, in HEK cells over-expressing TRPC3 channels (HEKT3), over-expression of junctate induces extensive proliferation of the ER resulting in significantly larger and more frequent couplings between the ER and the plasma membrane (Treves *et al.* 2004). The induction of ER plasma membrane couplings by junctate is in agreement with co-immunoprecipitation data showing that junctate forms a supramolecular complex with $InsP_3R$ and TRPC channels. These structural changes are paralleled by alterations of Ca^{2+} homeostasis, specifically by increased peak Ca^{2+} release and store depletion activated Ca^{2+} influx; on the other hand, knocking down junctate results in diminished agonist induced peak $[Ca^{2+}]_i$ transients and store depletion activated Ca^{2+} influx (Treves *et al.* 2000, 2004). The increase of store depletion activated Ca^{2+} influx is mediated by the short cytoplasmic NH_2-terminal domain of the protein, while the luminal carboxy-terminus Ca^{2+} binding domain of junctate (and thus also of humbug) increases the Ca^{2+} content of ER/SR stores and affects calcium transients evoked by SERCA inhibitors.

As to the effect of chronic over-expression of junctate, some discrepancies have arisen from the transgenic mouse models. Over-expression in skeletal muscles does not lead to an overt phenotype but is accompanied by a small increase in Ca^{2+} loading and Ca^{2+} storage of the SR resulting in a significant increase in RyR1 mediated Ca^{2+} release and an increased Ca^{2+} influx following depletion of intracellular Ca^{2+} stores (Divet *et al.* 2007). These changes were attributed to the over-expression of junctate's Ca^{2+} binding sites since the expression levels of other SR Ca^{2+} handling proteins such as SERCA, calsequestrin or sarcalumenin were not changed. Interestingly, the increased Ca^{2+} cycling across the SR membrane was accompanied by an adaptive increase in the number of mitochondria in fast fibres of Extensor Digiforum Longus (EDL) (but not soleus) muscles, which was not due to fast-to-slow fibre type transition (Divet *et al.* 2007). Junctate over-expression in the heart, on the other hand, leads to severe cardiac hypertrophy, bradycardia and arrythmias as well as alterations in the expression level of the SR proteins SERCA2, calsequestrin-2 and calreticulin. This decreased SR content of Ca^{2+} handling proteins is accompanied by an up-regulation of the Na^+/Ca^{2+} exchanger and plasmalemma calcium pump, two component of the cardiac sarcolemma involved in extrusion of Ca^{2+} from the cytoplasm. The decrease of the major calcium binding proteins of cardiac SR is paralleled by a decrease in caffeine induced Ca^{2+} release indicating a lower cardiac Ca^{2+} SR loading. At the moment the reasons for these apparent opposite effects of junctate over-expression in the heart and in skeletal muscle have not yet been elucidated.

Conclusions

The past three decades have seen major advancements in our understanding of the role of skeletal muscle SR

proteins in excitation–contraction coupling. The use of genetically modified animal models has also taught us that few of these proteins, namely the ryanodine receptor, Cav1.1 and junctophilin, are essential for EC coupling. On the other hand, the minor protein components seem to be important for the regulation of the EC coupling machinery. Mouse and cellular models have also shown that acute and/or chronic over-expression/depletion of a variety of minor components do not result in lethal phenotypes and/or in severe damage of to the EC coupling machinery, suggesting that its fine regulation is provided by functionally redundant minor components. The comprehension of EC coupling and its involvement in the pathophysiology of neuromuscular disorders awaits the identification and functional characterisation of the complete array of proteins of the transverse tubule and junctional face membrane compartments.

References

Anderson AA, Treves S, Biral D, Betto R, Sandonà D, Ronjat M & Zorzato F (2003). The novel skeletal muscle sarcoplasmic reticulum JP-45 protein. Molecular cloning, tissue distribution, developmental expression, and interaction with α1.1 subunit of the voltage-gated calcium channel. *J Biol Chem* **278**, 39987–39992.

Anderson AA, Altafaj X, Zheng Z, Wang ZM, Delbono O, Ronjat M, Treves S & Zorzato F (2006). The junctional SR protein JP-45 affects the functional expression of the voltage-dependent Ca^{2+} channel Cav1.1. *J Cell Sci* **119**, 2145–2155.

Berchtold MW, Brinkmeier H & Müntener M (2000). Calcium ion in skeletal muscle: its crucial role for muscle function, plasticity and disease. *Physiol Rev* **80**, 1215–1265.

Bleunven C, Treves S, Jinyu X, Leo E, Ronjat M, De Waard M, Kern G, Flucher BE & Zorzato F (2008). SRP-27 is a novel component of the supramolecular signalling complex involved in skeletal muscle excitation-contraction coupling. *Biochem J* **411**, 343–349.

Block BA, Imagawa T, Campbell KP & Franzini-Armstrong C (1988). Structural evidence for direct interaction between the molecular components of the transverse tubule/sarcoplasmic reticulum junction in skeletal muscle. *J Cell Biol* **107**, 2587–2600.

Brandt N, Franklin G, Brunschwig JP & Caswell A (2001). The role of mitsugumin 29 in transverse tubules of rabbit skeletal muscle. *Arch Biochem Biophys* **385**, 406–409.

Campbell KP, Franzini-Armstrong C & Shamoo AE (1980). Further characterization of light and heavy sarcoplasmic reticulum vesicles. Identification of the sarcoplasmic reticulum feet associated with heavy sarcoplasmic reticulum vesicles. *Biochim Biophys Acta* **602**, 97–116.

Costello B, Chadwick C, Saito A, Chu A & Fleischer S (1986). Characterization of the junctional face membrane from terminal cisternae of sarcoplasmic reticulum. *J Cell Biol* **103**, 741–753.

Delbono O, O'Rourke KS & Ettinger WH (1995). Excitation-calcium release uncoupling in aged single human skeletal muscle fibres. *J Membr Biol* **148**, 211–222.

Delbono O, Xia J, Treves S, Wang ZM, Jimenez-Moreno R, Payne AM, Messi ML, Briguet A, Schaerer F, Nishi M, Takeshima H & Zorzato F (2007). Loss of skeletal muscle strength by ablation of the sarcoplasmic reticulum protein JP45. *Proc Natl Acad Sci U S A* **104**, 20108–20113.

Dinchuk JE, Henderson NL, Burn TC, Huber R, Ho SP, Link J, O'Neil KT, Focht RJ, Scully MS, Hollis JM, Hollis GF & Friedman PA (2000). Aspartyl β-hydroxylase (Asph) and an evolutionarily conserved isoform of Asph missing the catalytic domain share exons with junctin. *J Biol Chem* **275**, 39543–39554.

Divet A, Paesante S, Bleunven C, Anderson A, Treves S & Zorzato F (2005). Novel sarco(endo)plasmic reticulum proteins and calcium homeostasis in striated muscles. *J Muscle Res Cell Motil* **26**, 7–12.

Divet A, Paesante S, Grasso C, Cavagna D, Tiveron C, Paolini C, Protasi F, Huchet-Cadiou C, Treves S & Zorzato F (2007). Increased Ca^{2+} storage capacity of the skeletal muscle sarcoplasmic reticulum of transgenic mice over-expressing membrane bound calcium binding protein junctate. *J Cell Physiol* **213**, 464–474.

Feriotto G, Finotti A, Volpe P, Treves S, Ferrari S, Angelelli C, Zorzato F & Gambari R (2005). Myocyte enhancer factor 2 activates promoter sequences of the human AβH-J-J locus, encoding aspartyl-β-hydroxylase, junctin, and junctate. *Mol Cell Biol* **25**, 3261–3275.

Feriotto G, Finotti A, Breveglieri G, Treves S, Zorzato F & Gambari R (2006). Multiple levels of control of the expression of the human AβH-J-J locus encoding aspartyl-β-hydroxylase, junctin, and junctate. *Ann NY Acad Sci* **1091**, 184–190.

Feriotto G, Finotti A, Breveglieri G, Treves S, Zorzato F & Gambari R (2007). Transcriptional activity and Sp 1/3 transcription factor binding to the P1 promoter sequences of the human AβH-J-J locus. *FEBS J* **274**, 4476–4490.

Flucher BE, Weiss RG & Grabner M (2002). Cooperation of two-domain Ca^{2+} channel fragments in triad targeting and restoration of excitation-contraction coupling in skeletal muscle. *Proc Natl Acad Sci U S A* **99**, 10167–10172.

Franzini-Armstrong C & Jorgensen AO (1994). Structure and development of E-C coupling units in skeletal muscle. *Annu Rev Physiol* **56**, 509–534.

Gillespie D & Fill M (2008). Intracellular calcium release channels mediate their own countercurrent: the ryanodine receptor case study. *Biophys J* **95**, 3706–3714.

González E, Messi L, Zheng Z & Delbono O (2003). Insulin-like growth factor-1 prevents age-related decrease in specific force and intracellular Ca^{2+} in single intact muscle fibres from transgenic mice. *J Physiol* **552**, 833–844.

Gouadon E, Schuhmeier RP, Ursu D, Anderson AA, Treves S, Zorzato F Lehmann-Horn F, & Melzer W (2006). A possible role of the junctional face protein JP-45 in modulating Ca^{2+} release in skeletal muscle. *J Physiol* **572**, 269–280.

Gronke RS, VanDusen WJ, Garsky VM, Jacobs JW, Sardana MK, Stern AM & Friedman PA (1989). Aspartyl β-hydroxylase: in vitro hydroxylation of a synthetic peptide based on the structure of the first growth factor-like domain of human factor IX. *Proc Natl Acad Sci U S A* **86**, 3609–3613.

Hong CS, Kwak YG, Ji JH, Chae SW & Kim DH (2001). Molecular cloning and characterization of mouse cardiac junctate isoforms. *Biochem Biophys Res Commun* **289**, 882–887.

Hong CS, Kwon SJ, Cho MC, Kwak YG, Ha KC, Hong B, Li H, Chae SW, Chai OH, Song CH, Li Y, Kim JC, Woo SH, Lee SY, Lee CO & Kim do H (2008). Overexpression of junctate induces cardiac hypertrophy and arrhythmia via altered calcium handling. *J Mol Cell Cardiol* **44**, 672–682.

Ito K, Komazaki S, Sasamoto K, Yoshida M, Nishi M, Kitamura K & Takeshima H (2001). Deficiency of triad junction and contraction in mutant skeletal muscle lacking junctophilin type 1. *J Cell Biol* **154**, 1059–1067.

Jay SP, Grupp IL, Luo W & Kranias EG (1997). Phospholamban ablation enhances relaxation in the murine soleus. *Am J Physiol Cell Physiol* **42**, C1–C6.

Jones LR, Zhang L, Sanborn K, Jorgensen AO & Kelley J (1995). Purification, primary structure, and immunological characterization of the 26-kDa calsequestrin binding protein (junctin) from cardiac junctional sarcoplasmic reticulum. *J Biol Chem* **270**, 30787–30796.

Kagari T, Yamaguchi N & Kasai M (1996). Biochemical characterization of calsequestrin-binding 30-kDa protein in sarcoplasmic reticulum of skeletal muscle. *Biochem Biophys Res Commun* **227**, 700–706.

Komazaki S, Ito K, Takeshima H & Nakamura H (2002). Deficiency of triad formation in developing skeletal muscle cells lacking junctophilin type 1. *FEBS Lett* **524**, 225–229.

Leberer E, Timms BG, Campbell KP & MacLennan DH (1990). Purification, calcium binding properties, and ultrastructural localization of the 53,000- and 160,000 (sarcalumenin)-dalton glycoproteins of the sarcoplasmic reticulum. *J Biol Chem* **265**, 10118–10124.

Lee JH (2008). Overexpression of humbug promotes malignant progression in human gastric cancer cells. *Oncol Rep* **19**, 795–800.

Liu Y, Kranias EG, Schneider MF (1997). Regulation of Ca^{2+} handling by phosphorylation status in mouse fast- and slow-twitch skeletal muscle fibres. *Am J Physiol Cell Physiol* **273**, C1915–C1924.

MacLennan DH, Asahi M & Tupling AR (2003). The regulation of SERCA-type pumps by phospholamban and sarcolipin. *Ann NY Acad Sci* **986**, 472–480.

Meissner G, Conner GE & Fliescher S (1973). Isolation of sarcoplasmic reticulum by zonal centrifugation and purification of Ca^{2+} pump and Ca^{2+}-binding proteins. *Biochim Biophys Acta* **298**, 246–269.

Melzer W, Hermann-Frank A & Luttgau HC (1995). The role of Ca^{2+} ions in excitation-contraction coupling of skeletal muscle fibres. *Biochim Biophys Acta* **1241**, 59–116.

Mitchell RD, Saito A, Palade P & Fleischer S (1983). Morphology of isolated triads. *J Cell Biol* **96**, 1017–1029.

Monkovic DD, VanDusen WJ, Petroski CJ, Garsky VM, Sardana MK, Zavodszky P, Stern AM & Friedman PA (1992). Invertebrate aspartyl/asparaginyl β-hydroxylase: potential modification of endogenous epidermal growth factor-like modules. *Biochem Biophys Res Commun* **189**, 233–241.

Nagaraj RY, Nosek CM, Brotto MA, Nishi M, Takeshima H, Nosek TM & Ma J (2000). Increased susceptibility to fatigue of slow- and fast-twitch muscles from mice lacking the MG29 gene. *Physiol Genomics* **4**, 43–49.

Nishi M, Mizushima A, Nakagawara K & Takeshima H (2000). Characterization of human junctophilin subtype genes. *Biochem Biophys Res Commun* **273**, 920–927.

Pan Z, Yang D, Nagaraj RY, Nosek TA, Nishi M, Takeshima H, Cheng H & Ma J (2002). Dysfunction of store-operated calcium channel in muscle cells lacking mg29. *Nat Cell Biol* **4**, 379–383.

Pan Z, Hirata Y, Nagaraj RY, Zhao J, Nishi M, Hayek SM, Bhat MB, Takeshima H & Ma J (2004). Co-expression of MG29 and ryanodine receptor leads to apoptotic cell death: effect mediated by intracellular Ca^{2+} release. *J Biol Chem* **279**, 19387–19390.

Paolini C, Protasi F & Franzini-Armstrong C (2004). The relative position of RyR feet and DHPR tetrads in skeletal muscle. *J Mol Biol* **342**, 145–153.

Peachey LD (1965). The sarcoplasmic reticulum and transverse tubules of the frog's sartorius. *J Cell Biol* **25S**, 209–231.

Renganathan M, Messi ML & Delbono O (1997). Dihydropyridine receptor-ryanodine receptor uncoupling in aged skeletal muscle. *J Membr Biol* **157**, 247–253.

Rios E & Pizarro G (1991). Voltage sensor of excitation-contraction coupling in skeletal muscle. *Physiol Rev* **71**, 849–908.

Saito A, Seiler S, Chu A & Fleischer S (1984). Preparation and morphology of sarcoplasmic reticulum terminal cisternae from rabbit skeletal muscle. *J Cell Biol* **99**, 875–885.

Schneider MF & Chandler WK (1972). Voltage dependent charge movement of skeletal muscle: a possible step in excitation-contraction coupling. *Nature* **242**, 244–246.

Shimuta M, Komazaki S, Nishi M, Iino M, Nakagawara K & Takeshima H (1998). Structure and expression of mitsugumin 29 gene. *FEBS Lett* **43**, 263–267.

Slack JP, Grupp IL, Luo W & Kranias EG (1997). Phospholamban ablation enhances relaxation in the murine soleus. *Am J Physiol Cell Physiol* **273**, C1–C6.

Somlyo AV, Gonzalez-Serratos HG, Shuman H, McClellan G & Somlyo AP (1981). Calcium release and ionic changes in the sarcoplasmic reticulum of tetanized muscle: an electron-probe study. *J Cell Biol* **90**, 577–594.

Stenflo J, Holme E, Lindstedt S, Chandramouli N, Huang LH, Tam JP & Merrifield RB (1989). Hydroxylation of aspartic acid in domains homologous to the epidermal growth factor precursor is catalyzed by a 2-oxoglutarate-dependent dioxygenase. *Proc Natl Acad Sci U S A* **86**, 444–447.

Takeshima H, Komazaki S, Nishi M, Iino M & Kangawa K (2000). Junctophilins: a novel family of junctional membrane complex proteins. *Mol Cell* **6**, 11–22.

Treves S, Feriotto G, Moccagatta L, Gambari R & Zorzato F (2000). Molecular cloning, expression, functional characterization, chromosomal localization, and gene structure of junctate, a novel integral calcium binding protein of sarco(endo)plasmic reticulum membrane. *J Biol Chem* **275**, 39555–39568.

Treves S, Franzini-Armstrong C, Moccagatta L, Arnoult C, Grasso C, Schrum A, Ducreux S, Zhu MX, Mikoshiba K, Girard T, Smida-Rezgui S, Ronjat M & Zorzato F (2004). Junctate is a key element in calcium entry induced by activation of $InsP_3$ receptors and/or calcium store depletion. *J Cell Biol* **166**, 537–548.

Volpe P & Simon BJ (1991). The bulk of Ca^{2+} released to the myoplasm is free in the sarcoplasmic reticulum and does not unbind from calsequestrin. *FEBS Lett* **278**, 274–278.

Wang J, de la Monte SM, Sabo E, Kethu S, Tavares R, Branda M, Simao L, Wands JR & Resnick MB (2007). Prognostic value of humbug gene overexpression in stage II colon cancer. *Hum Pathol* **38**, 17–25.

Weisleder N, Takeshima H & Ma J (2008). Immuno-proteomic approach to excitation–contraction coupling in skeletal and cardiac muscle: molecular insights revealed by the mitsugumins. *Cell Calcium* **43**, 1–8.

Yazawa M, Ferrante C, Feng J, Mio K, Ogura T, Zhang M, Lin PH, Pan Z, Komazaki S, Kato K, Nishi M, Zhao X, Weisleder N, Sato C, Ma J & Takeshima H (2007). TRIC channels are essential for Ca^{2+} handling in intracellular stores. *Nature* **448**, 78–82.

Yoshida M, Minamisawa S, Shimura M, Komazaki S, Kume H, Zhang M, Matsumura K, Nishi M, Saito M, Saeki Y, Ishikawa Y, Yanagisawa T & Takeshima H (2005). Impaired Ca^{2+} store functions in skeletal and cardiac muscle cells from sarcalumenin-deficient mice. *J Biol Chem* **280**, 3500–3506.

Zhang L, Kelley J, Schmeisser G, Kobayashi YM & Jones LR (1997). Complex formation between junctin, triadin, calsequestrin, and the ryanodine receptor. Proteins of the cardiac junctional sarcoplasmic reticulum membrane. *J Biol Chem* **272**, 23389–23397.

Zorzato F, Margreth A & Volpe P (1986). Direct photoaffinity labelling of junctional sarcoplasmic reticulum with [^{14}C]doxorubicin. *J Biol Chem* **261**, 13252–13257.

Zorzato F, Anderson AA, Ohlendieck K, Froemming G, Guerrini R & Treves S (2000). Identification of a novel 45 kDa protein (JP-45) from rabbit sarcoplasmic-reticulum junctional-face membrane. *Biochem J* **351**, 537–543.

Acknowledgements

This work was supported by the Swiss National Science Foundation (SNF grant number SNF 3200BO-114597), by the Fondation Suisse de Recherche sur les maladies musculaires, by the Association Française contre les Myopathies and by Telethon Italy.